
# 20th International Symposium on Intercalation Compounds

June 2-6, 2019

CDC - UNICAMP - Campinas - Brazil

# Proceedings brochure

Realization

UNICAMP

USP

Organization

ACQUAVIVA EVENTOS

Support

FAPESP

CNPq
Conselho Nacional de Desenvolvimento Científico e Tecnológico

CAPES

International Zeolite Association

ROYAL SOCIETY OF CHEMISTRY

aipea
ASSOCIATION INTERNATIONALE POUR L'ETUDE DES ARGILES

GASART

ACIL Weber

GRUPO guaçu

SHIMADZU
Excellence in Science

# Plenary Lectures

## Plenary Lecture: Layered Double Hydroxide Based Photocatalysts for Efficient Solar Fuels

**Tierui Zhang -** *Key Laboratory of Photochemical Conversion and Optoelectronic Materials, Technical Institute of Physics and Chemistry (TIPC), Chinese Academy of Sciences (CAS), Beijing, China*

Layered double hydroxide (LDH)-based materials have emerged as one of the most promising photocatalysts for water splitting into hydrogen, $CO_2$ photoreduction into fuels and photofixation of $N_2$ into $NH_3$, owing to their unique layered structure, compositional flexibility, controllable particle size, low manufacturing cost and ease of synthesis. Herein, some very recent research progress in my group has been summarized on the rational design of LDH-based photocatalysts for above-mentioned reactions by enhancing the light absorbance and separation of electron-hole pairs of photocatalysts. For instance, I) by creating more oxygen defects in ultrathin ZnAl-LDH nanosheets, the photocatalytic reduction of $CO_2$ with water over ZnAl-LDH exhibited stable activity of ≈7.6 μmol $g^{-1}$ $h^{-1}$; in ultrathin ZnAl-LDH nanosheets $N_2$ can be efficiently reduced into $NH_3$ under visible-light irradiation; II) By constructing heterogeneous interface structure, NiO/Ni nanocatalysts exhibited an unexpectedly high selectivity of 60% for $C_2$-$C_7$ hydrocarbons in the CO hydrogenation reaction under visible-light irradiation.[1-8]

### References

**(1)** Zhang, Tierui, et al., *Adv. Mater.* **2018**, 30 (3), 1704663.

**(2)** Zhang, Tierui, et al., *Adv. Mater.* **2017**, 29 (42), 1703828.

**(3)** Zhang, Tierui, et al., *Adv. Mater.* **2017**, 29 (27), 1700803.

**(4)** Zhang, Tierui, et al., *Adv. Mater.* **2017**, 29 (16), 1605148.

**(5)** Zhang, Tierui, et al., *Adv. Mater.* **2016**, 28 (43), 9454-9477.

**(6)** Zhang, Tierui, et al., *Angew. Chem. Int. Ed.* **2016**, 55 (13), 4215-4219.

**(7)** Zhang, Tierui, et al., *Adv. Energy Mater.* **2016**, 6 (3), 1501241.

**(8)** Zhang, Tierui, et al., *Adv. Mater.* **2015**, 27 (47), 7824-7831.

**Plenary Lecture: The versatile world of clays: from early studies to innovative applications**

**C. Bisio**, G. Gatti, F. Carniato, L. Marchese - *Dipartimento di Scienze e Innovazione Tecnologica, Università del Piemonte Orientale, Alessandria, Italy*

The use of clay minerals has ancient origin and nowadays these natural materials are extensively employed for a great number of environmental and engineering applications. The major advantages in the use of natural clays are associated to their large availability and low price. However, their use requires several extensive purification steps. In addition, depending on the genesis process and on the provenance site, the chemical composition of natural materials can be extremely variable. This variability represents a strong limitation for their application, especially when surface properties have to be strictly controlled. These reasons have stimulated scientists to develop synthetic materials whose structure and properties mimic those of natural layered materials. Through designed synthesis procedures it is possible to obtain lamellar solids with controlled chemical compositions, tunable layer dimensions and enhanced physico-chemical features. The modification of the inorganic clays by insertion of specific ions in the tetrahedral sheets (*i.e.* transition metal species), and/or the substitution of cations located in the interlayer space by organic surfactants, ions or hybrid compounds, make clays promising matrices for several applications spanning from from heterogeneous catalysis to polymer science (*see Figure*). In this respect, examples of the possible modification of synthetic clays will be given starting from early studies (for instance concerning the use of clays as heterogeneous catalysts or as fillers for the preparation of polymer nanocomposites) to more recent applications especially focusing to the development of solids for environmental purposes. Results obtained in our research group and related to the possible

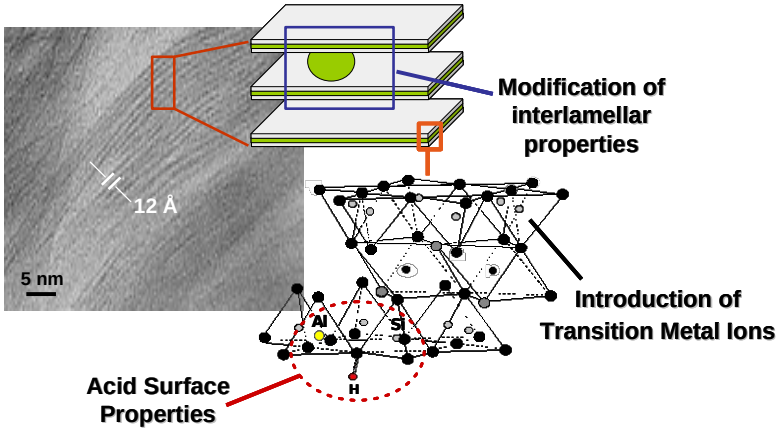

modification of the framework and/or interlayer properties of synthetic saponite clays to extend their application fields will be also discussed.

## Plenary Lecture: Advances of Zirconium Phosphate and Phosphonate Chemistry for new Applications

**Morena Nocchetti** - *Dipartimento di Scienze Farmaceutiche, Università degli Studi di Perugia (Perugia, Italy)*

Zirconium phosphate and phosphonate chemistry has grown considerably in recent years, due to the increased demand of new functional solids for application in many fields of materials chemistry. Inorganic–organic functional derivatives have been prepared by the modification of layered α- and γ-phases, with formula α-$Zr(HPO_4)_2 \cdot H_2O$, and γ-$ZrPO_4(H_2PO_4) \cdot 2H_2O$, by means of intercalation, topotactic exchange or ion-exchange reactions, carried out in soft conditions. Moreover, Zr phosphonates with organic functional groups covalently bonded to the inorganic layers and with structures related to those of their parent compounds, can be easily obtained by direct synthesis. More recently many new compounds, essentially based on aminophosphonate derivatives, have been discovered and their structures were solved mostly from powder diffraction data. In particular, the use of selected aminodiphosphonate building blocks, that can connect both phosphonic groups to metal atoms on the same side of layers, allowed to obtain compounds with reduced crowding of organic groups with different reactivity in the interlayer space. [1,2]. Finally, the combination of proper aminodiphosphonate and phosphate building blocks yielded compounds with a highly accessible interlayer region, that could accommodate a range of polar guest species, up to their complete exfoliation. The possibility to obtain single-layer nanosheets with a given structure is an ambitious and highly desirable goal because monolayers, or packets of few layers, can lead to the preparation of low-dimensional compounds in which the number of accessible functional sites on the surface of layers is largely increased. Moreover, the large number of polar amino, carboxylic, and free P-OH groups on the surface of these layers resulted very efficient to firmly immobilize metal nanoparticles, with catalytic or bioactive properties, such as gold, silver, palladium, or nickel [3,4].

[1] R. Vivani, F. Costantino, M. Taddei in “Metal Phosphonate Chemistry: From Synthesis to Applications”, A. Clearfield and K. Demadis (Eds), (The Royal Society of Chemistry, Cambridge, 2012) Chap 2, p 45-86.
[2] R. Vivani, F. Costantino, G. Alberti, M. Nocchetti, Micropor. Mesopor. Mater, 2008, 107, 58–70.
[3] F. Costantino, R. Vivani, M. Bastianini, L. Ortolani, O. Piermatti, M. Nocchetti, L. Vaccaro, Chem. Commun., 2015, 51, 15990—15993.
[4] F. Costantino, M. Nocchetti, M. Bastianini, M. Caporali, F. Liguori, ACS Applied Nano Materials, 2018, 1, 1750–1757.

## Plenary Lecture: Hydrous Layered Silicates

**Bernd Marler -** *Department of Geology, Mineralogy and Geophysics, Ruhr University Bochum, Germany*

The layer silicates considered as “Hydrous Layer Silicates” (HLSs) consist of a tetrahedral silicate layer and an inter-layer region where cations of low charge density (predominantly organic cations) and water molecules are located. Only weak interactions exist between neighbouring layers and between layers and the constituents of the inter-layer region. HLSs can be made by i) classical hydrothermal synthesis using organic cations or hydrated alkali metal ions {e.g. $[Na(H_2O)_6,]^+$}, ii) by acid leaching of layered alkali silicates, or iii) using the ADOR method (first step). Also, some natural HLSs like the mineral Kanemite, $Na_4[H_4Si_8O_{20}] \bullet 12\ H_2O$, exist. HLSs have been used as adsorbents and also for the preparation of composite materials by intercalating the materials with various organic molecules and cations. In particular, HLSs are interesting materials to serve as precursors for the synthesis of micro- and mesoporous framework silicates while preserving their layer topology. Initially, an overview on the HLSs materials known so far will be presented with a focus on structural aspects. The structures of the silicate layers show a remarkable relation to layer-like building blocks of zeolite frameworks. Therefore, HLSs are also often named “layered zeolites” or “two-dimensional zeolites”. A database on well characterized HLSs which is available online will be presented. This database also includes a compilation of some relevant features of the silicate layers. So far, silicate layers of 16 different layer topologies (= layer types) have been identified as being part of an HLS structure. The structure solution of HLS materials proved in most cases to be quite difficult because of the limited crystallinity of the materials leading to low resolution powder diffraction data. Various methods had to be used to solve the structures. Among those, FTIR spectroscopy turned out to be a useful tool to develop a first structure model of a HLS with a, so far, unknown structure. In contrast to many other silicates, the fingerprint region of the FTIR spectrum of a HLS (ca. 400 - 1500 $cm^{-1}$) gives a clear indication on the layer type of the material. Furthermore, some recent research results will be presented. This comprises i) the syntheses and structures of two fairly well ordered Crystalline Silicic Acids, ii) the structures of hydrated and dehydrated PREFER, and iii) a study on a “phyllo-tecto pair” of materials being closely related to each other and belonging to the Silica-X family of materials: RUB-6, a hydrous layer silicate and

RUB-5, a silica zeolite with a very high framework density. Moreover, the structure and some properties of the mineral magadiite will be presented. Magadiite, $Na_2[H_2Si_{14}O_{30}] * 8\ H_2O$ is known as a mineral since 1967 and has frequently been synthesized in the lab. The structure, however, remained unsolved for a long time, because of its complex nature and since magadiite typically shows considerable structural disorder.

# Keynote Lectures

## Keynote Lecture: The structure and ion-exchange properties of layered double hydroxides on the atomic level

**Ulla Gro Nielsen** - Department of Physics, Chemistry and Pharmacy, University of Southern Denmark, Odense, Denmark

Layered double hydroxides (LDH), anionic clays, find application within, e.g., environmental remediation, catalysis and as energy materials due to their flexible chemistry and ion-exchange properties. However, LDH materials are notorious for their poor crystallinity and frequent stacking faults, which render structural characterization challenging. Their general chemical composition is $[M(II)_{1-x}M(III)_x(OH)_2A_y\ nH_2O]$, where possible M(II) and M(III) cations include Mg(II), Ca(II), Zn(II), Ni(II), Al(III), Ga(III), and Fe(III). A is an anion needed for charge balance and is located in the interlayer along with interlayer water. The LDH properties and hence function are controlled by the choice of metal ions and anion. Especially, the distribution of metal ions in the cation layer has a large impact on the properties, but this information is difficult to obtain by diffraction techniques due to the large number of stacking faults in the LDHs. Structural characterization of LDH from the atomic level to the bulk composition has been obtained by combining multiple experimental techniques (PXRD, solid state NMR, vibrational spectroscopy, electron microscopy and ICP), which has advanced our understanding of the atomic level structure of LDH.[1-4] Furthermore, LDH are extensively tested for application in water remediation due to their ion-exchange properties. Detailed insight into the ion-exchange properties has been obtained using SSNMR in combination with adsorption studies.

1. Jensen, N. D.; Forano, C.; Pushparaj, S. S. C.; Nishiyama, Y.; Bekele, B.; Nielsen, U. G., *Physical Chemistry Chemical Physics* **2018,** *20*, 25335.
2. Pushparaj, S. S. C.; Forano, C.; Prevot, V.; Lipton, A. S.; Rees, G. J.; Hanna, J. V.; Nielsen, U. G., *Journal of Physical Chemistry C* **2015,** *119*, 27695.
3. Pushparaj, S. S. C.; Jensen, N. D.; Forano, C.; Rees, G. J.; Prevot, V.; Hanna, J. V.; Ravnsbæk, D. B.; Bjerring, M.; Nielsen, U. G,. *Inorganic Chemistry* **2016,** *55*, 9306.

4. Staal, L. B.; Charan Pushparaj, S. S.; Forano, C.; Prevot, V.; Ravnsbæk, D. B.; Bjerring, M.; Nielsen, U. G., *Journal of Materials Chemistry A* **2017,** *5* (41), 21795.

## Keynote Lecture: Layered double hydroxide and layered hydroxide salts as cationic exchangers!?

**Fernando Wypych - Department of Chemistry - Federal University of Paraná - - Curitiba - PR - Brazil.**

Layered double hydroxides (LDHs) and layered hydroxide salts (LHSs), with the respective generic formulas $[M^{+2}_{1-x}M^{+3}_{x}(OH)_2](A^{-n})_{x/n}.yH_2O$ and $[M^{+2}(OH)_{2-x}](A^{-n})_{x/n}.yH_2O$ ($M^{+2}$ and $M^{+3}$ = cation metal and $(A^{-n})_{x/n}.yH_2O$ = intercalated hydrated anion) are very well known as anionic exchangers. When some sulfate intercalated LDHs and LHSs are analyzed as minerals, like Natroglaucocerinite ($[Zn_6Al_3(OH)_{18}(SO_4)_2.6H_2O].Na(H_2O)_6$) and Gordaite ($[Zn_4(OH)_6(SO_4)Cl].Na(H_2O)_6$), a mismatch occurs during the neutralization of the hydroxide layers. In the case of Natroglaucocerinite, between the triple positive Zn/Al hydroxide layers are intercalated two hydrated sulfate anions, resulting in an excess of negative charge, which is counterbalanced with the intercalation of a hydrated sodium cation. In the case of Gordaite, the double positive zinc hydroxide layers are grafted with one sulfate and one chloride anion, resulting again in negatively charged layers, which can be counterbalanced with the intercalation of hydrated sodium cations. The objective of the present talk is to present the synthesis and characterization of different LDHs ($(M^{+2}_6M^{+3}_3(OH)_{18}(SO_4)_2.6H_2O].B^+(H_2O)_6$; $M^{+2}$= Mn, Mg, Zn, Co, Ni; $M^{+3}$= Al, Cr; $B^+$= Li, Na, K) and LHSs ($[M^{+2}_4(OH)_6(SO_4)Cl].B^+(H_2O)_6$; $M^{+2}$= Mg, Zn, Co, Ni; $B^+$= Li, Na, K) in the form of minerals. The results obtained when these materials are submitted to cation and anion exchange reactions are described.

| | ID | TITLE | PRESENTATION | THEME | AUTHORS |
|---|---|---|---|---|---|
| | - | Designing Hybrid Materials with Two-Dimensional Nanostructures for Energy Applications | Invited oral speaker | - | Camila M. Maronese |
| | - | Examples of Energetic and Environmental applications of Pillared Clays | Invited oral speaker | - | Karim Sapag |
| | - | Organophilic clays: preparation and uses | Invited oral speaker | - | Francisco R. Valenzuela Diaz |
| | - | Milestones of LDHs in benchmarking (bio-based) Polymer Performances | Invited oral speaker | - | Fabrice Leroux |
| 1 | 371 | Recent Development on Long-afterglow Phosphorescent Organic-inorganic Hybrids | Oral | Inorganic and hybrid layered materials | Yan Dongpeng |
| 2 | 377 | High oxygen barrier coating using non-toxic nanosheet dispersions for flexible food packaging film | Oral | Inorganic and hybrid layered materials | jingfang yu,Kanittika Ruengkajorn,Dermot OHare,Jean-Charles Buffet,Dana-Georgiana Crivoi, Chunping Chen |
| 3 | 408 | EXFOLIATION OF LAYERED METAL ORGANOPHOSPHONATES | Oral | Inorganic and hybrid layered materials | Vítezslav Zima,Klara Melanova,Katerina Kopecka,Ludvik Benes,Petr Knotek |
| 4 | 419 | Obtaining Al-3D-solids from the layered silicate Na-RUB-18: pillarization and hydrothermal transformation | Oral | Microporous and mesoporous materials | Gabriel de Biasi Báfero,Erica Cristina de Oliveira Munsignatti,Heloise Pastore |
| 5 | 430 | DIVALENT METAL-BASED SUPERCONDUCTING GIC PREPARED BY A SOLID-LIQUID REACTION IN MOLTEN SALTS | Oral | Graphite, carbon, and graphene intercalation compounds | Sebastien CAHEN |
| 6 | 438 | Study of the surface properties of clays and intercalated clays by inverse gas chromatography | Oral | Advanced characterization methods (in situ, in operando) | Jocelyne Brendlé |
| 7 | 451 | Novel 2D Materials from Exfoliation of Layered Hydroxide Salts | Oral | Theory and modelling | Sergio Tavares,Alexandre Leitão,Rodrigo Capaz,Pedro Ivo Rodrigues Moraes |
| 8 | 453 | Intercalated Catalysis: the hydrolysis of disaccharides in H-[Al]-magadiite | Oral | Heterogeneous catalysis | Guilherme Pires de Campos,Elise Albuquerque,Marco Fraga,Heloise Pastore |
| 9 | 460 | Investigation of structural models of Magadiite-type layered compounds by ab initio DFT calculations. | Oral | Theory and modelling | Bruna Nádia Silva,Heloise Pastore,Alexandre Leitão,Viviane Vaiss |
| 10 | 472 | Electron-phonon and electron-electron interactions in electron doped aromatic hydrocarbons viewed from electrical transport | Oral | Theory and modelling | Katsumi Tanigaki |
| 11 | 475 | Organically modified alpha-type zirconium phosphate by reaction with mono- and di-alkylepoxides | Oral | Inorganic and hybrid layered materials | Monica Pica |
| 12 | 488 | Extraction of Lanthanide Ions from Aqueous Solutions with Synthetic Saponite Clays | Oral | Inorganic and hybrid layered materials | Chiara Bisio |
| 13 | 499 | PREPARATION OF HETEROSTRUCTURES FORMED BY LAYERED DOUBLE HYDROXYDES COATED WITH MESOPOROUS SILICA | Oral | Inorganic and hybrid layered materials | Lister Pronestino Bianconi,Marcos Bizeto,Vera Regina Leopoldo Constantino,TAVIOT-GUEHO Christine |
| 14 | 511 | LIPOIC ACID AND LAYERED DOUBLE HYDROXIDE: EXPERIMENTAL AND IN VIVO TESTS APPROACHES | Oral | Biomaterials and drug delivery systems | Vanessa Rodrigues da Cunha,MARTA NAOMI NAKAMAE,Ye Ram kang,Fabrice Leroux,ivan HJ koh,Vera Regina Leopoldo Constantino,Rodrigo DE SOUZA,TAVIOT-GUEHO Christine,Ana Maria Cristina Rebello Pinto da Fonseca Martins |
| 15 | 517 | HYDROTHERMAL SYNTHESIS OF LIGHT-HARVESTING ORGANIC-INORGANIC HYBRID MATERIALS | Oral | Materials for electronic, magnetic or optical applications | Hipassia Moura, Miriam Unterlass |
| 16 | 539 | SYNTHESIS, STRUCTURE AND LUMINESCENCE STUDIES OF 2D EUROPIUM METAL-ORGANIC FRAMEWORKS | Oral | Metal-organic frameworks | Caroline Silva |
| 17 | 383 | BASICITY AND ACIDITY STUDY OF SOLVENT TREATED LAYERED DOUBLE HYDROXIDES (LDHS) | Poster | Inorganic and hybrid layered materials | Doy Why Justin Leung,Kanittika Ruengkajorn,Dermot OHare |
| 18 | 389 | Host-guest association of coumarin 343 with ß-cyclodextrin: experimental induced circular dichroism (ICD) and computer simulation studies (TD-DFT/PBE1) | Poster | Theory and modelling | Aguinaldo Robinson de Souza,Nelson Morgon,Valdecir Ximenes |
| 19 | 395 | SILICA@LAYERED DOUBLE HYDROXIDE CORE-SHELL HYBRID MATERIALS | Poster | Inorganic and hybrid layered materials | Wing Lam Joyce Kwok,Dana-Georgiana Crivoi,Jean-Charles Buffet,Dermot OHare |
| 20 | 398 | SELECTIVE TRANSFORMATION OF ACETONITRILE TOWARD N2 OVER (Cu, Co and Fe)-OXIDE CATALYSTS. | Poster | Heterogeneous catalysis | Paulo Henrique Silva,Jéssica Ponciano,Marcelo Batista |
| 21 | 402 | RGO-TIN OXIDE NANOCOMPOSITES FOR PHOTOELECTROCHEMICAL APPLICATIONS | Poster | Heterogeneous catalysis | Fernanda Romeiro,Gabriel Facheti,Alysson Martins,Maria Boldrin,Marcelo Orlandi |
| 22 | 406 | SILANE MODIFICATION OF LAYERED DOUBLE HYDROXIDES | Poster | Inorganic and hybrid layered materials | Chunping Chen,Jean-Charles Buffet,Dermot OHare |
| 23 | 413 | NEW SULFONATED ZIRCONIUM AND TITANIUM ORGANOPHOSPHONATES PREPARED BY TOPOTACTIC REACTIONS | Poster | Inorganic and hybrid layered materials | Klara Melanova,Vítezslav Zima,Jiri Brus,Ludvik Benes,Jan Svoboda |
| 24 | 416 | MOLECULAR SIMULATIONS OF THE CRYSTAL STRUCTURE OF ZIRCONIUM SULFOPHENYLPHOSPHONATES INTERCALATED WITH DERIVATES OF | Poster | Inorganic and hybrid layered materials | Ludvik Benes,Jan Svoboda,Klara Melanova,Vítezslav Zima,Petr Kovar,Miroslav Pospisil |
| 25 | 423 | CATALYCTIC COMBUSTION OF ACETONITRILE OVER COPPER-BASED CATALYSTS | Poster | Heterogeneous catalysis | Jéssica Ponciano,Marcelo Batista |
| 26 | 427 | CATALYTIC COMBUSTION OF ACETONITRILE OVER (CU, CO OR FE)-ZSM-5 CATALYSTS | Poster | Heterogeneous catalysis | Bruna Carla Santos Silveira,Marcelo Batista |
| 27 | 428 | DECOMPOSITION OF N2O OVER (CO, FE)-BETA CATALYSTS - INFLUENCE OF CO-FED GASES | Poster | Heterogeneous catalysis | Bruna Carla Santos Silveira,Nayara Biturini,Marcelo Batista |
| 28 | 429 | SYNTHESIS OF HALLOYSITE-LIKE NANOTUBES FROM CLAY MINERALS PRESENT IN IRON ORE TAILINGS | Poster | Intercalation mechanisms | Manoel Vítor Borel Gonçalves |

| | | | | | |
|---|---|---|---|---|---|
| 29 | 432 | NANOHYBRID FILMS OF ALGINATE AND LAYERED DOUBLE HYDROXIDE INTERCALATED WITH 1-NAPHTHALENEACETIC ACID: HORMONE DELIVERY CARRIER FOR PLANT GROWTH | Poster | Inorganic and hybrid layered materials | Vander Alencar de Castro,Vera Regina Leopoldo Constantino,Jairo Tronto,Danubia Nobre, Frederico Garcia Pinto,Willian Macedo,Geraldo Silva,Valber Duarte |
| 30 | 433 | Synthesis and Characterisation of LDH-based Core-Shell Composites | Poster | Inorganic and hybrid layered materials | Meng Lyu,Chunping Chen,Jean-Charles Buffet,Dermot OHare |
| 31 | 437 | DTF STUDY OF LAYERED DOUBLE HYDROXIDES WITH CATIONIC EXCHANGE CAPACITY: (A+ (H2O)6)[M2+6AL3(OH)18(SO4)2]·6H2O (M2+ = MG, ZN AND A+ = NA, K) | Poster | Theory and modelling | Pedro Ivo Rodrigues Moraes,Fernando Wypych ,Alexandre Leitão |
| 32 | 441 | 2D AURIDE SHEETS: STRUCTURAL AND SPECTROSCOPIC STUDY OF POTASSIUM-GOLD ALLOYS INTERCALATED INTO GRAPHITE | Poster | Graphite, carbon, and graphene intercalation compounds | Sebastien CAHEN |
| 33 | 442 | ENHANCING THE FIBROUS ASPECTS OF LAYERED CERIUM IV HYDROGENPHOSPHATE MEMBRANE FOR HEAVY METAL REMOVAL FROM CONTAMINATED EFFLUENTS | Poster | Inorganic and hybrid layered materials | João Paulo Pereira Duarte |
| 34 | 445 | EFFECTS OF ULTRASOUND AND PVP ASSISTED SYNTHESIS ON THE PROPERTIES OF EUROPIUM-BASED NANOSIZED MOFS | Poster | Metal-organic frameworks | Claudia Manuela Santos Calado,Thatiane Veríssimo dos Santos,Cintya Barbosa |
| 35 | 446 | SYNTHESIS AND CHARACTERIZATION OF NANOHYBRIDS BASED ON CARBON DOTS/EU-MOFS | Poster | Metal-organic frameworks | Kleyton Ritomar Monteiro da Silva ,Claudia Manuela Santos Calado,Thatiane Veríssimo dos Santos,Cintya Barbosa |
| 36 | 447 | ALGINATE BEADS AND KAOLINITE INCORPORATED WITH AGROCHEMICALS: EVALUATION OF FORAGING ACTIVITY OF LEAFCUTTER ANT OF GENRE ATTA SPP. | Poster | Inorganic and hybrid layered materials | Valber Duarte,Addila Gabriela Salgado,Danubia Nobre,Victor dos Santos Azevedo Leite,Allan Moraes,FLÁVIO FERNANDES,Frederico Garcia Pinto,Jairo Tronto |
| 37 | 450 | Oxygen Vacancy-Mediated Gas Barrier from the Nanoplatelet-Filled Polymer Film with Brick-Mortar-Sand Structure | Poster | Intercalation mechanisms | Wenying Shi |
| 38 | 452 | LAYERED DOUBLE HYDROXIDES (LDHS) AS CARRIER OF PENTAVALENT ANTIMONY: PREPARATION AND CHARACTERIZATION | Poster | Biomaterials and drug delivery systems | Tamires Silva,Giselle Paixão,Carmem Zanta,Thiago Aquino,Josué Santos,Mario Meneghetti, Luciano Grillo,Phabyanno Lima,Jonas Sousa,Camila Dornelas |
| 39 | 463 | ZN-AL LAYERED DOUBLE HYDROXIDE INTERCALATED WITH L-ASPARTIC: DISSOLVABLE ADSORBENT FOR CR (VI) DETERMINATION USING DISPERSIVE SOLID PHASE EXTRACTION | Poster | Host-guest interactions | Victor dos Santos Azevedo Leite,Vera Regina Leopoldo Constantino,Celly Mieko S. Izumi,Jairo Tronto,Frederico Garcia Pinto |
| 40 | 464 | BORON RELEASE AND LEACHING FROM BORATE INTERCALATED IN LAYERED DOUBLE HYDROXIDES FERTILIZER DURING CONSECUTIVE CULTIVATIONS | Poster | Host-guest interactions | Jader Ferreira,Gustavo Franco de Castro,Matheus Siqueira ,Lincoln Zotarelli,Edson Mattiello, Jairo Tronto |
| 41 | 466 | LAYERED DOUBLE HYDROXIDES AND SODIUM ALGINATE: FERTILIZER FOR CONTINUED RELEASE OF BORON | Poster | Host-guest interactions | Jader Ferreira,Gustavo Franco de Castro,Isabela Costa,Christian Fernandes,Lincoln Zotarelli, Edson Mattiello,Jairo Tronto |
| 42 | 469 | SELF-TEMPLATING SYNTHESIS OF 3D HIERARCHICAL NICO2O4@NIO NANOCAGE CATALYST FOR TOLUENE OXIDATION FROM HYDROTALCITES | Poster | Heterogeneous catalysis | Shuangde Li,Yunfa Chen |
| 43 | 473 | SIMPLE THERMAL REDUCTION OF GRAPHENE OXIDE | Poster | Graphite, carbon, and graphene intercalation compounds | Ana Paula Benevides |
| 44 | 479 | LAYERED DOUBLE HYDROXIDES: STUDIES ABOUT INTERCALATION AND RELEASE OF N-ACETYL-L-CYSTEINE | Poster | Biomaterials and drug delivery systems | Denise Eulálio,TAVIOT-GUEHO Christine,Fabrice Leroux,Dalva Faria,Vera Regina Leopoldo Constantino |
| 45 | 481 | DFT STUDY OF THE ACTIVATED MONTMORILLONITE AS SOLID ACID CATALYSTS IN BIODIESEL PRODUCTION CONTEXT | Poster | Theory and modelling | Carla Grijó Fonseca,Viviane Vaiss,Fernando Wypych ,WLADMIR SOUZA,Sandra S X Chiaro, Alexandre Leitão |
| 46 | 485 | SIMULATION, STRUCTURE AND PROPERTIES OF LI-AL-X (X= CL-, BR-, F-, I-, OH-, NO3-) HYDROTALCITE-LIKE COMPOUNDS BY AB INITO METHODS. | Poster | Theory and modelling | Carla Grijó Fonseca,Anna Barbosa,Fernando Wypych ,Alexandre Leitão |
| 47 | 491 | DEVELOPMENT OF NOVEL FUNCTIONALIZED SYNTHETIC SAPONITE CLAYS CONTAINING LN (III) IONS | Poster | Inorganic and hybrid layered materials | Chiara Bisio |
| 48 | 493 | NANOCOMPOSITES BENTONITE/TITANIUM DIOXIDE/NIOBIUM | Poster | Heterogeneous catalysis | Larissa Bonfim,Eduardo Nassar,Emerson Henrique De Faria,Tiago Honorato da Silva |
| 49 | 495 | SYNTHESIS OF MICROSPHERES USING KAOLIN CHITOSAN AND POLYVINYL ALCOHOL BY MECHANICAL DRIPPING PROCESS | Poster | Inorganic and hybrid layered materials | Suelen Souza,Eduardo Nassar,Emerson Henrique De Faria |
| 50 | 497 | DFT INVESTIGATION OF BENZOPHENONE ADSOLUBILIZED INTO ZN3AL-LDH INTERCALATED WITH DODECYLSULFATE | Poster | Theory and modelling | Sergio Tavares,Alexandre Leitão,Inna Nangoi,Fernando Wypych |
| 51 | 501 | A COMPARATIVE STRUCTURAL STUDY OF DIFFERENT SYNTHETIC ROUTES TO LDH-GLYPHOSATE MATERIALS | Poster | Inorganic and hybrid layered materials | Emanoel Hottes,Rosane Nora Castro,Rosane A S San Gil,André Marques dos Santos,Marcelo Herbst |
| 52 | 504 | NATURAL DITERPENE COPALIC ACID INCORPORATION AND RELEASE STUDIES IN NATURAL AND ORGANOPHILIC SEPIOLITE FIBROUS CLAY | Poster | Biomaterials and drug delivery systems | Eliene Santos,Vanessa Alves,Vladimir Heleno,Emerson Henrique De Faria |
| 53 | 505 | ELECTRONIC PROPERTIES OF SOME ZIRCONIUM AMINOPHOSPHONATES INVESTIGATED BY DFT CALCULATIONS | Poster | Theory and modelling | Bruna Nádia Silva,Sergio Tavares,Alexandre Leitão |
| 54 | 507 | LAYERED DOUBLE HYDROXIDES WITH THE CHEMICAL COMPOSITION ([A(H2O)6]MN6AL3 (OH)18[SO4]2·6H2O; A= NA OR K) AS PICKERING EMULSIFIERS. | Poster | Inorganic and hybrid layered materials | Lilian Amaral,Anne Raquel Sotiles,Fernando Wypych ,Rilton Alves de Freitas |

| | | | | | |
|---|---|---|---|---|---|
| 55 | 510 | Chemical steps for generation of meso-macoporous titania templated by latex beads synthesized without N2 gas. | Poster | Microporous and mesoporous materials | DJALMA BARROS FILHO,Antony Maik Correia da Silva,GISELLY CAVALCANTE,ANTONY ERNESTO DOS SANTOS SILVA,Jonas Sousa,Johnnatan Duarte Freitas,Antonio Osimar S. Silva, MAXIMILIA Frazão de Souza Degenhardt,Cristiano Oliveira,LARISSA OTUBO,João Vitor Ferreira,Phabyanno Lima,ALAN JOHN DUARTE |
| 56 | 512 | LAYERED DOUBLE HYDROXIDES FOR DRUG RELEASE OF CIPROFLOXACIN | Poster | Biomaterials and drug delivery systems | TAVIOT-GUEHO Christine |
| 57 | 524 | OXIDATIVE DEGRADATION OF HERBICIDE DCMU OVER LAYERED DOUBLE HYDROXIDES | Poster | Heterogeneous catalysis | Danilo Caiado,Alessandro Silva de Oliveira,Renato Rosseto |
| 58 | 525 | UPCONVERSION PHOSPOR BASED ON YB;ER DOPED DION-JACOBSON LAYERED PEROVSKITE KCA2NB3O10 | Poster | Materials for electronic, magnetic or optical applications | Victor Vendruscolo,Luidgi Giordano,Vera Regina Leopoldo Constantino,Lucas Carvalho Veloso Rodrigues |
| 59 | 527 | COMPARATIVE CHARACTERIZATION OF M2+/M3+ (M2+= MG2+ OR ZN2+ AND M3+= AL3+ OR GA3+) CARBONATE-INTERCALATED LAYERED DOUBLE HYDROXIDES | Poster | Inorganic and hybrid layered materials | Vagner Magri,Paulo Loureiro,Vera Regina Leopoldo Constantino |
| 60 | 535 | MATERIALS DERIVED FROM THERMAL DECOMPOSITION OF HYDROCALUMITE-TYPE COMPOUNDS: CATALYSTS FOR TRANSESTERIFICATION REACTIONS | Poster | Heterogeneous catalysis | Jairo Tronto,Roberta Prado,Addila Gabriela Salgado,Joyce Fabiula Rodrigues,Cristiane Scaldaferri,Fabiana Sousa,Vânya Pasa,Vera Regina Leopoldo Constantino,Frederico Garcia Pinto |
| 61 | 537 | TERBIUM (III) BASED INFINITE COORDINATION POLYMER COMPOSITE FILMS FOR LIGHT-EMITTING APPLICATIONS | Poster | Metal-organic frameworks | Guilherme Arroyos,Regina Frem |

# Recent Development on Long-afterglow Phosphorescent Organic-inorganic Hybrids

Dongpeng Yan[1]*

[1]Department of Chemistry, Beijing Normal University, Beijing, 100875, China

email: yandp@bnu.edu.cn

**Keywords:** layered double hydroxides; metal-organic frameworks; phosphorescence; sensor; smart materials

**Abstract.**

Luminescent Organic-inorganic Hybrids (such as layered double hydroxides (LDHs) and metal-organic frameworks (MOFs)) have received much attention due to their wide structural tunability and potential applications in sensors, biomedical imaging, photocatalysis, nonlinear optics and light emitting devices. Compared with the typical ligand-based, metal-active (noble metal (e.g., Pt and Ir) and rare-earth (e.g., Eu and Tb)) LDHs and MOFs with the excitation-state lifetime at nanosecond and/or microsecond levels, long-lasting phosphorescence systems usually feature much prolonged lifetimes (millisecond (ms) to second level). Therefore, the development of phosphorescent LDHs and MOFs can not only supply new understanding on the relationship between structure and long-lived excitation-state, but also construct new types of long-afterglow (also known as long-lasting phosphorescence or persistent luminescence) materials. In this work, recent long-afterglow phosphorescent LDHs and MOFs systems will be introduced, and their further applications in logic gate and smart materials will be discussed.[1-5]

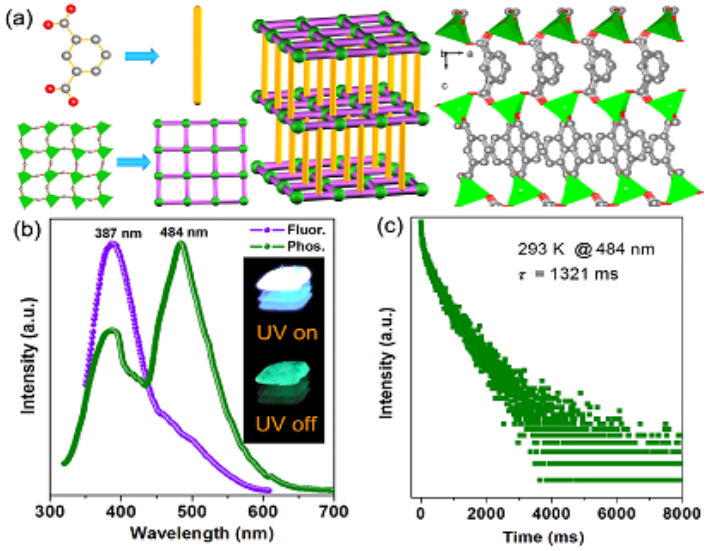


**Fig. 1** (a) Crystal structure of Zn-IPA. (b) Luminescence spectra. Insets show photographs taken before/after the excitation is turned off. (c) Time-resolved emission decay curve.

## References:

[1] X. Yang and D. Yan, *Chem. Sci.* 2016, 7, 4519; *Adv. Opt. Mater.* 2016, 4, 897; *Chem. Commun.* 2017, 53, 1801; *J. Mater. Chem. C* 2017, 5, 7898.

[2] R. Gao and D. Yan, *Chem. Sci.* 2017, 8, 590; *Chem. Commun.* 2017, 53, 5408; *Nano Research*, 2017, 10, 3606.

[3] Y. Yang, K. Z. Wang, D. P. Yan. *ACS Appl. Mater. Interfaces* 2016, 8, 15489; *ACS Appl. Mater. Interfaces* 2017, 9, 17399; *Chem. Commun.* 2017, 53, 7752.

[4] X. Yang, X. Lin, Y. Zhao, Y. S. Zhao, D. Yan, *Angew. Chem. Int. Ed.* 2017, 56, 7853.

[5] R. Gao, X. Mei, D. P. Yan, R. Liang, M. Wei, *Nat. Commun.* 2018, 9, 2798.

# High oxygen barrier coating using non-toxic nanosheet dispersions for flexible food packaging film

**JINGFANG YU, KANITTIKA RUENGKAJORN, DANA GEORGIANA CRIVOI, CHUNPING CHEN, JEAN-CHARLES BUFFET, DERMOT O'HARE***

Chemistry Research Laboratory, Department of Chemistry, University of Oxford, 12 Mansfield Road, Oxford, OX1 3TA, UK.
(*)Prof. Dermot O'Hare, Tel: +44 (0) 1865 272686; E-mail: dermot.ohare@chem.ox.ac.uk

## ABSTRACT

One of the major challenges in the circular economy relating to food packaging is the elimination of metallised film which is currently the industry standard approach to achieve the necessary oxygen barrier performance. There is an urgent unmet need for scalable solutions that can replace this aluminium coating with a solution-deposited or coextruded layer that can be recycled without separation from the rest of the packaging materials. Two-dimensional (2D) inorganic nanosheets are impermeable to gas molecules so exploiting their potential for high aspect ratio platelet structures is an effective approach to construct tortuous pathways to lower molecular diffusion rate through polymeric materials. The key challenges for high gas barrier food packaging materials are (i) the preparation of stable, high aspect ratio non-toxic 2D nanosheet dispersions and (ii) the use of an existing commercial coating technique. Here, we report the synthesis of high aspect ratio 2D non-toxic layered double hydroxide (LDH) nanosheet dispersions using a non-toxic exfoliation method in aqueous amino acid solution. High gas barrier coating films can be prepared using this food safe liquid dispersions through a bar coating process. The oxygen transmission rate (OTR) of 12 μm PET coated film can be reduced from 133.5 cc/$m^2$/day to below the instrument detection limit (<0.005 cc/$m^2$/day). The $O_2$ permeability of this film is estimated to be below 0.0007 x $10^{-16}$ $cm^3$(STP)·cm/$cm^2$·s·Pa, giving a barrier improvement factor (BIF) of 24640. In comparison, a commercially available 12 μm metallised PET has an $O_2$ permeability of 0.0349 x $10^{-16}$ $cm^3$(STP)·cm/$cm^2$·s·Pa. Most importantly, these coated films are also transparent and mechanically robust, making them suitable for flexible food packing while also offering new recycling opportunities.

**Keywords**: Coating, Oxygen barrier, Food packaging, LDH.

# EXFOLIATION OF LAYERED METAL ORGANOPHOSPHONATES

**V. ZIMA[1], K. MELÁNOVÁ[1], K KOPECKÁ[2], L. BENEŠ[2], P. KNOTEK[2]**

[1] Institute of Macromolecular Chemistry, AS CR, Heyrovsky sq. 2, 162 06 Prague 6, Czech Republic; [2] Faculty of Chemical Technology, University of Pardubice, 532 10 Pardubice, Czech Republic; vitezslav.zima@upce.cz, klara.melanova@upce.cz, st53267@student.upce.cz, ludvik.benes@upce.cz, petr.knotek@upce.cz

## ABSTRACT

Several procedures for the exfoliation of layered metal arylphosphonates with general formula $Me(C_6H_5PO_3)$ (Me = Ca, Sr, Ba) and $Zr(HO_3SC_6H_4PO_3)_2 \cdot 2H_2O$ were investigated with the aim to obtain material with the highest yield and the highest degree of delamination. The methods for characterization of these exfoliated materials were suggested and tested.

Keywords: metal phosphonates; exfoliation; nanosheets

## INTRODUCTION

Layered metal organophosphonates belong to a large group of hybrid organic-inorganic materials. They benefit from a well-defined structure of their inorganic part in combination with organic moieties, which can be modified to obtain desired properties. Thanks to their structure, with strong covalent bonds between the atoms in the layers but with rather weak interactions between the layers, these compounds can be used as host materials in intercalation reactions or as starting materials for production of 2D nanosheets by exfoliation.

## ALKALINE-EARTH PHENYLPHOSPHONATES

In this work we studied exfoliation of layered phenylphosphonates of alkaline-earth metals with general formula $MeC_6H_5PO_3 \cdot 2H_2O$ (Me = Ca, Sr, Ba).[1] These layered phenylphosphonates are hybrid organic-inorganic materials, which exhibit a hydrophobic character due to the presence of phenyl groups on the surface of the layers. Thanks to its hydrophobic character, these materials can be promising fillers for a series of polymer matrices. Production of nanosheets was performed by a so-called liquid-based exfoliation.[2] This technique is based on dispersing layered solids in a suitable solvent followed by application of normal and shear forces, which cause separation of individual layers from the bulk. The first step consisted in finding the most suitable solvent, in which the exfoliation can proceed. From the several solvents chosen for the testing of the exfoliation process, propan-2-ol (isopropylacohol, IPA) showed to be the most suitable, together with butan-1-ol.[3] With regards to the use of the phenylphosphonates

as filler in polymeric systems, IPA was used for further testing thank to its lower boiling point, which allows easier removal of this solvent from the reaction system during the preparation of the composite.

Several methods for the exfoliation of the calcium phenylphosphonate, which showed to be the most suitable phosphonate for the exfoliation, are also described and methods for the determination of the character and degree of the exfoliation are discussed.

## ZIRCONIUM 4-SULFOPHENYLPHOSPHONATE

In contrast to phenylphosphonates, which have no reactive functional group, zirconium 4-sulfophenylphosphonate (ZrSPhP) has an active acidic sulfo group,[4, 5] which can be employed in the process of exfoliation. In this contribution the exfoliation in the presence of amino alcohols is described and the exfoliated particles are characterized by a combination of several methods.

## ACKNOWLEDGMENT

This work was supported by the Czech Science Foundation (project No. 17-10639S) and the Czech Technology Agency (project No. TH02020201).

## REFERENCES

1. K. Melánová, L. Beneš, J. Svoboda, V. Zima, M. Pospíšil and P. Kovář, *Dalton Trans.*, 2018, **47**, 2867-2880.
2. V. Nicolosi, M. Chhowalla, M. G. Kanatzidis, M. S. Strano and J. N. Coleman, *Science*, 2013, **340**, 1420.
3. K. Kopecká, L. Beneš, K. Melánová, V. Zima, P. Knotek and K. Zetková, *Beilstein J. Nanotech.*, 2018, **9**, 2906-2915.
4. V. Zima, J. Svoboda, K. Melánová, L. Beneš, M. Casciola, M. Sganappa, J. Brus and M. Trchová, *Solid State Ionics*, 2010, **181**, 705-713.
5. J. Škoda, M. Pospíšil, P. Kovář, K. Melánová, J. Svoboda, L. Beneš and V. Zima, *J. Mol. Model.*, 2018, **24,** 10.

# Obtaining Al-3D-solids from the layered silicate Na-RUB-18: pillarization and hydrothermal transformation

**G.B. BÁFERO[1], E.C.O. MUNSIGNATTI[1], H.O. PASTORE[1]**

[1]Institute of Chemistry, University of Campinas, Monteiro Lobato St., 270, 13085-862, Campinas, SP, Brazil. E-mail: gpmmm@iqm.unicamp.br (H.O. Pastore)

## ABSTRACT

Layered silicates are well known for their low acidity and surface area, while the reactivity of their silanol groups allows the most different modifications in the lamella. In this work, two post-syntheses procedures were studied using the layered silicate Na-RUB-18 as the precursor of 3D materials containing structural Al, thus broadening its spectrum of applications. After the Al incorporation, confirmed by $^{27}$Al NMR analysis, the layered material was ion-exchanged with $CTA^+$ ions and the pillarization was conducted for 18 h using octylamine as the hydrolizing agent and tetraethylorthosilicate (TEOS) as the pillaring agent. The final material presented BET surface area of 223 $m^2$ $g^{-1}$ and mesopores in the range of 2-4 nm. Also, the XRD profile showed a significant crystallinity drop due to the amorphous $SiO_2$ pillars in the interlamellar space. In turn, the hydrothermal conversion of Na-RUB-18 led to the mordenite zeolite structure (MOR). The synthesis gel was obtained from the mixture of the precursor Na-RUB-18, the Al source and a NaOH solution. After 24 h, the treatment at 140 °C resulted in the desired material with Si/Al molar ratio of 6. The changes observed in the XRD profiles during crystallization suggested a conversion free of amorphization steps. The presence of $^{29}$Si NMR signals of silicon connected to Al and $^{27}$Al NMR signals of tetrahedrally coordinated Al atoms both confirmed the formation of the new structure.

Keywords: Na-RUB-18, pillarization, hydrothermal transformation, mordenite zeolite

## RESULTS AND DISCUSSION

Figure 1, curves a-b, shows the XRD profiles of the layered silicate Na-RUB-18 and the Al-incorporated sample, respectively. The comparison makes it clear that the post-synthesis procedure did not compromise the precursor structure and further promoted the aluminum insertion reaching a Si/Al molar ratio of 22, determined by ICP-OES analysis. In addition, the $^{27}$Al NMR spectrum clearly showed the presence of Al tetrahedral sites; and also a small signal related to octahedral or partially extra-framework Al [1,2].

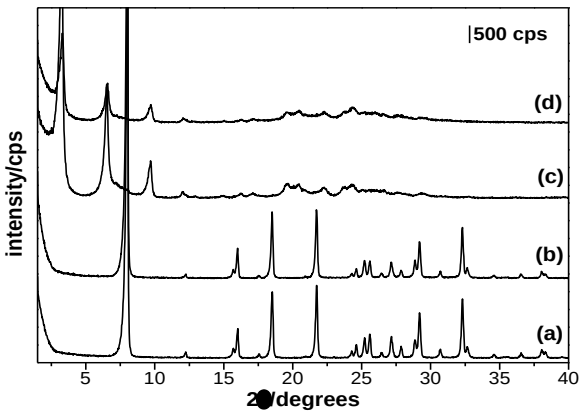


**Figure 1.** XRD profiles of (a) Na-, (b) Na-[Al]-, (c) CTA-[Al]- and (d) pillared-[Al]-RUB-18.

In the next step, the Na-[Al]-RUB-18 sample was ion exchanged with $CTA^+$ ions in order to promote the expansion of the interlamellar space. The XRD profile shown in Figure 1, curve c, shows that the diffraction peak for lamellar stacking was shifted from ~ 8° 2θ (d = 1.02 nm) in the sodium sample to 3.24° 2θ (d = 2.73 nm) in the CTA-[Al]-RUB-18 sample, which confirms the expansion [2]. Additionally, two more low-angle reflections are observed, corresponding to the peaks in 6.52° 2θ (d = 1.35 nm) and 9.70° 2θ (d = 0.91 nm). These peaks follow the d/2 and d/3 correlations as previously observed in the literature [2].

Finally, Figure 1, curve d, shows the XRD profile of the CTA-[Al]-RUB-18 sample after the pillarization using octylamine and TEOS. The diffraction pattern of this material is very similar to the precursor one, presenting only a slight decrease in the overall intensity. Such behaviour can be attributed to the silica species present in the solid interlamellar space. These species are the precursors of the amorphous pillars formed during the calcination step, which leads to the dilution of the crystalline material and to a pronounced loss of peaks intensity in the range of 20-30° 2θ [2].

The $^{29}$Si NMR spectrum showed a wide signal in the region of $Q^4$ sites and a shoulder in the region of $Q^3$ sites. In turn, the $^{27}$Al NMR spectrum showed the maintenance of tetrahedral Al sites. Elemental analysis provided a Si/Al molar ratio of 41, consistent with the addition of silica during pillarization. The BET surface area jumped from 7 $m^2$ $g^{-1}$ to 223 $m^2$ $g^{-1}$ in the final material, which also presented mesopores between 2-4 nm [2].

Figure 2, curves b-f, presents the XRD profiles of the samples synthesized trying to reach the MOR structure starting from Na-RUB-18 and using a Si/Al ratio of 10. The sequence of profiles follows the increase in crystallization time and shows a gradual transformation until the final material. Figure 2, curves b-d, shows that the Na-RUB-18 structure is present until 12 h of reaction. After 18 h, curve e, there are peaks of the precursor and also of the zeolitic material, i.e., the two phases coexist. Finally, above 18 h of hydrothermal treatment, curves f-g, crystalline MOR was obtained and the profiles were comparable to the literature [3]. Nevertheless, some MOR diffraction planes presented intensities slightly different than expected, a feature frequently dependent of the Si/Al molar ratio [3]; determined here by elemental analysis to be equal to 6. No extensive dissolution of the precursor followed by crystallization of the intended zeolite could be seen; an evidence of the surface-localized character of the transformation.

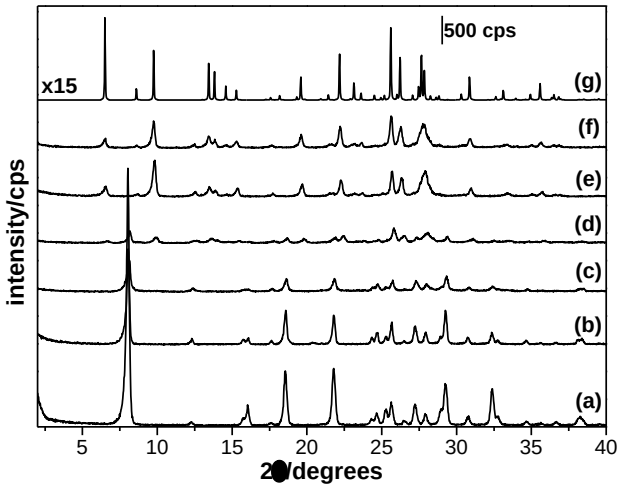


**Figure 2.** XRD profiles of (a) Na-RUB-18 and samples synthesized after (b) 6, (c) 12, (d) 18, (e) 24, (f) 48 h and (g) the MOR pattern.

$^{29}$Si NMR analysis showed that throughout the transformation, the $Q^4$ signal of the precursor decreased steadily, while the $Q^3$ signal remains a little displaced from its position in Na-RUB-18. A new signal between these two is possibly assigned to (1Al)-Si-$(SiO_4)_3$ groups, an evidence of the presence of structural Al [3]. A few intermediate samples showed also a signal in the $Q^2$ site region that can be attributed to (2Al)-Si-$(SiO_4)_2$ groups. The $^{27}$Al NMR spectrum of the MOR obtained showed tetrahedrally coordinated Al atoms. Again, the intermediate samples presented some particularities: this signal was slightly distorted and there was also evidence of octahedral Al sites, which is expected for materials in process of transformation.

## ACKNOWLEDGMENTS

This study was financed in part by the Coordenação de Aperfeiçoamento de Pessoal de Nível Superior – Brasil (CAPES) Finance Code 001. The authors are grateful to Fundação de Amparo à Pesquisa de São Paulo for the financial support (2014/06942-0). HOP acknowledges CNPq for the fellowship.

## REFERENCES

[1] G.B. Superti, E.C. Oliveira, H.O. Pastore, C. Bisio, L. Marchese, *Chem. Mater.* **83**, 201-211 (2005).
[2] F.S.O Ramos, H.O. Pastore, *Dalton Trans.* **46**, 11728-11737 (2017).
[3] F.S.O Ramos, E.C.O. Munsignatti, H.O. Pastore, *Microporous Mesoporous Mater.* **177**, 143-150 (2013).

# DIVALENT METAL-BASED SUPERCONDUCTING GIC PREPARED BY A SOLID-LIQUID REACTION IN MOLTEN SALTS

**EL HAJJ I., CAHEN S., SPEYER L., LAGRANGE P., HEROLD C.**

Institut Jean Lamour, UMR 7198 CNRS – Université de Lorraine
Campus Artem, 2 allée André Guinier, BP 50840, 54011 Nancy Cedex, France
Sebastien.cahen@univ-lorraine.fr

## ABSTRACT

The solid-liquid molten salts method has been employed in order to synthesize alkaline-earth metals and lanthanides Graphite Intercalation Compounds (GIC). By optimization of the synthesis parameters, several GIC have been successfully prepared. For the first time, it has been possible to prepare binary $SrC_6$ intercalated into the bulk, characterized by 00*l* and *hk*0 X-ray diffraction. Using the same way, bulk $BaC_6$ has also been successfully synthesized and characterized. Finally, even ytterbium has been partially intercalated into graphite. XRD, SEM/EDXS, ion beam analysis and magnetic measurements confirmed this observation. Currently, our efforts are focused on bulk intercalation of ytterbium and other lanthanides.

**Keywords**: Graphite Intercalation Compound, X-ray diffraction, molten salts, superconductivity

## INTRODUCTION

Especially due to their superconducting properties, $MC_6$ compounds (with M = alkaline-earth metal or lanthanide) have been extensively studied using various characterization techniques [1,2]. However, most of these studies are performed on samples prepared by solid-gas reaction where metal in the gaseous phase reacts on graphite powder at high temperature. By such a technique, metal is partially intercalated into graphite so that pristine graphite remains. Moreover, regarding the high temperatures employed, spurious metal carbides can be formed. Considering these facts, we have developed an original solid-liquid method in LiCl-KCl molten salts [3,4]. After a comprehensive study of the chemical mechanisms in different metal-LiCl-KCl mixtures, different $MC_6$ intercalation compounds have been prepared and characterized using X-ray diffraction, SEM/EDXS observations, ion beam analyses and magnetic measurements.

## RESULTS AND DISCUSSION

In this solid-liquid method, a LiCl-KCl eutectic mixture with a low melting point (353°C) is prepared and heated in a glove-box under argon atmosphere. Then, the metal desired to be intercalated into graphite is solubilized into the reaction medium thanks to a redox phenomenon. Finally, a highly oriented pyrolytic platelet of graphite is immersed in the liquid and the reaction is performed for a given duration (from 30 minutes to 10 days) in the temperature 400-450°C. After reaction, the intercalated sample is recovered in a glove-box and finally placed in an air-tight sample-holder for further characterizations.

Using strontium, we have successfully synthesized for the first time a high-quality $SrC_6$ bulk intercalation compound. The 00*l* X-ray diffraction pattern is given figure 1.

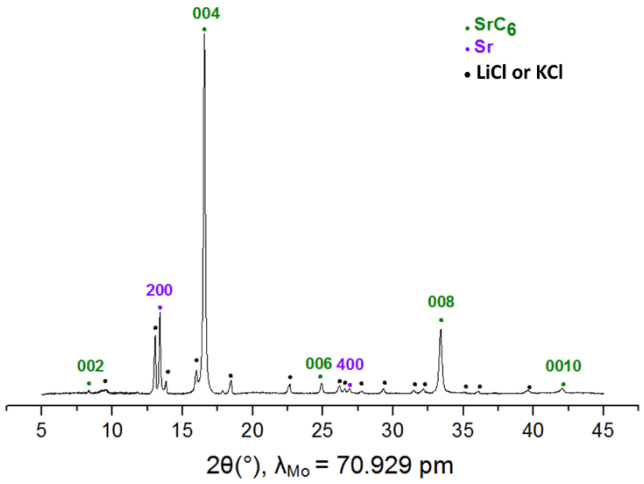


*Figure 1: 00l X-ray diffraction pattern of $SrC_6$*

It can be indexed as a first stage compound with a repeat distance of 494 pm without any residual graphite. By quantitative analysis of the 00*l* reflexions, it has been possible to calculate the 1D electronic density profile along the **c**-axis given figure 2.

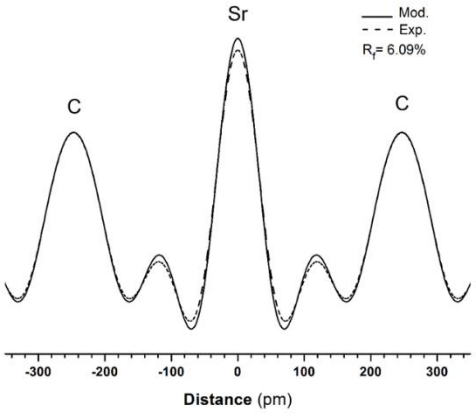


*Figure 2: 1D electronic density profile along the **c**-axis of $SrC_6$*

In a same manner, we have successfully prepared a $BaC_6$ bulk intercalation compound and performed itscharacterization by XRD. Finally, intercalation of ytterbium has been tested. For the moment, only partially intercalated samples have been obtainedbut the synthesis parameters are currently modified separately in order to prepare superconducting bulk $YbC_6$ intercalation compound.

## References

[1] M.P.M. Dean, C.A. Howard, S.S. Saxena, M. Ellerby, Phys. Rev. B 81 (2010) 045405.
[2] R.P. Smith, T.E. Weller, C.A. Howard, M.P.M. Dean, K.C. Rahnejat, S.S. Saxena, M. Ellerby, Physica C, 514 (2015) 50.
[3] M. Bolmont, S. Cahen, M. Fauchard, R. Guillot, G. Medjahdi, P. Berger, G. Lamura, P. Lagrange, C. Hérold, Carbon 133 (2018), 379.
[4] M. Fauchard, S. Cahen, M. Bolmont, G. Medjahdi, P. Lagrange, C. Hérold, Carbon 145 (2019), 501.

# Study of the surface properties of clays and intercalated clays by inverse gas chromatography

J. Brendlé[1], E. Brendlé[2]

[1]Institut de Science des Matériaux de Mulhouse, UMR CNRS 7361, Université de Haute-Alsace, Université de Strasbourg, 15 rue J. Starcky, 68057 Mulhouse Cedex, France: jocelyne.brendle@uha.fr
[2]Adscientis, Parc Sécoia, 1 rue A. Kastler, 68310 Wittelsheim, France, e.brendle@adscientis.com

## ABSTRACT

In this work a series of clays (natural and synthetic ones) and intercalated clays (i.e. organically modified by alkylammonium ions or a fungicide) were characterized by inverse gas chromatography,enabling gathering information on the numerous surface characteristics like the surface energy ($\gamma_s^d$), the surface nanoroughness, the acid-base character and the surface morphology**.**It is worthy to note that the dispersive component of the surface energy **($\gamma_s^D$)** decreases strongly after organic treatment, whatever the clay, meaning a lowering of the surface interactivity. The determination of the morphology indices indicates also a decrease of the surface roughness.

## INTRODUCTION

At the origin, the chromatographic analysis has been developed as a direct method, allowing the separation, the quantification and the identification of the components of a complex mix. This technique was then developed in order to determine the thermodynamic properties of a melted polymer impregnated on a finely divided solid (powder). This is the founding idea of the principle of inverse gas chromatography today called IGC. IGC measurements are realized by injecting chosen and known molecules, called molecular probes, in order to get chromatograms. The measured retention times, as well as the shape of the obtained peaks, are depending on the interactions occurring between the molecular probes and the investigated material (stationary phase). If the amount of injected probes is very low, the degree of dilution is such that the intermolecular interactions between the adsorbed molecules can be neglected, in this case, IGC is performed at Infinite Dilution ( ID-IGC)The exploitation of measured retention times and/or of the shape of the chromatograms gives access to numerous physicochemical properties of the analysed materials such as surface energy ($\gamma_s^d$)the surface nanoroughness, the acid-base character and the surface morphology. The goal of this determine the influence of the intercalation of organic moieties in the interlayer space of the natural of synthetic clays on the surface properties. A series of compounds have been prepared and fully characterized by conventional methods such as X-ray diffraction, thermal analysis and solid state nuclear magnetic resonance ($^{13}C$ and $^{19}F$) prior being characterized by ID-IGC.

## MATERIALS

A synthetic beidellite ($Na_{0.6}(Al_2)$ ($Si_{3.4}$ $Al_{0.6}$) $O_{10}(OH,F)_2$), was used as host to guest hexadecyltrimethylammonium ions ($C_{16}TMA^+$) and a natural Patagonian Na-montmorillonite($Na_{0.41}[(Si_{3.89}Al_{0.11})(Al_{1.43}Fe_{0.28}Mg_{0.30})O_{10}(OH)_2]$ (PatMt) was used to host octadecyltrimethylammonium ions ($C_{18}TMA^+$) (PatOD ) as well as fludioxonil (PatFX), a

widely used fungicide and both $C_{18}TMA^+$ and fludioxonil (PatODFX) [1]. Each sample used as chromatographic stationary phasewas introduced in a stainless steel column. All the samples were conditioned at 130 °C over night, using dry He as carrier gas. The measurements were performed at 110 °C.Several molecular probes (*n*-alkanes (from $C_2$ to $C_{12}$)), branched and cyclic alkanes (isooctane and cyclooctane respectively), polar molecules (acetonitrile, acetone, tetrahydrofuran (THF), ether, chloroform, methyl-acetate, benzene) were injected at infinite dilution conditions (< 1 µL).

## RESULTS AND DISCUSSION

The $\gamma_s^d$ value was determined starting from the slope of the straight line obtained from the plot of the *n*-alkane $\Delta G_a$ versus their number of carbon atoms. It was shown that the value decreases from 192 $mJ.m^{-2}$ to 50 $mJ.m^{-2}$ for the synthetic and modified beidellite, respectively, meaning a reducing of the surface interactivity. Injection of cyclooctane and isooctane also allows concluding that the intercalation of $C_{16}TMA^+$ ions in the interlayer space induce a lowering of the nanoroughness. In the same way, the results showed that the organo-treatment of Patagonian montmorillonite decrease significantly the surface energy values (from 170 $mJ.m^{-2}$ to 41 $mJ\ m^{-2}$ respectively), whereas the fludioxonil adsorption seemed not influence the measured surface energy of the samples. Information on the acid-base character were obtained by using a series of polar probes. Only the most acidic probes were eluted ($CHCl_3$ and benzene) on samples PatMt and PatFX. All the basic and amphoteric probes were not eluted. This is explained by the strong surface acidity (Lewis type).On the opposite, all the probes were eluted on samples (PatOD) and PatODFX meaning that the organo-treatment shields the surface acidity of the PatMt.

## CONCLUSION

It is worthy to note that organic treatment greatly affected the surface properties of the both beilleite and montmorillonite as nicely showed by inverse gas chromatography. Indeed the dispersive component of the surface energy strongly decreased as well as the nanoroughness and the surface acidity.

### Citations and References

[1] F.M.Flores, M.Gamba, R.M. Torres Sánchez, J. Brendlé, E. Brendlé, Microelectrophoresis and inverse gas chromatography as tools to study the surface interactions between a fluorinated fungicide and a raw or organically modified Patagonian Montmorillonite, Applied Clay Science (2016), 134(2), 83-88.

# Novel 2D Materials from Exfoliation of Layered Hydroxide Salts

**SÉRGIO R. TAVARES[A], PEDRO IVO R. MORAES[A], RODRIGO B. CAPAZ[B], ALEXANDRE A. LEITÃO[A]**

**[A]Departamento de Química, Universidade Federal de Juiz de Fora, Juiz de Fora, MG, 36036-330, Brazil**
**[B]Instituto de Física, Universidade Federal do Rio de Janeiro, Caixa Postal 68528, Rio de Janeiro, RJ 21941-972, Brazil**

## ABSTRACT

The electronic and structural properties of monolayer and few-layer 2D materials obtained from the exfoliation of four zinc-based layered hydroxide salts (LHSs) were investigated via DFT calculations. The exfoliation energies in the range of 30 meV/Å$^2$ were found for all cases. Monolayer structures remained semiconducting like the respective bulk compounds, although in some cases the band gap changes its character from indirect to direct. The effects of dehydration were also explored in terms of the electronic structure. It could be observed that the anion or cation removal from the interlayer region can turn the monolayer systems into metallic, by means of electron and hole doping, respectively.

## INTRODUCTION & THEORETICAL METHODOLOGY

The successful mechanical exfoliation of graphite into 2D graphene[1] opened up the field of 2D materials. Since then, a plethora of novel materials in monolayer or few-layer forms have emerged. 2D materials hold the promise to provide truly disruptive applications, with the potential to revolutionize many different fields, such as energy, health, electronics, space and many other more.

Many 2D materials can be obtained by exfoliation of layered or lamellar materials. Particularly interesting classes of layered materials which have not been extensively explored as platforms for 2D materials are layered double hydroxide (LDHs) and LHSs. Many LDHs have been successfully exfoliated into 2D form, but in comparison 2D LHSs have been less studied.

In this work, we used first-principles calculations based on density-functional theory (DFT) in order to explore different properties of the exfoliated forms of four representative examples of zinc-based LHSs: $Zn_3(OH)_4(NO_3)_2$, $Zn_5(OH)_8Cl_2.H_2O$, $Zn_5(OH)_8(NO_3)_2.2H_2O$ and $NaZn_4(OH)_6SO_4Cl.6H_2O$. In particular, $NaZn_4(OH)_6SO_4Cl.6H_2O$ is an interesting case to consider because it has Na cations in the interlayer region, which allows for hole-doping by ion removal.

All *ab initio* calculations were performed using the codes available in the Quantum Espresso package, which implements the DFT under periodic boundary conditions with plane wave functions as a basis set. The exfoliated forms of these structures were simulated by the insertion of a vacuum layer along the z-direction. Each of these 2D forms was studied by considering 1, 2 and 3 layers for each structure and also by the optimization of the layer parameters in the lateral directions, while the cell size along the z-direction was kept frozen during the geometry optimizations.

## RESULTS AND DISCUSSION

The exfoliation energies of the multilayer structures present the following energetic order: $NaZn_4(OH)_6SO_4Cl.6H_2O$ and $Zn_5(OH)_8Cl_2.H_2O$ > $Zn_5(OH)_8(NO_3)_2.2H_2O$ and $Zn_3(OH)_4(NO_3)_2$. The exfoliation energies fall near 30 meV/Å$^2$, which sets the boundary between “easily exfoliable” and “potentially exfoliable” materials, according to the classification of Mounet et al.[2] This is also

suggestive of the important contribution of electrostatic interactions – and not only van der Waals - in determining the strength of layer binding in these systems.

The band structures of the studied materials show that the bulk forms of the investigated compounds present an indirect band gap. In the case of $NaZn_4(OH)_6SO_4Cl.6H_2O$, even the exfoliated forms present this type of band gap. On the other hand, the monolayer structures of $Zn_3(OH)_4(NO_3)_2$, $Zn_5(OH)_8Cl_2.H_2O$ and $Zn_5(OH)_8(NO_3)_2.2H_2O$ present direct band gaps. The same holds true for the bilayer and trilayer structures of $Zn_3(OH)_4(NO_3)_2$ and $Zn_5(OH)_8Cl_2.H_2O$. In the case of $Zn_5(OH)_8(NO_3)_2.2H_2O$, the bilayer and the trilayer forms displayed, respectively, a direct and indirect band gap. Changes from indirect to direct gap as the number of layers is reduced occur in many 2D materials. Perhaps, the most well-known example is $MoS_2$, which has remarkable optical properties in the 2D form due to the direct gap[3].

The band gaps tend to be lower for the bulk forms of $Zn_3(OH)_4(NO_3)_2$ and $Zn_5(OH)_8Cl_2.H_2O$ than for those observed in their exfoliated forms. This is the expected behavior in terms of quantum confinement arguments. On the contrary, in the case of $Zn_5(OH)_8(NO_3)_2.2H_2O$ and $NaZn_4(OH)_6SO_4Cl.6H_2O$, the band gap of the bulk form is higher than those calculated for the multilayer systems.

Exfoliated LHSs may offer an extra degree of freedom for controlling their electronic structure and screening of Coulomb interactions, which is the possibility of adding or removing water molecules in their structure. The band structures of these dehydrated structures were also constructed in order to verify if the gaps are direct or indirect. In the case of $NaZn_4(OH)_6SO_4Cl$ and $Zn_5(OH)_8Cl_2$, the gaps are direct at Γ, while the gap of $Zn_5(OH)_8(NO_3)_2$ is indirect. Therefore, the direct band gap of the LHS monolayer containing $Cl^-$ ($Zn_5(OH)_8Cl_2.H_2O$) remains even when the dehydration occurs. On the other hand, the band structure of LHS monolayer containing nitrate anions is modified by the dehydration process, leading to an indirect band gap. The opposite occurs for the dehydration of $NaZn_4(OH)_6SO_4Cl.6H_2O$. The hydrated monolayer presents an indirect band gap, whereas the water removal makes it a direct band gap semiconductor. These changes in the electronic structure upon insertion or removal of water molecules is uncommon in other 2D materials and they certainly add flexibility and novel possibilities in exploring the optical properties of this class of materials.

LHSs may also offer the flexibility of tuning the electronic structure upon removal of cations and anions. As a matter of fact, charge conservation considerations suggest that one may be able to convert semiconducting monolayers to metallic ones by changing the ion concentration in the monolayers. The band structures clearly show that the nitrate removal generates metallic donor states, as the Fermi level is now pinned to the bottom of the conduction band. The removal of hexacoordinated sodium cations also leads to the generation of metallic acceptor states, with the Fermi level at the top of the valence band. The PDOS (Projected Density of States) analysis also shows that the projected states of the remaining ions (nitrate, and chloride and sulfate) tend to occur at the Fermi level for the two studied scenarios. Therefore, our analysis shows that indeed one may dope LHS monolayers by playing with the ion concentration.

## Citations and References


1 - Novoselov, K. S.; Geim, A. K.; Morozov, S. V.; Jiang, D.; Zhang, Y.; Dubonos, S. V.; Grigorieva, I. V.; Firsov, A. A. Science 2004, 306, 666 - 669.

2 - Mounet, N.; Gibertini, M.; Schwaller, P.; Campi, D.; Merkys, A.; Marrazzo, A.; Sohier, T.; Castelli, I. E.; Cepellotti, A.; Pizzi, G.; Marzari, N. Nature Nanotechnolog 2018, 13, 246 - 252.

3 - Mak, K. F.; Lee, C.; Hone, J.; Shan, J.; Heinz, T. F. Phys. Rev. Lett. 2010, 105, 136805.


## Acknowledgements


This work has been supported by CAPES, CNPq, FAPEMIG, Brazilian agencies and the enterprise Petrobras S/A (CENPES). We also acknowledge the CENAPAD-SP computational center.

# Intercalated Catalysis: the hydrolysis of disaccharides in H-[Al]-magadiite

**G. P. CAMPOS[1], E. M. ALBUQUERQUE[2], M. A. FRAGA[2], H. O. PASTORE[1]***

[1]Micro and Mesoporous Molecular Sieves Group, Institute of Chemistry, University of Campinas, 270 Monteiro Lobato St., University of Campinas, 13083-862, São Paulo, Brazil. E-mail: lolly@iqm.unicamp.br (H. O. Pastore).

[2]National Institute of Technology/MCTIC, Laboratory of Catalysis, Venezuela Av. 82/518, Saúde, 20081-312, Rio de Janeiro, Brazil. E-mail: marco.fraga@int.gov.br (M. A. Fraga).

## ABSTRACT

The hydrolysis of disaccharides is of great interest due to the possibility of obtaining platform chemicals such as glucose or hydroxymethylfurfural (HMF) from renewable feedstock[1].

Layered materials such as H-[Al]-magadiite were options as catalysts since the insertion of Al in their structures generates acid sites that are sufficiently strong to hydrolyze the glicosidic bonds while their interlamellar space (1.1 nm) allows the sugars to reach the active sites of the catalyst, by intercalation. Higher concentrations of aluminum inserted into the lamella led to a larger amounts of acid sites in the material, reflecting in higher conversions. The catalyst also showed good stability, since its structure did not change after 7 h of reaction, at temperatures around 473 K, in aqueous medium.

Among the disaccharides studied, cellobiose and lactose were hydrolyzed in the presence of H-[Al]-magadiite, while maltose presented low conversion values at the temperatures analyzed. This shows that the catalyst exhibits selective reactivity for glycosidic β(1→4) bond.

Keywords: [Al]-magadiite, disaccharide conversion, continuous process, layered solid.

## EXPERIMENTAL

The magadiite and [Al]-magadiites were prepared according to the literature[2] with different Si/Al (ratio ∞ ,8, 9 and 22) and transformed to the acid forms where the number in the parentheses indicates the Si/Al of the solids. All the samples were characterized by XRD, FTIR, NMR of the nuclei of $^{27}Al$ and $^{29}Si$ and ICP OES. The activity of the catalysts was evaluated in a continuous flow reactor with a space velocity of 0,026 $s^{-1}$, applying 25 MPa (25 bar) of pressure for 25.200 s (7 h) in different temperatures and the products analyzed by HPLC.

## RESULTS AND DISCUSSION

The characterization showed that the Al incorporated in the catalyst is stable in the framework, no structural alteration was observed after deammoniation. The first disaccharide studied was cellobiose at 473 K. It is formed by two units of glucose linked by the β-1,4-glycosidic bond. The reactions without catalyst and using H-maga showed very similar results: 23% and 20% of conversion (Figure 1), respectively. These results confirm that silicates are not acid and the products identified came from the homogeneous phase hydrolysis promoted by the temperature. Conversions of 81%, 67% and 32% were reached over the catalysts H-[Al]-maga(8), H-[Al]-maga(9) and H-[Al]-maga(22), in this order. The conversions increased as the concentration of framework Al also increased. For this substrate, the main product from the hydrolysis in Bronsted acid sites is glucose, but fructose was also identified in the analysis which shows that all three catalysts have active Lewis acid sites. The formation of HMF, levulinic and formic acids were identified in the samples. These three catalysts presented selectivity for glucose around 55-50% with yields varying from 16 to 45%: larger Al concentration in the layers led to a larger number of acid sites and higher conversion and selectivity in the reaction. Different disaccharides were used as substrates to analyze the strength of the glycosidic bond. Lactose (glucose and galactose linked by β-1,4-glycosidic bond) was also tested at 453 K with initial conversions of 53%, 42% and 50% for catalysts with Si/Al ratio of 8, 9 and 22 (Figure 2). Different from cellobiose, the reactions with lactose led to a small deactivation of all catalysts. These results were expected since both substrates present the same type of glycosidic bond. Lastly, maltose (two units of glucose linked by α-1,4-glycosidic bond) was tested at 383 K and, different from the other two disaccharides, it could not adsorb properly on the catalysts, resulting in a low conversion (10%). This substrate should have hydrolyzed more easily because its glycosidic bond is less stable than lactose and cellobiose. Therefore, [Al]-magadiite is a selective catalyst for β-1,4-glycosidic bond with an interlayer space large enough to allow the intercalation with the disaccharides for subsequent hydrolysis reaction.

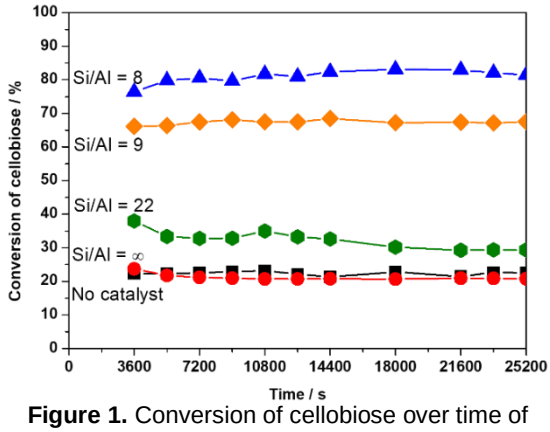


**Figure 1.** Conversion of cellobiose over time of reaction at 473 K.

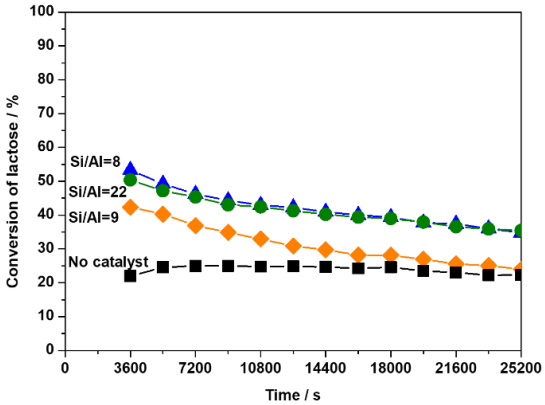


**Figure 2.** Conversion of lactose over time of reaction at 453 K.


## Acknowledgements

This study was financed in part by the Coordenação de Aperfeiçoamento de Pessoal de Nível Superior – Brasil (CAPES) -Finance Code 001. The authors are grateful to Fundação de Amparo à Pesquisa de São Paulo for the financial support to this work (2014/06942-0). HOP and MAF acknowledges CNPq for the fellowships. EMA is thankful to PCI/CNPq for her post-doctoral grant (Proc. 313014/2016-7).


## References


[1] Ennaert *et al*, *Chemical Society Reviews,* 2016, **45,** 584-611.
[2] H. M. Moura *et al*, *CrystEngComm*, 2011, **13**, 5428-5438.

# Investigation of structural models of Magadiite-type layered compounds by ab initio DFT calculations.

**BRUNA NÁDIA N. SILVA[1], VIVIANE S. VAISS[1], HELOISE O. PASTORE[2], ALEXANDRE A. LEITÃO[1]**

[1]*Departamento de Química – ICE, Universidade Federal de Juiz de Fora, CEP 36036-330 Juiz de Fora - MG -Brasil. Email:* brunaneves@ice.ufjf.br*;* vivianevaiss@ice.ufjf.br*, alexandre.leitao@ufjf.edu.br*

[2] *Instituto de Química, Universidade Estadual de Campinas, CEP: 13083-970, Campinas – SP. Email: lolly@iqm.unicamp.br*

## ABSTRACT

Magadiite is a layered silicate with many applications such as ion exchange and heterogeneous catalysis[1,2]. Its structure is yet unknown and several authors suggested some models based on the experimental characterizations[3,4,5]. The goal of this work is to study layered models of hydrated and dehydrated H-Magadiite by DFT calculations. The geometry of all the models were optimized and the XRD and $^{29}$Si NMR spectra were simulated for comparison with experimental data. The results show that the models based on Pinnavaia *et.al.* and Garcés *et.al.* works present the best similarities with the experimental data. Calculations of vibrational structure, phase diagram and thermodynamic analyses are expected as next steps of this work.

## INTRODUCTION AND COMPUTATIONAL METHODOLOGY

Magadiite is a layered silicate formed by $SiO_4$-rings. Although widely applied, this material present small crystals with low crystallinity and many defects, consequently, its structure was not yet refined. Experimentally, the models suggested for some authors are not completely proven. We proposed in this work to investigate this material using *ab initio* calculations which are based on the density-functional theory (DFT). Periodic boundary conditions were used, the exchange-correlation potential was described by the PBE-GGA and the core electrons were treated with Vanderbilt Ultrasoft pseudopotentials. The Kohn-Sham orbitals were expanded in a plane wave basis set up to a kinetic energy cutoff of 60 Ry and k-point grid of 4×3x1 was used to sample the first Brillouin zone for all cells.

Layered models of hydrated H-Magadiite (with 4 water molecules) and dehydrated one based on published reports (Rojo *et.al.*, Pinnavaia *et.al*., Garcés *et.al.*) were built. The geometry of all the models were optimized using the QUANTUM ESPRESSO package[6], the XRD and $^{29}$Si NMR spectra were simulated for comparisons with experimental data.

## RESULTS AND DISCUSSION

For all the hydrated models (Figure 1), we noticed that the water molecules interacting mainly between themselves than with layer hydroxyl groups. The simulated XRD patterns (Figure 2) show the sensible reduction of the basal spacings in all models, comparing the displacement of peak close to 10º in 2$\theta$, from hydrated to dehydrated samples, caused by approximation of the layers due the interaction of layer hydroxyl groups upon dehydration. For the values of basal spacing peak, the hydrated model from Garcés suggests the best approximation (7.44º) with the previous experimental work (6.55º)[7].

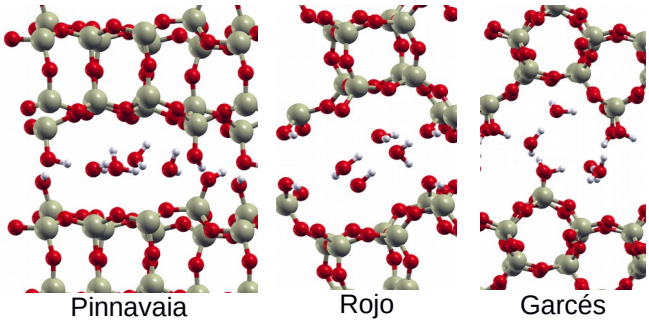


*Figure 1 : Simulated models of hydrated H-Magadiite*

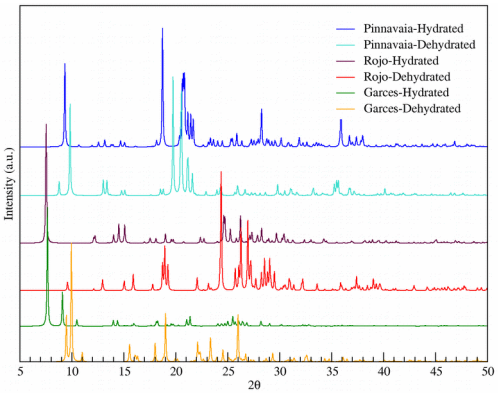


*Figure 2: Simulated XRD of Magadiite.*

We also calculated the $^{29}$Si chemical shifts and simulated the NMR spectrum for all the compounds, thereby identified the $Q_3/Q_4$ ratio (Figure 3A). The convolution of the signs shows appreciable difference between the hydrated and dehydrated models. However, the spectra of hydrated sample based on Pinnavaia and Garcés models indicate better similarities with the experimental results (Figure 3B).

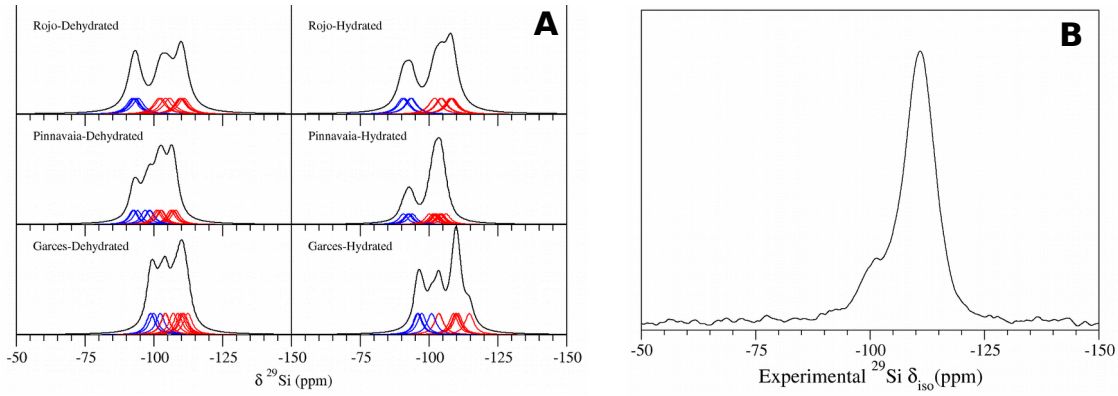


*Figure 3: $^{29}$Si NMR spectra of Magadiite (A) simulated and (B) experimental. Blue: $Q_3$ sites and red: $Q_4$ sites.*

As the next steps, we want to obtain the simulated IR spectra, perform the thermodynamic analysis of the dehydration reaction and study the phase diagram for each material.

**Support:** This work has been supported by CAPES, CNPq, FAPEMIG and FAPESP, Brazilian agencies and the Petrobras S/A (CENPES). We also acknowledge the CENAPAD-SP computational center.

## Citations and References

[1] H.M. Moura, et. al., CrysEngComm, 13, 5428-5438 (2011).
[2] G.L. Paz, et. al., J. Molec. Catal. A: Chem., 422, 43-50 (2016).
[3] J.M. Rojo, et. al., Zeit. Anorg. Allg. Chem., 540, 227-233 (1986).
[4] T.J. Pinnavaia, et. al., J. Sol. St. Chem., 63, 118-121 (1986).
[5] J.M Garces, et. al., Clays Clay Miner., 36, 409-418 (1988).
[6] P. Giannozzi, et. al., J. Phys.: Cond. Matter., 21, 395502 (2009).
[7] J.M.S. Silva, et. al., PCCP, 15, 13434-13445 (2013).

# Electron-phonon and electron-electron interactions in electron doped aromatic hydrocarbons viewed from electrical transport

K. Tanigaki[1,2], S. Heguri[2], Y. Matsuda[2]

*[11]AIMR, Tohoku University, Sendai 980-8577, Japan*
*[2]Department of Physics, Graduate School of Science, Sendai 980-8578, Japan*
*tanigaki@m.tohoku.ac.jp*

Unconventional superconductors, such as cuprates, Fe pnictides, and organic conductors have similarity to electron-doped aromatic hydrocarbon, such as antracene, tetracene, pentacene, and expanded $C_{60}$ [1-4] as well as even in graphene [5]. Electron-electron (e-e) correlations are thought to be the very important origin of their high Tc superconductivity. On the other hand, the highest superconductivity surpassing the cuprates recently found in $H_2S$ under high pressure gives the discussion back to the electron-phonon (e-ph) mediated superconductivity for achieving extremely high $T_c$. Although, relatively high $T_c$ in superconductivity was once claimed for simple aromatic hydrocarbons with electron carrier filling into their bands by alkali-metal insertion, the real electronic states have not yet been understood so far. This is partly because important scientific discussions have been made based on only limited magnetic and optical probes. The Fermi surface of $A_3C_{60}$ (A=alkali metals: K, Rb, Cs) superconductors with expanded cell ($V_{cell}(C_{60}^{3-})$) provides an intriguing research platform for both e-e and e-ph interactions. Being different from other unconventional superconductors, electrical transport measurements, however, had been very difficult in expanded $A_3C_{60}$ and they are made only for $K_3C_{60}$ and $Rb_3C_{60}$ with small cell size far apart from the Mott boundary. Here, we give experimental results that accurate electrical resistivity ($\rho(T,P)$) can be achieved for a variety $A_3C_{60}$ with expanded $V_{cell}(C_{60}^{3-})$ near the Mott boundary under various temperature (T) and pressure (P). Electrical transport was carefully measured as a function of T and P, straddling the phase boundary between the Mott insulator and the metallic/superconducting phase. A new phase diagram is proposed, which unambiguously shows an unprecedented new metallic state existing in the universal T-$V_{cell}(C_{60}^{3-})$ phase diagram. The new phase is interpreted to be generated by interplay between e-ph interactions via dynamic Jahn-Teller phonons and relatively large e-e correlations, showing a strong T-evolution of $\rho(T)$.

[1]. S. Heguri and K. Tanigaki, Dalton Transactions, 47, 2881 (2018).

[2]. Q. TN Phan, S. Oikawa, S. Heguri, Y. Matsuda, K. Tanigaki, Dalton Tranations, 46, 6715 (2017)

[3] Q. TN Phan, S. Heguri, H. Tamura, T. Nakano, Y. Nozue, K. Tanigaki, Phys. Rev. B 93, 075130 (2016).

[4] S. Heguri, M. Kobayashi, K. Tanigaki, Phys. Rev. B 92, 014502 (2015)

[5] S. Heguri, N. Kawada, T. Fujisawa, A. Yamaguchi, A. Sumiyama, K. Tanigaki, M. Kobayashi, Phys. Rev. Lett. 114, 247201 (2015).

# Organically modified α-type zirconium phosphate by reaction with mono- and di-alkylepoxides

Monica Pica[1*], Anna Donnadio[1] and Mario Casciola[2]

[1]*Department of Pharmaceutical Sciences, University of Perugia, Via del Liceo, 1, 06123 Perugia (Italy)*

*2 Department of Chemistry, Biology and Biotechnologies, University of Perugia, Via Elce di Sotto, 8, 06123 Perugia (Italy)*

* *monica.pica@unipg.it*

It is well known that α-type zirconium phosphates, both micro- and nano-crystalline materials, react with alkylepoxides. The reaction takes place between the –POH group of ZrP and the carbon atoms of the epoxide ring, provoking the ring opening and the formation of P-O-C bonds.

In light of these findings, it seemed of interest to study the reaction of α-ZrP with a diepoxide. The idea was to promote the formation of P-O-C bonds connecting adjacent layers, so as to covalently crosslink the layers. This contribution deals with the reaction of nanocrystalline ZrP with 1,2,7,8-diepoxyoctane (hereafter diepoxy), by using the same procedure used for the reaction with monoepoxides. A gel in THF of nanocrystalline ZrP was reacted with the diepoxy and several materials were prepared, by changing the diepoxy/ZrP molar ratio in the range 0.25 – 1.0.

The corresponding organophosphates, were characterized for their composition, thermal behavior and structural features. Moreover, the uptake of aliphatic alcohols, both from the liquid and vapour phases, was also investigated, showing that these materials have a quite agood ability to intercalate high percentages of alcohols, up to 60% in weight, with respect to the dry compound, in the case of ethanol.

# Extraction of Lanthanide Ions from Aqueous Solutions with Synthetic Saponite Clays

**S. MARCHESI[1], F. CARNIATO[1], M. BOTTA[1], L. MARCHESE[1], M. GUIDOTTI[2], C. BISIO[1]**

[1]*Dipartimento di Scienze e Innovazione Tecnologica, Università degli Studi del Piemonte Orientale "Amedeo Avogadro", Viale Teresa Michel 11, 15121-Alessandria, Italy.*
[2]*CNR-Istituto di Scienze e Tecnologie Molecolari, Via C. Golgi 19, 20133-Milano, Italy.*
stefano.marchesi@uniupo.it, fabio.carniato@uniupo.it, mauro.botta@uniupo.it, leonardo.marchese@uniupo.it, m.guidotti@istm.cnr.it, chiara.bisio@uniupo.it

## ABSTRACT

Due to their unique electronic, magnetic, optical and catalytic properties, rare-earth elements (REEs) have been extensively used in the last decades in renewable energy systems and hi-tech products [1]. Thus, the recycling of REEs is of great importance to reduce costs related to their use in the industry and to mitigate the dependence linked to the strategic import of these essential raw materials from remote countries. The traditional processes employed in the recovery of lanthanides are based on solvent extraction, which requires several steps and large amounts of solvents. The development of recovery methods with higher efficiency, lower costs and reduced environmental impact is an important challenge. Different solid sorbents based on carbon, porous silica and natural layered materials have been study for this purpose, due to high chemical affinity for *f*-block species. In this work, we explored two $Na^+$-exchanged synthetic saponite clays (Na-SAP-*n*, gel composition: [$SiO_2$:MgO:$Al_2O_3$:$Na_2O$:$H_2O$] 1:0.835:0.056:0.056:*n*, *n* = 20, 110) as alternative synthetic solid sorbents for the extraction of lanthanide ions, with different ionic radius ($La^{3+}$, $Gd^{3+}$ and $Lu^{3+}$), from aqueous solutions. The saponites were characterized by different particle size and cation exchange capacity (CEC), equal to 32.6 mmol/100 g and 87.9 mmol/100 g for Na-SAP-110 and Na-SAP-20, respectively. The uptake studies of $Gd^{3+}$ were performed in pure water and in simulated freshwater and seawater solutions, in different lanthanide concentrations (0.1-10 mM). Both solids showed high effective sorption capacity in the first 30 min - 1 h, followed by a plateau-*like* adsorption up to 5-24 hours. The amount of $Gd^{3+}$ captured (as 'mg of ion on gram of clay') indicates a strong relationship between the uptake and the CEC of clays: indeed, Na-SAP-20 extracted almost a double amount (*ca.* 49 mg/g) of $Gd^{3+}$ compared to Na-SAP-110 (*ca.* 26 mg/g). The uptake values, indicated in terms of mass-weighted distribution coefficient ($K_d$), are comparable to the ones of other layered and microporous materials reported in literature, especially for Na-SAP-20 (Figure 1). The same extraction behavior was found for $La^{3+}$ and $Lu^{3+}$, with a higher amount of $Lu^{3+}$ extracted by both saponites. The clays were finally tested in the presence of an equimolar mixture of all the three ions (3.33 mM of each), both in pure water and freshwater, showing a marked selectivity for $Lu^{3+}$, due to its lower ionic radius.

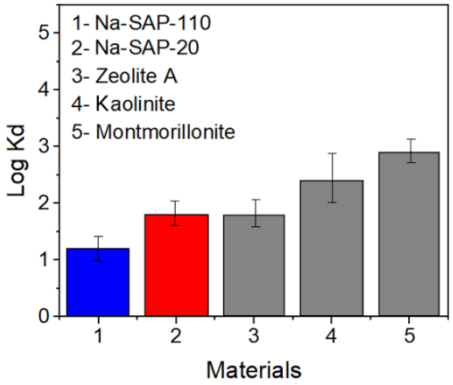


**Figure 1.** $Gd^{3+}$-uptake sorption performance of two synthetic saponites and of reference layered and porous materials (commercial LTA zeolite; kaolinite and montmorillonite). *Experimental conditions*: 15 mg of clay (Na-SAP-20/110) were added to a 1 mL of the test solution (pure water, [$Gd^{3+}$] = 10 mM), at 298 K.

**Keywords**

Saponite – REE – Extraction – Pollution – Environmental

## Citations and References

[1] C R. Ronda *et al.*, *J. Alloys Compd.*, **1998**, 275-277, 669-676.

# PREPARATION OF HETEROSTRUCTURES FORMED BY LAYERED DOUBLE HYDROXYDES COATED WITH MESOPOROUS SILICA

**LISTER PRONESTINO BIANCONI[1,2], CHRISTINE TAVIOT-GUEHO[3], VERA R. L. CONSTANTINO[2], MARCOS AUGUSTO BIZETO[1]**

[1]Universidade Federal de São Paulo (UNIFESP) – Instituto de Ciências Ambientais, Químicas e Farmacêuticas, R. São Nicolau, 210, 09913-030, Diadema – SP, Brazil, lister.bianconi@unifesp.br, mabizeto@unifesp.br
[2]Universidade de São Paulo (USP) – Instituto de Química, Av. Professor Lineu Prestes, 748, 05508-000, São Paulo – SP, Brazil, vrlconst@iq.usp.br
[3]Université Clermont Auvergne (UCA) – CNRS, Institut de Chimie de Clermont-Ferrand, F-63000, Av. Blaise Pascal, 24, Clermont-Ferrand - France, christine.taviot-gueho@uca.fr

## ABSTRACT

Layered double hydroxides (LDH) and mesoporous silicas (MS) are promising inorganic solids to be used as drug carriers due to their structural porosity and chemical properties. In this study, LDH with composition $[M_4Al_2(OH)_{12}]CO_3$ ($M = Mg^{2+}$ or $Zn^{2+}$) were combined to MS in order to produce heterostructures composed of LDH core coated by MS shell ($M^{II}_4Al_2$-$CO_3$@*m*$SiO_2$). The better experimental parameters were pursued to get ordered architectures after and before the template removal from the silica shell. Synthetized materials were characterized by X ray diffractometry (XRD), small angle X ray scattering (SAXS), elemental chemical analysis, infrared (IR) vibrational spectroscopy, specific surface area (SSA) and scanning electron microscopy (SEM). Applying surfactant elimination by calcination, memory effect permitted the structural reconstruction of magnesium based LDH core. On the other hand, surfactant extraction with aqueous solution kept the layered structure of both LDH core. SEM images showed significant morphological modifications after LDH covering by porous silica. The strategy evaluated in this work opens the possibility to prepare heterostructures of LDH intercalated with species besides carbonate and covered by mesoporous silica.

Keywords: layered double hydroxides, mesoporous silica, heterostructures

## INTRODUCTION

Several drugs have restrictions on the form of administration. Porous inorganic solids have emerged as promising alternatives for replacing conventional drug carriers. Among the universe of these inorganic carriers, layered double hydroxides (LDH) [1] and mesoporous silicas (MS) [2] deserve special mention, because they are biocompatible, biodegradable and show low toxicity. In order to improve the LDH properties regarding intercalation, storage and transport, it was proposed to join the properties of MS to this material producing a single heterostructure [3].

## EXPERIMENTAL

LDH samples were prepared by coprecipitation method at constant pH value. Next $M^{II}_4Al_2$-$CO_3$ materials were vigorously dispersed in aqueous mixture of ammonium hydroxide, hexadecyltrimethylammonium cation, and tetraethylorthosilicate. The material

was isolated, dried and redispersed in organic solvent having trimethylchlorosilane before template extraction. Finally, the surfactant in the porous silica shell was removed by calcination or by extraction with an aqueous solution. The heterostructures submitted to calcination were rehydrated to regenerate the LDH core [4]. Synthetized samples were characterized by structural, textural, and spectroscopic techniques.

## RESULTS AND DISCUSSION

XRD patterns and chemical analysis of LDH samples indicated the formation of typical hydrotalcite-type materials. Samples isolated after the silica covering presented an extra XRD peak at low angle region due to the presence of the porous silica amorphous structure. The calcination process promoted the layered structural collapse as it is expected. After rehydration, LDH structure reconstruction was observed partially only for $Mg_2Al@mSiO_2$ sample. In contrary, the solvent extraction did not compromise any the LDH core structure as all the main diffraction peaks remained after the template extraction. SEM images showed markedly differences in the particle's morphology after the formation of mesoporous silica shell (Figure 1). $M^{II}_4Al_2$-$CO_3$ materials presented circular arrangement of flat particles known as *sand rose* while the $M^{II}_4Al_2$-$CO_3@mSiO_2$ derived heterostructures showed quite regular spherical particles. Small angle X ray scattering were also used to investigate the core-shell structure in detail.

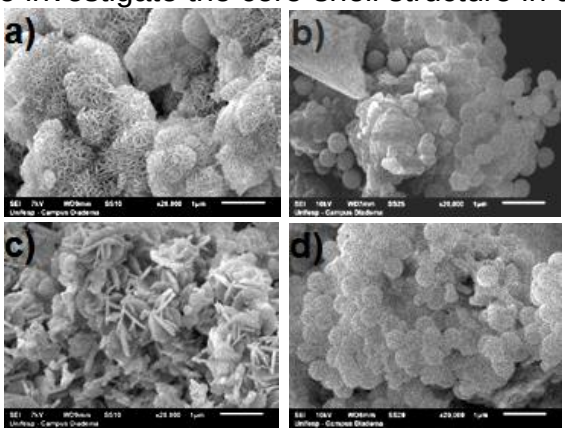


Figure 1: SEM images of ***i***. $Mg_4Al_2$-$CO_3$ and ***i***. $Zn_4Al_2$-$CO_3$ (a and c), and their respective heterostructures calcined after silica coating (b and d).

## CONCLUSIONS

Efficient experimental parameters were achieved to prepared core-shell structures of LDH covered by mesoporous silica as confirmed by a set of physical chemistry techniques used to their characterization. The removal of the template of silica pores by calcination promoted the collapse of LDH layered structure. The layered reconstruction by rehydrating the heterostructures (memory effect) was achieved partially for $Mg_2Al@mSiO_2$ material. Surfactant extraction by solvent was successful. The strategy evaluated in this work opens the possibility to prepared heterostructures of LDH intercalated with species besides carbonate and covered by mesoporous silica.

## REFERENCES

[1] Cunha et al., Quím. Nova 33, 159-171 (2010).
[2] Fonseca et al., Microporous Mesoporous Mater. 159, 24–29 (2012).
[3] Bao et al., Nanoscale 3, 4069-4073 (2011).
[4] Mascolo, G.; Mascolo, M. C., Microporous Mesoporous Mater. 214, 246–248 (2015).

# LIPOIC ACID AND LAYERED DOUBLE HYDROXIDE: EXPERIMENTAL AND *IN VIVO* TESTS APPROACHES

**VANESSA R. R. CUNHA,[1] MARTA N. NAKAMAE,[2] YE R. KANG,[2] RODRIGO B. SOUZA,[3] ANA MARIA C. R. P. F. MARTINS,[4] FABRICE LEROUX,[5] CHRISTINE TAVIOT-GUEHO,[5] IVAN H. J. KOH,[2] VERA R. L. CONSTANTINO[1]**

[1]Departamento de Química Fundamental, Instituto de Química, Universidade de São Paulo, USP, Av. Prof. Lineu Prestes 748, 05508-000, São Paulo, São Paulo, Brazil, vanrrc@gmail.com; vrlconst@iq.usp.br.
[2]Departamento de Cirurgia, Universidade Federal de São Paulo - UNIFESP, Rua Botucatu 740, CEP 04023-900, São Paulo, SP, Brazil, ivankoh@terra.com.br, mnakamae@gmail.com; yeram806@gmail.com.
[3]Departamento de Morfologia e Genética, Universidade Federal de São Paulo –UNIFESP, Rua Botucatu 740, CEP 04023-900, São Paulo, SP, Brazil, rodrigo.barbosa72@yahoo.com.
[4]Instituto Biológico, Secretaria da Agricultura e Abastecimento, Av. Conselheiro Rodrigues Alves 1252, CEP 04014-002, São Paulo, SP, Brazil, crisfm@biologico.sp.gov.br.
[5]Université Clermont Auvergne, Institut de Chimie de Clermont-Ferrand, BP 10448, F-63000 Clermont-Ferrand, France, christine.taviot-gueho@uca.fr, fabrice.leroux@uca.fr

## ABSTRACT

The antioxidant lipoic acid is slightly soluble in water, sensitive to light and heat and exhibits low bioavailability. One strategy to surpass such physicochemical and pharmacological limitations is to design and develop drug delivery systems. This work shows the physicochemical characterization of magnesium-aluminium and zinc-aluminium Layered Double Hydroxides (LDHs) containing the anion form of lipoic acid (Lip) (abbreviated $M_2$Al-Lip, M=$Zn^{2+}$ or $Mg^{2+}$) obtained by coprecipitation and ion exchange methods, as well as the biocompatibility assays by *in vivo* protocol. It was also explored different Lipoate/$Al^{3+}$ molar ratio (5, 8 and 10). Samples were characterized by elemental chemical analysis, X-ray diffraction (XRD), thermal analysis, and spectroscopic techniques (IR and solid state $^{13}$C NMR). The intercalation of lipoate anion into $Zn_2$Al and $Mg_2$Al LDH was successful using both the coprecipitation and anion exchange methods. X-ray diffraction patterns clearly showed an increase of the interlayer distance to 21.3 Å, indicating a bilayer inter penetrating interlayer arrangement of the antioxidant anions. Pair distribution function analysis was used to describe more detailed the arrangement of lipoate between the LDH layers. Spectroscopic data attested the structural integrity of the antioxidant after intercalation process. The biocompatibility of $M_2$Al-Lip samples was evaluated by *in vivo* assays *via* intramuscular tablets implantation in mice abdominal wall. The histological analysis suggested that $Mg_2$Al-Lip drug delivery system provided a more effective anti-inflammatory action than the $Zn_2$Al-Lip.

**Keywords:** Layered Double Hydroxides, Lipoic acid, antioxidant.

## INTRODUCTION

Design and development of drug delivery systems are topics of great interest to surpass the traditional drugs physicochemical limitations (such as solubility) and toxicological properties, and/or physiological barriers for the drug release [1]. The inorganic nanocarriers Layered Double Hydroxides (LDHs) have been having attention since they are known to be biocompatible and to present antacid activity [2].

The antioxidant lipoic acid is slightly soluble in water, sensitive to light and heat and exhibits low bioavailability (20-30 %) [3] which makes it a good candidate to be

intercalated between the LDH layers to improve its physicochemical and pharmacological properties.

## EPERIMENTAL

$M_2Al$-Lip samples were synthesized by coprecipitation and ion exchange methods and characterized by elemental chemical analysis, structural, thermal and spectroscopic analysis. The biocompatibility of the materials was assessed by *in vivo* assays *via* intramuscular tablets implantation in mice abdominal wall, as previously reported [4].

## RESULTS AND DISCUSSION

The intercalation of lipoate anion into $Zn_2Al$ and $Mg_2Al$ LDH was successful using both the coprecipitation and anion exchange method. The X-ray diffraction patterns clearly showed an increase of the interlayer distance to 21.3 Å in presence of lipoate anion. This distance value indicates a bilayer inter penetrating interlayer arrangement of the antioxidant anions into LDH, considering the acid form dimensions (Figure 1). The analysis of the Pair Distribution Function (PDF) revealed a distance at 4.8 Å that may be attributed to a S---S distance between closest neighbouring lipoate anions in the middle of LDH gallery. Vibrational IR and solid state $^{13}C$ NMR spectroscopies showed that lipoate structure is kept after intercalation process.

The histological analysis showed that the amount of defense cells presents in the material $Mg_2Al$-Lip is lower than the results obtained for the zinc analogous material. Therefore, it suggests that the matrix $Mg_2Al$-Lip provided a more effective anti-inflammatory action than the $Zn_2Al$-Lip.

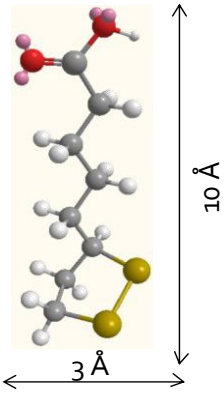


Figure 1 – Molecular structure of lipoic acid, $C_8H_{14}O_2S_2$

## CONCLUSION

LDHs are potential carriers for lipoate storage and delivery in the organism. The different physiological activity presented by $Mg_2Al$-Lip and $Zn_2Al$-Lip materials suggests that the carrier chemical composition may contribute to the modulation of the lipoate activity.

## REFERENCES

1.Choi, G., Kim, T.H., Oh, J.M., Choy, J.H., Coord. Chem. Rev., 359: 32-51, 2018.
2. Li, Z., Ye, E., David, Lakshminarayanan, R., Loh, X.J., Small, 12: 4782-4806, 2016.
3. Durrani, A.I., Schwartz, H., Nagi, M., Sontag, G., Food Chem., 120: 1143-1148, 2010.
4. Cunha, V.R.R., Souza, R.B., Martins, A.M.C.R.P.F., Koh, I.H.J., Constantino, V.R.L., *Sc. Reports*, 6: 1-10, 2016.

# ONE-POT HYDROTHERMAL SYNTHESIS OF LIGHT-HARVESTING ORGANIC-INORGANIC HYBRID MATERIALS

***Hipassia M. Moura*[1,2] *and Miriam M. Unterlass*[1,2,3*]**

[1] Institute of Materials Chemistry, Technische Universität Wien, Vienna, Austria
[2] Institute of Applied Synthetic Chemistry, Technische Universität Wien, Vienna, Austria
[3] CeMM - Research Center for Molecular Medicine of the Austrian Academy of Sciences, Vienna, Austria
*miriam.unterlass@tuwien.ac.at

**ABSTRACT**

Perylene diimides (PDIs) are an important class of high-performance dyes, with intriguing optoelectronic properties. PDIs recently draw great attention as light-harvesting materials. [1] Here, one great challenge is to avoid the formation of large PDI aggregates, which is crucial when high transparency and high fluorescence are needed for realistic device applications.

One possibility to avoid the formation of large PDI aggregates is to embed them in an inorganic matrix, *i.e.* to synthesize hybrid materials (HMs). In the best-case, one obtains PDIs that are finely dispersed in the matrix, and additionally improves their thermo-chemical stability. Moreover, when using inorganic matrices that structurally impart defined spaces for host incorporation – such as in layered clays – one may force the embedded PDIs to adopt a preferred orientation. Thereby highly organized photoactive HMs may be created. Yet, PDIs/layered materials HMs are relatively unexplored. [2-3] Moreover, the few existing routes suffer from severe drawbacks, including multistep syntheses under harsh conditions, and poor dispersibility and/or leaching of the PDI component.

To overcome these drawbacks, we have developed a green and efficient one-pot approach towards optoelectronically active PDI HMs. Our approach consists of simultaneously synthesizing the organic PDIs and inorganic silicate matrices by hydrothermal synthesis (HTS). HTS is a classical method for generating various inorganic compounds *e.g.* gemstones and zeolites. Recently, we showed that organic high-performance dyes can be prepared by HTS. [4-5] Yet, the simultaneous synthesis of organic dyes and inorganic matrices remains to date unexplored.

Here, we discuss the major advantages and challenges of the concomitant preparation of organic PDIs and silicates regarding *(i)* PDI intercalation, *(ii)* HM crystallinity, *(iii)* thermal and chemical stability of HMs, *(iv)* PDI dispersion within matrix, and *(v)* fluorescence properties. The HMs here obtained benefit strongly from both components: While the inorganic host structure gives stabilization and generates order, the organic part contributes to the opto-electronic, color and fluorescence properties.

***Keywords:*** *perylene diimides, hybrid materials, fluorescent solids*

**References**

[1] T. Nguyen, J. Wu, V. Doan, B. J. Schwartz, S. H. Tolbert. *Science* **2000**, *288*, 652-656.
[2] D. K. Bhowmick, L. Stegemann, M. Bartsch, C. A. Strassert, H. Zacharias. *J. Phys. Chem. C* **2016**, *120*, 3275–3288.
[3] K. K. R. Datta, A. Achari, M. Eswaramoorthy. *J. Mater. Chem. A* **2013**,*1*, 6707-6718.
[4] B. Baumgartner, A. Svirkova, J. Bintinger, C. Hametner, M. Marchetti-Deschmann, M. M. Unterlass. *Chem. Commun.* **2017**, *53*, 1229-1232.
[5] M. J. Taublaender, F. Glöcklhofer, M. Marchetti-Deschmann, M. M. Unterlass. *Angew. Chem. Int. Ed.* **2018**, *58*, 12270-12274.

# SYNTHESIS, STRUCTURE AND LUMINESCENCE STUDIES OF 2D EUROPIUM METAL-ORGANIC FRAMEWORKS

**CAROLINE MORAES DA SILVA, REGINA CÉLIA GALVÃO FREM**

Department of General and Inorganic Chemistry, Institute of Chemistry, São Paulo State University (UNESP), Araraquara, Brazil. E-mail: Caroline_moraesilva@hotmail.com

## ABSTRACT

MOFs have been drawing increasing interest as one of the most versatile materials with permanent porosity, despite other porous inorganic materials such as silica and zeolites. This class of metalorganic frameworks shows unique properties such as high crystallinity, high surface area, good thermal stability as well the possibility of chemical functionalization.[1] They are defined as bi- or three-dimensional coordination polymers with empty cavities and are constructed from multitopic ligands coordinated to metallic ions or clusters by strong covalent interactions.[2] In addition, luminescent properties can also be introduced to the MOFs if they are synthesized with lanthanide ions as metal centers (named LnMOFs) and, for this reason, other applications can be exploited as luminescent sensors, biosensors, biomarkers, light emitting devices, among others. In this context, this work starts with the preparation of the **EUPDC** sample, a 2D MOF based on trivalent europium ion and 2,6-pyridinedicarboxilate linker (PDC) and the investigation of the potential properties. The work also investigated the chemical stability of this material in aqueous phase. When in the presence of water, the compound **EUPDC** undergoes a reversible reaction generating the luminescent 2D coordination polymer $[Eu(PDC)(HPDC)(H_2O)_2]\cdot 4H_2O$ (**EUPDCW**). In addition to modifying the coordination environment of the europium ion, this structural modification caused by the presence of the solvent, led to the protonation of the PDC linker. The reversibility of the system **EUPDC-EUPDCW** was confirmed by powder X-ray diffraction studies as well chemical exfoliation processes.

*Keywords*: LnMOFs, lanthanides, luminescence, two-dimensional materials.

## INTRODUCTION

The Metal-Organic Frameworks (MOFs) are crystalline solids constructed from multitopic ligands bridged coordinated to metallic ions or clusters by strong covalent interactions, forming coordination networks containing voids (cavities).[1] The main interest in this type of material is related to the set of unique properties such as: permanent porosity, high crystallinity, high surface area, good thermal stability and the possibility of chemical functionalization.[2]

These networks can be two-dimensional (MOF 2D) or three-dimensional (MOF 3D). The two-dimensional MOFs are layered with strong coordinate bonds in the plane, and weak interactions between layers. In addition to the inherent properties of MOFs, 2D MOFs also have high surface area, more accessible active sites and ultrafine (nm) thickness and possibilities of isolating the monolayers by exfoliation methods.[3]

The luminescent MOFs, like some lanthanide metal-organic frameworks, have advantages and characteristics as high optical purity, sharp emission peaks, long luminescence lifetimes, which arise from *f-f* transitions via an "antenna effect". This event consists of the absorption of ultraviolet radiation by the chromophore groups of the linker followed by the transfer of energy to the emissive levels of the lanthanide ion populating the levels resulting in the *f-f* forbidden transitions observable, with potential for luminescent sensors.[4]

## EXPERIMENTAL

*Synthesis of **EUPDC***. The **EUPDC** compound was obtained by hydrothermal synthesis. 1,3,5-benzenetricarboxylic acid was dissolved in water, followed by the addition of NaOH to adjust pH. Then, was addition 2,6-pyridinedicarboxylic acid and europium (III) chloride hexahydrate. The

mixture was stirred further in a polytetrafluoroethylene (PTFE)-lined steel autoclave, and was subsequently heated to 150ºC for 3 days. After cooling and filtering, single crystals were isolated which were suitable for X-ray single crystal diffraction.

*Chemical stability.* The **EUPDC** powder was simply immersed in water for 24 hours. After that, the material was washed with water, centrifuged, dried in a vacuum and characterized by powder X-ray diffraction.

*Chemical exfoliation.* The **EUPDC** powder was dispersed in water. The mixture was then sonicated for 30 min before UV-Vis transmittance measurements.

## RESULTS AND DISCUSSION

The X-ray single crystal diffraction of **EUPDC** compound revealed self-organized two-dimensional structures in the solid state by intermolecular hydrogen bonding interactions, forming a three-dimensional structure with stacking of the monolayers. The luminescence studies show intense emission in the red region. The excitation spectrum ($\lambda_{em}$ = 611nm) shows a broad band in region 250-350 nm and bands of the intraconfigurational transition of the europium (III). The emission spectrum show the characteristic transitions of the europium (III) ion, from the excited level $^5D_0 \rightarrow {}^7F_J$, with an intensity maximum at 611 nm.

The **EUPDC** powder sample, when in the presence of water, undergoes a reversible reaction generating the luminescent 2D coordination polymer $[Eu(PDC)(HPDC)(H_2O)_2]\cdot 4H_2O$ (**EUPDCW**), proved by powder X-ray diffraction and elemental analysis. The chemical exfoliation proves the instability of the **EUPDC** sample. In aqueous solution, the low percentage of transmittance indicates the inefficiency of the exfoliation as a consequence of the recrystallization of the **EUPDC** compound, that is, the formation of the **EUPDCW**. The **EUPDCW** sample activated at 120ºC in vacuum, releases the water molecules organizing in the original conformation (**EUPDC**), as can been in Fig.1. With FT-IR, it is possible to infer that the water molecules interact by hydrogen bonding with the carbonyl of the structure of the **EUPDC** compound. The presence of the $\upsilon$(OH) broad band at 3438 $cm^{-1}$ and the absence of the $\upsilon$(C=O) band in 1740 $cm^{-1}$. After band activation process $\upsilon$(C=O) is strong at 1746 $cm^{-1}$.

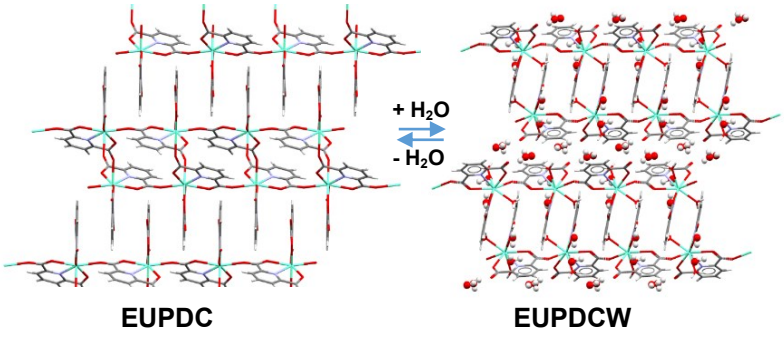


**Figure 1.** Reversible behavior of the **EUPDC** compound in aqueous solution.

## CONCLUSION

A two-dimensional **EUPDC** was obtained. The compound showed instability (reversible) in aqueous solution, becoming the **EUPDCW** compound. **EUPDC** compound shows potential application as a luminescent sensor in solutions, with the exception of aqueous systems. It is believed that the obtainment of nanosheets (monolayers) from the two-dimensional MOF might have promising applications in several areas, especially in sensoring.

### Citations and References

[1] BATTEN, S. R. *et al*. **Pure and Applied Chemistry**, 85, 2013.
[2] ZHOU, H. J., KITAGAWA, S. **Chem. Soc. Rev.**, 43, 2014.
[3] Zhang, H. *et al.* **Small Methods**, 1, 2017.
[4] Li, J. *et al*. **Chem. Soc. Rev.**, 43, 2014.

# Basicity and Acidity Study of Solvent Treated Layered Double Hydroxides (LDHs)

**DOY LEUNG, KANITTIKA RUENGKAJORN, CHUNPING CHEN AND DERMOT O'HARE**

Chemistry Research Laboratory, Department of Chemistry, University of Oxford, Oxford, OX1 3TA, United Kingdom. doy.leung@chem.ox.ac.uk

Keywords: Layered double hydroxides, basicity, acidity

## ABSTRACT

LDHs and their partially calcined derivatives, layered double oxides (LDOs), have been developed for use as heterogeneous catalysts due to their high basicity.[1] Recently, further enhancements to their basicity can be achieved by alkali-metal doping of LDHs.[2]

We have recently discovered that by re-dispersing LDHs in organic solvents, a new family of LDHs can be synthesised: aqueous miscible organic and aqueous immiscible organic LDHs (termed: AMO-LDHs and AIM-LDHs respectively, Figure 1a)[3,4]. These new families display an increase in surface area as well as an improved hydrophobicity, leading to improved dispersibility in non-polar solvents.

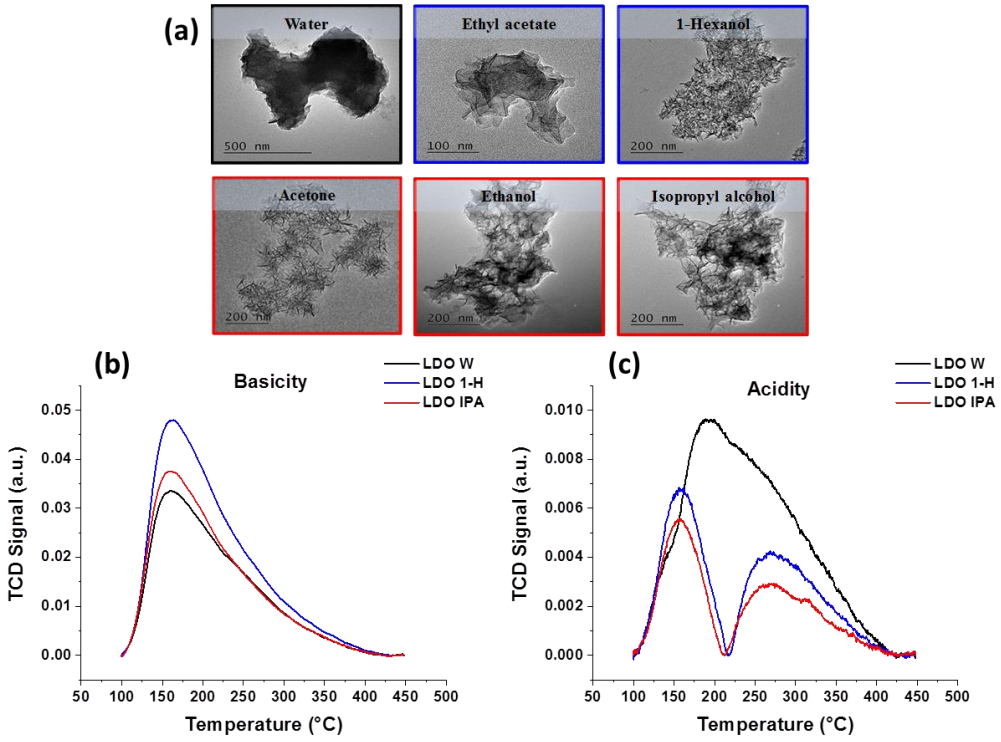


**Figure 1**: (a) TEM images of solvent treated $Mg_3Al$-$CO_3$ LDHs (black: conventional, blue: AIM- and red: AMO-) used in this study; (b) basicity data obtained from $CO_2$-TPD and (c) acidity data obtained from $NH_3$-TPD (W: water, 1-H: 1-hexanol and IPA: isopropyl alcohol.).

We have discovered that by dispersing conventional water-washed LDHs in organic solvents, the acidity and basicity of the compound were altered. The LDO prepared from an LDH dispersed in IPA (LDO-IPA) to an LDO derived from a conventional water washed LDH (LDO-W) were very different. While the basicity measured using temperature programmed desorption (TPD) remains similar (1.97 and 1.95 mmol $g^{-1}$ respectively), the acidity of LDO IPA dramatically decreased. LDO IPA shows an acidity of 0.16 mmol $g^{-1}$ while that of LDO W is 0.58 mmol $g^{-1}$.

## Citations and References

[1] W. Kagunya, Z. Hassan and W. Jones, *Inorg. Chem.*, 1996, **35**, 5970–5974.
[2] E. L. G. Oliveira, C. A. Grande and A. E. Rodrigues, *Sep. Purif. Technol.*, 2008, **62**, 137–147.
[3] K. Ruengkajorn, V. Erastova, J.-C. Buffet, H. C. Greenwell and D. O'Hare, *Chem. Commun.*, 2018, **54**, 4394–4397.
[4] C. Chen, A. Wangriya, J.-C. Buffet and D. O'Hare, *Dalton Trans.*, 2015, **44**, 16392–16398.

# Host-guest association of coumarin 343 with β-cyclodextrin: experimental induced circular dichroism (ICD) and computer simulation studies (TD-DFT/PBE1)

**XIMENES, V.F.[1], DE SOUZA, A.R.[1], MORGON, N.H.[2]**

[1] Department of Chemistry, Faculty of Sciences, UNESP – São Paulo State University, 17033-360, Bauru, São Paulo, Brazil.
[2] Department of Physical Chemistry, Institute of Chemistry, Campinas State University, UNICAMP, 13083-861, São Paulo, Brasil.

## ABSTRACT

The inclusion of coumarin 343 into β-cyclodextrin was studied by both experimental Induced Circular Dichroism (ICD) and computer simulation studies in order to understand the photophysical properties upon the formation of the complex. The coumarin molecule shows a peak in the ICD spectra at 450 nm only in the presence of β-cyclodextrin. This result was confirmed by calculations at the PBE1PBE level of theory for the singlet multiplicity and number of states equal to 15.

## INTRODUCTION

The phenomena of host-guest association have attracted scientific interest as a basic concept in the fields of supramolecular chemistry, molecular biology and nanotechnology [1]. Cyclodextrins are macrocyclic sugar molecules composed of α-1,4-glycosidic linkages of either 6, 7, or 8 glucose units, and are denoted as α-, β-, and γ-cyclodextrin, respectively. β-Cyclodextrin possess a hydrophobic central cavity that enable it to accommodate different organic, inorganic, neutral or charged molecules with many applications in the field of pharmaceutical and food chemistry, catalysis, synthesis, and development of biosensors [2,3]. The photophysical properties of coumarin 343 (C343) are very sensitive to solvent polarity, different pH values and H-bond association. This characteristic of C343 enables them to be used as a molecular probe for sensing micro and nano environments present in proteins [4], DNA and inclusion phenomena. C343 and β-cyclodextrin forms a host-guest complex where the former binds into to the cavity of the macromolecular host resulting in interesting spectroscopic effects and one of the most studied is the fluorescent enhancement of the guest. In this work we aim to elucidate the conformation of C343 and the mode of binding with β-cyclodextrin.

## RESULTS AND DISCUSSION

The interaction between C343 and β-cyclodextrin was studied by the induction of chirality in the former. The reaction medium was composed of β-cyclodextrin (5 mmol $L^{-1}$) in the absence or presence of 30 μmol $L^{-1}$ C343 in 50 mmol $L^{-1}$ phosphate buffer, pH 7.0, 25°C. The ICD studies were performed in a Jasco J-815 spectropolarimeter (Jasco, Japan) equipped with a thermostatically controlled cell holder. The spectra were obtained with 1 nm step resolution, response time of 1 s and scanning speed of 50 nm/min. A 3 mL quartz cuvette with a 10 mm path length and a magnetic stirrer were used for the measurements in the near-UV-CD range. The baseline (buffer) was subtracted from all measurement.

The computer simulation of the host-guest system was carried out at the PM6/IEFPCM level of theory. We considered the translational movement of the guest from 5 Å, at intervals of 0.1 Å from bellow and up the mass center of the host structure along with the rotational movements of the guest (center of mass) at intervals of 30 degrees. From the obtained energies we proceed to calculate the Boltzmann distribution between the most stable structures. At the most relevant obtained structures we obtained 15 most stable singlet electronic states at the TD-DFT/PBE1/6-31G(2d,p) level of theory, and thus obtaining the respective electronic transitions with the oscillatorr and rotational strength. The most stable structure of the host-guest complex is present at Figure 1 at different angles of view.

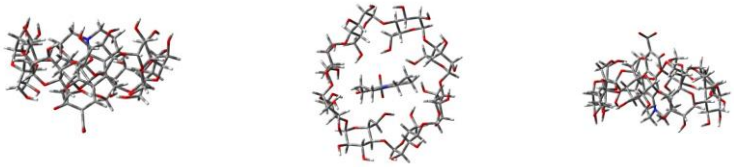

Figure 1. Most stable structure of the host-guest complex.

The experimental absorbance and ICD of the host-guest complex are presented at Figure 2(a), were we can observe a maximum at 450 nm at both spectra and the appearance of a positive Cotton effect in the ellipticity of coumarin 343. In Figure 2(b) we can observe that the calculated absorbance and ICD spectra of coumarin 343 are in good agreement with the experimental one.

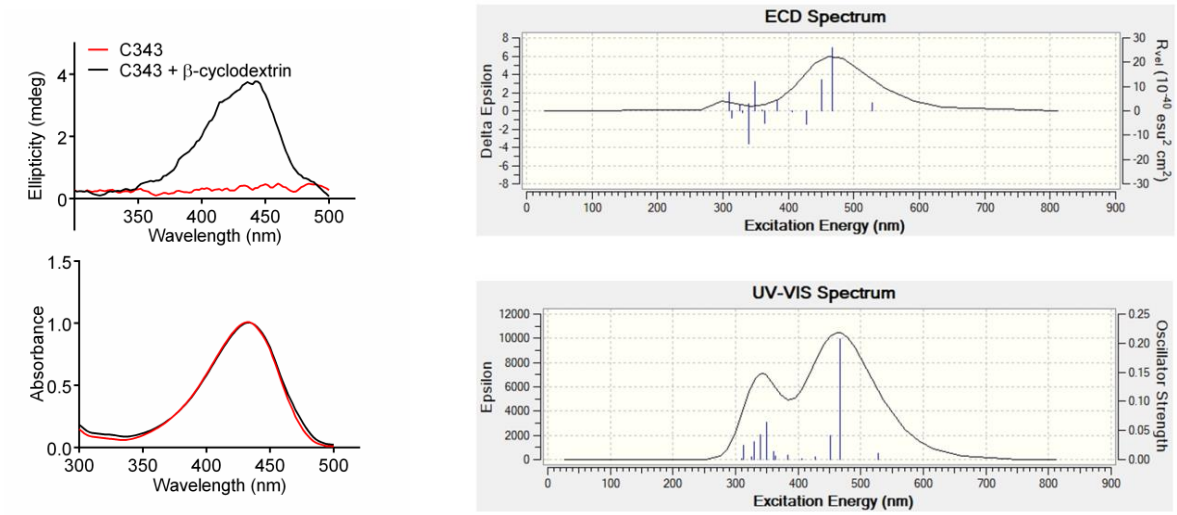


(a) (b)

Figure 2. (a) Experimental and (b) theoretical (PBE1PBE) UV-Vis and ICD spectra.

## REFERENCES


1. Lehn, J-M, “Supramolecular Chemistry: Concepts and Perspectives”, VCH, Weinheim, 1995.
2. Edetsberger, M.; Knapp, M.; Gaubitzer, E.; Miksch, C.; Gvichiya, K. E; Köhler, G. *J. Incl. Phenom. Macrocycl. Chem*. **2011**, 70, 327-331.
3. Scypinski, S.; Drake, J.M. *J. Phys. Chem.* **1985**, 89, 2432-2435.
4. Garg, A.; Manidhar, D.M.; Gokara, M.; Malleda, C.; Reddy, C. S.; Subramanyam, R , R. *PLoS ONE* **2013**, 8(5), 1-17.

# Silica@Layered Double Hydroxide Core-shell Hybrid Materials

**WING LAM JOYCE KWOK, DANA-GEORGIANA CRIVOI, CHUNPING CHEN, JEAN-CHARLES BUFFET AND DERMOT O'HARE***

Chemistry Research Laboratory, Department of Chemistry, University of Oxford, 12 Mansfield Road, Oxford, OX1 3TA, UK. Email: wing.kwok@balliol.ox.ac.uk

Keywords: layered double hydroxides, core-shell, silica.

## ABSTRACT

A series of silica@layered double hydroxides ($SiO_2$@$Mg_2Al$-$CO_3$-AMO-LDHs) have been synthesised by *in-situ* nucleation and growth of $Mg_2Al$-$CO_3$-LDH platelets in the presence of amorphous spherical silica particles (~500 nm).[1,2] We have systematically investigated a number of synthetic parameters in order to evaluate their effects on the composition, morphological and physical properties of the isolated core@shell materials.

Syntheses carried out at moderate stirring speeds (*e.g.* 500 rpm) were found to promote the formation of vertically aligned LDH platelets with respect to the silica surface. Addition rates of the metal solutions slower than 0.43 mmol $h^{-1}$ were found to create a thicker LDH shell consisting of vertically aligned LDH platelets. When the metal solutions were added rapidly (0.86 mmol $h^{-1}$), we observed that for both slow and fast stirring speeds the synthesised core-shell materials had thin LDH shells and the majority of the LDH precipitated independent of the silica, forming unbound "free" LDH.

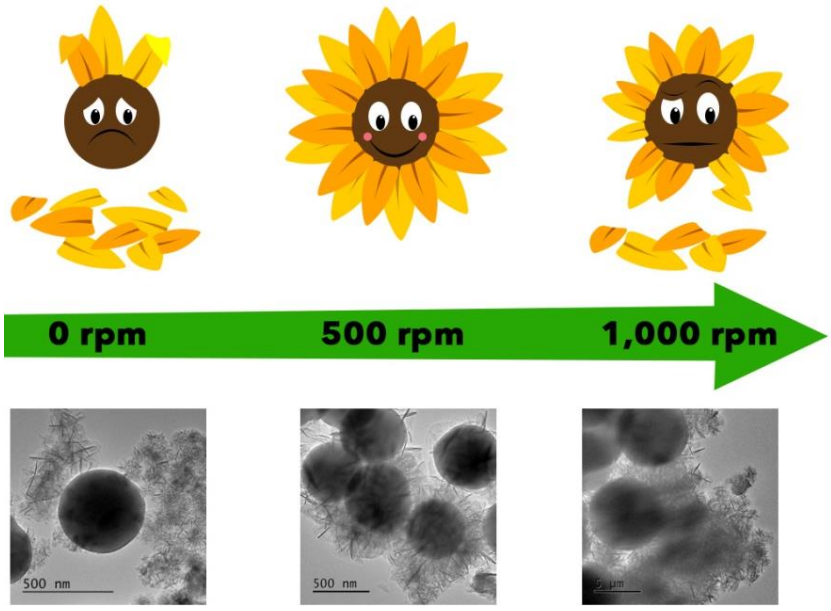


**Figure 1.** TEM images of $SiO_2$@$Mg_2Al$-$CO_3$-AMO-LDHs synthesised with metal addition rate 0.11 mmol $h^{-1}$ at different stirring speeds.

The experiments indicate that preparing high quality core@LDH needs detailed attention to the synthesis conditions. We found that for core-shell $SiO_2$@$Mg_2Al$-$CO_3$-AMO-LDH materials, the use of moderate stirring speeds and slow metal addition rates produced samples with an optimal honeycomb-like morphology and the highest surface area.

### Citations and References

[1] C. Chen, R. Felton, J.-C. Buffet and D. O'Hare, *Chem. Commun.*, 2015, **51**, 3462.
[2] W. L. J. Kwok, D.-G. Crivoi, C. Chen, J.-C. Buffet and D. O'Hare, *Dalton Trans.*, 2018, **47**, 143.

# SELECTIVE TRANSFORMATION OF ACETONITRILE TOWARD $N_2$ OVER (Cu, Co and Fe)-OXIDE CATALYSTS.

**PAULO HENRIQUE DA SILVA, JÉSSICA A. P. PONCIANO, MARCELO S. BATISTA***

Chemical Engineering Department, Federal University of São João Del Rei, Campus Alto Paraopeba, Minas Gerais, Brazil. *e-mail: marcelobatista@ufsj.edu.br

## ABSTRACT

CuO, $Co_3O_4$ and $Fe_2O_3$ catalysts were prepared, characterized by XRD and $H_2$-TPR and investigated for the selective catalytic combustion of acetonitrile ($CH_3CN$-SCC). The XRD patterns of the catalysts confirmed the CuO, $Co_3O_4$ and $Fe_2O_3$ crystalline structures. All catalysts showed lower temperature (~400$^oC$) for $CH_3CN$-SCC than without catalyst (~800$^oC$). CuO and $Co_3O_4$ catalysts had lower temperature for total reduction and higher $CH_3CN$ conversion. CuO, $Co_3O_4$ and $Fe_2O_3$ catalysts were selective to $N_2$ and $N_2O$, $N_2$ and $NO_x$ and, $N_2$ and HCN, respectively.

**Keywords:** pollution, acetonitrile, combustion, catalyst.

## INTRODUCTION

Acetonitrile ($CH_3CN$) mainly comes from the tail gas of industrial acrylonitrile plants in significant amounts, and its removal has attracted attention due to its potential hazard. $CH_3CN$ can be readily decomposed into the highly toxic HCN in the body once it directly contacts humans [1].

Treatment of acetonitrile gases by traditional thermal combustion at elevated temperatures (above 800$^oC$) often lead to formation undesirable of large amounts of nitrogen oxides and the HCN amount depends on the reaction conditions [2]. On the other hand, selective catalytic combustion (SCC) uses much lower temperature and is the most efficient route and suitable to transformation of $CH_3CN$ into $N_2$ and $CO_2$ [3]. In this study, CuO, $Co_3O_4$ and $Fe_2O_3$ catalysts were investigated for $CH_3CN$-SCC.

## MATERIALS AND METHODS

CuO, $Co_3O_4$ and $Fe_2O_3$ catalysts were prepared by calcination of metal nitrate at 650°C with the rate of 10$^oC$/min for 2 h. These catalysts were characterized by XRD (40 KV, 15 mA and CuKα radiation) and $H_2$-TPR (10°C/min and 30 mL/min from mixture of 2 vol.% $H_2$ in Ar). The catalysts were evaluated in the $CH_3CN$-SCC using a quartz wool-type "U" reactor and 8.6 mg of metal in the sample, fed with continuous flow of 50 mL/min of a mixture containing 2.8 vol.% $CH_3CN$ in synthetic air. The reactor was coupled in line to a mass spectrometer (THERMO) for gas analysis: $N_2$ (m/z = 28), $O_2$ (m/z = 32 and 16), NO (m/z = 14), $N_2O$ (m/z = 44 and 30), $NH_3$ (m/z = 17), $CH_3CN$ (m/z = 41) and $CO_2$ (m/z = 44).

## RESULTS AND DISCUSSION

The XRD patterns of the catalysts showed all characteristics peaks of CuO (PDF 41-0254), $Co_3O_4$ (PDF 01-1152) and $Fe_2O_3$ (PDF 01-1053) crystalline structures (Fig. 1). TPR profiles of CuO presents one reduction peak at 343$^oC$, corresponding to the reduction of CuO to $Cu^0$ (Fig. 2). $Co_3O_4$ shows pratically one peak at 360ºC which was

assigned to the reduction of $Co^{3+}$ to $Co^{o}$. Reduction of the $Fe_2O_3$ occurs in more than one stage. The first peak corresponds to the reduction of $Fe_2O_3$ to $Fe_3O_4$ occurs around 295°C. The reduction of $Fe_3O_4$ to $Fe^0$ can be observed in the range of 330°C to 700°C, which can occur via FeO ($Fe_3O_4$→FeO→$Fe^{o}$).

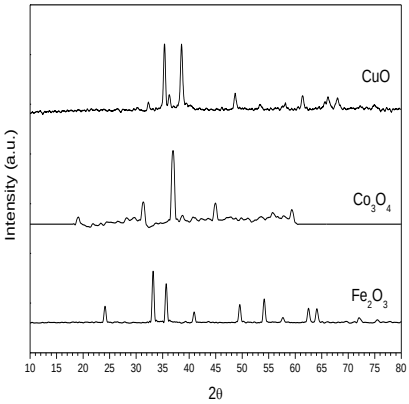


Fig. 1: XRD patterns.

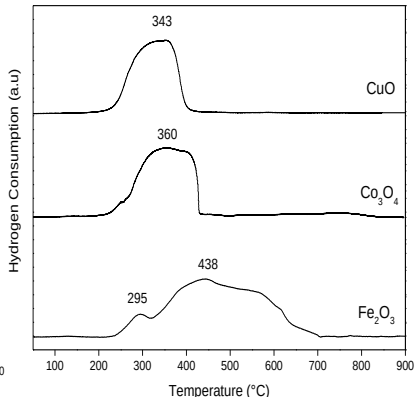


Fig. 2: $H_2$-TPR profiles.

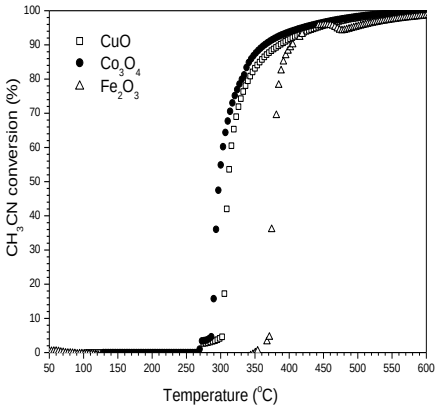


Fig. 3 – $CH_3CN$ conversion

Fig. 3 shows the $CH_3CN$ conversions on CuO, $Co_3O_4$ and $Fe_2O_3$ catalysts as a function of reaction temperature. It was found that the $CH_3CN$ initial conversion rises rapidly upon the temperature and almost kept stable at temperature range of 500–600°C on all catalysts. The copper, cobalt and iron oxides are active sites for the $CH_3CN$-SCC reaction and the comparison of the catalysts was performed with the same mass of metal into reactor. CuO and $Co_3O_4$ catalysts showed similar activities and were more actives than $Fe_2O_3$ catalyst in lower temperature. According to these results, the CuO and $Co_3O_4$ catalysts had lower temperature for total reduction and higher $CH_3CN$ conversion.

Apart from high conversion of $CH_3CN$, the high yield of $N_2$ and $CO_2$ is another important criterion for choosing the ideal catalyst due to the possible releasing of other undesirable byproducts ($NH_3$, $N_2O$, HCN, NO and $NO_2$) during $CH_3CN$ combustion. $Fe_2O_3$ catalyst was selective to $N_2$ and HCN. $Co_3O_4$ catalyst was selective to $N_2$ and $NO_x$. On the other hand, $CH_3CN$ was largely transformed into $N_2$ and undesirable byproducts ($N_2O$ and NO+$NH_3$ traces) above 320°C over CuO catalyst (no shown). These undesirable by-products and the $N_2$ yield observed for the CuO catalyst are very similar to those found in the literature for the CuO supported on SBA-15 catalyst [3]. CuO showed the highest $N_2$ yield, which started from 300°C, increased progressively upon the reaction temperature and almost kept stable at temperature range of 400–600°C. In addition, acetonitrile was oxidized directly to $CO_2$ on all catalysts.

## CONCLUSIONS

The XRD patterns of the catalysts confirmed the CuO, $Co_3O_4$ and $Fe_2O_3$ crystalline structures. All catalysts showed lower temperature (~400°C) for $CH_3CN$-SCC than without catalyst (~800°C). CuO and $Co_3O_4$ catalysts had lower temperature for total reduction and higher $CH_3CN$ conversion. CuO, $Co_3O_4$ and $Fe_2O_3$ catalysts were selective to $N_2$ and $N_2O$, $N_2$ and $NO_x$ and, $N_2$ and HCN, respectively.

## REFERENCES


[1] ZHANG, R.; LIU, N.; LEI, Z.; CHEN, B. Chemical Reviews 116, p. 3658–3721, 2016.
[2] BRITT, P. F. Pyrolysis and Combustion of Acetonitrile. Oak Ridge TN: Oak Ridge National Lab, 2002.
[3] ZHANG, R.; SHI, D.; LIU, N.; CAO, Y.; CHEN, B. Appl. Catal. B: Env. 146, p. 79–93, 2014.

# rGO-tin oxide nanocomposites for photoelectrochemical applications

**Fernanda C. Romeiro*, Gabriel Facheti, Alysson S. Martins, Maria Valnice B. Zanoni, Marcelo O. Orlandi***

Instituto de Química, Universidade Estadual Paulista, 14800-900, Araraquara-SP, Brazil.
*costaromeirof@yahoo.com, marcelo.orlandi@unesp.br

## ABSTRACT

In this work, $Sn_3O_4$ and its nanocomposite with reduced graphene oxide (rGO) were synthesized using the one step microwave hydrothermal method. Raman spectroscopy indicated the successful synthesis of rGO-tin oxide nanocomposite. The presence of abundant functional groups in the GO precursor has played a crucial role in the chemical composition and morphology of the nanocomposite. Due to the synergistic effect, the resulting nanocomposite exhibited high electronic interaction between tin oxide and rGO sheets, which improved the photoelectrochemical hydrogen ($H_2$) evolution and its stability during electrolysis.

Keywords: photoelectrocatalytic properties, $Sn_3O_4$, reduced graphene oxide; microwave hydrothermal method.

## INTRODUCTION

In order to reduce the environmental effects from the use of fossil fuels, hydrogen is considered as one of the most important energy sources, presenting advantages such as high energy density; besides being considered a clean energy fuel. [1] In this way, the development of efficient catalysts to produce hydrogen is one of the most promising challenges in recent years. [1] Among the studied photoelectrocatalysts, mixed valence tin oxide ($Sn_3O_4$) has emerged as one promising ecofriendly alternative, due to the co-existence of $Sn^{2+}$ and $Sn^{4+}$ ions, which leads to a desirable band structure for photocatalytic $H_2$ evolution from water solution. [2] However, up to date, there are only few results regarding $Sn_3O_4$ for $H_2$ evolution reaction. In order to improve the photoelectrochemical applications, the graphene, a high surface area carbonaceous material, can increase the electron-hole separation and simultaneously promotes the control of composition and morphology of semiconductors materials. [3] In this work we report a simple one-step synthesis rGO-tin oxide nanocomposite for photoelectrochemical $H_2$ evolution applications.

## METHODOLOGY

Pure $Sn_3O_4$ was obtained from the addition $SnF_2$ in a water/ethanol and addition of NaOH solution (1.0 mol $L^{-1}$) until pH = 6.0. To obtain the nanocomposite, a dispersion containing 32 mg of graphite oxide in a water/ethanol mixture was added to the previous dispersion. The final solutions were transferred into a teflon autoclave and placed in the microwave-assisted reactor (150 °C, 2h). The obtained materials were deposited on titanium plates surfaces and submitted under spin coating methodology with posterior calcination at 400 °C, in order to obtain their respective films. The photoelectrochemical tests were measured using $Na_2SO_4$ 0.5 mol $L^{-1}$ (pH=6) as electrolyte support. An artificial sunlight simulator of 300 W was employed for the photoelectrochemical tests.

## RESULTS AND DISCUSSION

As observed in Fig. 1a, the pure $Sn_3O_4$ presented Raman bands characteristic of the $Sn_3O_4$ triclinic structure (indicated by *) and a broad band around 466 and 619 $cm^{-1}$ ascribed to small portion of $SnO_2$. In the nanocomposite it was observed the co-existence of the Raman modes of $Sn_3O_4$ and $SnO_2$, and the additional presence of the D and G bands assigned to the defects within the hexagonal graphitic structures and phonon vibration of $sp^2$ bonded carbon atoms in rGO sheets, respectively. The $Sn_3O_4$ sample presented well-defined plate-like morphology, as shown in Figure 1b. In the nanocomposite, the morphology was modulated by GO precursor, which the definition of the plate-like morphology decreased and the rGO covered the tin oxide nanoparticles (Fig. 1c).

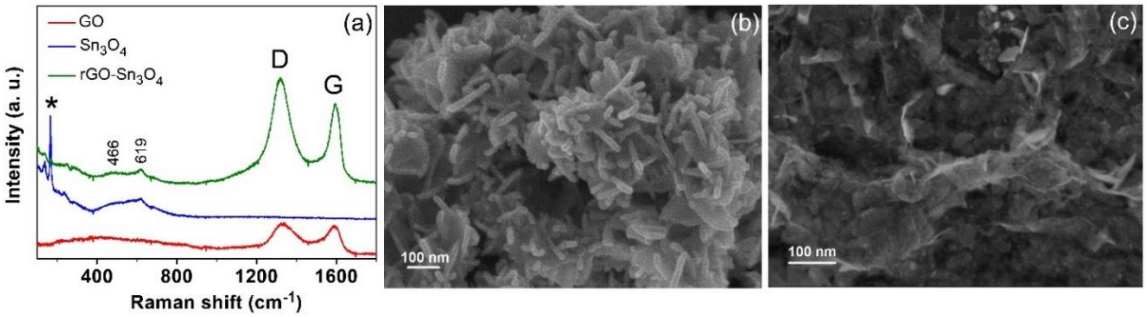


Fig. 1. (a) Raman spectra of the GO, $Sn_3O_4$ and rGO-$Sn_3O_4$ nanocomposite (b) FE-SEM image of $Sn_3O_4$ and (c) of rGO-$Sn_3O_4$ nanocomposite**.**

The rGO-$Sn_3O_4$ material presented higher current density at lower potential under the light as observed in Fig. 2a, which can be related to the favorable reduction of $H^+$ ions to $H_2$ molecules. Additionally, the nanocomposite exhibited higher stability and higher current density as observed by the chronoamperometry measurement in Fig. 2b, when compared to the pure $Sn_3O_4$. The high activity of the nanocomposite for hydrogen evolution can be attributed to the synergistic effect between tin oxide nanostructures and the rGO sheets, which promoted photoelectrocatalytic stability and fast ion/electron transfer at the film surface. This work presents the development of new materials for photocathodic processes.

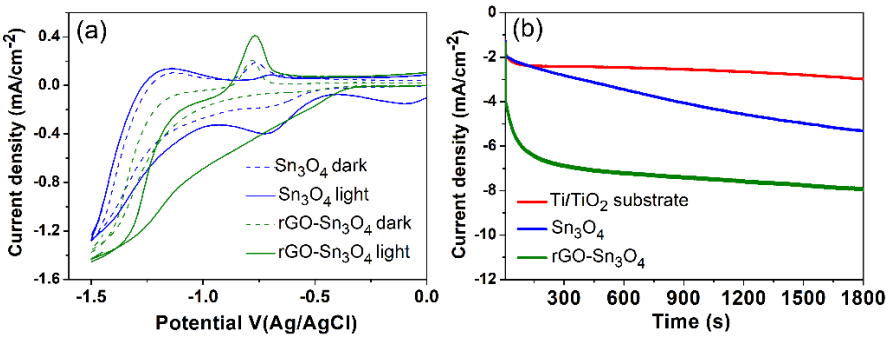


Fig. 2. (a) CVs and (b) chronoamperometry measurement (at -1.5 V, under artificial sunlight simulator) of $Sn_3O_4$ and rGO-$Sn_3O_4$ nanocomposite in $Na_2SO_4$ (0.5 $mol.L^{-1}$), pH = 6.

### Citations and References


[1] Morales-Guio, C. G, *et al*., Chem. Soc. Rev. 2010, 43, 6555.
[2] Manikandan, M. *et al*., ACS Appl. Mater. Interfaces, 2014, 6, 3790.
[3] Geim, A. K, *et al*., Nat. Mater. 2007, 6, 183.

# Silane modification of layered double hydroxides

**CHUNPING CHEN, JEAN-CHARLES BUFFET AND DERMOT O'HARE***

Chemistry Research Laboratory, Department of Chemistry, University of Oxford, Oxford, OX1 3TA, United Kingdom. Chunping.chen@chem.ox.ac.uk.

Keywords: Layered double hydroxides, silane modification, water vapor resistance.

## ABSTRACT

Silane modification of layered double hydroxide (LDH) plays an important role in improving the compatibility with non-polar materials and increasing their water vapor resistance of LDH.[1-3] However, the surface modified LDH via aqueous routes normally shows self-condensation, aggregated morphology and poor porosity, which hinder their applications. In this study, we applied an anhydrous synthesis method to obtain silane grafted LDHs without losing pristine properties. A series of silane coupling agents (triethoxyvinylsilane (TEVS), triethoxyoctylsilane (TEOS), and (3-glycidyloxypropyl) trimethoxysilane (TMGPS)) were chose to study surface modification on $ZnMg_2Al\text{-}CO_3$ LDH in acetone medium. In situ NMR measurement proved the condensation reaction and the formation of a by-product (methanol or ethanol). The silane treated LDH kept similar structure, morphology, surface area and relatively enlarged pore volume. Solid state $^{13}C$ NMR and $^{27}Al$ NMR spectroscopy indicated that the silanes have been successfully grafted on the surface of $ZnMg_2Al\text{-}CO_3$ LDH. The TGA and water vapor uptake studies confirmed that the modified LDHs exhibited low water content and low water vapor capacity in relative humidity (RH70) at 20 °C.

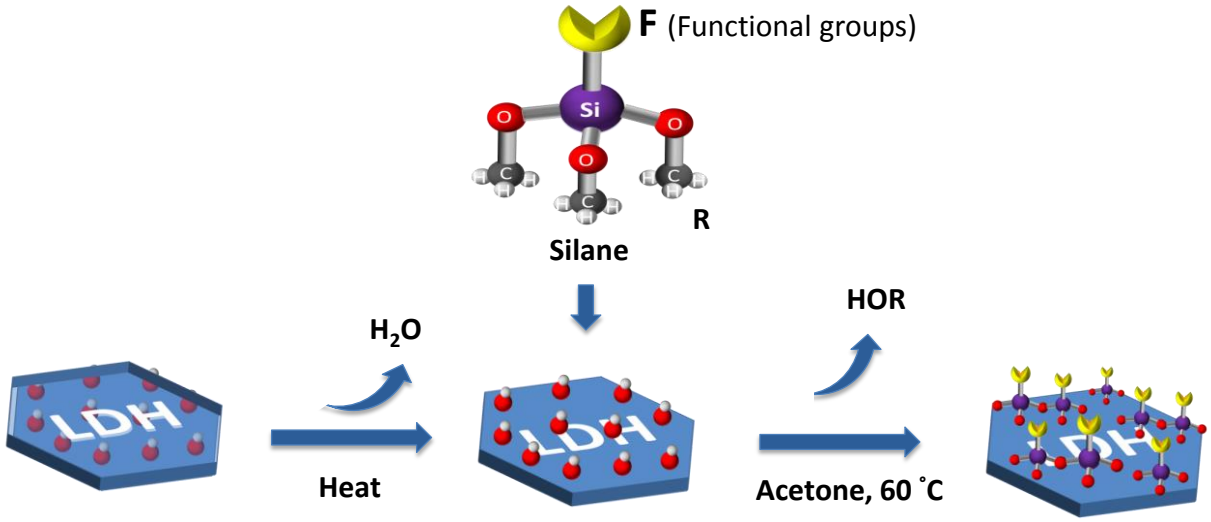


Fig. 1 Scheme of silane reactions with hydroxyl groups on LDH surface.

## Citations and References

1. C. Zhang, J. Yu, L. Xue and Y. Sun, *Materials*, 2017, 10, 78.
2. Q. Tao, H. He, T. Li, R. L. Frost, D. Zhang and Z. He, *J. Solid State Chem.*, 2014, 213, 176-181.
3. A. Y. Park, H. Kwon, A. J. Woo and S. J. Kim, *Adv. Mater.*, 2005, 17, 106-109.

# New sulfonated zirconium and titanium organophosphonates prepared by topotactic reactions

K. Melánová[1], V. Zima[1], J. Brus,[1] L. Beneš[2], J. Svoboda[2]

[1] Institute of Macromolecular Chemistry, AS CR, Heyrovsky sq. 2, 162 06 Prague 6, Czech Republic; [2] Faculty of Chemical Technology, University of Pardubice, 532 10 Pardubice, Czech Republic; klara.melanova@upce.cz, vitezslav.zima@upce.cz, jiri.brus@imc.cas.cz, ludvik.benes@upce.cz, jan.svoboda@upce.cz

**Abstract**

Compounds with a formula $M(PO_4)(H_2PO_4)_{1-x}\cdot(HO_3SC_2H_4N(CH_2PO_3H)_2)_{x/2}\cdot yH_2O$, where M = Zr or Ti, were formed by topotactic reaction of γ-zirconium or titanium hydrogen phosphate with 2-bis(phosphonomethyl)aminoethane-1-sulfonic acid. In the case of zirconium compounds, coefficient *x* depends on the amount of the acid used and on reaction time. In the case of titanium phosphonate the coefficient *x* does not depend on the amount of the acid used. Basal spacing of the prepared compound increases with increasing *x* and relative humidity. Replacement of dihydrogen phosphate with phosphonate anions was confirmed by infrared and $^{31}P$ solid NMR spectroscopies. The electrical conductivity of the prepared materials and their ability to intercalate basic molecules was also studied.

Key words: γ-zirconium hydrogen phosphate; topotactic reaction; solid state NMR; phosphonate

The structure of gamma modification of zirconium or titanium hydrogen phosphate (**γ-ZrP, γ-TiP)** consists of a rigid framework of $ZrO_8$ octahedra joined to each other with tetradentate $PO_4$ groups inside and $H_2PO_4$ groups outside these planes.[1,2] The interlayer $H_2PO_4$ can be replaced by anions of mono- or diphosphonic acids forming a layered inorganic-organic hybrids with a general formula $ZrPO_4(O_2PRR')$, where R and R´ can be H, OH or organic group.[3] Recently, zirconium R-amino-N,N´-bis(alkylphosphonates) were prepared by reaction of $ZrOCl_2$ with corresponding acid in the presence of HF.[4]

In this contribution, new phosphonates were prepared by a reaction of gamma-modification of zirconium or titanium hydrogen phosphate with 2-bis(phosphonomethyl)-aminoethane-1-sulfonic acid (**$H_4$TDP**).

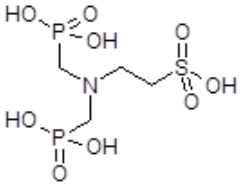

**$H_4$TDP**

In the case of **γ-ZrP** the topotactic reactions were done by refluxing the **γ-ZrP** host in an acetone-water solution of **$H_4$TDP**; **γ-ZrP** delaminates under reflux[3] and subsequently reacts with **$H_4$TDP**. The phosphonate content depends on the amount of the acid used (see Table 1). The basal spacing of the phosphonates prepared increases

with increasing *x*. On the other hand, **γ-TiP** does not delaminate under reflux; the anion exchange was therefore done by hydrothermal treatment. The phosphonate content is nearly the same in the **Ti-B** to **Ti-D** products regardless the amount of the acid used and also the basal spacing of all three compounds differs only slightly.

Table 1. The denotation, formulas and basal spacing of the samples prepared together with the amount of $H_4TDP$ used for synthesis

| Sample | Formula | $n_{H4TDP}$ [mmol] | Basal spacing [Å] |
|---|---|---|---|
| **γ-ZrP** | $Zr(PO_4)(H_2PO_4)\cdot yH_2O$ | 0 | 12.26 |
| **Zr-A** | $Zr(PO_4)(H_2PO_4)_{0.70}(H_2TDP)_{0.15}\cdot 2H_2O$ | 0.5 | 13.34 |
| **Zr-B** | $Zr(PO_4)(H_2PO_4)_{0.32}(H_2TDP)_{0.34}\cdot 2H_2O$ | 1.0 | 15.42 |
| **Zr-C** | $Zr(PO_4)(H_2PO_4)_{0.10}(H_2TDP)_{0.45}\cdot 1.5H_2O$ | 2.0 | 17.12 |
| **γ-TiP** | $Ti(PO_4)(H_2PO_4)\cdot 2H_2O$ | 0 | 11.59 |
| **Ti-A** | - | 0.52 | 16.29 + 11.59 |
| **Ti-B** | $Ti(PO_4)(H_2PO_4)_{0.20}(H_2TDP)_{0.40}\cdot 1.3H_2O$ | 1.03 | 16.05 |
| **Ti-C** | $Ti(PO_4)(H_2PO_4)_{0.16}(H_2TDP)_{0.42}\cdot 1.5H_2O$ | 1.55 | 15.80 |
| **Ti-D** | $Ti(PO_4)(H_2PO_4)_{0.18}(H_2TDP)_{0.41}\cdot 1.5H_2O$ | 2.06 | 16.21 |

In the IR spectra of **Zr-A, Zr-B** and **Zr-C**, bands at 504, 1406, 1458, 2860 and 2962 $cm^{-1}$ appear corresponding to rocking $CH_2$ vibration, symmetric and asymmetric $CH_2$ deformation vibrations and symmetric and asymmetric stretching C-H vibrations. Intensity of these bands increases with increasing number of $H_2TDP^{2-}$ anions present in the compound. The intensity of the band at about 1240 $cm^{-1}$, which corresponds to δ(P-OH) vibration,[5] is significantly lower than that in the spectrum of pure **γ-ZrP**.

$^{31}P$ MAS NMR and $^{31}P$-$^{31}P$ SQ/DQ MAS NMR spectra also confirm the gradual replacement of dihydrogen phosphate with phosphonate anions in the samples **Zr-A** to **Zr-C.**

All compounds prepared show ionic conductivity. Their conductivity decreases with increasing *x*, but compounds **Zr-A** and **Zr-B** are more conductive than parent **γ-ZrP.**

All compounds are able to intercalate butylamine. The basal spacing of these intercalates is larger than that of the corresponding host, but they are not stable and decompose during washing.

This work was supported by the Czech Science Foundation (grant number 17-10639S).

## References

1. D. M. Poojary, B. L. Zhang, Y. P. Dong, G. Z. Peng, A. Clearfield, J. Phys. Chem. 981 *(1994)* 13616-13620.
2. A. N. Christensen, E. K. Andersen, I. G. K. Andersen, G. Alberti, M. Nielsen, M. S. Lehman, Acta Chem. Scand. 44 (1990) 865-872.
3. R. Vivani, F. Costantino, M. Taddei, in *Metal Phosphonate Chemistry: From Synthesis to Applications,* A. Clearfield, K. Demadis, Eds. (RSC Publishing, Cambridge 2012), pp. 45-86.
4. R. Vivani, F. Costantino, M. Taddei, in *Metal Phosphonate Chemistry: From Synthesis to Applications,* A. Clearfield, K. Demadis, Eds. (RSC Publishing, Cambridge 2012), pp. 67-75.
5. P. L. Stanghellini, E. Boccaleri, E. Diana, G. Alberti, R. Vivani, Inorg. Chem., 43 (2004) 5698-5703.

# Molecular simulations of the crystal structure of zirconium sulfophenylphosphonates intercalated with derivates of 4-4'-dipyridylamine

L. Beneš[1], J. Svoboda[1], K. Melánová[2], V. Zima[2], P. Kovář[3], M. Pospíšil[3]

[1] Faculty of Chemical Technology, University of Pardubice, 532 10 Pardubice, Czech Republic; [2] Institute of Macromolecular Chemistry, AS CR, Heyrovsky sq. 2, 162 06 Prague 6, Czech Republic; [3] Charles University, Faculty of Mathematics and Physics, Ke Karlovu 3, 121 16 Prague 2, Czech Republic; ludvik.benes@upce.cz, jan.svoboda@upce.cz, klara.melanova@upce.cz, vitezslav.zima@upce.cz, kovar@karlov.mff.cuni.cz, pospisil@karlov.mff.cuni.cz,

**Abstract**

Three push-pull molecules based on aminopyridine, N-(pyridin-4-yl)pyridin-4-amine (**A**) and its derivatives 3-methyl-N-(pyridin-4-yl)pyridin-4-amine (**B)** and 3-nitro-N-(pyridin-4-yl)pyridin-4-amine (**C**), were intercalated into zirconium 4-sulfophenylphosphonate (**ZrSPhP**). The intercalates prepared were characterized by elemental and thermo-gravimetric analyses, powder X-ray diffraction, and IR and UV-vis spectrosopies. Classical molecular simulation methods were used for a description of an arrangement of intercalated guest molecules within a layered structure of the host.
Key words: zirconium sulfofphenylphosphonate; intercalation; molecular modeling

Materials having nonlinear optical properties are of great interest for optical signal processing.[1] Among them, an important position belongs to organic push-pull molecules containing donor and acceptor groups - push-pull chromophores. Optical properties of these chromophores can be improved by their incorporation into a rigid environment, e.g. in an interlayer space of a layered compound (a host). Recently, we have succeeded in intercalation of several push-pull molecules based on aminopyridine into this zirconium sulfophenylphosphonate.[2] One of them is N-(pyridin-4-yl)pyridin-4-amine (**A**), see Scheme 1. We found that the second order susceptibility as a measure of the nonlinear optical property increases from 1.56 to 1.89 pm/V, when **A** is incorporated in **ZrSPhP**.[2]

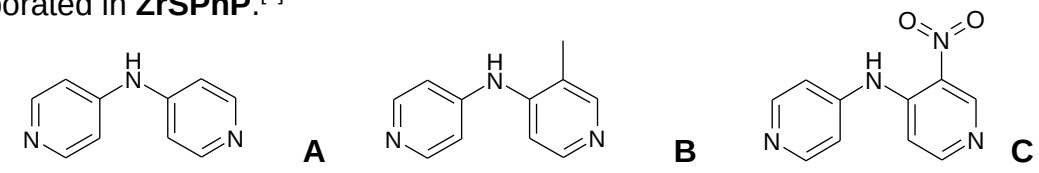


Scheme 1. Optically active molecules intercalated into **ZrSPhP**

All three guests were intercalated into **ZrSPhP** by treatment of the host with an ethanolic solution of corresponding guest at room (**A**) or elevated temperature (**B**, **C**). As follows from elemental and thermogravimetric analyses, all three intercalates contain 0.5

guest molecule per formula unit and interlayer water (1.5 $H_2O$ per formula unit for **ZrSPhP-A** and 0.7$H_2O$ for **ZrSPhP-B** and **ZrSPhP-C**).

The IR spectra of all three intercalates in the region from 1800 to 600 $cm^{-1}$ represent a superposition of the peaks found in the host and guest molecules. In the region of the pyridine ring stretching vibrations, bands corresponding to protonated pyridine appeared, indicating that the guest molecules are at least partially protonated in the intercalates.

As follows from UV-vis spectra of **ZrSPhP-A** and **ZrSPhP-B**, the absorption maxima are shifted to the higher wavelength in comparison with pure guests and the values of these maxima are close to that obtained for **A** and **B** protonated by exposition of this compound to HCl vapors. The UV-vis spectrum of **ZrSPhP-C** is more complicated and values of its maxima are more similar to unprotonated **C**.

Materials Studio modelling environment was used for the molecular calculations.[3] The initial model of **ZrSPhP** was used based on the results of our previously performed geometry optimization which were published by Škoda et al.[4] The calculation shows that most of the guest molecules are positioned in parallel orientation but some guests can also adopt a tilted orientation with respect to the host layers. The water molecules present in the interlayer space are not located among the sulfo groups as it was in the case of parent **ZrSPhP**[4] but are shifted towards the middle of the interlayer space. The water and the guest molecules create a net of hydrogen bonds (see Figure 1).

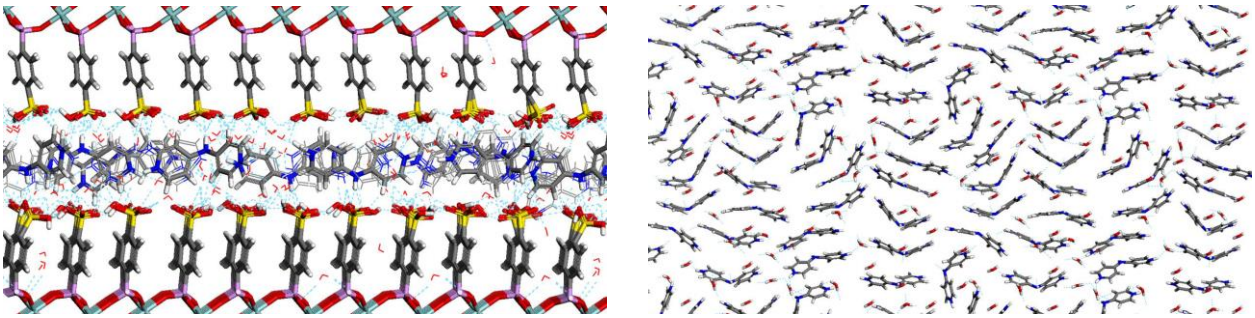

Figure 1. Side view (left) and top view (right) of the **ZrSPhP-A** structure

This work was supported by the Czech Science Foundation (grant number 17-10639S).

## References

1. P. N. Prasad and D. J. Williams, Introduction to Nonlinear Optical Effects in Molecules and Polymers, Wiley, New York, 1991.
2. F. Bureš, D. Cvejn, K. Melánová, L. Beneš, J. Svoboda, V. Zima, O. Pytela, T. Mikysek, Z. Růžičková, I. V. Kityk, A. Wojciechowski and N. AlZayed, J. Mater. Chem. C, 2016, 4, 468-478.
3. Materials Studio Modeling Environment, Release 4.3 Documentation, Accelrys Software Inc., San Diego, CA, 2003.
4. J. Škoda, M. Pospíšil, P. Kovář, K. Melánová, J. Svoboda, L. Beneš and V. Zima, J. Mol. Model. 2018, 24, 10.

# CATALYCTIC COMBUSTION OF ACETONITRILE OVER COPPER-BASED CATALYSTS

**JÉSSICA A. P. PONCIANO, MARCELO S. BATISTA***

Chemical Engineering Departament, Federal University of São João Del Rei, Campus Alto Paraopeba, Minas Gerais, Brazil, CEP 36420-000. *e-mail: marcelobatista@ufsj.edu.br

## ABSTRACT

Cu-ZSM-5, $La_2CuO_4$ and CuO catalysts were prepared, characterized by XRD and $H_2$-TPR and investigated for the selective catalytic combustion of acetonitrile ($CH_3CN$-SCC). The XRD patterns of the catalysts confirmed the CuO, MFI and $La_2CuO_4$ crystalline structures. $CH_3CN$ conversion rises rapidly with temperature and copper species are the active sites. Cu-ZSM-5 catalyst was more active than CuO and $La_2CuO_4$ catalysts showing that copper species in zeolite were more actives for the $CH_3CN$-SCC reaction. These results showed that the zeolite-based catalyst was quite advantageous for the $CH_3CN$-SCC.

**Keywords:** acetonitrile, combustion, catalyst, copper.

## INTRODUCTION

Acetonitrile ($CH_3CN$) is a gas present in the industrial exhaust plant in the production of acrylonitrile and has a high risk, because it can easily decompose into HCN. This pollutant in the gas phase is able to affect human beings and even be lethal at ppm levels in air. Their effective removals by either incineration or catalytic combustion thus become necessary in order to control the air quality of our surviving environments. However, the extremely high temperature (>850°C) for combustion readily leading to the NOx (NO, $NO_2$) formation and the requirement of additional fuel consumption made this approach rather unattractive [1]. On the other hand, selective catalytic combustion ($CH_3CN$-SCC) uses much lower temperature and is the most efficient route and suitable to transformation of gaseous acetonitrile. The literature reports some studies on the performed of catalysts prepared via impregnation for the acrylonitrile-SCC and rare works related to $CH_3CN$-SCC [2]. In addition, the combustion of acetonitrile follows different routes depending on the catalyst structure [3]. In this study, Cu-ZSM-5, $La_2CuO_4$ and CuO catalysts were investigated for $CH_3CN$-SCC.

## MATERIALS AND METHODS

Cu-ZSM-5 catalyst was prepared by ion-exchange methods using commercial NH4-ZSM-5 (Si/Al=12) and, then calcined at 650°C for 2 h. CuO catalyst was prepared by calcination of cupric nitrate at 650°C. $La_2CuO_4$ catalyst was prepared by the Citrate method. Copper and lanthanum nitrates in the stoichiometric quantity were dissolved in water; then citric acid and ethylene glycol were added in equimolar amounts. The mixture was stirred and the excess water was evaporated at 80°C. The resin-like material was formed after dried at 110°C overnight. The material was deagglomerated and calcined at 550°C for 3 h and 800°C for 5 h (heating rate 5°C $min^{-1}$) in static air.

All catalysts were characterized by X-ray diffractometry (XRD) and temperature-programmed reduction by hydrogen ($H_2$-TPR). Finally, the catalytic test was performed

using U-shaped reactor, 8.6 mg of metal in the sample and flow of 50 mL/min of a mixture containing 2.8 vol.% $CH_3CN$ in synthetic air. The reactor was coupled in line to a mass spectrometer (THERMO) for gas analysis.

## RESULTS AND DISCUSSION

Fig. 1 shows the XRD analysis of all catalysts. Cu-ZSM-5 catalyst presented characteristic peaks of MFI structure (PDF 37-0359) and copper oxide (2θ = 35.5, 38.7 and 48.7°). This indicates that during ion exchange occurred precipitation of copper species. CuO catalyst showed all characteristic peaks of copper oxide (PDF 41-0254). In its turn, $La_2CuO_4$ catalyst showed peaks of the perovskite structure (PDF 70-0449) and copper oxide. This shows that part of the copper is outside the perovskite structure.

Cu-ZSM-5 presented TPR profile with two reduction peaks (Fig. 2). The peak at 238°C was assigned to partial reduction of copper exchanged ($Cu^{2+} \rightarrow Cu^{+}$) and reduction of CuO (observed by XRD) to $Cu^0$. The peak at 356°C was attributed to successive reduction of $Cu^+$ to $Cu^0$. As shown in Fig. 2, the reduction of CuO catalyst presents one reduction peaks at 296°C ($Cu^{2+} \rightarrow Cu^0$). $La_2CuO_4$ showed reduction peak at 287°C together with a shoulder at 333°C, which was assigned to reduction of $Cu^{2+}$ (present in CuO and $La_2CuO_4$) to $Cu^0$; another reduction at 401°C is due to the reduction of $Cu^+$ to $Cu^0$, which was not totally reduced in the previous step.

Fig. 3 shows the $CH_3CN$ conversions on Cu-ZSM-5, CuO and $La_2CuO_4$ catalysts as a function of reaction temperature. $CH_3CN$ conversion rises rapidly with temperature and copper species are the active sites. In this way, Cu-ZSM-5 catalyst was more active than CuO and $La_2CuO_4$ catalysts showing that copper species in ion-exchange position are more actives for the $CH_3CN$-SCC reaction.

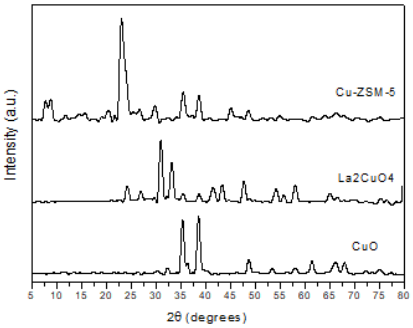


Fig. 1: XRD patterns.

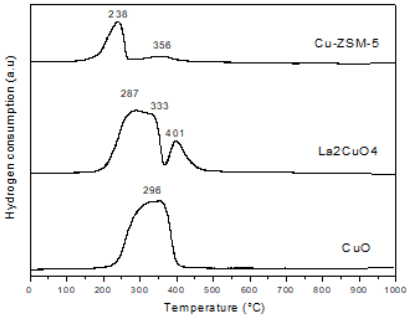


Fig. 2: $H_2$-TPR profiles.

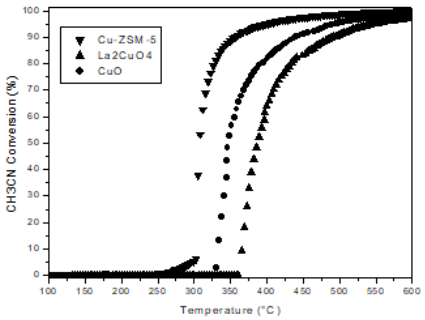


Fig. 3 – $CH_3CN$ conversion

## CONCLUSIONS

Cu-ZSM-5, CuO and $La_2CuO_4$ catalysts were investigated for the $CH_3CN$-SCC. $CH_3CN$ conversion rises rapidly with temperature and copper species are the active sites. Cu-ZSM-5 showed the highest acetonitrile conversion making it an excellent candidate to catalyse $CH_3CN$-SCC.

## REFERENCES

[1] Zhang R, Liu N, Lei Z et al. Chemical Reviews 116, p. 3658-3721, 2016.
[2] Zhang R, Shi D, Liu N et al. Applied Catal. B Environmental 146, p. 79-93, 2014.
[3] Zhang R, Shi D, Liu N et al. Catalysis Today 258, p.17-27, 2015.

# CATALYTIC COMBUSTION OF ACETONITRILE OVER (Cu, Co or Fe)-ZSM-5 CATALYSTS

**BRUNA CARLA S. SILVEIRA, MARCELO S. BATISTA***

Chemical Engineering Department, Universidade Federal de São João del Rei. Campus Alto Paraopeba, Minas Gerais, Brazil. ***e-mail: marcelobatista@ufsj.edu.br.

## ABSTRACT

(Cu, Fe, Co)-ZSM-5 catalysts were studied for the selective catalytic combustion of acetonitrile (SCC-$CH_3CN$). These catalysts prepared by ion exchange method and characterized by XRD and $H_2$-TPR. The XRD patterns showed peaks of MFI structure and also CuO and $Fe_2O_3$. The $H_2$-TPR profiles of the catalysts corroborated the XRD results. All catalysts showed that the $CH_3CN$ conversion rises rapidly with temperature. Cu-ZSM-5 showed the highest acetonitrile conversion and selectivity to $N_2$ for the $CH_3CN$-SCC.

**Keywords:** acetonitrile, combustion, zeolite, ZSM-5.

## INTRODUCTION

Acetonitrile is an organic compound predominantly emitted by biomass burning and industrial exhaust gases. Classified as a volatile organic compound (VOC), it is a hazardous chemical due to carcinogenic potential [1]. The combustion of acetonitrile requires high temperatures and leads to formation of nitrogenous compounds (NOx). On the other hand, selective catalytic combustion of acetonitrile (SCC-$CH_3CN$) for $N_2$ and $CO_2$ is an interesting alternative.

Zhang group [2] studied the $CH_3CN$-SCC over M/SBA-15 (M = Cu, Co, Fe, V, Mn, Pd, Ag, Pt) catalysts prepared via impregnation. $CH_3CN$ conversion follows a trend of Pt/ > Pd/ > Cu/ > Co/ > Fe/ > V/ > Ag/ > Mn/ > SBA-15. Moreover to the desired main product of $N_2$, harmful byproducts (NO, $NO_2$, $N_2O$, $NH_3$, and CO) were observed during this catalytic combustion. Pd and Pt are often used for oxidation reactions and are considered to be the most active catalysts for catalytic oxidation. However, $CH_3CN$ was mainly converted into NOx over Pd/ and Pt/SBA-15. Meantime, Cu/SBA-15 exhibited a nearly complete conversion of $CH_3CN$ together with $N_2$ selectivity of 80% (>350°C). It was founded that the $CH_3CN$ conversions follow a decreasing order of Cu/ > Co/ > Fe/ > V/ > Mn/SBA-15. In this work, (Cu, Co, Fe)-ZSM-5 catalysts were prepared by ion-exchange method using ZSM-5 zeolite, characterized by XRD and TPR, and evaluated for the $CH_3CN$-SCC.

## MATERIALS AND METHODS

(Cu, Co, Fe)-ZSM-5 catalysts were prepared by three consecutive ion-exchanges using ZSM-5 zeolite and aqueous solution (0.1 mol/L) of nitrates of: copper II, cobalt II and iron III. These catalysts were characterized by XRD (40 KV, 15 mA and CuKα radiation) and $H_2$-TPR (10°C/min and 30 mL/min from mixture of 2 vol. % $H_2$ in Ar). Catalytic evaluates were carried out in U-shaped quartz reactor, fed with a continuous flow of 50 mL/min of a mixture containing 2.8 vol. % $CH_3CN$ in synthetic air.

## RESULTS AND DISCUSSION

The XRD patterns of the catalysts showed characteristics peaks of ZSM-5 zeolite (PDF 37-0359), CuO (PDF 41-0254) and $Fe_2O_3$ (PDF 01-1053) crystalline structures (Fig. 1). This indicates that during ion exchange occurred precipitation of copper and iron species. $H_2$-TPR profiles of Fe-ZSM-5 showed three reduction peaks (Fig. 2). The peak at 359°C was attributed to the reduction of $Fe_2O_3$ to $Fe_3O_4$ and the peak at 770°C correponds to the reduction of $Fe_3O_4$ to $Fe^0$. The peak at 486°C was assigned to partial reduction of iron exchanged in ZSM-5 ($Fe^{3+}$ to $Fe^{2+}$). In Cu-ZSM-5 the peak at 238°C was assigned to partial reduction of copper exchanged ($Cu^{2+} \rightarrow Cu^{+}$) and reduction of CuO (observed by XRD) to $Cu^0$. The peak at 356°C was attributed to successive reduction of $Cu^+$ to $Cu^0$. The absence of peaks in Co-ZSM-5 comfirmed the absence of cobalt oxide on the surface of the catalyst and presence of cobalt species exchanged in the zeolite. These results are also consistent with the XRD measurement. Most Co species exist in the form of $Co^{2+}$ at the ion exchange sites and the further reduction of $Co^{2+}$ into $Co^0$ occurred above 1000°C [3].

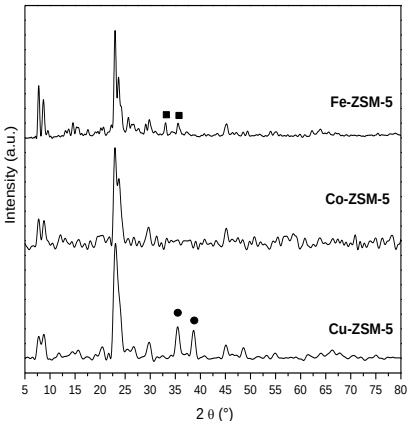


Fig. 1: XRD patterns.

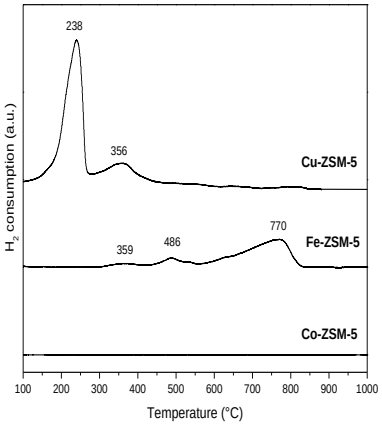


Fig. 2: $H_2$-TPR profile

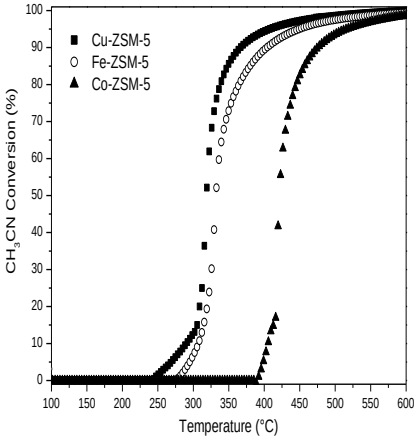


Fig 3.: $CH_3CN$ conversion

Fig. 3 shows the $CH_3CN$ conversions on (Fe, Co, Cu)-ZSM-5 catalysts as a function of reaction temperature. All catalysts showed that the $CH_3CN$ initial conversion rises rapidly upon the temperature and almost kept stable at temperature range of 500–600°C. Cu-ZSM-5 catalyst was more active than Co-ZSM-5 and Fe-ZSM-5 catalysts, showing that copper species are more actives for the $CH_3CN$-SCC reaction. Cu-ZSM-5 showed also the highest selectivity to $N_2$.

## CONCLUSIONS

(Fe, Co, Cu)-ZSM-5 catalysts were investigated for the $CH_3CN$-SCC. The XRD patterns showed peaks of MFI structure and also CuO and $Fe_2O_3$. All catalysts showed that the $CH_3CN$ conversion rises rapidly with temperature. Cu-ZSM-5 showed the highest acetonitrile conversion and selectivity to $N_2$ for the $CH_3CN$-SCC.

## REFERENCES

[1] Zhang R, Liu N, Lei Z et al. Chemical Reviews 116, p. 3658-3721, 2016.
[2] Zhang R, Shi D, Liu N et al. Applied Catal. B Environmental 146, p. 79-93, 2014.
[3] Biturini N, Santos A, Batista M S. Reac Kinet Mech Cat 126, p. 341-352, 2019.

# DECOMPOSITION OF $N_2O$ OVER (Co, Fe)-BETA CATALYSTS - INFLUENCE OF CO-FED GASES

**BRUNA CARLA S. SILVEIRA, NAYARA F. BITURINI, MARCELO S. BATISTA***

Chemical Engineering Department, Federal University of São João Del Rei, Campus Alto Paraopeba, Minas Gerais, Brazil. *e-mail: marcelobatista@ufsj.edu.br

## ABSTRACT

Co-BETA and Fe-BETA catalysts were prepared by ion exchange and characterized by XRD and $H_2$-TPR. The influence of co-fed gases ($O_2$, $CO_2$, $CH_4$, and $H_2O$) on the $N_2O$ decomposition over (Co or Fe)-BETA catalysts was investigated. The results showed that $Co^{2+}$ and $Fe^{3+}$ exchanged were observed in Co-BETA and Fe-BETA catalysts, respectively. In addition, $Fe_2O_3$ particles were found on surface of the Fe-BETA catalysts. Co-BETA was more actives than Fe-BETA for the direct decomposition of $N_2O$. Conversion of $N_2O$ over Fe-BETA was remained stable when co-fed $O_2$, $CO_2$, and $CH_4$, but decreases slightly with $H_2O$. On the other hand, Co-BETA was very stable when co-fed $O_2$, $CO_2$, $CH_4$, and especially $H_2O$.

**Keywords:** $N_2O$ decomposition, co-fed gases, catalyst, BETA zeolite.

## INTRODUCTION

Nitrous oxide ($N_2O$) is a potent greenhouse-effect gas. Recent progress in the $N_2O$ decomposition reaction (de-$N_2O$) has been studied with the focus on transition-metal (Cu, Fe, Co)-modified zeolite catalysts. Efforts dedicated to Cu-ZSM-5 have shown that de-$N_2O$ is inhibited by $O_2$ or $H_2O$ co-fed [1]. On the other hand, Fe-zeolite catalysts have been outstanding due to their high activity and resistance in co-fed of $CH_4$, CO, $O_2$ and $SO_2$ [2]. Furthermore, it is also notable that Co-sites were more active than Fe-sites for the direct de-$N_2O$. Therefore, the objective of this work was to study the influence of co-fed $O_2$, $CO_2$, $H_2O$ and $CH_4$ on the de-$N_2O$ over (Co or Fe)-BETA catalysts.

## MATERIALS AND METHODS

Co-BETA and Fe-BETA catalysts were prepared by ion-exchange methods using $NH_4$-BETA (TRICAT, Si/Al=12) zeolite. These catalysts were characterized by XRD (40 KV, 15 mA and CuKα radiation) and $H_2$-TPR (10°C/min and 30 mL/min from mixture of 2 vol.% $H_2$ in Ar). In the catalytic tests of de-$N_2O$, 50 mL/min of 10 vol.% $N_2O$ in He was flowed continuously over 50 mg of sample. The effect of co-fed gases was studied by adding 10 vol.% $O_2$, 10 vol.% $CO_2$, 10 vol.% $CH_4$ and 10 vol.% $H_2O$ vapor.

## RESULTS AND DISCUSSION

Fig. 1 shows that the BEA crystalline structure (PDF 48-0074) was well preserved even after exchange with Fe or Co ions. Fe-BETA catalyst shows slight reductions in the peak intensities due to the higher X-ray absorption coefficient of Fe compounds. Fe-BETA shows also characteristics peaks of $Fe_2O_3$ (■) (PDF 01-1053). The absence of $Co_3O_4$ peaks in Co-BETA diffractogram indicates the presence of Co-exchanged species in the zeolite structure.

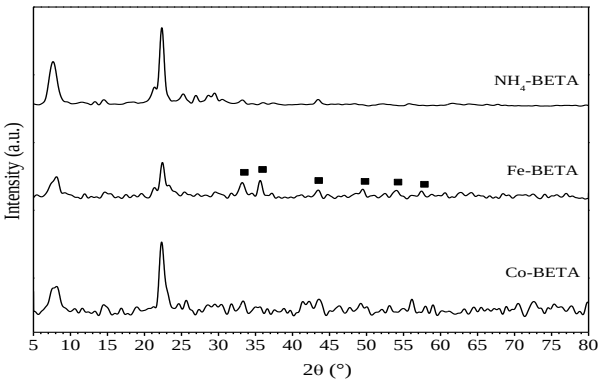


Fig. 1: XRD of BETA and (Co, Fe)-BETA catalysts.

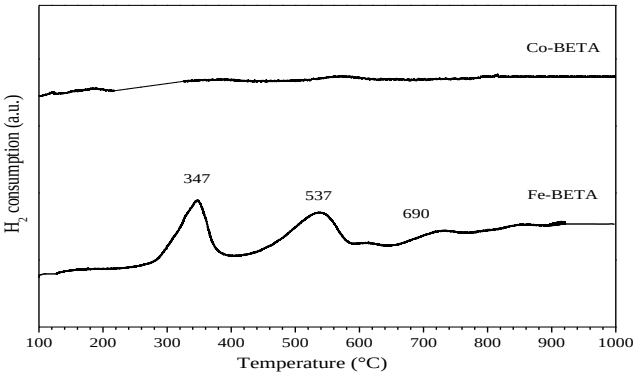


Fig. 2: $H_2$-TPR profiles of (Co, Fe)-BETA catalysts.

No reduction peaks was observed in TPR profiles of Co-BETA, confirming the absence of cobalt oxides (Fig. 2). The further reduction of $Co^{2+}$ exchanged into $Co^0$ occurred above 1000°C. The first two peaks (347 and 537°C) of Fe-BETA were mainly assigned to reduction of $Fe^{3+}$ exchanged to $Fe^{2+}$. A slight shoulder at 690°C was attributed to the reduction of FeO to $Fe^0$, confirming $Fe_2O_3$ on surface. Further reduction of $Fe^{2+}$ exchanged into $Fe^0$ occurred above 1000°C and causes the collapse of the zeolite structure [3]. $N_2O$ conversion rises very rapidly with the temperature on Co-BETA, but much more smoothly on Fe-BETA (Fig. 3). Co-BETA was more active than Fe-BETA. The conversion of $N_2O$ over Fe-BETA practically remained stable in the presence of $O_2$, $CO_2$, and $CH_4$ (Fig. 4). The decreases slightly (~ 6%) in the presence of $H_2O$ was associated with the hydroxylation of the active iron sites. The $N_2O$ conversion over Co-BETA was maintained after the introduction of all gases ($O_2$, $CO_2$, $CH_4$ and $H_2O$). These results indicated that cobalt sites were more resistant to hydroxylation than the iron sites exchanged in BETA.

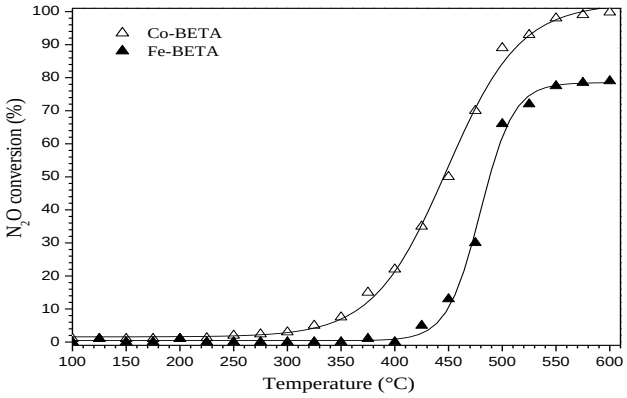


Fig. 3: De-$N_2O$ over (Co, Fe)-BETA catalysts.

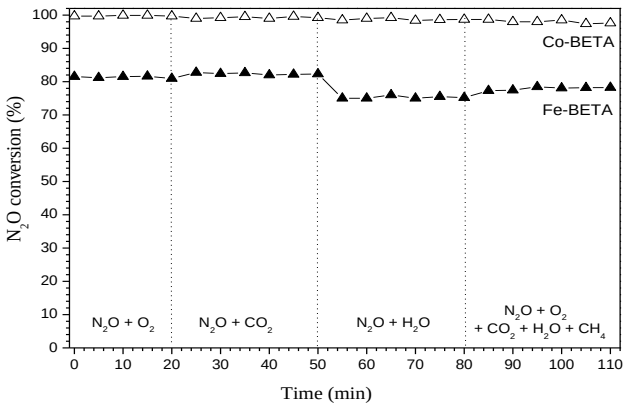


Fig. 4: Effect of co-fed gases on the $N_2O$ conversion.

## CONCLUSIONS

$Co^{2+}$ and $Fe^{3+}$ exchanged were observed in Co-BETA and Fe-BETA catalysts, respectively. In addition, $Fe_2O_3$ particles were found on Fe-BETA catalysts. Co-BETA was more actives than Fe-BETA for the direct de-$N_2O$. Conversion of $N_2O$ over Fe-BETA was stable when co-fed $O_2$, $CO_2$, and $CH_4$, but decreases with $H_2O$. However, Co-BETA was very stable when co-fed $O_2$, $CO_2$, $CH_4$, and especially $H_2O$.

## REFERENCES

[1] Meng T, Ren N, Ma Z (2015) Journal of Molecular Catalysis A: Chemical 404:233-9.
[2] Debbagh MN, Lecea CSM, Pérez-Ramírez J (2007) Applied Catalysis B: Environmental 70:335-341.
[3] Feng XD, Hall WK (1997) Journal of Catalysis 166:368-376.

# SYNTHESIS OF HALLOYSITE-LIKE NANOTUBES FROM CLAY MINERALS PRESENT IN IRON ORE TAILINGS

**MANOEL VÍTOR BOREL GONÇALVES[1], ANTÔNIO VALADÃO CARDOSO[2], FABRÍCIO VILELA PARREIRA[3]**

[1]REDEMAT, Universidade Federal de Ouro Preto, Praça Tiradentes, 20, Centro, Ouro Preto/MG, 35400-000, Brazil. e-mail: m.vitorbg@gmail.com

[2]Escola de Design - Universidade do Estado de Minas Gerais, Av. Antônio Carlos, 7545, São Luiz, Belo Horizonte/MG, 31270-010, Brazil. e-mail: antonio.cardoso@uemg.br

[3]Centro de Tecnologia de Ferrosos/Vale S.A., Av. Dr. Marco Paulo Simon Jardim, 3580, Bairro Mina de Águas Claras, Nova Lima/MG, 34006-270, Brazil. e-mail: fabricio.parreira@vale.com

## ABSTRACT

The major aim of this work was to evaluate a methodology of segregation of kaolinite present in iron ore tailings (IOT) and using it in the synthesis of halloysite nanotubes (HNT). The segregation of kaolinite was performed by acid leaching of the IOT. Samples of high purity kaolinite and halloysite were used as reference materials. Three steps were strictly controlled for efficacy of the synthetic procedure: (i)pre-intercalation of the clay mineral using dimethyl sulfoxide (DMSO); (ii)obtaining the methoxy-modified kaolinite; (iii)intercalation of the methoxy kaolinite with suitable organic molecules. Cetyltrimethylammonium chloride (CTMACl) and cetyltrimethylammonium bromide (CTAB) were used when adopting the one-step method. Hexylamine (C6N) was used for the two-step procedure. X-ray diffraction results showed that the reference sample and the product obtained from the IOT were composed essentially of kaolinite. The pre-intercalation procedures showed very promising to intervene in the kaolinite structure, where the $d_{001}$ value increased from 7.09Å to 11.40Å, with no evidence of loss of crystallinity. The results of Mössbauer spectroscopy of kaolin indicated the occurrence of $Fe^{2+}$ and structural $Fe^{3+}$ in kaolinite. Apparently the contamination of $Fe^{3+}$ ions did not interfere in the synthetic process. SEM images indicated the morphological transformation of plate-like kaolinite for kaolinite nanotubes with halloysite-like structure.
*Keywords: iron ore tailings, kaolinite, intercalation, nanotubes*

## INTRODUCTION

HNT is a natural clay mineral exhibiting a 1:1 layered structure of the kaolin group. Although kaolinite occurs naturally in the plate form, it has been shown to be susceptible to transformation into nanotubes by means of intercalation/deintercalation methods. The 1:1 kaolinite layers curls to compensate the lateral misfit between the tetrahedral and octahedral sheets when the hydrogen bonds between the layers are sufficiently weakened. The layer delamination and curl procedure can be performed in one-step, where intercalation and swelling occur at the same time, or two-steps, where intercalation and swelling occur separately.

Thus, the objective of this study is to segregate kaolinite from the other mineral components present in the IOT, to use it as a raw material for the synthesis of halloysite-like nanotubes and to compare its performance with high purity products.

## EXPERIMENTAL PROCEDURE

In order to segregate the kaolinite from the IOT, acid leaching was performed using hydrochloric acid solution and distilled water at 120ºC for 2h.

To prepare DMSO-intercalated kaolinite (kaolinite-DMSO), 10g of kaolinite (high purity and IOT secreted) was added into a mixture of 60mL DMSO and 10mL distilled water, stirred and refluxed at 150ºC for 7h. The solid in the mixture was separated by centrifugation and washed three times using 1,4-dioxane and isopropanol. The product was dried at 60ºC for 24h.

To prepare methoxi-modified kaolinite (kaolinite-MeOH), 5g of kaolinite-DMSO was added into 100mL of methanol (MeOH) and stirred for 7 days, at room temperature. The solid in the mixture was separated by centrifugation and used while wet for the synthesis process.

To prepare halloysite-like nanotubes in one-step route, approximately 1g of kaolinite-MeOH wet was added into a 40ml MeOH solution of CTMACl 1M and 40ml MeOH solution of CTAB 1M and both stirred at 80ºC for 24 h. The solid in the mixture was separated by centrifugation, washed six times with ethanol and then dried at room temperature. To prepare halloysite-like nanotubes in two-step route, approximately 0,5g of kaolinite-MeOH wet was added into 15ml of C6N. The intercalation compounds where redispersed in 1,4-dioxane (20ml) and sonicated for 10 min for the swelling. The process was repeated three times.

## RESULTS

The product obtained presented major kaolinite composition, with typical basal reflection of 7.09Å, equal to that measured for the high purity reference product. Kaolinite-DMSO presented a typical diffraction pattern with the $d_{001}$ value for kaolinite-DMSO environment and kaolinite-DMSO reflux is 11.40Å. SEM image of the plate-like kaolinite particles have a typical pseudo-hexagonal morphology. SEM images of kaolinite intercalated with CTAB, CTMACl and C6N showed the presence of nanotubes. There was effective formation of the methoxy-modified kaolinite, since the intercalating molecules inhabited the interlayer region, resulting in the delamination and curl of the kaolinite layers and the formation of halloysite-like nanotubes.

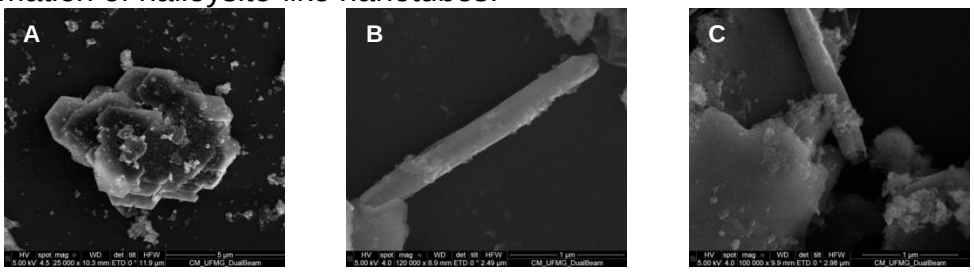


Fig 1: SEM images of kaolinite obtained from IOT (A) and halloysite-like nanotubes synthetized using this raw material (B,C).

## CONCLUSIONS

The morphological transformation of kaolinite plates to nanotubes can be achieved by the one or two step method of intercalating the methoxy-modified kaolinite. The method of kaolinite segregation from the IOT proved to be efficient, providing a product with high purity and crystallinity. As these are two basic prerequisites for the feasibility of clay as a raw material for this synthesis, it can be stated that it will be possible to synthesize nanotubes with high added value with the kaolinite obtained from the IOT.

# NANOHYBRID FILMS OF ALGINATE AND LAYERED DOUBLE HYDROXIDE INTERCALATED WITH 1-NAPHTHALENEACETIC ACID: HORMONE DELIVERY CARRIER FOR PLANT GROWTH

**CASTRO V.A.[1], DUARTE V.G.O.[1], NOBRE D.A.C.[1], SILVA G.H.[1], CONSTANTINO V.R.L.[2], PINTO F.G.[1], MACEDO W.R.[1] and TRONTO J.[1]**

[1] Federal University of Viçosa - Rio Paranaíba Campus. MG-230 Highway. Km 7. Rio Paranaíba - MG. Brazil. CEP: 38810-000. E-mail: vanderalencar.castro@ufv.br
[2] Department of Fundamental Chemistry. Institute of Chemistry. University of São Paulo, Professor Lineu Prestes Avenue. 748. São Paulo - SP. Brazil. CEP: 05508-000.

## ABSTRACT

Auxins are an important class of plant hormones responsible for the physiological development of plants[1]. The use of auxins in agriculture has been highlighted due their advantages such as the longer action and stability of the active agents, minimization of the effects of biotic and abiotic stresses, etc. The production of nanohybrid films, derived from the interaction between alginate biopolymer and layered double hydroxides (LDHs) intercalated with auxins, presented an alternative to improve the effectiveness of compounds as plant growth hormone. The goals of this work were: (*i*) synthesis of nanohybrid films of sodium alginate polymer and LDH intercalated with 1-naphthaleneacetic acid (abbreviated $Zn_2Al$-NAA-LDH); (*ii*) application of these films as a coating on beans seeds (*Phaseolus vulgaris* L.); (*iii*) investigation of the regulation of plant growth promoted by these treatments. The $Zn_2Al$-NAA-LDH was synthetized by a coprecipitation method at a constant pH[2,3]. The synthesized LDH was characterized by X ray diffraction (XRD), vibrational spectroscopy (FTIR-ATR), thermogravimetric analysis coupled to mass spectrometry (TGA-DSC-MS), among other techniques. The bean seeds coated with films of alginate containing $Zn_2Al$-NAA-LDH were evaluated in bioassays performed in greenhouse (pots filled with substrate) and laboratory (sand trays). The greenhouse bioassay showed that seeds coated with films were efficient to improve root fresh matter, whereas the laboratory bioassay indicated that seeds coated with films presented significant effects on bean root length. Hence the nanohybrid film improves the plant physiological development, to be efficient in growing plants.

***Keywords:*** layered double hydroxides, auxins, 1-naphthaleneacetic acid, nanohybrid films.

## INTRODUCTION

Auxins, plant hormones, have functions in the regulation of physiological processes, from embryogenesis to the formation of new organs. The main auxins that promote plant growth are 1-naphthaleneacetic acid (NAA), indolyl-3-acetic acid (IAA), and indolyl-3-butyric acid (IBA). Currently, the application of these auxins in agriculture has been highlighted, due to the advantages they provide, such as the longer action and stability of the active agents, minimizing the effects of biotic and abiotic stresses. An interesting alternative to improve the effectiveness of auxins as plant growth hormone, providing a physical and chemical protection of these compounds, it is the preparation of nanohybrid films of alginate biopolymer with Layered Double Hydroxides (LDHs) intercalated with auxins.

In this sense, the goals of this work were: (*i*) synthesis of nanohybrid films derived from the interaction between sodium alginate polymer and zinc-aluminium LDH intercalated with 1-naphthaleneacetic acid ($Zn_2Al$-NAA-LDH); (*ii*) application of these films as a coating on beans seeds (*Phaseolus vulgaris* L.); (*iii*) investigation of the growth of these plants by bioassays.

## EXPERIMENTAL

The $Zn_2Al$-NAA-LDH was synthetized by coprecipitation method at constant pH value (9.5 ± 0.5). This material was characterized by a set of analytical techniques: XRD, FTIR-ATR, TGA-DSC-MS, specific surface area and and scanning electron microscopy (SEM). Bean seeds were coated with different types of films, all of them produced from aqueous sodium alginate solutions (Table 1). The seeds were immersed in the alginate systems and then in a $Ca(NO_3)_2$ solution for the formation of the films on their surfaces.

**Table 1:** Composition of films

| Film | $V_{H2O}$ (L) | Alginate (mg) | [$Zn_2Al$-$CO_3$-LDH] (mg/L) | [NAA] (mg/L) | [$Zn_2Al$-NAA-LDH] (mg/L) |
|---|---|---|---|---|---|
| *M1* | 0.025 | 500 | -- | -- | -- |
| *M2* | 0.025 | 500 | $1.0x10^{-3}$ | -- | -- |
| *M3* | 0.025 | 500 | -- | $1.0x10^{-3}$ | -- |
| *M4* | 0.025 | 500 | -- | -- | $2.7x10^{-3}$ |

## RESULTS

The $Zn_2Al$-NAA-LDH presented a basal spacing of 19.2 Å, a *d* value reported in the literature for NAA intercalated in LDH [2]. ATR-FTIR spectrum presented bands related to the presence of NAA in the material: The band at 1750 $cm^{-1}$ is attributed to axial stretching of carbonyl (C=O) and the band at 1550 $cm^{-1}$ is assigned to the C=C bond of aromatic ring.

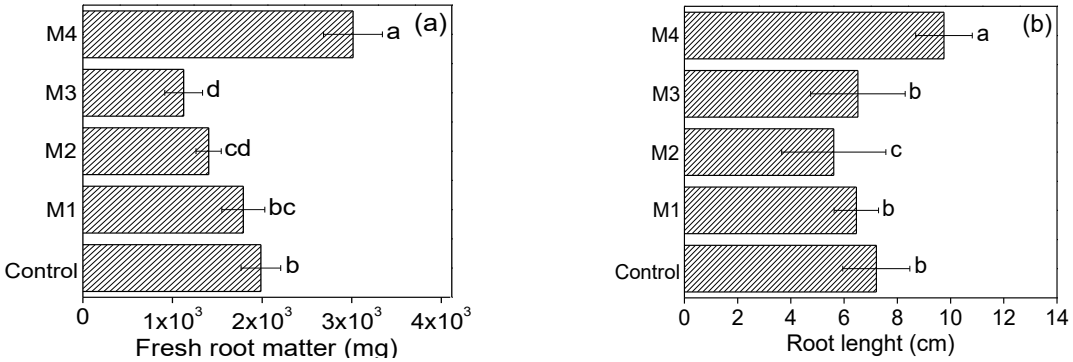


**Figure 1:** Values of (a) fresh root matter performed in greenhouse (pots filled with substrate) and (b) root length performed in laboratory (sand trays).

The bioassay results presented in Fig. 1 show that the seeds coated with the *M4* film ($Zn_2Al$-NAA-LDH) have superior performance compared to the other films for the analyzed parameters, *i.e.* moist root matter and root length.

## CONCLUSIONS

The preparation of the nanohybrid films and the seeds coating process were effective. The seeds coated with films of $Zn_2Al$-NAA-LDH (*M4*), presented higher values of moist root matter and root length, which suggests the slow release of NAA. Furthermore, a low phytotoxic effect of dosage was shown in the seed coated with *M3* film. The results showed that nanohybrid films can be used as carriers of plant hormones.

### REFERENCES

[1]. Perrot-Rechenmann, C. Cellular responses to auxin: division versus expansion. *Cold spring harbor perspectives in biology.* 2, (2010): a001446.
[2]. Williams, G. R.; O'Hare, D. Towards understanding, control and application of layered double hydroxide chemistry. *J. Mater. Chem.* 16, (2006): 3065.
[3]. Taviot-Guého, C.; Prévot, V.; Forano, C.; Renaudin, G.; Mousty, C.; Leroux, F. Tailoring hybrid layered double hydroxides for the development of innovative applications, *Adv. Funct. Mater*. 28, (2018): 1703868.

***Acknowledgments:*** FAPEMIG, CAPES and CNPq.

# DTF study of layered double hydroxides with cationic exchange capacity: $(A^{+}(H_2O)_6)[M^{2+}{}_6Al_3(OH)_{18}(SO_4)_2]\cdot 6H_2O$ ($M^{2+}$ = Mg, Zn and $A^{+}$ = Na, K)

**PEDRO IVO R. MORAES[1], FERNANDO WYPYCH[2], ALEXANDRE A. LEITÃO[1]**

[1]Departamento de Química, Universidade Federal de Juiz de Fora, Juiz de Fora, MG, CEP 36036-330, Brazil, pedroivo@ice.ufjf.br, alexandre.leitao@ufjf.edu.br

[2]Departamento de Química, Universidade Federal do Paraná, Curitiba, PR, CEP 81531-980, Brazil, wypych@ufpr.br

## ABSTRACT

Layered double hydroxides (LDH) with molar ratio $M^{2+}$:$Al^{3+}$ of 2:1, correspondent to the minerals Motukoreaite ($M^{+2}$= Mg) and Natroglaucocerinite ($M^{+2}$= Zn) structures were investigated by DFT calculations. The layer domain of this minerals contains three positive charges ($[M^{2+}{}_6M^{3+}{}_3(OH)_{18}]^{3+}$) which are counterbalanced with two sulphate anions resulting $([M^{2+}{}_6M^{3+}{}_3(OH)_{18}](SO_4)_2)^{-}$ and these compound are intercalated with hydrated sodium cation. Structures with different layer compositions (Mg/Al and Zn/Al) and intercalated cation ($Na^{+}$ and $K^{+}$) were built. The structural, electronic and thermodynamic properties were investigated. The thermodynamic of the cation exchange reaction was performed replacing sodium cation with potassium cation, maintainig the intercalated sulfate. LDH are traditionally studied as anion exchangers but these compositions of LDH can also exchange cations.

Keywords: Layered Double Hydroxides, DFT, Cation Exchange Reactions, Thermodynamics.

## INTRODUCTION

Layered double hydroxides (LDH) or hydrotalcite-like compounds are natural or synthetic layered materials whose structure is similar to Brucite ($Mg(OH)_2$) and are very well known as anionic exchangers. LDHs can be described by a general formula $[M^{2+}{}_{1-x}M^{3+}{}_x(OH)_2][(A^{n-})_{x/n}\cdot yH_2O]$. Motukoreaite ($(Na(H_2O)_6)[Mg_6Al_3(OH)_{18}(SO_4)_2]\cdot 6H_2O$)[1], Natroglaucocerinite ($(Na(H_2O)_6)[Zn_6Al_3(OH)_{18}(SO_4)_2]\cdot 6H_2O$)[2] are LDHs minerals with a $M^{2+}$:$M^{3+}$ 2:1. These materials are intercalated with sulfate anions and hydrated sodium cations. Recently cationic exchange reactions were study in this family of compounds. The cations were exchanged without exchange the sulfate anions[3].

Density Functional Theory (DFT) calculations are reliable tool to provide electronic properties and assist the experimental data. The aim of this work is investigate the electronic structure of Motukoreaite and Natroglaucocerinite with chemical formulas $[Mg_6Al_3OH)_{18}][Na(H_2O)_6(SO_4)_2]\cdot 6H_2O$ and $[Zn_6Al_3(OH)_{18}][K(H_2O)_6(SO_4)_2]\cdot 6H_2O$ and with the 1H and 3R polytypes. It is also a target to evaluate thermodynamically a possible cationic exchange. For the sake of simplicity these models will be called as: M-Al-($NaSO_4$) and M-Al-($KSO_4$), M = Mg and Zn.

The DFT calculations were performed using the codes available in the Quantum Espresso package[4]. We used the generalized gradient approximation, GGA-PW91 for the exchange-correlation (XC) functional, and ultrasoft pseudopotentials. Kohn-Sham one electron states were expanded in a planewave basis set with a kinetic cutoff energy of 60 Ry(480 Ry for the density). A Monkhorst-Pack mesh of 2x2x2 k-point sampling

was used. The structures were built correspond to a 3x3 in 3R and 1H polytype as reported by Costa *et al*.[5].

## RESULTS

The simulated structures cell parameters for both 3R and 1H polytypes show a good agreement with the experimental data. Figure 1 show the optmized structures for LDHs. The structures intercalated with $K^+$ show a higher basal spacing than $Na^+$ and the layer composed by Zn showed a higher *a* and *b* parameters than the Mg compounds, but the structures with Mg shows higher *c* parameter for both polytypes. The electronic total energy shows that the most stable polytype is the 3R for both compositions. The increments of ΔG show that both polytypes could be accessed experimentally, since the average differences between the 1H and 3R polytypes curves are 11.15, 18.22, 13.11 and 16.21 kJ $mol^{-1}$ for Mg-Al-($NaSO_4$), Mg-Al-($KSO_4$), Zn-Al-($NaSO_4$) and Zn-Al-($KSO_4$) respectively as can be seen in the Figure 1.

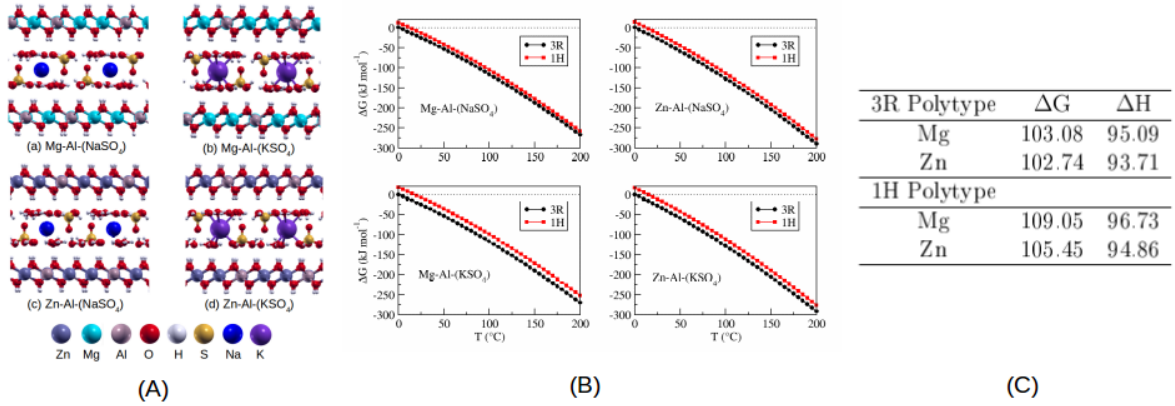


| 3R Polytype | ΔG | ΔH |
|---|---|---|
| Mg | 103.08 | 95.09 |
| Zn | 102.74 | 93.71 |
| 1H Polytype | | |
| Mg | 109.05 | 96.73 |
| Zn | 105.45 | 94.86 |

(C)

Figure 1: (A) Optimized structures of 3R polytype (upper line) and 1H polytype (bottom line). (B) Gibbs free energy increments for the LDHs. (C) Thermodynamic potentials for the cationic exchange reactions (M-Al-($NaSO_4$)→M-Al-($KSO_4$)) at 298.15 K (kJ $mol^{-1}$).

The thermodynamic for the cationic exchange reactions indicate that the cation $K^+$ can be thermodynamically replaced by $Na^+$ keeping the sulfate anions. The Gibbs free energy and the enthalpy for the cation exchange reaction are shown in Figure 1. The reaction rates of those processes play a major in the ion selectivity, however our study takes into account only thermodynamic potentials, the ion exchange kinetics is not regarded. The same behaviour was observed for both polytypes. The electronic analyses were performed for the 3R stacking. The main difference in the electronic density was observed when the layer composition change. The hydroxide anions in Zn/Al layer showed a basic behaviour while for Mg/Al compositions the most basic sites are the sulfate anions. This is also explained by the difference between the Mg and Zn calculated Bader charges.

**Support:**This work has been supported by CAPES, CNPq, FAPEMIG, Brazilian agencies and the enterprise Petrobras S/A (CENPES). We also acknowledge the CENAPAD-SP computational center.

### Citations and References

[1] Rodgers, K. A., *et al*. Mineral. Mag. 1977, 41 ,389-390.
[2] Witzke, T., *et al*. Zeit. Kristal. 1995, 9, 252.
[3] Sotiles, A. R., *et al*. J. Am. Chem. Soc. 2019, 141, 531-540.
[4] Giannozzi, P., *et al*. J. Phys.: Condens. Matter 2009, 21, 395502.
[5] Costa, D. G., *et al*. J. Phys. Chem. C 2010, 114, 14133-14140.

# 2D AURIDE SHEETS: STRUCTURAL AND SPECTROSCOPIC STUDY OF POTASSIUM-GOLD ALLOYS INTERCALATED INTO GRAPHITE

**SPEYER L., CAHEN S., EL HAJJ I., LAGRANGE P., HEROLD C.**

Institut Jean Lamour, UMR 7198 CNRS – Université de Lorraine
Campus Artem, 2 allée André Guinier, BP 50840, 54011 Nancy Cedex, France
Sebastien.cahen@univ-lorraine.fr

## ABSTRACT

Regarding its lamellar structure, graphite can accommodate various chemical species in its van der Waals gaps thanks to redox intercalation reactions. The present work is focused on the intercalation of potassium-gold alloys using a solid-liquid method in alkali-based molten alloy medium. Several graphite-potassium-gold compounds have been prepared, especially a pure ternary graphite intercalation compound (GIC) with a $K_{1.3}Au_{1.5}C_4$ formula and presenting poly-layered intercalated sheets. This compound has been characterized regarding its structural and physical properties using several complementary techniques. The quantitative analysis of the 00*l* reflections recorded by X-ray diffraction allowed to determine a C-K-Au-Au-Au-K-C stacking sequence along the *c*-axis. In order to probe the valence of gold in the intercalated sheet, $^{197}$Au gold Mössbauer spectroscopy has been carried out and a negative valence has been evidenced for intercalated gold. This remarkable result can be correlated with the high electronegativity value of gold on the Pauling's scale, explaining the possibility to form auride anion especially when associated with electropositive alkali metals.

**Keywords**: Graphite Intercalation Compound, X-ray diffraction, gold, Mössbauer spectroscopy

## INTRODUCTION

Using potassium-based molten alloys, several poly-layered graphite intercalation compounds were synthesized with mercury or thallium [1,2]. The corresponding compounds exhibit superconducting properties with enhanced critical temperature compared to binary $KC_8$ GIC [3,4]. Considering the fact that gold is the neighbour of Hg and Tl in the periodic table, we have realized an in-depth exploration of the graphite-potassium-gold system using the solid-liquid method in K-Au molten alloys. The impact of the experimental synthesis parameters has been investigated, leading to the possible synthesis of three potassium-gold intercalation compounds.

## RESULTS AND DISCUSSION

Using the combination of X-ray diffraction and ion beam analysis, three compounds have been evidenced: $K_{1.3}Au_{1.5}C_4$ with five-layered intercalated sheets, $K_{1.6}Au_{0.7}C_4$ exhibiting three-layered intercalated sheets and metastable $KAu_{0.7}C_4$ with two K-Au intercalated planes in each intercalated sheet. The intercalation mechanisms for preparing such compounds have been carefully investigated in a recent work [5]. The first compound denoted gamma appears remarkably stable and high-quality GIC can be synthesized, allowing to perform in-depth investigations using various characterization

techniques. The structural study of this compound indicates a C-K-Au-Au-Au-K-C stacking sequence (Fig. 1) in agreement with the $K_{1.3}Au_{1.5}C_4$ chemical formula.

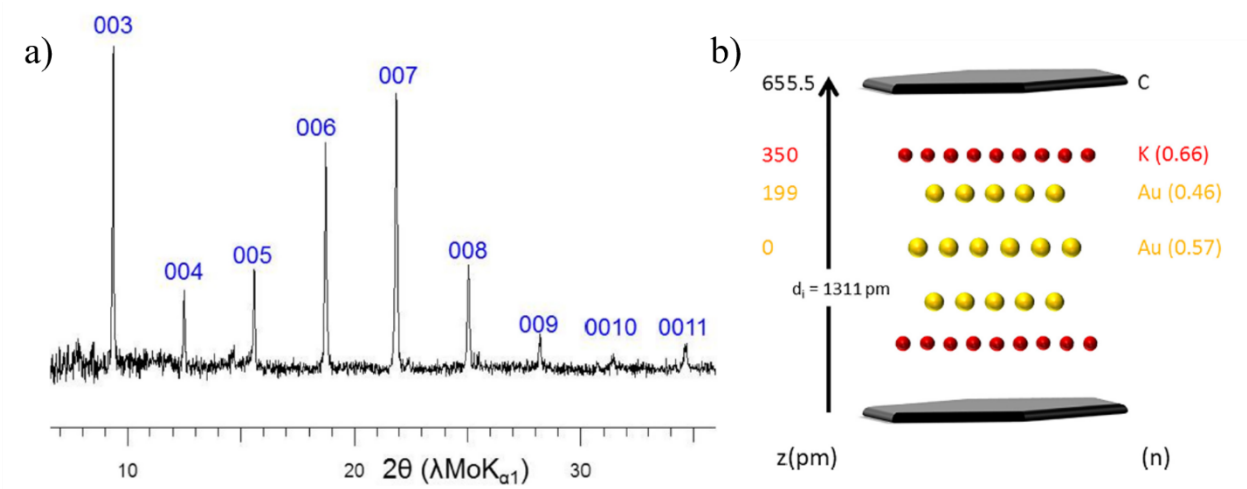


Fig.1. a) 00*l* XRD pattern b) Stacking sequence along *c*-axis for the gold-potassium γ-GIC [6].

Such a structure can be related to the charge transfer between the different constitutive elements. Potassium layers are positively charged, as in the binary $KC_8$ compound, due to the low electronegativity of potassium. Then, it is possible to postulate, for the gold layers, a negative charge which would be stabilized by the adjacent positive potassium layers. Recent $^{197}$Au Mössbauer measurements have been carried out on this compound and actually highlight a negative oxidation state for intercalated gold, giving two-dimensional auride anions sheets. This is a remarkable result, supported by the proven existence of auride anions, especially in gold-alkali metal compounds [7,8].

## References


[1] M. El Makrini, P. Lagrange, D. Guérard, A. Hérold, Carbon, 18 (1980) 211-6.
[2] B. Outti, P. Lagrange, C. R. Acad. Sci. Paris, 313 (1991) 1135-9.
[3] R. A. Wachnik, L. A. Pendrys, F. L. Vogel, P. Lagrange, Solid State Comm., 43 (1982) 5-8.
[4] L. A. Pendrys, R. A. Wachnik, F. L. Vogel, P. Lagrange, Synth. Metals, 5 (1983) 277-90.
[5] M. Fauchard, S. Cahen, P. Lagrange, P. Berger, C. Hérold, Carbon, 145 (2019) 501-6.
[6] M. Fauchard, S. Cahen, P. Lagrange, G. Medjahdi, P. Berger, C. Hérold, Carbon 140 (2018) 182-8.
[7] C. Koenig, N. E. Christensen, J. Kollar, Phys. Rev. B, 29 (1984) 6481-8.
[8] R. E. Watson, M. Weinert, Phys. Rev. B, 49 (1994) 7148-54.

# ENHANCING THE FIBROUS ASPECTS OF LAYERED CERIUM IV HYDROGENPHOSPHATE MEMBRANE FOR HEAVY METAL REMOVAL FROM CONTAMINATED EFFLUENTS

**DUARTE J.P.P.[1], ROCHA L.D.S. [1], SOUZA R.M. [1], MEDEIROS M.E. [1], MALTA L.F.B. [1]**

1- Instinto de Química, Universidade Federal do Rio de Janeiro (Avenida Athos da Silveira Ramos, nº 149, Bloco A – 7º andar, Rio de Janeiro (RJ) - Brasil). Email: diretoria@iq.ufrj.br

## ABSTRACT

Cerium (IV) hydrogenphosphate (CeP) belongs to the class of acid phosphates of tetravalent metals. In particular, this material assumes the form of fibrous self-supported sheets [1]. It presents the property of ion-exchange towards cations. In the present work it is intended to study incorporation of heavy metals in layered matrix of varying cristallinities as an effort to obtain an efficient metal remover for contaminated aqueous efluents.

CeP was synthesized according to previous work [2]. 6 mol $L^{-1}$ $H_3PO_4$ aqueous solution was added dropwise to a 0.05 mol $L^{-1}$ $(NH_4)_2Ce(NO_3)_6$ aqueous solution at 90ºC and the mixture was kept at this temperature for 4h, 8h, 16h and 24h. The solids were characterized by XRD, SEM and BET.

This material's fibrous texture increased proportionally with hydrothermal treatment (HT) time until 16h, as visualized by SEM images (Figure 1). Also crystallinity increased, according to the mean crystallites sizes (from 15 to 17.6 nm), based on x-ray diffraction pattern (Figure 2). The surface area measured by BET analyzer for CeP with 8 hours of HT was 23,075 $m^2$ / g. Further characterizations are underway.

Ion-exchange with palladium, lead and cadmium has been started.

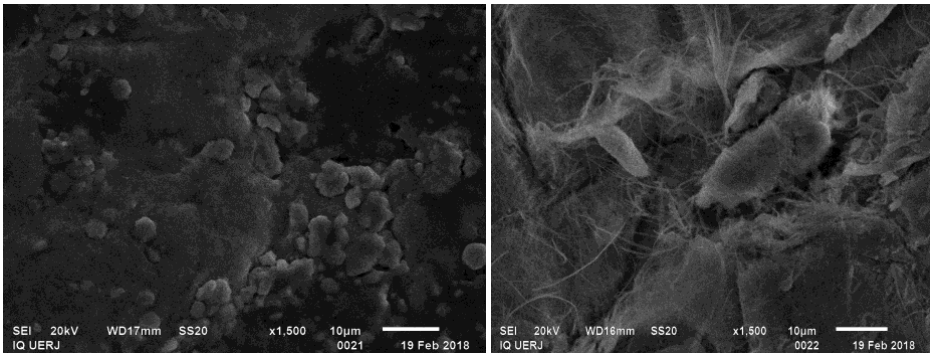


**Figure 1.** SEM images at 1500x magnification of CePs hydrothermally treated by 4 (left) and 16 hours

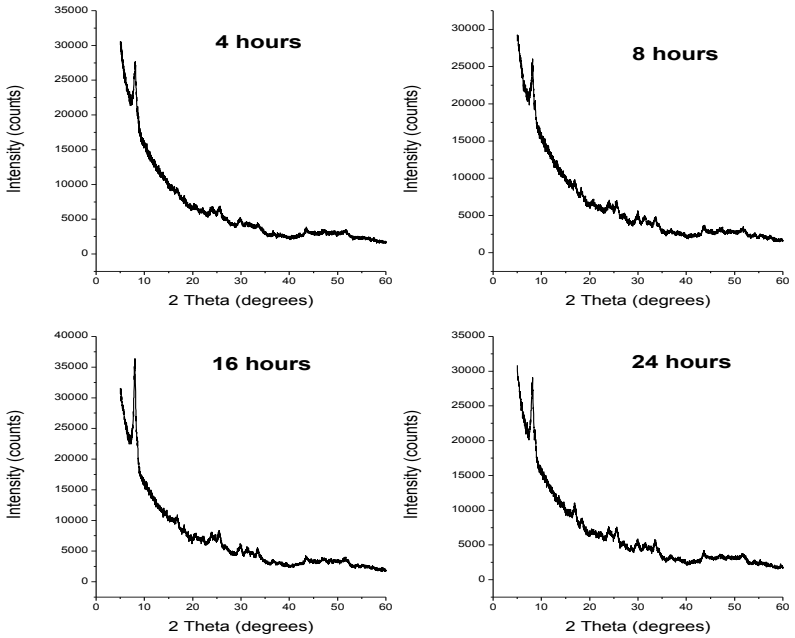


**Figure 2.** XDR plot of distinct CEPs synthetised, vaying HT time

## REFERENCES

[1] G. Alberti, M.A. Massucci, and E. Torracca: J. Chromatography 30, 579 (1967).
[2] H. Hayashi, K. Torii and S. Nakata: Hydrothermal Treatment and strontium ion sorption properties of cerium (IV) hydrogenphosphate (1996)

# EFFECTS OF ULTRASOUND AND PVP ASSISTED SYNTHESIS ON THE PROPERTIES OF EUROPIUM-BASED NANOSIZED MOFS

**CLAUDIA M. S. CALADO, THATIANE V. SANTOS AND CINTYA D. A. E. S. BARBOSA**

Instituto de Química e Biotecnologia. Universidade Federal de Alagoas, Av. Lourival Melo Mota, S/N. Tabuleiro dos Martins, Maceió/AL. E-mail: cmsc.calado@gmail.com

## ABSTRACT

The nano-sized MOFs (NMOFs) $[Eu_2(BDC)_3(H_2O)_4]$ were prepared by ultrasound (US) assisted method without (EuNMOF) or with the presence of the stabilizing agent polyvinylpyrrolidone (PVP) (EuNMOF@PVP) in order to evaluate its influence on structural, morphological and photophysical properties. These NMOFs were characterized by XRD and proved to be isostructural to the microcrystalline compound previously reported in the literature. Based on SEM results, EuNMOFs showed to be flower-like, on the other hand, EuNMOF@PVP presented a nanoplate morphology with layer sizes varying in the range of 40–80 nm. Solid-state luminescent properties of these EuNMOFs were studied and exhibited similar profiles in relation to the europium transitions. Thus, obtaining EuNMOFs with different morphologies can lead to new or improved properties.
**Keywords:** Ultrasound, PVP, nano-MOFs, morphology.

## INTRODUCTION

The structural architecture of europium-based nano-sized metal-organic framework (EuNMOFs) associated with its inherent photoluminescent properties make it promising for applications in several fields.[1] In recent years, alternative approaches have been developed aiming to milder conditions than traditional methods and intending to improve modulation at the nanoscale. In this work, we present an easy ultrasonic assisted method to the synthesis of EuNMOFs ($[Eu_2(BDC)_3(H_2O)_4]$, BDC = 1,4-benzenedicarboxylic) with and without the presence of polyvinylpyrrolidone (PVP) as a passive agent.

## EXPERIMENTAL

### Synthesis of EuNMOF and EuNMOF@PVP

An aqueous solution of disodium terephthalate ($Na_2BDC$) was slowly dropped into a solution of $Eu(NO_3)_3.5H_2O$. Right after, the mixture was submitted to ultrasonic energy. The experimental procedure to the synthesis of EuNMOF@PVP was very similar, with the only difference of addition of PVP to the solution of $Eu(NO_3)_3.5H_2O$. The resulting products in both cases were centrifuged, washed with absolute ethanol three times and dried under high vacuum. All solutions were prepared with ultrapure water.

## RESULTS AND DISCUSSION

The materials here presented were characterized by XRD, FTIR, TGA, SEM and photoluminescence spectroscopy. According to the obtained diffractograms, both

EuNMOFs presented alike profiles, as well as luminescent properties and were assumed to be isoreticular to the micro-compound reported in the literature.[2] Conforming to SEM results, EuNMOFs showed a flower-like morphology; on the other hand, EuNMOF@PVP presented a nanoplate shape, with sizes varying in the range of 40–80 nm.

Figure 1 – a) XRD pattern of EuNMOFs, micro-compound and simulated. b) Excitation spectra monitoring the emission at 614 nm and c) emission spectra with excitation at 315 nm of EuNMOFs and micro-compound. d) SEM of i-ii) EuNMOF and iii) EuNMOF@PVP.

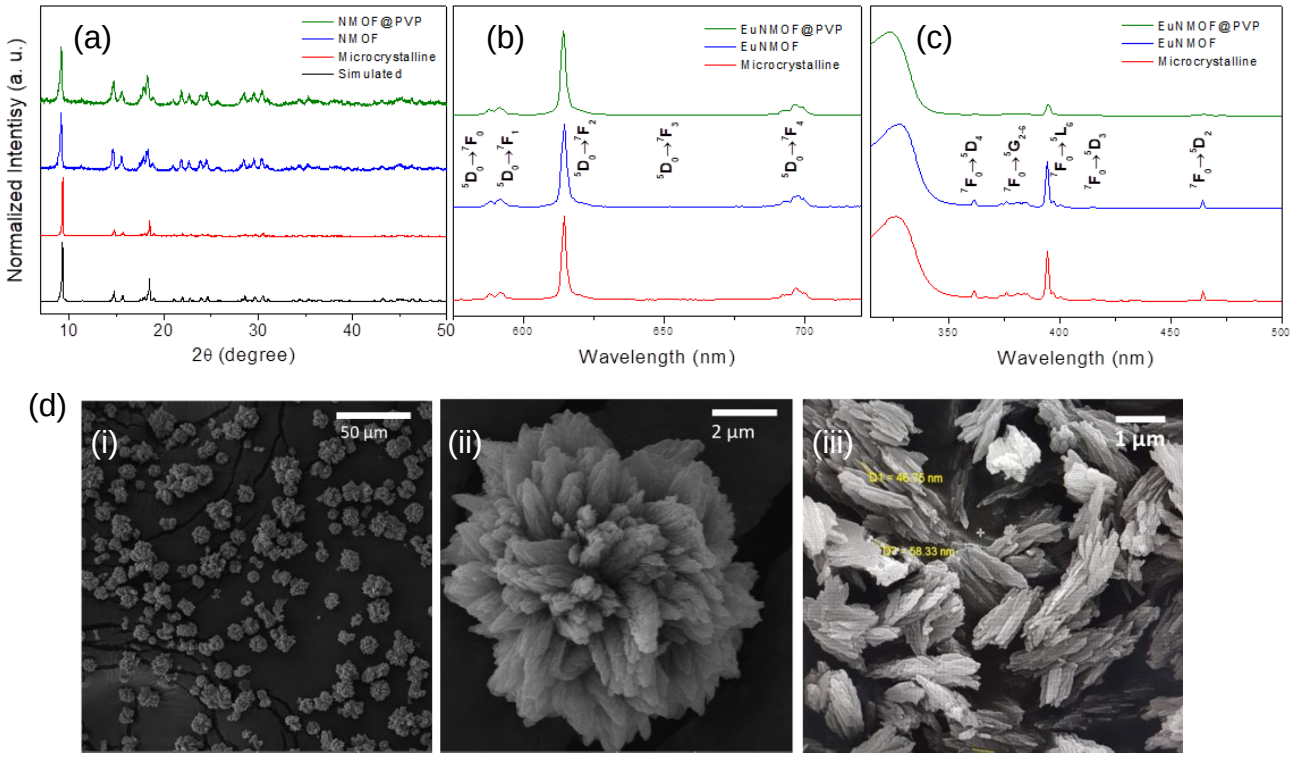


The effect of ultrasound on chemical reactions can be explained by the mechanism of acoustic cavitation, thence its use can accelerate nucleation and produce nanocrystals.[1] Associated with PVP, here applied as capping agent, this methodology allows a controlled growth of the nanostructure as much as in relation to the morphology.

## CONCLUSION

The nano-sized MOFs $[Eu_2(BDC)_3(H_2O)_4]$ were successfully synthesized by the ultrasonic method, with and without the presence of PVP, presenting one of its dimensions in the nanoscale. These materials were assumed to be isostructural to the micro-sized compound and presented different morphologies. Due to their size and properties, these results suggest that both materials may be promising for several applications.

**ACKNOWLEDGMENT:** UFAL, CNPq.

### Citations and References

[1] Barros, B. et al. Chemistry Select, 3, 7459 – 7471, 2018
[2] Daiguebonne, C. et al. Inorganic Chemistry, 47, 3700 – 3708, 2008

# SYNTHESIS AND CHARACTERIZATION OF NANOHYBRIDS BASED ON CARBON DOTS/EU-MOFs

**KLEYTON R. M. DA SILVA[1], CLAUDIA M. S. CALADO, THATIANE V. SANTOS[1] AND CINTYA D. A. E. S. BARBOSA[1]**

[1]Instituto de Química e Biotecnologia. Universidade Federal de Alagoas, Av. Lourival Melo Mota, S/N. Tabuleiro dos Martins, Maceió/AL. E-mail: ritomarmonteiro@gmail.com

## ABSTRACT

The development of hybrid compounds based on MOFs and other functional materials has been sought in order to obtain new properties and/or their tunability. Here, a new luminescent hybrid nanomaterial-based in carbon dots (C-Dots) encapsulated in europium metal-organic frameworks (C-Dots/EuMOFs) was synthesized by the ultrasonic method at room temperature and characterized according to structural, morphological and luminescent aspects. Chitosan gel was used as a precursor of C-Dots through hydrothermal synthesis. The C-Dots exhibited emission dependent on the excitation wavelength (with a maximum in green emission), a size below 10 nm and characteristic absorption peaks in 205 and 280 nm related to π-π* and *n*-π * transitions of the C=C bonds and amine groups on the surface, respectively. The nanohybrid (C-Dots/EuMOFs) presented to be isostructural to the microcrystalline phase $[Eu_2(BDC)_3(H_2O)_4]$ reported in the literature. SEM results showed that the morphology of the nanohybrid is plate-like. The fluorescence of C-Dots/EuMOFs exhibited dual emission, with well-defined emission wavelengths centered at 440 nm and 615 nm (when excited at 370 nm) attributed to characteristic peaks of C-Dots and Eu-MOFs, respectively. Thus, synthesizing luminescent materials with dual emission can be promising in fields like sensing, especially as ratiometric probes**.**

**Keywords:** Nanohybrids, carbon dots, EuMOFs, dual emission

## INTRODUCTION

Considered as emerging materials, metal-organic frameworks (MOFs) has attracted attention in various scientific and technological sectors due to their excellent structural and physicochemical properties. [1] In this sense, the development of hybrid materials based on MOFs and other functional materials, [2] as carbon dots (C-Dots) can lead to new and/or tunable properties. The C-Dots display high optical properties, easy preparation, low toxicity, and biocompatibility. Here, a new luminescent nanohybrid based in C-Dots encapsulated in $[Eu_2(BDC)_3(H_2O)_4]$ were synthesized by the ultrasonic method at room temperature, with the addition of polyvinylpyrrolidone (PVP) as a stabilizing agent and characterized by XRD, FTIR, TGA, SEM techniques and photoluminescence spectroscopy.

## RESULTS AND DISCUSSION

A simple and facile ultrasound-assisted synthesis of a new nanohybrid based carbon dots and europium MOFs was performed. The XRD pattern of the C-Dots/EuMOFs is well consistent with microcrystalline phase $[Eu_2(BDC)_3(H_2O)_4]$ reported in the literature, [3] showing that the encapsulation of C-Dots did not altered the structural properties (fig. 1a). SEM results showed that the morphology of the nanohybrid is plate-like (fig. 1b). The C-Dots exhibited excitation-dependent emission wavelength, a size below 10 nm and

characteristic absorption peaks in 205 and 280 nm related to π-π* and *n*-π * transitions of the C=C bonds and amine groups on the surface, respectively (fig. 1c). The excitation and emission spectrum showed that there is a relationship between the excitation wavelength and the emission of the CDs/EuMOFs (fig. 1d). When excited at 370 nm it is possible to see characteristic peaks of both C-Dots and Eu-MOFs. On the other hand, by exciting at 280 nm it is possible to see mostly the characteristic emissions of the europium transitions (fig. 1e).

**Figure 1:** (a) XRD simulated and C-Dots/EuMOFs, (b) SEM of C-Dots/EuMOFs (c) UV-Vis and emission dos C-Dots (excited at 290 – 410), (d) excitation spectra of C-Dots/EuMOF and (e) emission spectra of the C-Dots/EuMOFs and C-Dots.

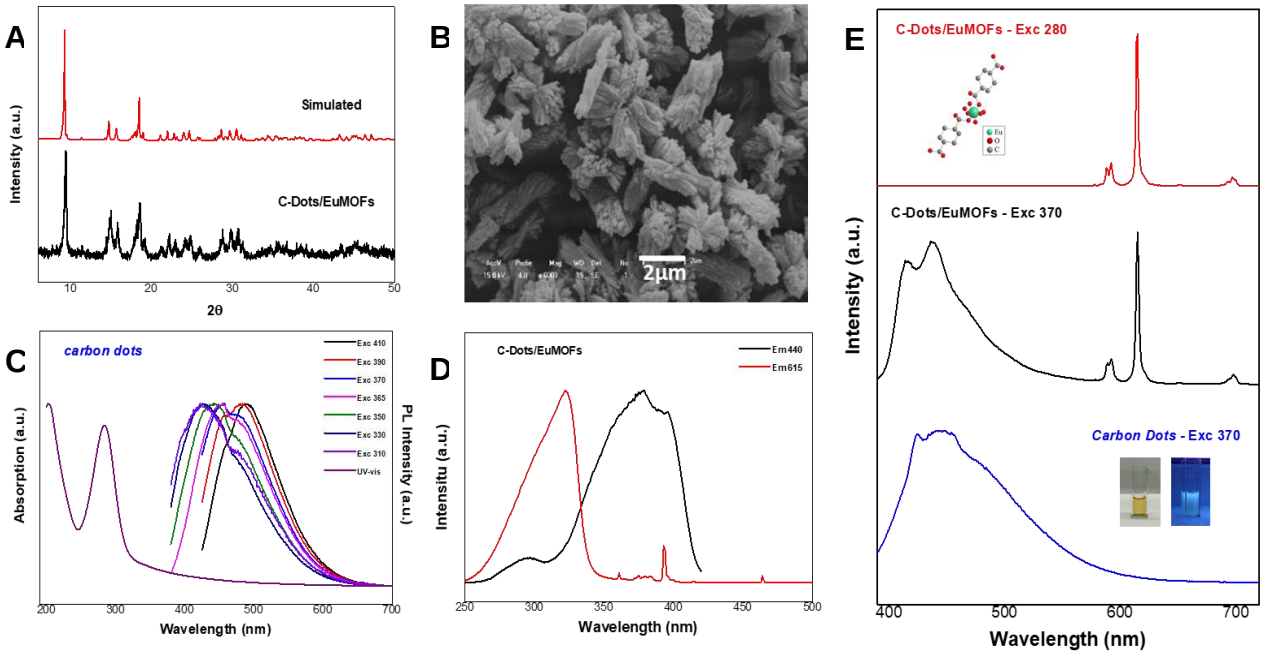


## CONCLUSION

The nanohybrid C-Dots/EuMOFs was successfully synthesized. This nanomaterial showed the plate-like morphology, maintained its structure after encapsulation of the carbon dots. Furthermore, exhibited an emission profile with characteristic peaks of both C-Dots and Eu-MOFs. These results showed that the nanohybrid C-Dots/EuMOFs can be assumed as promising ratiometric probes**.**

**ACKNOWLEDGMENT:** UFAL, FAPEAL, CNPq.

### References

[1] Kumar, P. et al. Trends in Anal. Chem. 2015, 73, 39-53.
[2] Xu, Xiao-Yu . J. Mater. C, 2016, 4, 1543-1549.
[3] Daiguebonne, C. et al. Inorg. Chem. 2008, 47, 3700-3708.

# ALGINATE BEADS AND KAOLINITE INCORPORATED WITH AGROCHEMICALS: EVALUATION OF FORAGING ACTIVITY OF LEAFCUTTER ANT OF GENRE *Atta* spp.

**DUARTE V.G.O.[1], CORRÊA A.G.S.[1], NOBRE D.A.C.[1], LEITE V.S.A.[1], MORAES A.R.F.[1], FERNANDES F.L. [1], PINTO F.G. [1], TRONTO J[1].**

[1] Universidade Federal de Viçosa - Campus Rio Paranaíba, Rodovia BR 354 km 310, CEP: 38810-000, Rio Paranaíba-MG, Brazil. E-mail: valber.g@hotmail.com

## ABSTRACT

The leafcutter ants, *Atta* spp. are severe pests that cause loss of billions of dollars on the forest plantations annually. Currently, the use of granulated baits and the thermal fogs application are options to control these pests. In this sense, new technologies are welcome to expand the control options. Therefore, the goals of this work were: (*i*) synthesize and characterize organic-inorganic hybrid materials derived of interaction between alginate beads and kaolinite clay incorporated with agrochemicals (e.g. sodium tetraborate, *Beauveria bassiana* spores, and chlorpyrifos); (*ii*) evaluate by bioassays the forage activity in the field and the toxicity of the bait in laboratory for leafcutter ants, after the application of granulated baits. The beads of alginate were characterized by a set of techniques: X ray diffraction (XRD), vibrational spectroscopy (ATR-FTIR), and thermogravimetric analysis coupled to mass spectrometry (TGA-DTA), etc. In the bioassays, a completely randomized design treatments was used, and the means compared by the Tukey test, at 5% probability. The characterization techniques provided information about the prepared materials, evidencing the presence of the precursors in the alginate beads. The bioassays allowed the toxicity and efficiency of the baits in activity to be verified. The most efficient baits for the control of these insects were the ones that presented in their composition the active chlorpyrifos insecticidal principle. Based on the results, we can conclude that the synthesis of the alginate beads containing the agrochemicals originated products with formicide potential, being them efficient as management technique.

*Keywords:* kaolinite clay, sodium alginate, agrochemicals, chemical control.

## 1. INTRODUCTION

In Brazil, there are two thousand different species of ants. Leafcutter ants of the genre *Atta* and *Acromyrmex* are severe pests that cause the loss of billions of dollars on the plantations annually, especially seedlings.

Currently, research has been directed towards the search for insecticides less aggressive to the environment, which may allow a better sustainability of fauna and flora. In this sense, new technologies that present the use of environmentally friendly materials have been developed. Hybrid organic-inorganic materials are a special class of materials prepared by the appropriate combination of organic and inorganic components. The synergistic effect between the parts gives rise to materials with unique properties, distinct from their isolated components. These materials represent not only a creative alternative to the search for new ecofriendly materials, but also allow innovative industrial applications. [1]

## 2. EXPERIMENTAL

The synthesis of the alginate beads was performed by adapting of the complex coacervation method described by Zhang et al. (2014). [2] The bioassays in the laboratory were performed according to the methodology adapted from Bueno et al. (1997). [3] The bioassays in the field were performed according to the methodology proposed by Mariconi (1970). [4]

## 3. RESULTS AND DISCUSION

The diffractograms of the synthetized beats are presented in Figure 1 (I). The presence of diffraction peaks, indicated by the Miller indices (*hkl*), are related to Kaolinite clay.

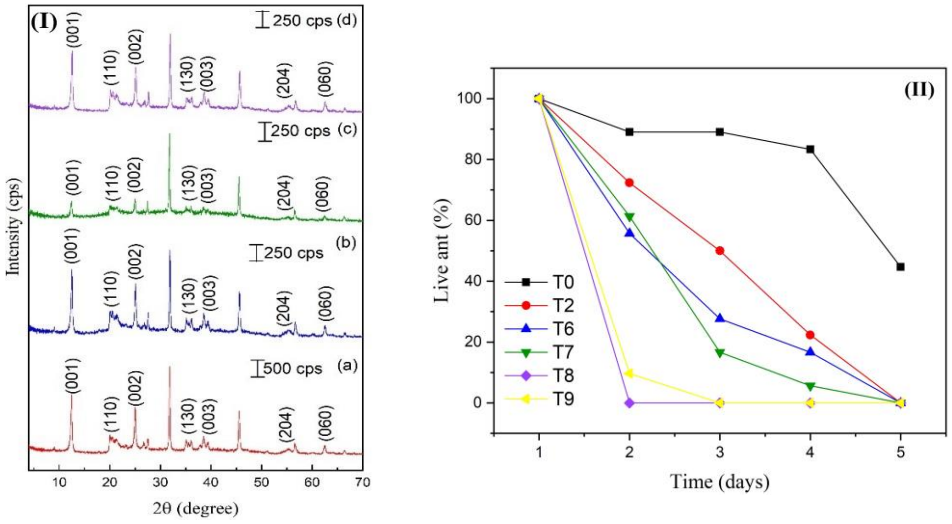


**Figure 1 (I):** XRD of the beats: (a) control with borate (T2); (b) 2.5 g borate and *B. bassiana* (T6); (c) 5 g borate and *B. bassiana* (T7) and (d) borate and chlorpyrifos (T8). **(II):** Percentage of live ants during the evaluation days. Treatments - T0: Witness, T2: control with borate, T6: 2.5 g borate and *B. bassiana*; T7: 5 g borate and *B. bassiana*, T8: Borate and chlorpyrifos and T9: Mirex®.

The results of laboratory bioassay presented in Figure 1 (II) showed a significant interaction between treatments versus days evaluated after the application of the baits. The T8 bait presented superiority over the commercial Mirex® bait (T9) (Tukey test at 0.05), causing the death of 100% of the insects in 24 h of evaluation. In the field, the averages of ant flux did not diverge among themselves that shows the toxic potential of these baits in the chemical control of these insects.

## 4. CONCLUSIONS

The synthesis of the alginate baits containing the agrochemicals were efficient, giving rise to products with potential formicide action. The characterization techniques used (XRD, ATR-FTIR and ATG-DTA) allowed the identification of chemical and physical characteristics of the synthesized baits. Based on the results obtained by statistical analyzes and experiments, the bait T8 presented the best chemical control of cutter ants of the genre *Atta*, with chlorpyrifos insecticide as active principle, causing a faster mortality compared to Mirex®.

## 5. REFERENCES


[1] SANCHEZ, C., SHEA, K.J., KITAGAWA, S. Recent progress in hybrid materials science. *Chem. Soc. Rev*, v.40, p. 471–472, 2011.

[2] ZHANG, Y.; LIANG, X.; YANG, X.; LIU, H.; YAO, J. An eco-friendly slow-release urea fertilizer based on waste mulberry branches for potential agriculture and horticulture applications. *ACS Sustain. Chem. Eng*, v.2, n.7, p.1871–1878, 2014.

[3] BUENO, O.C.; MORINI, M.S.C.; PAGNOCCA, F.C.; HEBLING, M.J.A.; SILVA, O. A. Sobrevivência de Operárias de *Atta sexdens* rubropilosa Forel (Hymenoptera: Formicidae) Isoladas do Formigueiro e Alimentadas com Dietas Artificiais. *An. Soc. Entomol*, v. 26, n. 1, p. 107-113, 1997.

[4] MARICONI, F. A. M. As saúvas. São Paulo: Agronômica Ceres, 1970. 167 p.



***Acknowledgments:*** CAPES, FAPEMIG and CNPq.

***Oxygen Vacancy-Mediated Gas Barrier from the Nanoplatelet-Filled Polymer Film with Brick-Mortar-Sand Structure***

**WENYING SHI***

State Key Laboratory of Chemical Resource Engineering, Beijing University of Chemical Technology, Beijing, 100029, P. R. China. E-mail: shiwy@mail.buct.edu.cn

**ABSTRACT**

The gas barrier film based on nanoplatelet-filled polymer composite (NFPC) have attracted wide consideration for a variety of applications s[1,2]. However, how to reduce the free volume and interfacial penetration of NFPC film still faces challenges[3,4]. Here, a three-component "brick–mortar–sand" structure film, where layered double hydroxide (LDH) nanoplatelet is used as brick, $O_2$ as sand and polymer as mortar, is constructed with a lower oxygen transmission rate (OTR) of ~ 1.62 $cm^3$ $m^{-2}$ $day^{-1}$ $atm^{-1}$. It is worth mentioning that the oxygen vacancies (Vo) on LDH layers serving as traps adsorb the $O_2$, accompanied by the formation of a three-component structure. Therefore, in this way, not only the barrier property of $O_2$ is improved, but also greatly simplifies the preparation process of the three-component film. Furthermore, the film has phosphorescence emission characteristics due to the introduction of carbon dots (CDs). The establishment of an indirect relationship between OTR and phosphorescence intensity enables simple spectral or even naked-eye detection of OTR.

**keywords: layered double hydroxide, gas barrier, oxygen vacancies, carbon dots**

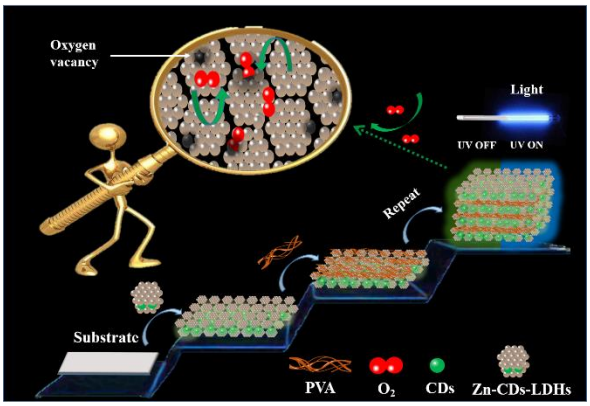


**Scheme 1**. Schematic representation for the fabrication of $(Zn\text{-}CDs\text{-}LDHs/PVA)_n$ multilayer film by spin coating and its gas barrier performance.

**Citations and References**

(1) J. Lange, Y. Wyser, Pack. Technol. Sci. 2003, 16, 149–158.
(2) O. C. Compton, S. Kim, C. Pierre, J. M. Torkelson, S. T. Nguyen, Adv. Mater. 2010, 22, 4759–4763.
(3) M. A. Priolo, D. Gamboa, K. M. Holder, J. C. Grunlan, Nano Lett. 2010, 10, 4970–4974.
(4) S. Logothetidis, Mater. Sci. Eng. B 2008, 152, 96–104.

# Layered Double Hydroxides (LDHs) as carrier of pentavalent antimony: preparation and characterization

**TAMIRES ANDRADE DA SILVA.[1], GISELLE ALVES DA PAIXÃO[1], CARMEM LÚCIA DE PAIVA E SILVA ZANTA.[1], THIAGO MENDONÇA DE AQUINO.[1], JOSUÉ CARINHANHA CALDAS SANTOS.[1], MARIO ROBERTO MENEGHETTI.[1], LUCIANO APARECIDO MEIRELES GRILLO.[1], PHABYANNO RODRIGUES LIMA.[2], JONAS SANTOS SOUSA.[2], CAMILA BRAGA DORNELAS.[1]**

[1] Federal University of Alagoas (UFAL), 57072-900 Maceió, AL, Brazil
[2] Chemistry department, Federal Institute of Alagoas (IFAL), 57020-600 Maceió, AL, Brasil
*tamires_a@hotmail.com

## ABSTRACT

As a major measure of control of leishmaniasis, the World Health Organization (WHO) advocates the use of antimonials, despite its significant limitations [1]. In this context, as an alternative to antimony loading, the preparation of nanostructured binary systems is predicted through the use of Layered double hydroxides (LDHs). For this, the precursors Mg, Al LDH and meglumine antimoniate (MA) were synthesized. The products were prepared by ion-exchange solution. Both the precursors and the products were analyzed by characterization techniques. Qualitative protocols were used to investigate the antimony speciation [2]. After the confirmation of the synthesis of the precursors, the thermogravimetry technique (Figure 1) showed that only the MA-LDH 3 product presented a new thermal profile, and the result of the scanning electron microscopy allied to the energy dispersive spectroscopy (Figure 2) revealed that the antimony is evenly distributed throughout the surface of the sample. Complementing this information, quantitatively, there is about 12% of antimony in the product and it has maintained its valence Sb (V). The result of the chemical oxygen demand and Fourier transform infrared spectroscopy indicated that the product is inorganic, added to nuclear magnetic resonance spectra (Figure 3) that were determinant to confirm the replacement of meglumine by LDH in the antimony carrier. Finally, the technique of X-ray powder diffraction (Figure 4) ratified the obtaining of a binary system of adsorvato type. In conclusion, this system may represent a new approach to targeted and promising leishmaniasis delivery.
Keywords: Antimony; Meglumine antimoniate; Layered double hydroxide.

Figure 1. Thermal analysis curves. (a): precursors, (b): products obtained.

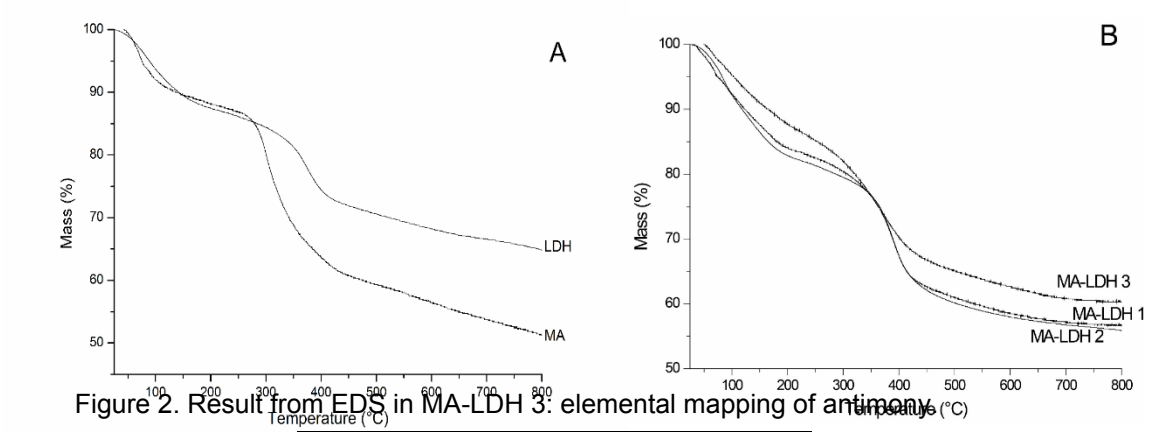


Figure 2. Result from EDS in MA-LDH 3: elemental mapping of antimony.

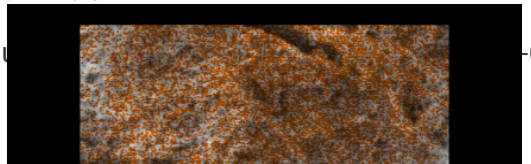

Figure 3. Partial $^{1}H$ NMR of NMG (a), MA (b) and first (c), second (d) and third (e) washes of the product MA-LDH 3, showing complete elimination of products of depolymerization of MA or NMG.

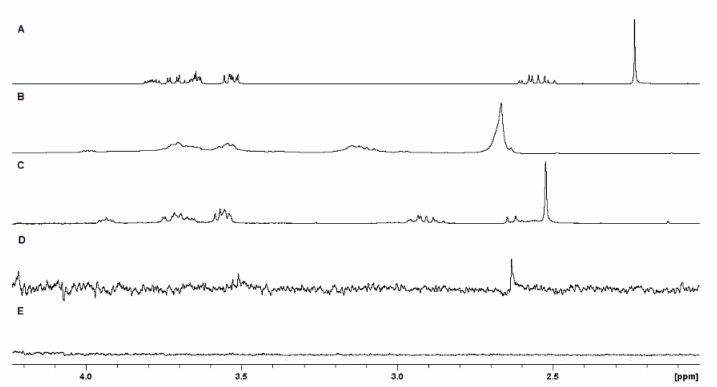


Figure 4. Diffractograms: (a) of the product MA- LDH 3 (•) planes coinciding with the ($KSb(OH)_6$), and (b) physical mixture.

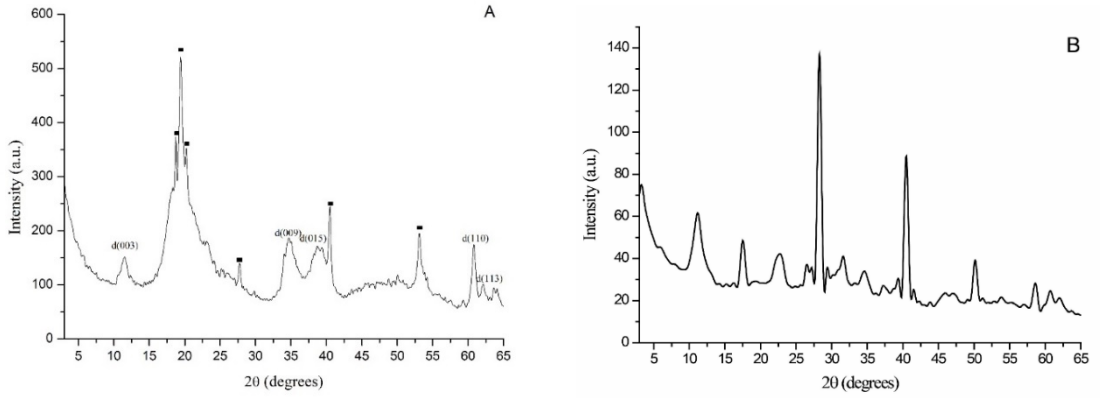


## Citations and References

[1] G. Verma, M.F Khan, W. Akhtar, M. Shaquiquzzaman, M. Akhter, A. Marella, T. Naved, S. Parvez, H. Kumar, S. Tauhid, M.M Alam, International Journal of Pharma and Bio Sciences 8 (2017) 1-7.

[2] F.B Martí, F.L Conde, S.A Jimeno, J.H Méndez, Paraninfo, Madrid (1992) ed.4.

# Zn-Al Layered Double Hydroxide Intercalated with L-Aspartic: dissolvable adsorbent for Cr (VI) determination using dispersive solid phase extraction

Leite V.S.A.[1], Constantino V.R.L.[2], Izumi C.M.S.[3], Tronto J.[1], Pinto F.G.[1]

1 – Universidade Federal de Viçosa, Instituto de Ciências Exatas e Tecnológicas, Campus de Rio Paranaíba, Rodovia BR 354 km 310, CEP 38810-000, Rio Paranaíba - MG, Brazil.*e-mail: frederico.pinto@ufv.br
2 – Universidade de São Paulo, Instituto de Química, Departamento de Química Fundamental, Av. Lineu Prestes 748, CEP 05508-000, São Paulo - SP, Brazil.
3 – Universidade Federal de Juiz de Fora, Departamento de Química, Rua José Lourenço Kelmer, s/n, CEP 36036-900, Juiz de Fora - MG, Brazil.

## ABSTRACT

In this work, a new analytical method was developed for the determination of Cr (VI) in aqueous solution using dispersive solid phase extraction (DSPE) and flame atomic absorption spectrometry (FAAS). In this method, Zn-Al layered double hydroxide intercalated with L-Aspartic (ZnAl-ASP-LDH) was used as adsorbent material. The parameters that influence the adsorption of Cr (VI) onto LDH in solution, such as the initial pH value, the contact time and the interfering ions were studied and optimized. After extraction of Cr (VI) from solution (pH = 5.5, 10 min) by ZnAl-ASP-LDH, the material was dissolved in $H_2SO_4$ and analyzed by FAAS. Thus, the maximum recovery of the analyte, decrease of the matrix effect and increase of the sensitivity of the analysis are assured. The method presented a linear range of 10 to 700 $\mu g \cdot L^{-1}$ and correlation coefficient $r^2$ = 0.999. The limits of detection (LOD) and limits of quantification (LOQ) were 3.13 $\mu g \cdot L^{-1}$ and 10.43 $\mu g \cdot L^{-1}$, respectively. The accuracy of the method was verified using certified water sample containing Cr (VI) [Cr (VI) -QC1453] and by recovery studies of the analyte in drinking $H_2O$ samples.

***Keywords:*** speciation; chromium (VI), layered double hydroxides, L-aspartic acid

## 1. INTRODUCTION

Cr (VI) is an element widely used in industry and is known in nature as oxyanions ($CrO_4^{2-}$ and $Cr_2O_7^{2-}$), however is an extremely carcinogenic agent. The World Health Organization (WHO) establishes a limit of 50 $\mu g \cdot L^{-1}$ Cr (VI) in drinking water [1].

Recent studies have demonstrated the potential of Layered Double Hydroxides (LDHs) as adsorbents for analytes of interest using the DSPE method [2].

The use of LDH intercalated with amino acids is an interesting strategy for speciation and preconcentration of Cr (VI), since at a certain pH, the amino group from amino acid molecule can be protonated and interacting electrostatically with the oxyanions of Cr (VI). The possibility of dissolution of the LDH in acid medium, after extraction of the analyte, eliminates the elution step. Thus, there is a simplification of the process and ensuring maximum recovery of the analyte [3].

## 2. EXPERIMETAL

ZnAl-ASP-LDH was synthesized by co-precipitation method at constant pH. It was characterized by X-ray diffraction (XRD), Raman spectroscopy and scanning electron

microscopy (SEM). The LDH was applied in Cr (VI) adsorption, evaluating maximum adsorption capacity, interfering ions and better pH value for speciation. Developing a new method for selective Cr (VI) separation. The analyte of interest was quantified flame atomic absorption spectrometry (FAAS).

## 3. RESULTS AND DISCUSSION

The diffractogram for ZnAl-ASP-LDH is presented in Figure 1 (a). The basal spacing found for this material was 12.4 Å. The Figure 1(b) shows the results of effect of pH on the adsorption of Cr (III) and Cr (VI) using ZnAl-ASP-LDH as adsorbent. In the pH = 5.5 there was simultaneous the highest adsorption of Cr (VI) and the lower adsorption to Cr (III). Thus, the pH value of 5.5 was chosen for the development of the method.

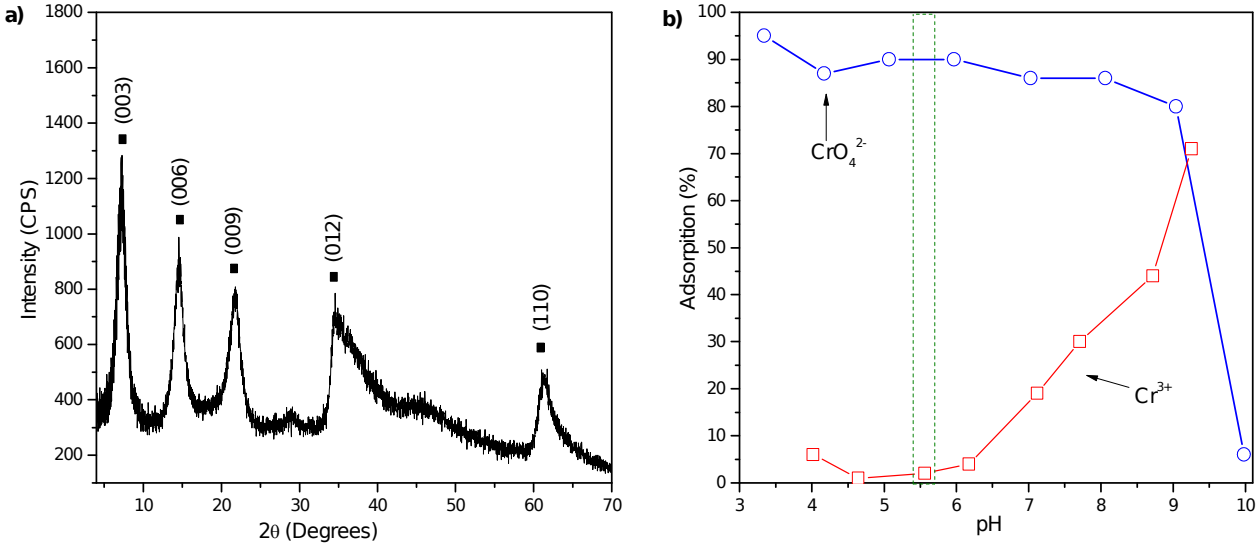


**Figure 1. a)** Diffractogram of ZnAl-ASP-LDH. **b)** Effect of pH on the adsorption of Cr (III) and Cr (VI) using ZnAl-ASP-LDH as adsorbent.

## 4. CONCLUSION

ZnAl-ASP-LDH showed good selectivity for Cr (VI) adsorption in the presence of interfering ions, including Cr (III) at pH = 5.5. ZnAl-ASP-LDH showed a maximum adsorption of Cr (VI) of 80.39 $mg \cdot g^{-1}$ (Langmuir isotherm model). The LOD for Cr (VI) determination was 3.13 $\mu g \cdot L^{-1}$.

## REFERENCES

[1] R. Rakhunde, L. Deshpande, H.D. Juneja, Chemical speciation of chromium in water: A review, Crit. Rev. Environ. Sci. Technol. 42 (2012) 776–810.

[2] S. Tang, G.H. Chia, Y. Chang, H.K. Lee, Automated Dispersive Solid-Phase Extraction Using Dissolvable $Fe_3O_4$ - Layered Double Hydroxide Core − Shell Microspheres as Sorbent, (2014).

[3] M. Sajid, C. Basheer, Layered double hydroxides: Emerging sorbent materials for analytical extractions, TrAC - Trends Anal. Chem. 75 (2016) 174–182.

***Acknowledgments*:** FAPEMIG, CAPES and CNPq.

# BORON RELEASE AND LEACHING FROM BORATE INTERCALATED IN LAYERED DOUBLE HYDROXIDES FERTILIZER DURING CONSECUTIVE CULTIVATIONS

**CASTRO G. F.[1], FERREIRA J. A.[2], SIQUEIRA M. T.[1], ZOTARELLI. L.[3], MATTIELLO E. M.[1], TRONTO J.[2]**

[1.] Federal University of Viçosa, Department of Soils, Viçosa - MG, Brazil. gustavofcastro@ymail.com
[2.] Federal University of Viçosa, Institute of Exact and Technological Sciences, Rio Paranaíba Campus, Rio Paranaíba - MG, Brazil. jaderalves@ufv.br
[3.] University of Florida, Horticultural Sciences Department, 1241 Fifield Hall, Gainesville – Florida, United States of America. E-mail: lzota@ufl.edu

## ABSTRACT

Conventional boron (B) fertilizers (e.g. $H_3BO_3$) can be easily leached due to its high solubility. A higher retention of B in the soil can be achieved using slow release sources such as layered double hydroxides (LDHs). The objectives of this study was i) to evaluate the release and leaching of B by two fertilizer sources in a column study without plants; ii) to evaluate the soil availability of the same two sources of B fertilizer for consecutive cultivations. For the leaching study two B fertilizers ($Mg_2Al$-B-LDH and $H_3BO_3$) were applied in soil columns and incubated for 1; 5; 10; 15; 20; 25 and 30 days before leaching. Sunflower plants were cultivated for two seasons in greenhouse under two sources of B ($Mg_2Al$-B-LDH and $H_3BO_3$) and six rates of B fertilizer in a factorial 2 x 6. Plants received a single application of B at the first cultivation. The amount of B leached was lower for $Mg_2Al$-B-LDH than $H_3BO_3$. There were no significant differences for sunflower aboveground biomass and total B accumulation for the two B sources and rates in the first cultivation. In the second cultivation, sunflower aboveground biomass and tissue B content increased quadratically and linearly for $H_3BO_3$ and $Mg_2Al$-B-LDH, respectively with the increase of B rate. The fast release of $H_3BO_3$ in the soil resulted in plant toxicity symptoms in the high rates, while the slow release of $Mg_2Al$-B-LDH promoted a steady release of B to the plants during first and second cultivations.

***Keywords:*** slow-release, layered double hydroxide, micronutrient.

## INTRODUCTION

Conventional boron (B) fertilizers (e.g. $H_3BO_3$) are very soluble and can be easily leached into the soil profile. B leaching is common in regions with high rainfall and sandy soils. A higher retention of B in the root zone can be achieved by using slow-release sources, such as layered double hydroxides (LDHs) [1]. The use of LDH may effectively reduce B leaching and increase the availability of B to plants. The objectives of this study was i) to evaluate the release and leaching of B by two fertilizer sources in a column study without plants; ii) to evaluate the soil availability of the same two sources of B fertilizer for consecutive cultivations.

## MATERIALS AND METHODS

Formulation, chemical and structural characterization of borate intercalated in layered double hydroxides of magnesium and aluminum ($Mg_2Al$-B-LDH) fertilizer were previously reported by Castro et al. [1].

The leaching test in soils columns was performed according to the method described by Abat et al. [2] using $Mg_2Al$-B-LDH and $H_3BO_3$ as sources. The leached of B was analyzed in different contact times (1; 5; 10; 15; 20; 25 and 30 days) between sources and soil.

Two sources of B ($Mg_2Al$-B -LDH and $H_3BO_3$) and six rates of total B (0.0, 0.5, 1.0, 2.0, 3.0 and 5.0 mg $dm^{-3}$) was applied on 2 $dm^3$ pots filled with soil in a factorial design (2 x 6). Pots received a single application of B, and sunflower was cultivated for two consecutive seasons in a greenhouse. The experiment was conducted in a randomized block design with four replications.

## RESULTS AND DISCUSSION

Overall, there was a lower B load in the leachate for $Mg_2Al$-B-LDH treatment compared to $H_3BO_3$ in the column leaching experiment. At first leaching collection, the total B leached from $H_3BO_3$ and $Mg_2Al$-B-LDH was equivalent to 39 % and 5 %, respectively of the total B applied. At the fifth leaching procedure at 20 days after fertilizer application, 100% of the B from the $H_3BO_3$ and 72 % $Mg_2Al$-B-LDH were leached.

There were no significant differences for sunflower aboveground biomass and total B accumulation for the two B sources and rates in the first cultivation. When analyzing the effect of doses on the contents, the model that best fit the two sources was the quadratic one. In the second cultivation, sunflower aboveground biomass and tissue B content increased quadratically and linearly for $H_3BO_3$ and $Mg_2Al$-B-LDH, respectively with the increase of B rate. The fast release of $H_3BO_3$ in the soil resulted in plant toxicity symptoms in the high rates, while for $Mg_2Al$-B-LDH the release was more sustainable, allowing a linear growth and accumulation of B by the plants. Similar results were found by Benício et al. [3], using LDH as the source of phosphorus (P). In this work, the LDH-P increased the productivity of corn plants, weight and P content in the aerial part of the plants.

## CONCLUSIONS

The $Mg_2Al$-B-LDH promoted a slower release of B to the soil solution, thus reduced initial leaching of B compared to $H_3BO_3$. The slower release of B by $Mg_2Al$-B-LDH can increase the retention of B in the soil consequently increasing the likelihood of B uptake by plants. The results of the second cultivation showed a linear growth and accumulation of B by plants when using $Mg_2Al$-B-LDH, indicating a more gradual release of B in the soil solution.

## REFERENCES


[1]. Castro GF, Ferreira JA, Eulálio D, de Souza SJ, Novais SV, Novais RF, Pinto FG, Tronto J. Layered double hydroxides: matrices for storage and source of boron for plant growth. Clay Minerals. 2018;1–27.

[2]. Abat M, Degryse F, Baird R, Mclaughlin MJ. Slow-release boron fertilisers: Co-granulation of boron sources with mono- ammonium phosphate ( MAP ). Soil Research. 2015; 53:505–511.

[3]. Benício LPF, Constantino VRL, Pinto FG, Vergutz L, Tronto J, Costa LM. Layered Double Hydroxides: New Technology in Phosphate Fertilizers Based on Nanostructured Materials. ACS Sustainable Chemistry & Engineering. 2017; 5:399-409.



***Acknowledgments:*** FAPEMIG, CAPES and CNPq.

# LAYERED DOUBLE HYDROXIDES AND SODIUM ALGINATE: FERTILIZER FOR CONTINUED RELEASE OF BORON

**CASTRO G. F. [1], FERREIRA J. A.[2], COSTA I. A. M..[1] FERNANDES C. N..[1], ZOTARELLI L..[3], MATTIELLO E. M..[1], TRONTO.J. [2]**

[1.] Federal University of Viçosa, Department of Soils, Viçosa - MG, Brazil. gustavofcastro@ymail.com
[2.] Federal University of Viçosa, Institute of Exact and Technological Sciences, Rio Paranaíba Campus, Rio Paranaíba - MG, Brazil. jaderalves@ufv.br
[3.] University of Florida, Horticultural Sciences Department, 1241 Fifield Hall, Gainesville – Florida, United States of America. E-mail: lzota@ufl.edu

## ABSTRACT

The production of sustained release fertilizers is a current alternative for the slower delivery of nutrients to plants, and also to reduce leaching losses to the environment. The production of microspheres of layered double hydroxides (LDHs) and sodium alginate is a viable option to obtain new fertilizers with delayed release of nutrients. The objectives of this study were to evaluate the "*in vitro*" release and boron (B) leaching from soil incubation of two sources of B, $H_3BO_3$ and microspheres produced in combination of LDH and sodium alginate. Synthesis microspheres of sodium alginate and LDH intercalated with B (LDH-B-ALG) was performed by the complex coacervation method. The study of the "*in vitro*" release and leaching of B in soil columns was performed by comparing the effect of two sources ($H_3BO_3$ and LDH-B-ALG) at different solution pH (5.5 and 7.5) and contact time. After 1 hour of contact between source and solution, $H_3BO_3$ released 100 % of the B present in its structure and LDH-B-ALG released on average 9 %, for both solution pHs. In the leaching study, the release of B by LDH-B-ALG was lower than $H_3BO_3$ in all contact times between source and soil in soil pH 6.5 and 7.5. Within 20 days of incubation, 100 % of B from $H_3BO_3$ and 50 % of B from LDH-B-ALG was leached. The low solubility and leaching potential of LDH-B-ALG used as source of B represents advantage in the use of in comparison to $H_3BO_3$.

Keywords: microspheres, LDH matrix, leaching, micronutrient.

## INTRODUCTION

Synchronized supply of nutrients with plant growth may increase fertilizer use efficiency by plants and reduces leaching losses to the environment. The production of microspheres of layered double hydroxides (LDHs) and sodium alginate is a viable option to obtain new fertilizers with delayed release of nutrients [1]. The combination of LHDs with the sodium alginate polymer, forming microspheres, can increase the efficiency of the product obtained. The objectives of this study were to evaluate the "*in vitro*" release and boron (B) leaching from soil incubation of two sources of B, $H_3BO_3$ and microspheres produced in combination of LDH and sodium alginate.

## MATERIALS AND METHODS

Synthesis microspheres of sodium alginate and LDH intercalated with B **(**LDH-B-ALG**)** was performed by the complex coacervation method [2]. The "*in vitro*" release study was performed in a 5.5 and 6.5 pH solutions and progressive contact times between source and solution (0; 1; 2; 4; 6 and 12 hours). The B leaching study in soil columns was conducted according to the method described by Abat et al [3], the release of B was analyzed in 6.5 and 7.5 soil pH incubated during 1; 5; 10; 15; 20; 25 and 30 days. The released of B from LDH-B-ALG was compared to a soluble source, $H_3BO_3$.

## RESULTS AND DISCUSSION

The release of B in solution at time 0, immediately after contact between source and solution at pH 5.5 was 4.1 % from B for $H_3BO_3$ and 0.7 % for LDH-B-ALG. After one hour of contact the $H_3BO_3$ was completely solubilized releasing 100 % of B in solution, while the release of B from LDH-B-ALG was 10 %, and 91 % after 12 hours of contact. There was no difference in B release at pH 7.5 and 5.5. Benicio et al. [4] reported a lower release of phosphorus by LDH because of the lamellar compounds compared to super triple superphosphate source.

The levels of B leached for LDH-B-ALG were lower than $H_3BO_3$ both soil pHs. Within one day of incubation, the release of B by $H_3BO_3$ was 37 %, and for LDH-B-ALG was 2 %. Within twenty days of incubation all B from $H_3BO_3$ was release to the soil solution and recovery in the leachate. After thirty days of incubation, 74 % of the total B from LDH-B-ALG was recovered. There was an effect of pH on B release. B leaching from both sources was lower at pH 7.5 than pH 6.5. These results suggest a higher formation of borate anions at alkaline pH, which resulted in a higher affinity with the solid phase of the soil.

## CONCLUSIONS

The results of B "in vitro" release and leaching by the sources suggest for LDH-B-ALG, a slow and continued release characteristics. Future research using the LDH-B-ALG microspheres as B source of nutrients to plants is needed.

## REFERENCES


[1] Castro GF, Ferreira JA, Eulálio D, de Souza SJ, Novais SV, Novais RF, Pinto FG, Tronto J. Layered double hydroxides: matrices for storage and source of boron for plant growth. Clay Minerals. 2018;1–27.

[2] Zhang Y, Liang X, Yang X, Liu H, Yao J. An eco-friendly slow-release urea fertilizer based on waste mulberry branches for potential agriculture and horticulture applications. ACS Sustainable Chemistry & Engineering. 2014; 2:1871-1878.

[3] Abat M, Degryse F, Baird R, Mclaughlin MJ. Slow-release boron fertilisers: Co-granulation of boron sources with mono- ammonium phosphate ( MAP ). Soil Research. 2015; 53:505–511.

[4] Benício LPF, Constantino VRL, Pinto FG, Vergutz L, Tronto J, Costa LM. Layered Double Hydroxides: New Technology in Phosphate Fertilizers Based on Nanostructured Materials. ACS Sustainable Chemistry & Engineering. 2017; 5:399-409.



***Acknowledgments:*** FAPEMIG, CAPES and CNPq.

***Self-templating synthesis of 3D hierarchical $NiCo_2O_4$@NiO nanocage catalyst for toluene oxidation from hydrotalcites***

**SHUANGDE LI., YUNFA CHEN**

State Key Laboratory of Multiphase Complex Systems, Institute of Process Engineering, Chinese Academy of Sciences, Beijing 100190, PR China, sdli@ipe.ac.cn, State Key Laboratory of Multiphase Complex Systems, Institute of Process Engineering, Chinese Academy of Sciences, Beijing 100190, PR China, chenyf@ipe.ac.cn.

## ABSTRACT

Rational design layered double hydroxides (LDHs) with 3D hierarchical hollow structures due to high complexity in shell architecture and composition have attracted tremendous interest for catalytic oxidation. Herein, we reported a facile two step method to fabricate a 3D hierarchical $NiCo_2O_4$/NiO nanocage using zeolitic imidazolate framework-67 (ZIF-67) as both a precursor and a self-sacrificing template, which contains in situ transformation of ZIF-67 into Co-NiLDH yolk-shelled structures following calcination. CoNi-yh-T (varied reaction time and calcination temperature) nanocages were investigated systematically by BET, XPS, H2-TPR, $NH_3$-TPD and studied for toluene oxidation. The CoNi-6h-350 sample possessed much higher activity with 90% toluene conversion (T90) at 229°C at a high space velocity (SV = 60 000 ml $g^{-1}$ $h^{-1}$) than other catalysts (T90 >240ºC). Abundant surface high valence Co ions due to the novel hierarchical nanostructures played key role for catalytic activities, together with adsorbed oxygen species and abundant medium-strength surface acid sites.

Keywords: layered double hydroxides; self-templating synthesis; catalytic oxidation;

## RESULTS

A series of hollow structured catalysts with high surface area and small size have been successfully fabricated on layered double hydroxide @zeolitic-imidazolate-framework-67 (LDH@ZIF-67) precursors. In order to accurate control of the balance between the rates of ZIF-67 template etching and CoNi-LDH formation, we take reaction time into consideration to attain perfect hollow dodecahedral structured precursors. The reaction time and calcination temperature will influence the textural and catalytic properties (Fig 1a). Among the samples, the CoNi-6h-350 sample exhibits best toluene oxidation performance. The CoNi-6h-350 in Fig1b, shows 3D hierarchical architectures, with uniformly distributed nanosheets of several hundreds of nanometers width interconnecting with each other to form a free-standing irregular mesh configuration.

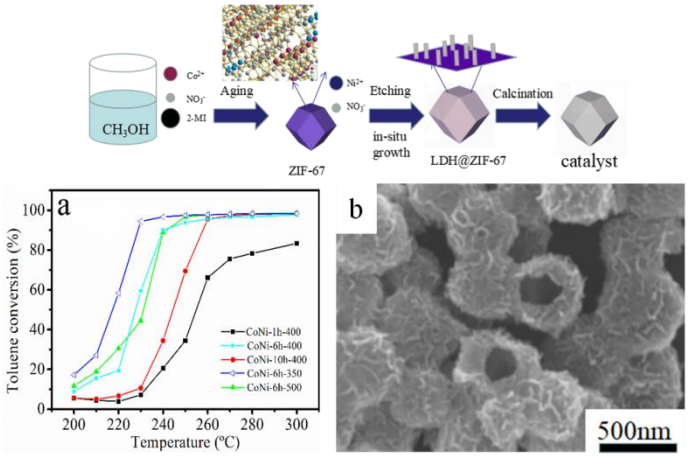

Fig.1 scheme of synthetic route, a) toluene conversion as a function of temperature, toluene =200 ppm, space velocity =60000 ml $g^{-1}$ $h^{-1}$, b) SEM image of CoNi-6h-350.

X-ray photoelectron spectroscopy (XPS) shown in Table 1 indicate that a higher Co species concentration in catalysts surface, which is beneficial for more active site exposed [1]. It can be explained that much high valence $Co^{3+}$ existed in CoNi-6h-350 catalyst, induce more surface oxygen vacancies, therefore $O_{ads}/O_{latt}$ ratio higher than other samples. Following the Mars-van Krevelen mechanism, surface oxygen vacancies plays an important role in toluene reactions, since the oxygen vacancies on catalyst surface may accelerate the adsorption and dissociation of oxygen molecules, resulting in the formation of highly active electrophilic oxygen molecules to attack nucleophilic toluene, which can totally increase catalyst activity.

Table 1 Physical characterization, catalytic activities, and surface elemental compositions of the samples

| sample | BET surface area ($m^2g^{-1}$) | Total pore volume ($cm^3g^{-1}$) | $T_{90}$(ºC) | Ni/Co | | $O_{ads}/O_{latt}$ | $Co^{3+}/Co^{2+}$ | $Ni^{3+}/Ni^{2+}$ |
|---|---|---|---|---|---|---|---|---|
| | | | | EDX | XPS | | | |
| CoNi-1h-400 | 85.5 | 0.66 | >300 | 2.1 | 1.1 | 1.04 | 0.61 | 2.28 |
| CoNi-10h-400 | 126.3 | 0.95 | 259 | 2.7 | 2.1 | 0.90 | 0.67 | 2.09 |
| CoNi-6h-400 | 98.4 | 0.67 | 240 | 2.0 | 1.8 | 1.01 | 0.82 | 2.28 |
| CoNi-6h-350 | 141.6 | 0.91 | 229 | 2.5 | 1.9 | 1.32 | 1.05 | 2.25 |
| CoNi-6h-500 | 64.9 | 0.30 | 244 | 2.8 | 1.6 | 1,30 | 0.56 | 2.20 |

**Citations and References**

[1] S. Mo, S. Li, J. Li, Y. Deng, S. Peng, J. Chen, Y. Chen, Nanoscale 8 (2016) 15763-15773.

# SIMPLE THERMAL REDUCTION OF GRAPHENE OXIDE

**ANA PAULA BENEVIDES, DEBORAH VARGAS CESAR**

Universidade do Estado do Rio de Janeiro, Rua São Francisco Xavier, 524, Maracanã, Rio de Janeiro – RJ, 20550-013, Brasil, ana.benevides@uerj.br, dvargas@uerj.br

## ABSTRACT

Reduced graphene oxide (RGO) was obtained by reducing graphene oxide (GO) using a thermal route. In this study, the thermal reduction of GO was evaluated to obtain RGO samples using a conventional muffle furnace, available in any laboratory. The proposed method is simple and has scalability. Two different drying temperatures for GO (60 and 150 °C), two different reduction temperatures (500 and 600 °C) and methods, named *standard* and *instantaneous*, were used. The evaluation of the samples by infrared spectroscopy indicated different reduction degree of the samples. GO precursor dried at 150 °C followed by the reduction at 600 °C exhibited the best degree of reduction, and scanning electron microscopy images revealed the formation of sheets of RGO with an average size of 120 μm.

Keywords: reduced graphene oxide; thermal reduction; characterization.

## INTRODUCTION

Graphene and graphene-based nanocomposites have received considerable attention from different areas, due to its unique properties. Typically, graphene is obtained by the reduction of graphene oxide, and the number of stacked sheets defines the material as graphene or RGO[1]. Among the different routes to obtain graphene, the thermal reduction is simpler and does not require toxic reagents[2]. Besides, it can be used for a large quantity of material. In general, the process uses a tubular furnace inserting the sample into the preheated furnace at the reduction temperature for a short time (as 30 s)[3] or by starting at room temperature and heating with a specific rate (as 5 °C/min)[2,4]. Studies in literature usually analyze different reduction temperatures, but do not compare these two different methods of heating. Thus, in this work, we present the evaluation of a different way to obtain RGO by thermal reduction using a conventional muffle furnace. Different conditions of drying and calcination temperature were applied to obtain the best condition to produce RGO by thermal treatment. The infrared spectroscopy (FTIR) and scanning electron microscopy (SEM) were used to evaluate the reduction process and the morphology of the samples synthesized.

## METHODOLOGY

Graphene oxide was obtained from Graflake 9950 (kindly provided by Nacional de Grafite) using the modified Hummers method[5]. The different reduction conditions tested are summarized in Table 1. The samples were named as RGO-**$T_d$Mt** where ***$T_d$*** is the drying temperature, ***M*** is the reduction method (**S**: standard; **I**: instantaneous) and ***t*** the time (in seconds) that the sample stayed in the reduction temperature into the furnace (Jung, model LF 00613). Samples were characterized by Fourier transform infrared spectroscopy (FTIR) using the spectrometer Spectrum One (Perkin Elmer), with

an accessory of attenuated total reflectance, 4 $cm^{-1}$ resolution; and by scanning electron microscopy (SEM), using a Jeol JSM-6701F (20 kV), without metal coating.

Table 1 - Reduction conditions of GO.

| RGO | $T_d$ (3 h) | Reduction method | Furnace temperature | Time |
|---|---|---|---|---|
| RGO-60**S**60 | 60 °C | *Standard* (30°C/min) | 600 °C | 60 s |
| RGO-50**S**60 | 150 °C | *Standard* (30°C/min) | 600 °C | 60 s |
| RGO-60**I**10 | 60 °C | *Instantaneous* | 600 °C | 10 s |
| RGO-150**I**10 | 150 °C | *Instantaneous* | 600 °C | 10 s |
| RGO-150**S**600* | 150 °C | *Standard* (30°C/min) | 500 °C | 600 s |
| RGO-150**I**60 | 150 °C | *Instantaneous* | 600 °C | 60 s |

(*) Reduction temperature of 500 °C

## RESULTS AND DISCUSSION

Results of infrared spectroscopy of GO showed characteristics bands corresponding to C=O, C-OH, and C-O-C of oxygen-containing groups introduced in the graphite structure[6]. The spectra of RGOs 60**S**60, 150**S**60, 150**I**10, 150**S**600* and 150**I**60 exhibited a decrease in the intensity of these bands, which suggests GO reduction. However, sample RGO-60**I**10 did not show any degree of reduction. Samples 150**S**60 and 150**S**600* exhibited a higher degree of reduction. Comparing RGO-60**S**60 with RGO-150**S**60 and RGO-60**I**10 with RGO-150**I**10, we concluded that the higher drying temperature favored a greater degree of reduction, which agrees with the literature[7]. The presence of water could delay the heating process, having a negative role in the thermal exfoliation and reduction process[7]. Comparing RGO 150**S**60 to RGO 150**I**10, the *standard* method favored a higher degree of reduction, showing that some oxygenated groups take more time to be reduced. SEM images of RGO-150**S**60 showed a lamellar morphology and sheets with an average size of 120 μm. RGO-60**I**10 that had a lower degree of reduction presented a morphology more similar to the GO precursor.

## CONCLUSIONS

Drying GO at 150 °C followed by the *standard* method of reduction at 600 °C in the muffle furnace favored the highest degree of reduction (samples RGO-150**S**60 and RGO-150**S**600*). The proposed method is simple and does not need a special furnace.

### Citations and References


1. International Union of Pure and Applied Chemistry. *Compendium of Chemical Terminology*. (IUPAC, 2014).
2. Botas, C. *et al. Carbon N. Y.* 52, 476–485 (2013).
3. McAllister, M. J. *et al. Chem. Mater.* 19, 4396–4404 (2007).
4. González, Z. *et al. Carbon N. Y.* 50, 828–834 (2012).
5. Hummers, W. S. & Offeman, R. E. *J. Am. Chem. Soc.* 80, 1339 (1958).
6. Guerrero-contreras, J. *Mater. Chem. Phys.* 153, 209–220 (2015).
7. Schniepp, H. C. *et al. J. Phys. Chem. B* 110, 8535–8539 (2006).

# LAYERED DOUBLE HYDROXIDES: STUDIES ABOUT INTERCALATION AND RELEASE OF *N*-ACETYL-L-CYSTEINE

**EULÁLIO D.[1], TAVIOT-GUEHO C.[2], LEROUX F.[2], FARIA D.L.A.[1], CONSTANTINO V.R.L.[1]**

[1.] Departamento de Química Fundamental, Instituto de Química, Universidade de São Paulo - USP, Av. Prof. Lineu Prestes 748, CEP 05508-000, São Paulo, SP, Brazil, deniseeulalio.de@usp.br, dlafaria@iq.usp.br, vrlconst@iq.usp.br

[2.] Université Clermont Auvergne, Institut de Chimie de Clermont-Ferrand, BP 10448, F-63000 Clermont-Ferrand, France, christine.taviot-gueho@uca.fr, fabrice.leroux@uca.fr

## ABSTRACT

This work aims the synthesis and characterization of a Layered Double Hydroxide (LDH) intercalated with N-acetyl-L-cysteine (NAC), an antioxidant species, as well as the investigation of *in vitro* release of the organic guest through two different methods (dynamic and static), in a simulated extracellular matrix fluid. LDH hybrid material was prepared by the coprecipitation method (abbreviated $Zn_2Al$-NAC) and characterized by X-ray diffraction (XRD), mass coupled thermal analyses (TG-MS), Fourier transform infrared (FT-IR) and Raman (FT-Raman) spectroscopies, scanning electron microscopy (SEM), and $^{13}C$ and $^{27}Al$ solid state NMR spectroscopy. XRD pattern of $Zn_2Al$-NAC showed basal spacing related to (003) plane of 16.3 Å, corresponding to a bilayer arrangement between the layers. Hybrid sample has flat-shaped particles and 27.4 wt% of NAC. TG-MS data indicated the $Zn_2Al$-NAC dehydroxylation at about 330ºC and the begin of $CO_2$, $NO_2$ and $SO_2$ release at 660ºC. NAC thermal stability is enhanced when in LDH confined structure. Spectroscopic data indicated the deprotonation of the carboxylic ($COO^-$ stretching modes at 1566 and 1392 $cm^{-1}$) and the thiol groups (absence of S-H stretching band), and along with $^{13}C$ NMR results, attested the chemical integrity of NAC after intercalation. $^{27}Al$ NMR spectrum showed an asymmetric peak assigned to more than one Al octahedral site. *In vitro* tests using $Zn_2Al$-NAC tablets suggested a modified (prolonged) guest release: 20-35 % after 96 h considering both used methods. The cations lixiviation was minimum (0.2% of zinc; aluminum was not detected). $Zn_2Al$-NAC hybrid material presents potential for application in the medicinal and agronomic fields.

**Keywords:** Layered Double Hydroxides, N-acetyl-L-cysteine, antioxidant.

## INTRODUCTION

LDHs comprises an extensive class of natural and synthetic materials, which structures and properties are often compared to those of the hydrotalcite mineral [1]. NAC is a L-cysteine derived amino acid (Figure 1) applied as mucolytic agent, in the treatment of paracetamol intoxication and in the control of the formation of bacterial biofilms caused by the bacterium *Xylella fastiodiosa* [2]. However, NAC presents a very low bioavailability (from 4 to 10%). The aim of this work is to investigate the intercalation and delivery of the antioxidant NAC into the LDH with zinc-aluminum composition ($Zn_2Al$-NAC).

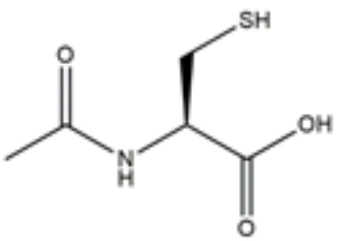


Figure 1 – Molecular structure of NAC.

## EXPERIMENTAL

$Zn_2Al$-NAC were synthesized by the coprecipitation method and characterized by structural, spectroscopic, thermal, textural and elemental chemical analysis. The release of the intercalated NAC was assessed by *in vitro* experiments in simulated biological medium, applying both the dynamic and static methods.

## RESULTS AND DISCUSSION

X-ray diffraction patterns presented $d_{003}$ basal spacing of 16.3 Å, suggesting a bilayer arrangement of the antioxidant species between the layers. Imagens from scanning electron microscopy showed the presence of flat particles with low degree of aggregation. $Zn_2Al$-NAC IR spectrum presented bands at 1566 ($\nu_{as}$ $COO^-$) and 1392 $cm^{-1}$ ($\nu_s$ $COO^-$); Raman spectrum showed bands at 2932 ($\nu$ CH), 1642 ($\nu$ C=O of amide group), 1429 ($\delta$ $CH_2$), 1399 ($\nu_s$ $COO^-$), 683 ($\nu$ CS) and 124 $cm^{-1}$ ($\delta$ O-Zn-O). S-H stretching band is absent in the vibrational spectra. The differences ($\Delta$) between the position of the bands related to the antisymmetrical and symmetrical stretching of the carboxylate group, $\Delta(COO^-)$, observed for $Zn_2Al$-NAC and for isolated sodium NAC salt at pH 11.0 were equal to 182 and 174 $cm^{-1}$, respectively, which can indicate a coordination of carboxylate group to the matrix layers as a bidentate ligand. However, a smaller value of $\Delta(CO_2^-)$ for the salt in comparison with the intercalated NAC does not always confirm a bidentate coordination. As it is observed for the $Cu_2(OH)_3CH_3COO$ mineral, acetate $\Delta(CO_2^-)$ increases after intercalation but crystal X-ray analysis showed a monodentate coordination. This behavior has been explained due to the hydrogen bonding between the neighboring hydroxyl and the free oxygen of the coordinated carboxylate [3].

The results of vibrational spectroscopy and $^{13}C$-NMR attested the structural integrity of the NAC after intercalation and suggest that the deprotonation of the carboxylic and thiol groups occurred. The layers presented distinct sites of hexacoordinate aluminum, according to the $^{27}Al$-NMR spectrum.

The set of characterization techniques indicates the partial substitution of hydroxide ions coordinated to the layers metal cations for the oxygen of NAC carboxylate group. From thermal and elemental analysis, it was proposed the following formula: $[Zn_{2.04}Al(OH)_{5.72}(C_5H_7NO_3S)_{0.18}]$ $(C_5H_7NO_3S)_{0.50}\cdot 1.6H_2O$. *In vitro* assay suggested a modified (prolonged) NAC release, since 35% of the antioxidant was released along 96 h applying the dynamic method, in contrast with 20% of release in the static approach. Raman stratigraphic analyzes of the tablets after the release test showed that ion exchange occurred only in its external regions after 96 h, evidenced by the appearance of a band at 973 $cm^{-1}$ assigned to stretching of $HPO_4^{2-}$ anions.

## CONCLUSION

$Zn_2Al$-NAC material presented potential for application in the medicinal and agronomic fields, once the antioxidant intercalation occurred in a satisfactory amount, and the application of LDH as a host propitiated a NAC modified release profile (prolonged).

## References


[1] Cavani, F.; Trifirò, F.; Vaccari, A. *Catal. Today* 1991, *11*, 173.
[2] Muranaka, L. S.; Giorgiano, T. E.; Takita, M. A.; Forim, M. R.; Silva, L. F. C.; Coletta-Filho, H. D.; Machado, M. A.; de Souza, A. A. *PLoS One* 2013, *8*, 1.
[3] Pereira, D. C.; Faria, D. L. A.; Constantino, V. R. L. *J. Braz. Chem. Soc.* 2006, *17*, 1651.

# DFT STUDY OF THE ACTIVATED MONTMORILLONITE AS SOLID ACID CATALYSTS IN BIODIESEL PRODUCTION CONTEXT

**CARLA G. FONSECA[1], VIVIANE S. VAISS[1], FERNANDO WYPYCH[2], WLADMIR F. SOUZA[3], SANDRA S.X. CHIARO[3], ALEXANDRE A. LEITÃO[1]**

[1]Departamento de Química, Universidade Federal de Juiz de Fora, Juiz de Fora, MG, 36036-330, Brazil. carla.grijo@ice.ufjf.br, vivianevaiss@ice.ufjf.br, alexandre.leitao@ufjf.edu.br

[2]CEPESQ – Research Center in Applied Chemistry – Departamento de Química, Universidade Federal do Paraná, P.O. Box 19032, 81531-980 Curitiba, PR, Brazil. wypych@ufpr.br

[3]PETROBRAS-CENPES, Rio de Janeiro, RJ 21941-915, Brazil. *wladmir@petrobras.com.br, sandrachiaro@petrobras.com.br*

## ABSTRACT

Heterogeneous catalysis based on clays such as Montmorillonite (Mt) has received considerable attention due to their environmental compatibility, low cost, selectivity, thermal stability and recyclability. The Mt is classified as a 2:1 mineral clay and many important properties of the Mt arise from their surface chemistry especially when this material is submitted to an acid activation process with inorganic acids (HCl, $H_2SO_4$ and $H_3PO_4$)[1].. The acid activation preferentially occurs on the edge surfaces, in this sense *ab initio* calculations were performed in order to determinate the most probable models for (010) and (110) surfaces. After, the acid-activated Mt surfaces were simulated and the reactivity of the surfaces was estimated. The calculations indicated that the acid character of the acid-activated Mt mainly comes from the H sites present in silanol and aluminol groups. The microstructural evolution of the Mt during the acid activation was investigated by $^{29}Si$ and $^{27}Al$ NMR simulations and these calculations could assist in the correct assignment of the silicon and aluminum chemical environments. The catalytic activity of the acid activated Mt was evaluated by means of esterification reaction and the reaction barriers were obtained for both surfaces. The dependence between the Gibbs free energy variation with the temperature can also be computed.

Keywords: Cationic Clay, Montmorillonite, Acid Activation, Biodiesel, Catalysis

## INTRODUCTION

Acid activation is a chemical treatment, typically used on clay minerals such as kaolinite, halloysite, and montmorillonite (Mt) in order to obtain materials with enhanced surface properties toward environmental, technological and industrial applications[2]. The resulting compounds present high surface area, pore volume and density of Lewis and Brönsted sites. Acid-activated Mt has proved to be effective catalysts in the methyl or ethyl esterification of free fatty acids (FFA) to obtain Biodiesel, a biodegradable and environment friendly fuel from effective renewable sources[1]. Crystallographic planes that contribute predominantly to Mt edge surfaces are (010) and (110) and they are the catalytically active plans in these applications. In the present work, a comprehensive DFT study on the edge surfaces of the acid-activated Mt is introduced in order to evaluate the reaction mechanism of the solid acid-catalyzed esterification of acetic acid.

The quantum mechanical calculations were performed using the codes available in Quantum ESPRESSO (QE) package[3]. Electronic structure calculations were based on density functional theory (DFT) implemented with periodic boundary conditions using plane wave functions as basis set. The electronic correlation and exchange terms were employed using GGA-PBE.

**RESULTS**

The acid-activated Mt surfaces were simulated, and the reactivity of the surface sites was checked by means of $NH_3$ adsorption. The results confirm the greater acidity of the sites from the (110) surface compared to (010) surface sites. The PDOS analysis showed that the acid character of the edge surfaces manly arises from the H sites in Si-OH and Al-OH groups. By means of NMR simulation of $^{27}Al$ and $^{29}Si$ it was possible to characterize both the $Al^{IV}$ and $Al^{V}$ sites on the edge surfaces in accordance with the propositions made in literature[2]. Based on the adsorption energies, we can infer that the esterification mechanism begins with the adsorption of acetic acid. The adsorption energy of acetic acid was the most negative, thus it is favored over the methanol.

Table 1: Adsorption energies of the reactants of the esterification reaction. The figure corresponds to the structure and charge density difference of the acid acetic adsorption.

| | (010) | (110) |
|---|---|---|
| Reactants | ΔE / kcal mol$^{-1}$ | ΔE / kcal mol$^{-1}$ |
| Methanol | -17.97 | -17.10 |
| Acetic acid | -23.31 | -25.38 |

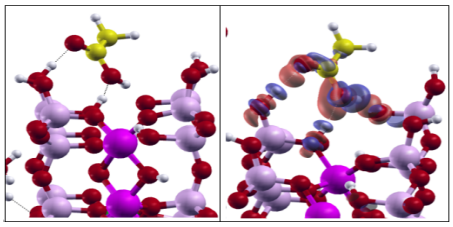

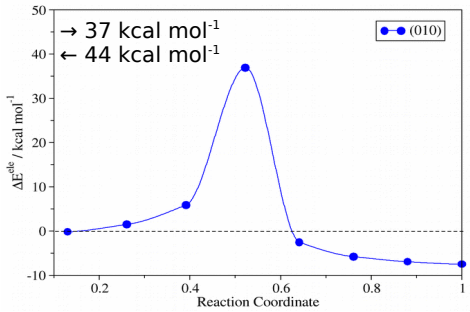


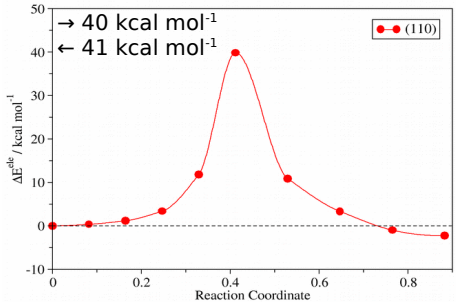


The figures above show the reaction paths (simulated using CI-NEB method) calculated for the esterification reaction from the adsorbed reactants on both edge surfaces. It was found that the reaction proceeds through a concerted mechanism with a single transition state (TS) and without the formation of a intermediate. It is expected that more extensive acid treatments can be better for catalysis applications. These calculations are being made.

**Support:** This work has been supported by CAPES, CNPq, FAPEMIG, Brazilian agencies and the enterprise Petrobras S/A (CENPES). We also acknowledge the CENAPAD-SP computational center.

**Citations and References**

[1] L. Zatta, L. P. Ramos, F. Wypych, App. Clay Sci., 80-81, 231, (2013).
[2] Fonseca, C.G.; Leitão, A.A.; *et al.*, App. Clay Sci. 170-178, 165, (2018).
[3] P. Giannozzi, S. Baroni, N., *et al.*, J. Phys. Condens. Matter., 21, 395502, (2009).

# Simulation, structure and properties of Li-Al-X (X= $Cl^-$, $Br^-$, $F^-$, $I^-$, $OH^-$, $NO_3^-$) hydrotalcite-like compounds by *ab inito* methods.

**ANNA CAROLINA DE A. BARBOSA[1], CARLA G. FONSECA[1], FERNANDO WYPYCH[2], ALEXANDRE A. LEITÃO[1]**

*[1]Chemistry Department, Federal University of Juiz de Fora, 36036-330, Juiz de Fora, MG, Brazil, annacarolina@ice.ufjf.br, carla.grijo@ice.ufjf.br, alexandre.leitao@ufjf.edu.br.*
*[2]CEPESQ – Research Center in Applied Chemistry – Chemistry Department, Federal university of Paraná, P.O. Box 19032, 81531-980 Curitiba, PR, Brazil, wypych@ufpr.br.*

## ABSTRACT

An important aspect in the layered double hydroxides (LDH) synthesis is the nature of the cations in the formula $M^{+2}_{1-x}M^{+3}_x(OH)_2(A^{-n})_{x/n}.yH2O$. Since the preparation of a new compound is based on the partial isomorphic substitution of the metal $M^{+2}$ by $M^{+3}$, the difference between the atomic radius cannot be very large[1]. It is known from the literature that a family of LDH is structurally related to the Gibbsite ($Al(OH)_3$). In Gibbsite structure, the layers are formed by octahedral aluminum sites coordinated by hydroxide anions at the vertices, occupying two-thirds of the octahedral sites. The alternance between occupied site and vacancy creates a small deformation of the octahedra. As a result, the vacancy is slightly wider compared to the occupied site. The octahedral vacancies of the gibbsite layer have the diameter comparable to small cations such as $Li^+$, without large deformations, once the atomic radius of $Li^{1+}$ and $Al^{3+}$ are close. In this case, the generated charge is counterbalanced by anions and water molecules in the interlayer space[2]. The treatment of gibbsite with lithium chloride (LiCl) and water ($H_2O$) allows the formation of LDH with an unusual molecular formula $[LiAl_2(OH)_6]$ $Cl.pH_2O$. This *ab initio* study discusses the thermodynamics and the structural modifications derived from anion exchange on LiAlCl. The $Cl^-$ ion in the LDH precursor was exchanged for a series of anions, $F^-$, $Br^-$, $OH^-$, $I^-$ and $NO_3^-$. The Gibbs energy, the enthalpy and the charge density difference were also evaluated.

*Keywords: LDH, Ab initio calculation, anion exchange, NMR.*

## Introduction

Layered double hydroxides (LDHs) have attracted considerable interest due to their potential applications as selective adsorbents, hosts for drugs and biomolecules, precursors for ceramics and polymer nanocomposite[3]. The family of LDHs Li-Al-X is the only set of LDHs to contain $1^+$ and $3^+$ cations. In this case the $Li^+$ cations occupy the octahedral vacancies within $Al(OH)_3$ layers, resulting in a positively charged layer. The interlayer anion ensures the charge balance. In the hydrated structures the water molecules form hydrogen bonds with the anion and layer hydroxyls. The understanding of the influence of different interlayer anions in the LDH structure have great importance to help on theoretical planning for technological applications, since the intercalation behavior is important in many processes[4].

All the calculations were performed using the Quantum ESPRESSO (QE) package[3]. Electronic structure calculations were based on density functional theory (DFT) implemented with periodic boundary conditions using plane wave functions as basis set. The electronic correlation and exchange terms were employed using GGA-PBE.

Interaction of valence electrons with nuclei and core electrons were treated by the projector augmented-wave (PAW) method [5].

## RESULTS AND DISCUSSION

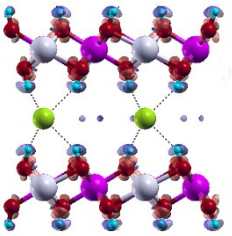

The objects of the study were both the dehydrated and hydrated structure of the layered double hydroxide Li-Al-X. We chose Li-Al-Cl as a precursor because *ab initio* calculations have shown a good reproducibility on the geometric parameters with a margin of error less than 3%. The $Cl^-$ anions share a single set site and have hydrogen bonds with the OH groups in the adjacent layers and with interlayer water molecules on the dehydrated and hydrated structures respectively.

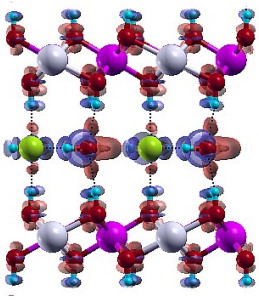

We investigated the possibility of the $^{27}Al$ and $^{7}Li$ nuclei having different NMR parameters in function of lithium arrangement in the layer and the chloride in the interlayer for the Li-Al-X (X= $Cl^-$, $Br^-$, $F^-$, $I^-$, $OH^-$, $NO_3^-$). $^{27}Al$ and $^{7}Li$ NMR spectra were simulated in a magnetic field of 7.04T. The references used were α-$Al(OH)_3$ for the $^{27}Al$ NMR and LiCl for the $^{7}Li$ one. On $^{27}Al$ NMR, the dehydrated structures have shown chemical shifts ranging between -4.05ppm and -8.27ppm while $^{7}Li$ NMR shows values between -5.02 and -5.84ppm. The same behavior was observed on the hydrated structures. While the $^{7}Li$ NMR showed chemical shifts between -5.32 and -5.83ppm, the values for $^{27}Al$ NMR was ranging between -4.55ppm and -6.28ppm. This result is interesting because while the substitution of the interlayer anion and the degree of hydration affect significantly the $^{27}Al$ spectra it does not happen to the $^{7}Li$ spectra.

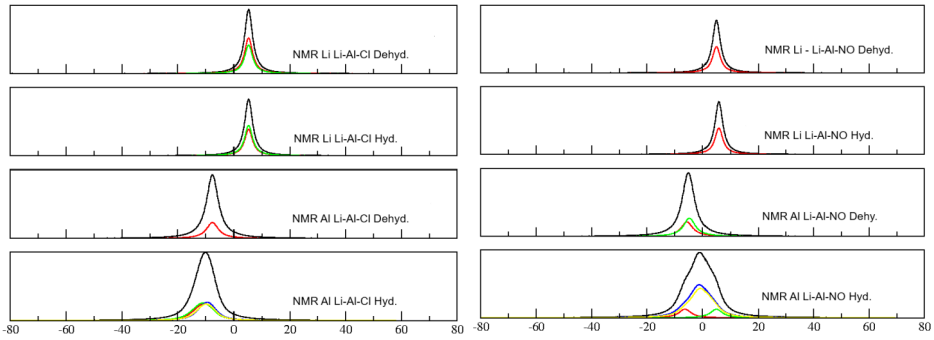


The figures above show the $^{27}Al$ and $^{7}Li$ simulated NMR for Li-Al-Cl and Li-Al-NO. The other monovalent anions spectra were also calculated, as well as their charge density difference. The free Gibbs energies related to thermodynamic study of exchange reactions were also calculated. The same calculations for the divalent anions $SO_4^{-2}$ and $CO_3^{-2}$ are being made.

**Support:** *This work has been supported by CAPES, CNPq, FAPEMIG, Brazilian agencies and the enterprise Petrobras S/A (CENPES). We also acknowledge the CENAPAD-SP computational center.*

### Citations and References

1. L. Crepaldi, *et al*., *Química Nova;***v.21**, 300 – 311, (1997)
2. V. P. Isupov, *et al*., *Journal of Structural Chemistry*; **v.39**, 362 – 366, (1998)
3. X. J. Hou, *et al*., *Applied Surface Science*, 416, 411-423 (2017)
4. D. G. Costa, *et al*, Applied Clay Science, **v.56**, 16-22 (2012)
5. P. Giannozzi, S. Baroni, N., *et al*., J. Phys. Condens. Matter., 21, 395502, (2009).

# Development of Novel Functionalized Synthetic Saponite Clays containing Ln(III) Ions

**S. MARCHESI[1], F. CARNIATO[1], M. BOTTA[1], L. MARCHESE[1], C. BISIO[1]**

[1]*Dipartimento di Scienze e Innovazione Tecnologica, Università degli Studi del Piemonte Orientale "Amedeo Avogadro", viale Teresa Michel 11, 15121-Alessandria, Italy*.
chiara.bisio@uniupo.it

## ABSTRACT

Synthetic layered clays of the family of smectites called saponites have stimulated particular interest over the past few decades due to their interesting properties, such as high thermal stability and excellent chemical versatility [1]. The introduction of *f*-block elements, as ions or complexes, in the clay framework may lead to the development of novel lamellar materials with interesting features such as electronic, magnetic, optical and catalytic properties.

Afterwards, we modified the hydrothermal synthetic method of saponites to introduce both $Gd^{3+}$ and $Eu^{3+}$ as ions directly into the inorganic framework, thus conferring both paramagnetic and luminescent properties to the final material (GdEuSAP, Figure 1). Samples containing only $Gd^{3+}$ or $Eu^{3+}$ ions have been prepared as references (GdSAP and EuSAP). The solids were submitted to a $Na^{+}$-exchange procedure to ensure a chemical uniformity of the exchange sites. The $Ln^{3+}$ loading in samples resulted to be 0.02 mmol/g. $^{29}$Al solid-state NMR showed that lanthanides tend to be incorporated more in the tetrahedral sites of the framework. The presence of lanthanides did not alter the general crystalline structure of saponite, as observed by XRD analyses, while SEM and TEM microscopies indicated the presence of different levels of spatial organization of lamellae, with a size of few ten nanometers. The luminescence spectrum of samples showed the characteristic peaks of the $Eu^{3+}$, with the presence of a $Gd^{3+}\rightarrow Eu^{3+}$ energy transfer process. The average hydration of the $Eu^{3+}$ ($q$), estimated through the radiative lifetimes ($\tau$) in $H_2O$ and $D_2O$, was found to be 4. The intrinsic quantum efficiency of $Eu^{3+}$ ($\Phi^{Eu}_{Eu}$) was establish to be 3.25% and 4.29% for Eu-SAP and Na-GdEuSAP, respectively, with high photostability under continuous irradiation. $1/T_1$ $^1$H-NMRD profiles of the aqueous suspensions showed the typical shape of slowly tumbling systems, with a broad hump at high magnetic fields and a maximum value of relaxivity ($r_1$) centered at 30-40 MHz, at 310 K. The $r_1$ is influenced by water diffusion phenomena through the interlayer, as suggested by the increase of $r_1$ with temperature. The suspensions were treated with EDTA ligand and no release of $Gd^{3+}$ ions in solution was observed in presence of high EDTA concentrations, demonstrating a high stability of the materials.

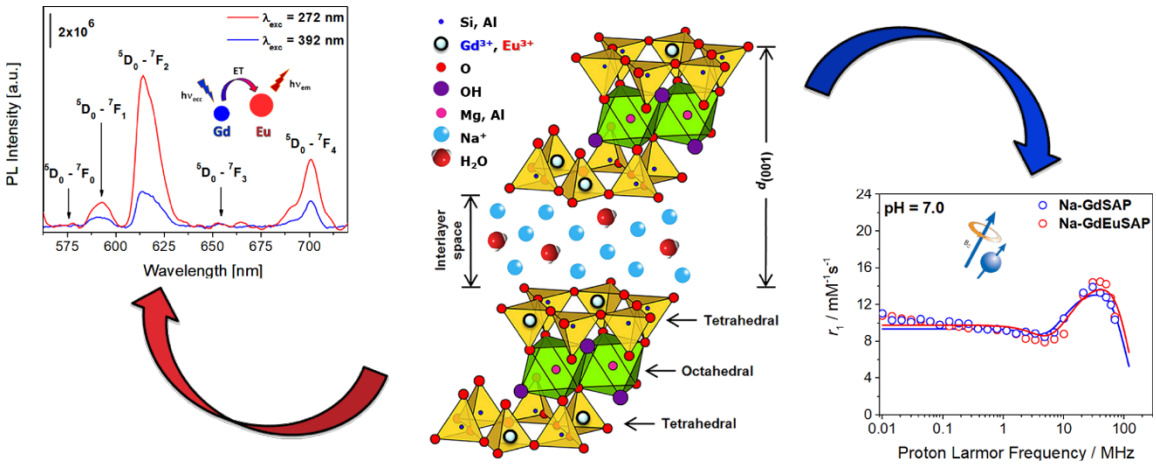


**Figure 1.** Luminescence and relaxometric properties of GdEuSAP sample.

**Keywords**

Saponite – Lanthanide – Intercalation – Luminescence – Relaxometry

## Citations and References

[1] D. Costenaro, G. Gatti, F. Carniato, G. Paul, C. Bisio and L. Marchese, M*icroporous and Mesoporous Materials*, **2012**, *162*, 159-167.

[2] S. Marchesi, F. Carniato, C. Bisio, L. Tei, L. Marchese and M. Botta, “Novel Paramagnetic Clays obtained through intercalation of $Gd^{3+}$-Complexes”. *Dalton Trans.*, **2018**, *47*, 7896-7904.

# Nanocomposites bentonite/titanium dioxide/niobium

**Bonfim, L.F., da Silva, T.H., Nassar, E.J., Ciuffi, K.J., de Faria, E.H.**

Universidade de Franca (UNIFRAN) - Grupo de Pesquisa em Materiais Lamelares Híbridos (GPMatLam), Av. Dr. Armando Salles Oliveira, 201, CEP 14.404-600, Franca, SP, Brasil.
larissa.fbonfim@outlook.com and/or emerson.faria@unifran.edu.br

## ABSTRACT

The goal of this work was the synthesis and characterization of nanocomposites bentonite/titanium dioxide doped with niobium oxide obtained via hydrolytic sol-gel methodology. The materials were several characterized by X-ray powder diffraction, ultraviolet/visible absorption spectroscopy, specific surface area analysis and cation exchange capacity. The presence of titanium dioxide on the bentonite surface could be verified after the calcination at 400 and 700ºC due the presence of the typical anatase phase. Is important remark that niobium oxide associated with clay mineral and $TiO_2$ semiconductor constitute a photocatalyst candidate to application under solar light because the absortion present a very broadner band confirming that clay mineral and niobium oxide could affect the band gap from semiconductor ($TiO_2$).

Keywords: clay minerals; semiconductor; niobium; photodegradation.

## Introduction

Conventional treatments are not effective for the removal of most of the contaminants from urban wastewater, so it's necessary to search for new materials that can oxidize these substances of interest. [1,2]. Among the different types of clays, the bentonite group, which consists in crystalline and lamellar particles, described as very thin, irregularly shaped or blades, disposed in a typical TOT (2:1) arrangement, constituted by two tetrahedral silica layers alternated by an octahedral Al, Fe and Mg hydroxyl layers [3].

A variety of semiconductors have been tested in photo assist techniques, among them, $TiO_2$ has been the most widely used because of its unique properties such as high chemical stability, non-toxicity, biocompatibility and strong reduction power[4]. Niobium based materials have received greater attention in the field of heterogeneous catalysis, being studied as catalyst and catalyst support in important chemical reactions[5].

Thus, the goal of this work was to evaluate the synthesis and characterization of nanocomposites using bentonite, titanium dioxide doped with niobium oxide, using the sol-gel methodology to better recover the clay mineral surface. The influence of temperature annealing to photocatalyst was also evaluated. All the heterogenenous photocatalysts obtained will be further employed to treatment of emerging organic pollutants in aqueous medium.

## Experimental

The synthesis of nanocomposites was based on the work of Barbosa, et al[6]. For this, was kept under constant mechanical stirring for 24 hours, initially 40 g of bentonite in 800 mL of isopropanol, after an hour was added 4 mL of acetic acid, 8 mL of titanium isopropoxide (IV) and ammonium niobite (V) oxalate (5%/mol relate to titanium dioxide content). The suspension was then centrifuged, and oven dried at 80 ºC for 24 hours. The synthesis of the nanocomposites denominated bentonite-niobium was carried out in the same way, but without the addition of titanium isopropoxide (IV). The obtained materials

were shared in four fractions, one not receiving heat treatment while the other three fractions were calcined at 400, 700 and 1000 ºC for 24 hours in a muffle, with air atmosphere, where the annealing temperatures adopted for the heating treatment were based on the allotropic changes of the titanium for anatase rutile and brookite, respectively.

## Results and Discussion

The X-ray powder diffraction shown that the materials maintain their crystallinities up to 700 ºC, indicating the characteristic peaks close to the natural bentonite, was evidenced that the basal spacings were smaller until there was no more crystallinity in the materials. Effect explained due the water elimination after calcination from the cation presents on bentonite interlayer spaces. In materials calcined at 1000 ºC, was possible observe peaks of niobium oxide, titanium niobium oxide, and anatase and brookite phases of titanium dioxide between 22 and 39 2θ degrees, which is very close to that found in the literature[6,7,8] confirming the presence of semiconductors.

Ultraviolet/visible spectroscopy shown also the presence of more broadner bands in the solids containing titanium dioxide and niobium oxide; confirming that the wavelength range with maximum absorption increase using the clay minerals as support, this point suggest that photocatalysts could be efficient also using sun light due the displacement of the semiconductor band with maximum centered at 325 nm to the visible region [9].

Cation exchange capacity and specific surface area, shown that the materials with bentonite present higher values (near to 1300 $m^2/g$ for materials prepared only with niobium oxide versus 700 $m^2/g$ for materials with titanium dioxide and niobium oxide heated at 400º C), the clay is already positively charged, expandable and presents smaller particle size and could result in a good arrangement of dioxide recover on the surface. Thermal analysis, on DSC curves, confirms also that anatase was obtained at 600 ºC due the presence of exothermic peak at 600 ºC on the samples containing titanium dioxide [10,11].

## Conclusion

Sol-gel methodology was efficiently applied to prepare heterogeneous photocatalysts, the efficient recovery of the bentonite surfaces was proven by various techniques that confirms also the interaction between bentonite with the titanium dioxide and niobium oxides, as well as the change in the absorption range, displaced to the visible region, which makes the materials prepared herein promising photocatalyst under solar light excitation and also the higher specific superficial area values maintained including after annealing to 700ºC induces the higher capability to generate hydroxyls radical under aqueous solution.

## Citations and References


[1] Daughton, C.G., Ternes, T., A. **Environmental Toxicology**, v. 28, n. 12, p. 2663-2670, 2009.

[2] Malaj, E. et al. **Proceedings of the National Academy of Sciences**, v.111, n.26, p.9549-9554, 2014.

[3] Melo, S.A.S et al. **Química Nova**, v. 32, n. 1, p. 188-197, 2009.

[4] Liu, L., Chen, X. **Chemical Reviews**, v. 114, n. 19, p. 9890-9918, 2014.

[5] Sturt, N.R.M., Vieira, S.S, Moura, F.C.C. **Journal of Environmental Chemical Engineering**, v. 7, n. 1, p. 102866, 2019.

[6]Barbosa, L.V. et al. **Catalysis Today**, v. 246, p. 133-142, 2015.

[7] Lopes, O.F. et al. **Química Nova**, v. 38, n. 1, p. 106-117, 2015.

[8] Hwang, K., Sohn, H., Yoon, S. **Journal of Power Sources**, v. 378, p. 225-234, 2018.

[9] Lim, M. et al. **Electrochemistry Communication**, v. 11, n. 3, p. 509-514, 2009.

[10] Chen, Y., Wang, K., Lou, L. **Journal of Photochemistry and Photobiology A: Chemistry**, v. 163, n. 1-2, p. 281-287, 2004.

[11] Rahim, S. et al. **Applied Surface Science**, v. 351, p. 175-187, 2015.

# Synthesis of microspheres using kaolin chitosan and polyvinyl alcohol by mechanical dripping process

**Souza, S.D., Nassar, E.J., Ciuffi, K.J., de Faria, E.H.**

Grupo de Pesquisa em Materiais Lamelares Híbridos (GPMatLam), Universidade de Franca (UNIFRAN), Av. Dr. Armando Salles Oliveira, 201, CEP 14.404-600, Franca, SP, Brasil. Suelendsouza11@gmail.com e/ou emerson.faria@unifran.edu.br

**ABSTRACT**

The goal of the present work was the synthesis and characterization of microspheres using natural materials (kaolin with higher kaolinite content) and polymeric compounds (chitosan and polyvinyl alcohol - PVAL) that is a promising alternative to increase the absorption capacity of chemical compounds in water. The materials were prepared by inversion (acidic to basic medium) using a peristaltic pump to obtain spheres with regular size distribution in short interval times. Swelling tests were performed on the microspheres. All the solids were characterized by the techniques X-ray powder diffraction (XRD), infrared absorption spectroscopy (FTIR), cation exchange capacity (CEC) and scanning electronic microscopy analysis. Results obtained through the XRD proved the addition of the polymers in the kaolin resulting in a typical conventional composite due to the presence of the diffraction halo characteristic of the amorphous polymers and characteristic peaks profile of kaolin with very lower intensity. FTIR shown all the typical vibrations of the chitosan and confirm the effective interaction of PVAL and chitosan resulting in a polymeric blend, some typical kaolinite stretching are also observed at 3620, 3690 $cm^{-1}$.This bands are not displaced compared to original kaolin FTIR confirming that only surface interaction are obtained in this composites.

**Keywords:** Adsorbents, kaolin, microspheres, biodegradable polymers.

## Introduction

Adsorption is a very simple, clean and fast process commonly employed for the removal of metals, dyes, drugs and other toxic residues present in lower or higher concentrations in gas or liquid phase. On the nature different type of clays are responsible for control the mobility of metals and other anthropogenic wastes present in soils or water. In this context, adsorbents based on clay minerals present an efficient removal for cationic charged species. Different techniques could be employed to develop and accelerates the process of microspheres synthesis [1], as is the case of peristaltic pump dripping, in addition to standardizing the samples, aid in the large-scale preparation.

Chitosan is an excellent biosorbent for the removal of metal ions because it possesses a unique combination of properties (such as biodegradability, bioactivity, biocompatibility and non-toxicity) and is the richest and cheapest biopolymer in nature [2]. In this context PVAL is a biodegradable synthetic polymer that is especially noteworthy because of its transparency, strength and biocompatibility [3].

Kaolin is a mineral rich in kaolinite that is an aluminosilicate with a dioctahedral structure, composed of structurally asymmetric layers of type TO or 1: 1. Thus, the structure of kaolin is basically composed of a simple tetrahedral sheet of silica bonded to a single octahedral sheet of alumina with exposed oxygen on one side of the layer, and hydroxyls on the other. [4].

Thus, the goal of this works was the combination of the properties of inorganic materials (natural kaolin rich in kaolinite and humic substances) and biopolymers

(chitosan and PVAL) that could be a very efficient strategy to development materials with new properties.

## Experimental

For the preparation of the kaolin-chitosan (KQ) and kaolinite-chitosan-PVAL (KQPVAL) microspheres, the chitosan powder was first solubilized in a 5% (v/v) aqueous acetic acid solution, remaining under stirring for 24 hours, for the formation of KQPVAL microspheres, 25 mL of the PVAL solution was added to 25 mL of 2% (w/v) chitosan solution, remaining under constant stirring and heating at 60 ºC after this process 7 g of kaolin was deposited in the solution with constant mechanical stirring for 24 hours. The solution thus obtained was mechanically dripped onto an 8% (w/v) sodium hydroxide solution under vigorous magnetic stirring, yielding the microspheres by phase inversion. The microspheres were washed with distilled water to pH 7.5. In the final step, the wet microspheres were taken to the vacuum oven at 30 ºC.

## Results and Discussion

XRPD confirmed the addition of the polymers in kaolin due to the presence of the diffraction halo characteristic of the amorphous polymers. Scanning electron micrographs show that the texture of solids KQ shown the typical tactoids on the polymer surfaces is similar to that from original kaolin structures. Is possible observe some kaolin aggregates. However for solid KQPVAL the surface are completely distinct more smoothly confirming that PVAL induces the better interaction between kaolin and chitosan. The presence of PVAL produces the better adhesion of the surface of clay crystals. This aggregation effect evidenced by increasing on rugosity of surface is always higher for the materials containing only kaolin and chitosan, in which more spongy particles are observed. FTIR show that the bands at 1648 $cm^{-1}$ were attributed to the C=O stretching of amide originating from chitosan. The bands located between 2900 and 2950 $cm^{-1}$ are related to C-H, and may be related to PVAL, and an overlap may occur between the bands of elements present between chitosan and PVAL. In the swelling test, it was possible to observe the maximum rate of 40 minutes for KQ, with maximum percentage of 220%. In the KQPVAL composite the maximum percentage of swelling was 322% in 20 minutes. This difference can be explained by the contact time between chitosan and PVAL in solution, contributing to the homogeneity between polymers and clay.

## Conclusion

The present study demonstrates that the preparation method used was promising for the production of microspheres with interesting properties. XRD results indicate the formation of an amorphous composites evidencing the good distribution of clay in polymeric matrix, from the technological viewpoint the method was interesting, since the ability of the hybrid to absorb molecules could be favoured by the decrease of the degree of crystallinity of its structure. Swelling tests showed that the microspheres have high capacity to absorb water.

## Citations and References


[1] Park, D.-H.; Hwang, S.-J.; Oh, J.-M.; Yang, J-H.; Choy, J.-H.; *Prog. Polym. Sci*. **2013**, *38*, 1442.
[2] ZHANG, L.; ZENG, Y.; CHENG, Z. Journal of Molecular Liquids, v. 214, p. 175–191, 2016.
[3] DE OLIVEIRA, M. J. A. Radiation Physics and Chemistry, v. 84, p. 111–114, 2013.
[4] UDDIN, M. K. Chemical Engineering Journal, v. 308, p. 438–462, 2017.

# DFT Investigation of benzophenone adsolubilized into $Zn_3Al$-LDH intercalated with dodecylsulfate.

**INNA M. NANGOI[A],SÉRGIO R. TAVARES[A], FERNANDO WYPYCH[B], ALEXANDRE A. LEITÃO[A]**

**[A]Departamento de Química, Universidade Federal de Juiz de Fora, Juiz de Fora, MG, 36036-330, Brazil**
**[B]CEPESQ - Research Center in Applied Chemistry, Universidade Federal do Parana - Departamento de Qumica, P.O. Box 19032, 81531-980 - Curitiba, PR, Brazil**

## ABSTRACT

DFT calculations were performed to gain insight of the interactions behind the benzophenone adsolubilization into $Zn_3Al$-LDH (Layered Double Hydroxide) intercalated with dodecylsulfate (DDS). Structurally, a modification of the DDS tilt angle is observed after dehydration, leading to a significant basal reduction. The charge density plots showed that the water molecules close to the anion heads tend to distribute the charge dipoles on the inorganic layer. Regarding the benzophenone adsolubilization, the interactions between guest molecule/hybrid host could be determined as well as the main geometric modications of the organic molecule. In terms of the electronic structure, after the benzophenone adsolubilization, a reduction of the energy band gap was observed along with an indirect-to-direct gap transition.

## INTRODUCTION & THEORETICAL METHODOLOGY

Intercalation chemistry is a very promising research field due to the possibility of tuning several properties, such as the chemical and thermal stability as well as the control of the release of different intercalated species.[1] LDHs are vastly studied in the literature as the inorganic hosts for various intercalation processes, especially because of its anion exchange properties. Many intercalated anions are reported in the literature, among them are the anionic organic linear surfactants such as DDS, dodecylbenzosulfonate (DBS), just to cite some examples.

One of the main purposes of surfactant intercalation in LDHs is to enable the adsolubilization of organic neutral molecules. For instance, Cursino *et al.* reported the adsolubilization of benzophenone in $Zn_xAl$-DDS.[2] The results showed that the synthesized materials presented good UV radiation absorption as well as the indication of dermal toxicity reduction.

In spite of this promising feature by the benzophenone adsolubilization, very little is known about the structural arrangement and the electronic properties of the confined molecule in the interlayer region. In this work, our main objective is to study the characteristic interactions between the organic molecule and the aliphatic chains of DDS in the interlayer region of LDHs. Furthermore, we also aim to elucidate the possible modifications of several electronic structure properties, such as the energy gaps, induced by the adsolubilization process.

All calculations were performed using the codes available in the Quantum Espresso package, which implements the DFT under periodic boundary conditions. The periodic structure of DDS-intercalated $Zn_3Al$-LDH, here simplied as $Zn_3Al$-DDS, was modelled using the brucite structure data, having a fraction of divalent cations replaced for $Al^{3+}$ cations. The $3R_1$ polytype was generated by the stacking vector (a/2, a$\sqrt{}$3/6, c/3).

## RESULTS AND DISCUSSION

The unit cell parameters *a* and *b* were very similar for both optimized structures (hydrated and dehydrated models), indicating that no bond and angle distortions of the layer octahedra occur after dehydration. A good agreement between the simulated and the experimental values of *a* and

*b* was also achieved, the relative deviation being of approximately 3%. On the other hand, a notable contraction (of approximately 18%) was observed for the basal spacing after dehydration. This behavior is expected, though, in the case of $Zn_2Al$-DDS, such decrease was not observed[3], suggesting that this basal reduction is specific to the $Zn_3Al$ compounds.

Regarding the influence of the water molecules on the charge redistribution, the charge density difference plots (Fig. 1) show that there is a greater concentration of dipole-like interactions in the dehydrated structure than in the hydrated one.

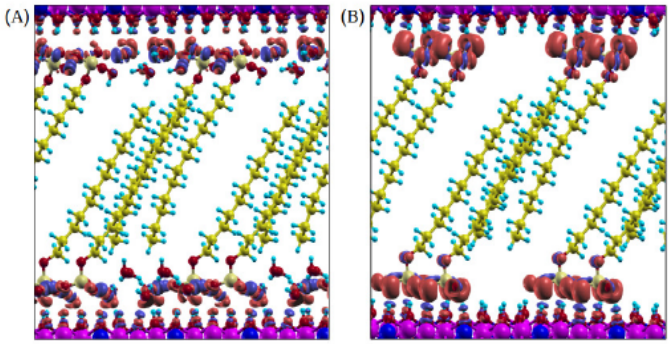


Figure 1: Charge density difference plots of (A) hydrated $Zn_3Al$-DDS and (B) dehydrated $Zn_3Al$-DDS.

Fig. 2 shows the most stable conformation of benzophenone interacting with the DDS chains. The mean distance between benzophenone and the DDS anion is about 3 Å. Benzophenone also suffers a torsion between the aromatic rings of about -10º, adopting almost a planar configuration after adsolubilization, while the optimized dihedral value in the solid state is of 32º.

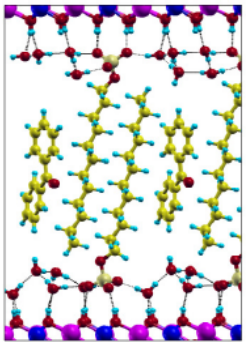

Figure 2: Snapshot of the benzophenone adsolubilization in hydrated $Zn_3Al$-DDS.

The band structures showed that a significant decrease of the energy gap occurs after the benzophenone adsolubilization, indicating that this process is able to tune the energy gap of surfactant-intercalated LDHs. Moreover, the gap transition also changes from an indirect gap to a direct gap when the benzophenone molecule is adsolubilized.

## Citations and References

1 - Kafunkova, E., Taviot-Gueho, C., Bezdicka, P., Klementova, M., Kovar, P., Kubat, P., Mosinger, J., Pospisil, M., Lang, K. Chemistry of Materials 22 (8), 2010, 2481-2490.

2 - Cursino, A. C. T., da Silva Lisboa, F., dos Santos Pyrrho, A., de Sousa, V. P., Wypych, F. Journal of Colloid and Interface Science 397, 2013, 88-95.

3 - Tavares, S. R., Wypych, F., Leitão, A. A. Applied Clay Science 143, 2017, 107-114.

## Acknowledgements

This work has been supported by CAPES, CNPq, FAPEMIG, Brazilian agencies and the enterprise Petrobras S/A (CENPES). We also acknowledge the CENAPAD-SP computational center.

# A comparative structural study of different synthetic routes to LDH-glyphosate materials

**EMANOEL HOTTES[a], ROSANE NORA CASTRO[a], ROSANE AGUIAR DA SILVA SAN GIL[b], ANDRÉ MARQUES DOS SANTOS[a], MARCELO HAWRYLAK HERBST[a]**

[a]Universidade Federal Rural do Rio de Janeiro, Instituto de Química, Seropédica – RJ. (emanoelhottes1986@hotmail.com)
[b]Universidade Federal do Rio de Janeiro, Instituto de Química, Rio de Janeiro – RJ.

## ABSTRACT

Herein we present a comparative investigation on the structural aspects of LDH-glyphosate materials prepared by two different routes, aiming the design of slow-release glyphosate formulations. We have compared a direct and an indirect preparation route, and the materials were characterized by FTIR, powder XRD and multinuclear solid-state NMR. The XRD patterns confirmed that the glyphosate molecules are intercalated in a tilted, near vertical orientation respective to the LDH lamella. FTIR spectra of the LDH-glyphosate materials show that the bands attributed to the carboxylate and phosphonate moieties of the glyphosate molecules were shifted to lower wavenumbers, and the $^{13}C$ CPMAS spectra of the LDH-glyphosate materials show that the peaks were split into two sets and shifted to higher frequencies when compared to pristine glyphosate, thus confirming that the glyphosate immobilization was successful.

## INTRODUCTION

Glyphosate is a post-emergent, systemic, non-selective and wide-spectrum world-wide used herbicide. When applied, a portion of it is absorbed by the plants and another significant portion goes to the soil. Once in the soil surface, glyphosate may suffer several chemical and physical processes, such as degradation, leaching, complexation and percolation. Once complexed with metal cations or metal oxides in the soil, glyphosate becomes inactive, unless physical processes change the equilibrium and mobilize the complexes, rendering active glyphosate species, that may reach the underwater deposits[1]. Thus, the continuous usage of glyphosate may cause several environment damages, and alternative formulations are needed. In this work, we have investigated the interaction of the glyphosate (glyP) with LDH, aiming to get new slow release systems. In LDH the brucite-like structure is partially occupied by trivalent cations, that is, the magnesium cations are substituted for e.g. aluminum cations, affording a liquid positive charge to the LDH lamella. Thus, anionic species may intercalate inside the lamella, for instance, glyphosate anionic species (figure 1c). Clearly, besides intercalation, glyP anions may also adsorb onto the LDH external surface. We have compared two preparations, one direct and another indirect. In the direct route glyP is added together with all other reagents, according to Meng *et al*.[2]. In the indirect route, an ordinary carbonate-LDH compound was calcined for 4h at 450ºC, and was subsequently stirred with an appropriate quantity of glyP in deionized water at 80ºC for 24h, following Constantino&Pinnavaia[3]. The two preparations were performed at pH=9, were the major anionic glyphosate species is glyP[2-4]. In either case, the LDH-glyP products were isolated, washed, dried and characterized by XRD (Rigaku Ultima IV diffractometer), FTIR (Bruker Vertex 70), and solid-state NMR ($^{27}Al$ spectra: Bruker Avance II 400NB, 4mm probe rotating at 8KHz in the magic angle; $^{13}C$ CPMAS spectra: Bruker Avance III 400WB, 4 mm probe rotating a 10 KHz in the magic angle). The interlamellar spacing of 0.69 nm (003 peak) was measured for the materials obtained by both routes, indicating that glyP anions are intercalated in an tilted, near vertical orientation respective to the LDH lamella. The higher crystallinity of the material obtained by the indirect route was evidenced by the narrower and more intense peak (003), when compared to the same peak in the diffractogram of the product obtained by the direct route. Figure 1 shows the diffractograms of the compounds obtained by direct and indirect routes, as well as the proposed intercalation mode for the glyphosate anions [2].

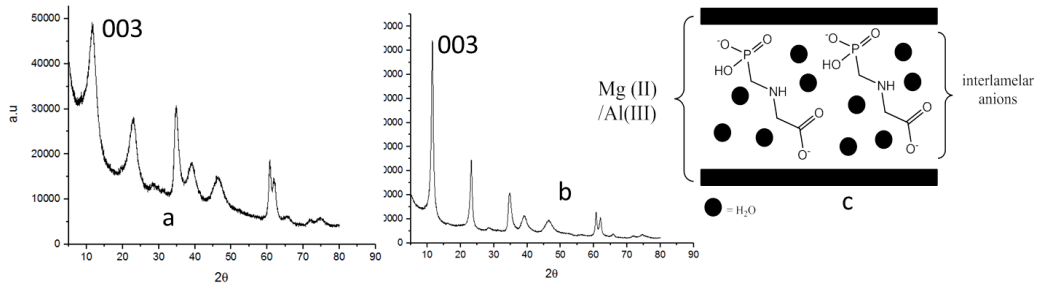


**Figure 1:** XRD profiles of the materials obtained by (a) direct and (b) indirect routes. Scheme (c) shows the intercalation mode proposed for the LDH-glyP materials prepared at pH 9.

The LDH-glyP interaction was confirmed by the FTIR spectra that show shifts of the bands attributed to the carboxylate and phosphonate groups of the glyphosate molecules. In the spectrum of pristine glyphosate the following bands were observed:at 1730-1712 and 1421 $cm^{-1}$ ($\upsilon_{as}$ $COO^-$ and $\upsilon_s$ $COO^-$), and at 1174 and 1094 $cm^{-1}$ ($\upsilon_{as}$ P-O and $\upsilon_s$ P-O), whereas in the LDH-GlyP spectra those bands were shifted to 1620 and 1370 $cm^{-1}$, and to 1100 and 980 $cm^{-1}$ respectively. The $^{27}$Al MAS spectra measured for the materials obtained from the direct and indirect routes showed only an intense and narrow signal in the octahedral Al range, close to 7 ppm. In both cases the symmetry of the signal indicated isotropic charge distribution around the Al core[5]. The $^{13}$C CPMAS spectra of the pristine glyphosate and LDH-GlyP compounds are depicted in Figure 2. Two sets of peaks are observed for the LDH-GlyP spectra, and the $^{13}$C chemical shifts of glyphosate (Figure 2-A) were shifted to higher frequencies for LDH-GlyP compounds, which indicates interaction of the glyphosate anions with the LDH. The broadened signal at 180 ppm was attributed to the C1 of the intercalated glyphosate, whereas the narrower signal at 170 ppm was attributed to the C1 of the adsorbed glyphosate. The narrower peak shows symmetry similar to the pristine glyphosate signal, suggesting that the interaction between the carboxylate group of the glyphosate with the LDH external surface causes the observed shift[6]. The results also suggest that the intercalated LDH-GlyP material was obtained in higher yield by the direct route (Figure 2-B), when compared with the indirect route (Figure 2-C).

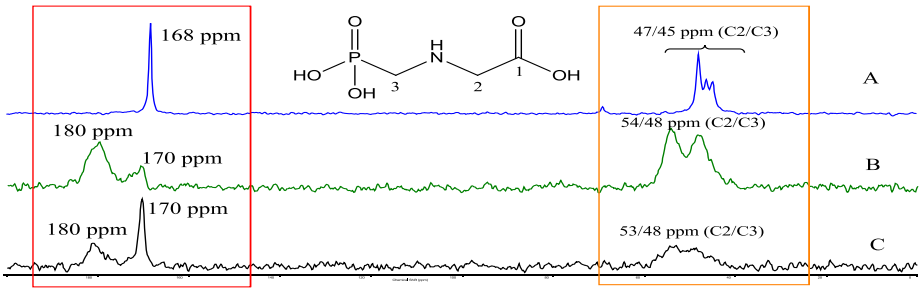


**Figure 2:** $^{13}$C CPMAS NMR spectra obtained for (A) pristine glyphosate; (B) LDH-GlyP prepared by the direct route; and (C) LDH-GlyP obtained by the indirect route.

Thus, it can be concluded from XRD, FTIR and $^{13}$C CPMAS NMR data that, in the experimental conditions employed in this work, the direct route favors the intercalation of glyphosate, although the product showed a lower degree of crystallinity when compared to that obtained by the indirect route.

## Citations and References

[1] Giesy, J. P.; Dobson, S.; Solomon, K. R. Rev. Environ. Contam. Toxicol. 2000, 167, 35 – 120.
[2] Meng, J., *et al*. Chinese Sci. Bull. 2005, 50, 745 – 751.
[3] Constantino, V. R. L., Pinnavaia, T. J. Inorg. Chem. 1995, 34, 883 – 892.
[4] Peixoto, M. M., *et al*. J. Phys. Chem. A. 2015, 119, 5241 – 5249.
[5] Sideris, P. J., *et al*. Chem. Mater. 2012, 24, 2449 – 2461.
[6] Christensen, M. A., Schaefer, J. Biochemistry. 1993, 32, 2868 – 2873.

# Natural diterpene copalic acid incorporation and release studies in natural and organophilic sepiolite fibrous clay

**SANTOS, E. S., ALVES, V.L., HELENO, V. C. G., DE FARIA, E.H.**

Núcleo de Pesquisas em Ciências Exatas e Tecnológicas, Universidade de Franca (UNIFRAN), Av. Dr. Armando Salles Oliveira, 201, CEP 14.404-600, Franca, SP, Brasil. eliene.silverio@gmail.com e/ou emerson.faria@unifran.edu.br

**ABSTRACT**

Sepiolite functionalization studies were carried out followed by the characterization of all inorganic materials. Kinetic and equilibrium studies were performed with the natural diterpene providing important information on equilibrium time, equilibrium concentration and other experimental conditions for the best adsorption condition and yield the hybrid material containing the active compound copalic acid. The solid was obtained after magnetic stirring at 25ºC for two hours with natural or organophilic (containing amine groups) sepiolite. The experiment with concentration of 1000 mg/L provided by the equilibrium, showed the better adsorption capacity. The solids were carefully characterized by X-ray powder diffraction, infrared absorption spectroscopy and thermal analysis. After the incorporation of the active compound copalic acid, the release in buffer pH=7.4 study was analysed by UV-Vis spectroscopy that showed the copalic acid release data. It was possible to define that equilibrium of active specie release was reached after 48 hours using organophilic sepiolite.

**Keywords:** copalic acid, fibrous clay mineral, adsorption, drug delivery.

## Introduction

The diterpenes or diterpenoids as they are also called, are a large and structurally diverse class of natural products, with skeletons of 20 carbons. [1] Diterpenes have a broad spectrum of important biological activities, such as antiparasitic, anti-inflammatory, cytotoxic, anticancer, among others. Copalic acid has a lipid-like skeleton, first described by Nakano and Djerassi in 1961. [2]

Hybrid materials represent a class of materials that have been widely used in adsorption processes. The multifunctionality of these materials enables a range of applications within the adsorption area allowing the removal of complex species such as toxic metals, drugs, organochlorine pesticides, among numerous other compounds. Besides this range of applications within the adsorption area, there are countless followings such as catalysis, sensors, controlled release of drugs, composites, nanocomposites, polymer loads, among others. [3] The objective of this work is to analyse the adsorption of active diterpenes in sepiolite (natural and organophilic), that is a fibrous clay mineral, and also verify the drug release profile of the adsorbed natural product on fibrous clay mineral.

## Experimental

Based on the work Moreira et al. 2016[3] the functionalization of sepiolite with the 3-aminopropyltriethoxysilane was made using the method with excess of the alkoxide in presence of dried sepiolite, under inert argon atmosphere. The resulting material was centrifuged and washed once with toluene, after which the material was subjected to the Soxhlet system to be washed with ethanol and then with water. The purified sepiolite was named Sep, while the functionalized was named Sep-APTES. Adsorption (kinetic and equilibrium) study, a solution with concentration of 30 $mg.L^{-1}$ of the copalic acid was initially prepared. Next, test tubes containing 50 mg of Sep and Sep-APTES were added

in each test tube for kinetic evaluation. Then 5 ml of the solution of the copalic acid was added to each test tube, which were taken into the batch reactor with temperature control and at the end of each desired time, the supernatant was separated from the solid adsorbents by centrifugation, and then analysed by UV-Vis spectrophotometry. The copalic acid release study was made using the dialysing membrane, 50 mg of each solid containing copalic acid (Sep and Sep-APTES), thus the material was weighed and adhered to the membrane along with 2 ml of pH 7.4 phosphate buffer solution. The membrane was then placed in a beaker and taken to the reactor under magnetic stirring, and at the interval times aliquots with 3mL were removed and analysed by UV-Vis spectroscopy; is important remark that during each aliquot removal, 3 mL of buffer phosphate solution was added to the release medium.

## Results and Discussion

X-ray powder diffraction shows the typical sepiolite diffraction pattern. The solids after copalic acid incorporation did not show any displacement, remarking the typical characteristic of fibrous clays that maintain the zeolitic cavities bonded by apical oxygen, resulting in a non-swollen clay mineral type. The infrared absorption spectroscopy evidenced the changes after sepiolite functionalization with the alkoxides and after copalic acid incorporation. The typical bands of the amine groups and carboxylic acids from diterpenes were observed at 1567-1411 and 1000-500 $cm^{-1}$. The kinetic study established that the equilibrium was reached at about two hours using the concentration of 1000 $mg.L^{-1}$. After the incorporation of the copalic acid the release in buffer pH=7.4 showed the typical profile of drug release for sample containing amine groups (maintenance of concentration release against intervals time analysed). However the purified sepiolite (Sep-Ac.Cop) presented a higher release rate reaching 30.78% in 48h. Natural sepiolite release the copalic acid in very short time intervals, thus the active substance do not reach the equilibrium of drug release. Some peaks with increase and decrease of concentration were observed confirming that only sepiolite could not guarantee the effective interaction with copalic acid. Functionalized sepiolite presented a lower percentage of release, presenting only 8.8% in 48h. However, it presented a certain equilibrium in the release, providing greater efficiency in the control of the release. Over time, the copalic acid concentration reaches the plateau and maintain constant until 10 days.

## Conclusion

Sepiolite was functionalized by 3-aminopropyltriethoxysilane and TG, FTIR and XRPD confirm the attachment of amine groups on fibrous clay. The experiments also confirm that the active diterpene was also incorporated. The typical adsorption experiment, kinetic and equilibrium studies shown that the time required to reach the equilibrium for Sep and Sep-APTES was 2 h. The optimal concentration employed 1000 mg/L (based on equilibrium study) evidenced the copalic acid incorporation into Sep and Sep-APTES 18,10 mg/g and 58,76 mg/g. The controlled release study established that the material Sep-APTES presented higher efficiency on copalic acid release.

## Citations and References

[1] Garcia, P.A.; Oliveira, A.B.; Batista, R. Occurrence, biological activities and synthesis of kaurane diterpenes and their glycosides. Molecules, 2007; 12, 455-483.
[2] Nakano, T.; Djerassi, C. Terpenoids.XLVI.Copalic acid. J. Org. Chem., 1961; 26(1), 167-173.
[3] Moreira, M.A.; Ciuffi, K.J.; Rives, V.; Vicente, M.A.; Trujillano, R.; Gil, A.; Korili, S.A.; Faria, E.H. Effect of chemical modification of palygorskite and sepiolite by 3-aminopropyltriethoxisilane on adsorption of cationic and anionic dyes. 2016.

# Electronic properties of some zirconium aminophosphonates investigated by DFT calculations

**BRUNA NÁDIA N. SILVA[1], SÉRGIO R. TAVARES[1], ALEXANDRE A. LEITÃO[1]**

*[1]Departamento de Química – ICE, Universidade Federal de Juiz de Fora, CEP 36036-330 Juiz de Fora - MG -Brasil. Email: brunaneves@ice.ufjf.br; sergiorodriguestavares@ice.ufjf.br, alexandre.leitao@ufjf.edu.br*

## ABSTRACT

The α-ZrP is a layered material well known in the literature and recently new structures are being proposed by modifications of its synthesis for different applications. To better understand these new systems, the goal of this work is to conduct a theoretical study of the structural and electronic properties of some zirconium aminophosphonates by DFT calculations. The geometry optimizations and the simulated XRD patterns show a good agreement compared to the experimental data. The $^{31}$P NMR simulation presented two distinct sites for each material. We also noticed from the projected density of states (PDOS) that the animo group is more acidic than all the other oxygen atoms. In addition, these amino groups present certain differences regarding the Bader charges of the nitrogen atoms. For the next steps, we will simulate the IR spectra and propose the exfoliation of all these materials.

## INTRODUCTION AND COMPUTATIONAL METHODOLOGY

The α-ZrP is a stable layered compound with several applications in biological systems and controlled release of species from the interlayer region[1,2]. Furthermore, modifications in its synthesis have recently been reported and may lead to other zirconium aminophosphonates with significant properties such as proton conductors, ion exchanges, heterogeneous catalysis, among others[3,4]. Hence, a theoretical study of the acidity and the distribution of charges in different sites will assist the understanding of the reactivity of these compounds.

The goal of this work is to study some zirconium aminophosphonates by DFT calculations. We simulated layered models of zirconium aminophosphonates wich were experimentally characterized by published reports (Taddei et.al., 2016): $ZrH[F_3(O_3PCH_2NH_2)]$ (ZAMPAF), $Zr_2H_2[(C_2O_4)_3(O_3PCH_2NH_2)_2]$ . $2H_2O$ (ZAMPAOX), $Zr(O_3PCH_2CH_2NH_3)_2Cl_2$ (ZAEPACl). We used the QUANTUM ESPRESSO package[6] to optimize the geometry of all the models and to simulate the XRD, $^{31}$P NMR, PDOS and the Bader charges.

## RESULTS AND DISCUSSION

For all the simulated layered materials, a good agreement with the experimental unit cell parameters was achieved, with the relative errors being lower than 3%. Figure 1 shows the geometry-optimized structures. The simulated XRD patterns (Figure 2) also demonstrate that the simulated and experimental basal spacing peaks overlap in all cases, except for ZAMPAF. Figure 3 depicts the $^{31}$P chemical shifts and the simulated the NMR spectra for all materials. ZAMPAF presented positive chemical shifts because the greatest shielding occour for the neighbours Zr-F in the $ZrO_2F_4$ and the $ZrO_4F_2$ coordination. ZAMPAOX gives two very different signals because the coordination of zirconium leads to a structural distortion in the aminophosphonates located between the oxalate groups. On the other hand, we can observe an alignment of the phosphorous in the ZAEPACl material when the chemical shifts are very close.

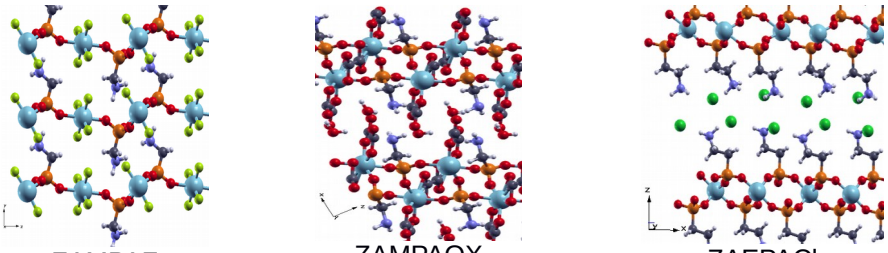


*Figure 1 : Simulated models of Zirconioum Aminophosphonates*

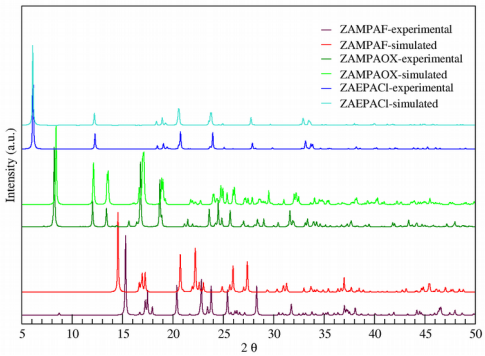


*Figure 2: XRD of Zirconioum Aminophosphonates.*

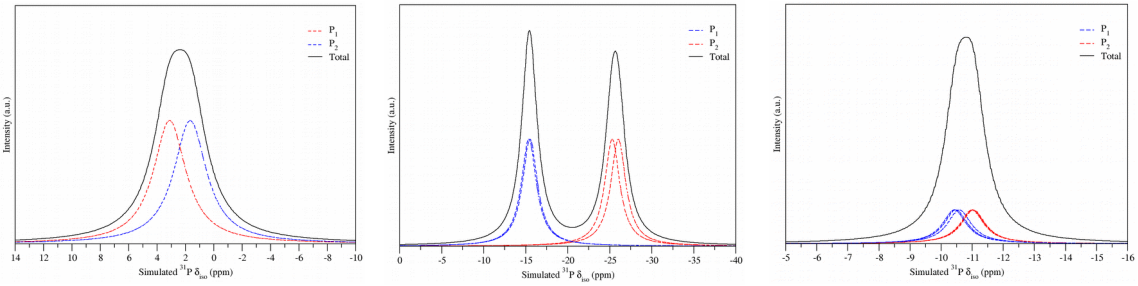


*Figure 3: Simulated $^{31}P$ NMR of Zirconioum Aminophosphonates.*

We could notice from the PDOS analysis that the animo group has a higher acidity than all oxygen atoms present in the layers. Bader charges confirme that the nitrogen atoms correspond to different chemical environments (ZAMPAF: -1.72, ZAMPAOX: -1.64, ZAEPACl: -1.24) and this feature occurs according to the interaction types in the amino groups between the layers. The next steps of this work are the simulation of the IR spectra and the energy *gap* analysis by their band structures. The study of the single-layer models (exfoliation) is also one of our goals in the future.

**Support:** This work has been supported by CAPES, CNPq, FAPEMIG, Brazilian agencies and Petrobras S/A (CENPES). We also acknowledge the CENAPAD-SP computational center.

## Citations and References

[1] A. Díaz, et al. Biomacrom., v.11.9 (2010); Chem. Commun., v.48.12 (2012).
[2] L. Chen, et al. Materials & Design, v.122, 247-254 (2017).
[3] M. Taddei, et. al. Inor. Chem., v. 55, n. 12, p. 6278-6285, (2016).
[4] M. Terban, et. al. Inor. Chem., v. 56, n. 15, p. 8837-8846, (2017).
[5] P. Gianozzi, et al., J. Phys.: Cond. Matter., 21, 395502 (2009)

# Layered double hydroxides with the chemical composition ($[A(H_2O)_6]Mn_6Al_3(OH)_{18}[SO_4]_2 \cdot 6H_2O$; A= Na or K) as Pickering emulsifiers.

**LILIAN F. M. DO AMARAL[1a], ANNE R. SOTILES[1b], FERNANDO WYPYCH[1c], RILTON A. DE FREITAS[1d].**

[1]Chemistry Department, Federal University of Paraná, P.O.Box 19032, Curitiba-PR, 81531-980, Brazil
[1a]lilianamaral08@gmail.com, [1b]anne_sotiles@hotmail.com, [1c]wypych@ufpr.br, [1d]rilton@ufpr.br

## ABSTRACT

Layered double hydroxides (LDH) with similar composition to the mineral Na-Shigaite ($[A(H_2O)_6]Mn_6Al_3(OH)_{18}[SO_4]_2 \cdot 6H_2O$; A= Na or K) were synthesized by co-precipitation with increasing pH and characterized with several instrumental techniques. The cation exchange reactions were performed in the presence of alkaline metal sulphates, using different instrumental techniques to show that the cations were completely exchanged without the removal of the intercalated sulphate anions. The synthesis was investigated considering the time and temperature of the hydrothermal treatment. The layered particles, when dispersed in water, have several characteristics of good Pickering emulsifiers as colloidal scale size, viscosity of aqueous dispersions and the possibility of exchange cations and anions in order to modulate particle hydrophobicity. We investigated the role of these particles in the stabilization of emulsions containing water and liquid paraffin, the interfacial properties and wettability of the particles associated to oil/water formulation constituents and their influence on the stability and type of emulsion formed using macroscopic analysis and confocal fluorescence microscopy.

Key words: Layered double hydroxides, particle size, emulsions of Pickering.

## INTRODUTION

In recent years, solid particles have been used as emulsifiers and layered double hydroxides (LDH) as an example of highly effective solids to stabilize emulsions [1]. The LDH uses can be related to the versatile properties in terms of chemical composition, basicity, high charge density and surface area, possibility of controlling its characteristics of hydrophilicity/hydrophobicity and layered morphology [2]. These compounds are represented by the general formula $[M^{+2}_{1-x}M^{+3}_x(OH)_2]^{x+}(A^{-n})_{x/n} \cdot yH_2O$, where $M^{2+}$ can be ($Mg^{2+}$, $Ni^{2+}$, $Co^{2+}$, $Zn^{2+}$ or $Cu^{2+}$) and $M^{3+}$ can be ($Al^{3+}$, $Cr^{3+}$ or $Fe^{3+}$), with "A" being the anion of the interlayer with charge (-n). The density of the intercalated species can be easily controlled, since they are proportional to the $M^{3+}$ in the layer [3,4].

In the present study, LDH with the composition of Shigaite were synthesized by co-precipitation by increasing the pH. Solutions of $MnSO_4$, $Al_2(SO_4)_3$, and $A_2SO_4$ ($A^+$ = Na or K) in 100 mL of Mili-Q water, with Mn, Al and alkaline molar ratios of 6:3:1, were slowly added to a solution of 1 mol $L^{-1}$ AOH ($A^+$ = Na or K) in an automatic glass titration reactor operating at 90 °C, under $N_2$ flow [5]. After the precipitation, the materials were maintained at 90 °C for 120 h, centrifuged at 4500 rpm, washed several times with purified water (MilliQ system), and kept under dispersion at 5 °C. The effect of the LDH particles as stabilizers of mixtures of mineral oil (paraffin) (density = 0.874 g·cm$^{-3}$ at 25 ºC) and purified water (density = 0.997 g·cm$^{-3}$) were investigated. It was evaluated the mass fractions (φ) of 0.8, 0.7, 0.5, 0.3, 0.2 and 0.1 of liquid paraffin in water and the LDH concentrations of 0.005 to 1.0% (m/m), dispersed previously in the aqueous phase. These mixtures were submitted to ultrasonic probe for 1 min and kept in environment with constant temperature

of 22°C. Thus, a macroscopic study of the emulsions was conducted by obtaining photographs as a function of time. The phase separation of mixtures promptly occurs, approximately 10 min after shaking, the tubes showed completely separated phases. The photos of the emulsion tubes in the presence of particles are shown in Figure 1.

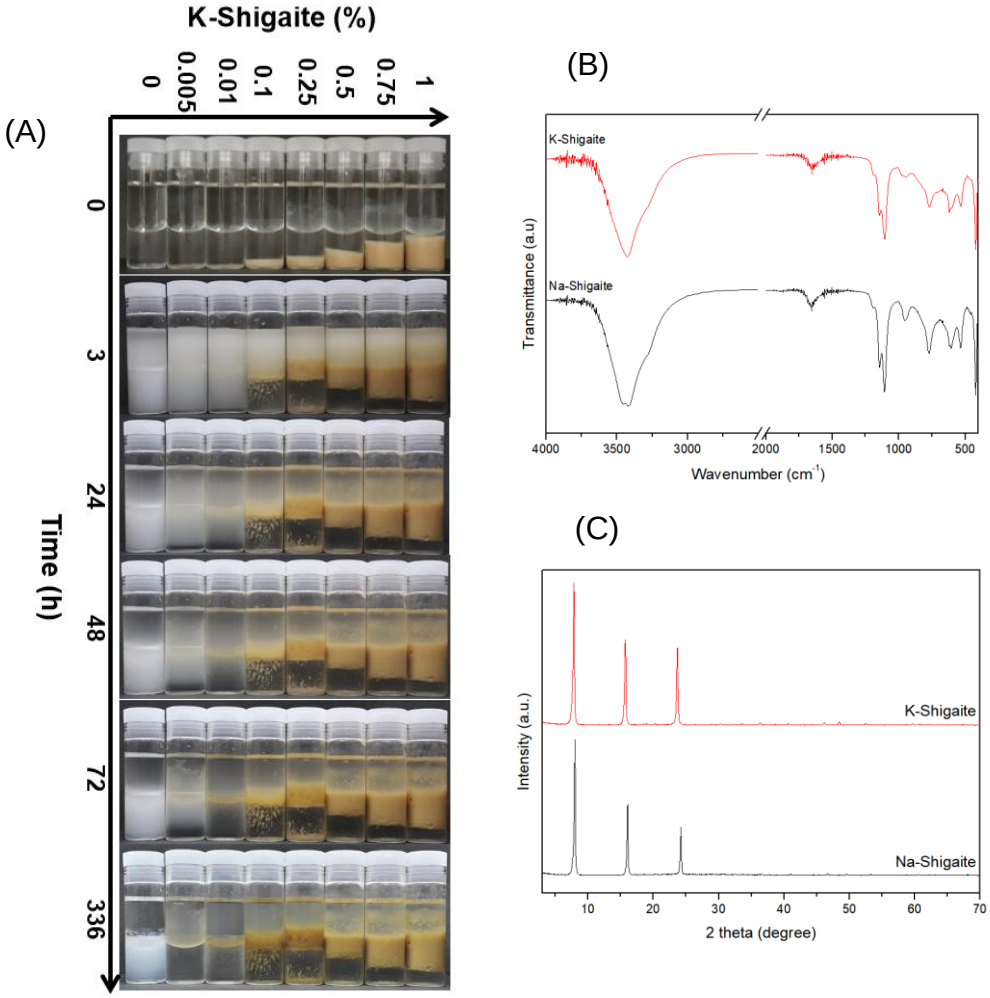


Figure 1: Photographs of the emulsions containing liquid paraffin (φ =0.5) and water phases as a function of K-Shigaite concentration and time (A). X-ray diffraction patterns (B) and Fourier transform infrared spectra (FTIR) (C) of K-Shigaite and Na-Shigaite.

## Citations and References


[1] W. J. Ganley, J. S. van Duijneveldt, Controlling the Rheology of Montmorillonite Stabilized Oil-in-Water Emulsions, Langmuir, 33 (2017) 1679–1686.

[2] H. Katepalli, V.T. John, A. Tripathi, A. Bose, Microstructure and rheology of particle stabilized emulsions: Effects of particle shape and inter-particle interactions, J. Colloid Interface Sci. 485 (2017) 11-17.

[3] F. Wypych, K.G. Satyanarayana, Clay surfaces : fundamentals and applications, Elsevier Academic Press, 2004.

[4] V. Rives, Layered double hydroxides: present and future, Appl. Clay Sci. 22 (2002) 75–76.

[5] A. R. Sotiles, L. M. Baika, M. T. Grassi, F. Wypych, Cation Exchange Reactions in Layered Double Hydroxides Intercalated with Sulfate and Alkaline Cations $(A(H_2O)_6)[M^{2+}\ 6Al_3(OH)_{18}(SO_4)_2]\cdot 6H_2O$ ($M^{2+}$ = Mn,Mg, Zn; $A^+$ = Li, Na, K), J. Am. Chem. Soc. 141 (2019) 531−540.

# Chemical steps for generation of meso-macoporous titania templated by latex beads synthesized without $N_2$ gas.


## AUTHORS

A. M.Correia da Silva[1], G. C. Cavalcante[1], J.V. Ferreira da Silva[1], A. E. Santos Silva[1], P.R. Lima[2], J. S. Sousa[1], A.J. D. Freitas[1], J. D. Freitas[1], A. O. S. Silva[3], M. F. S. Degenhardt[4], C. L. P. Oliveira[4], L. Otubo[5], D. A. Barros Filho[1*]

1 - IFAL – Maceió, Avenida do Ferroviário, 530, Centro, Maceió, Zip-Code: 57020-600, Brazil
anthony.de.2012@gmail.com; giselly.c.cavalcante@gmail.com; joaovitorf11@outlook.com; antonyessilva@gmail.com; jonas_sousa@hotmail.com; ajdfifal@gmail.com; johnnatandf@gmail.com;*djalneno@gmail.com - corresponding author

2 - IFAL - Marechal Deodoro, R. da Matança (Rua Lourival Alfredo), 176 - Poeira, Mal. Deodoro - AL, 57160-000, Brazil.
phaby.lima@gmail.com

3 - Laboratório de Síntese de Catalisadores (LSCat), Centro de Tecnologia, Universidade Federal de Alagoas, Maceió, 57072-900, Brazil.
osimar@yahoo.com

4 - Instituto de Física, Universidade de São Paulo, Rua do Matão, 1371, CEP 05508-090 , São Paulo, Brazil.
crislpo@if.usp.br;mfs@if.usp.br

5 - Laboratório de Microscopia e Microanálises (LMM), Instituto de Pesquisas Energéticas e Nucleares, IPEN-CNEN/SP, 05508-000, São Paulo – SP, Brazil
larissa.otubo@ipen.br



## ABSTRACT

The development of porous materials has been one of the goals of nanotechnology. There is an increasingly real need to understand the mechanisms that generate self-structured materials specifically those that originate from templates of colloidal particles such as polymers, silica, titania and silicon. The importance of these templates is to produce devices with industrial applications such as solar cells, desalinators, batteries and photonic crystals. One of the main difficulties encountered in the application of colloidal particles is to produce them in large scale with uniform size and deposit them on flat surfaces so that they can cover homogeneously a substrate forming crystallographic domains at micrometric scale. The focus of this work is to show how polymerization of styrene monomer (Figure 1A) and the formation of porous titania by bonding with $SO^{4-}$ ions originally present on its surface (Figure 1C) occurs. Latex beads were synthesized without the presence of the $N_2$ gas which resulted in an increase of surface charge with a strong tendency to aggregate. The generation of self-structured materials occurred by controlled evaporation of solvent as reported in the literature[1]. Titania precursor solution was used so that the mesometric pore architecture (<10 nm) was maintained even after heat treatment at 600°C for 1 hour[2]. These features become feasible to use latex beads as original material to generate meso-macroporous oxide materials in a fast and inexpensive route.



**Keywords:** nanotechnology, polymer particles, porous films; surface characterization

A ) -

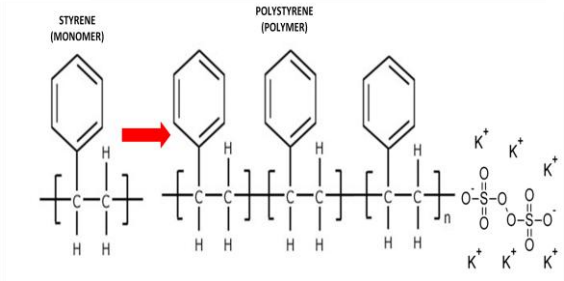


B ) -

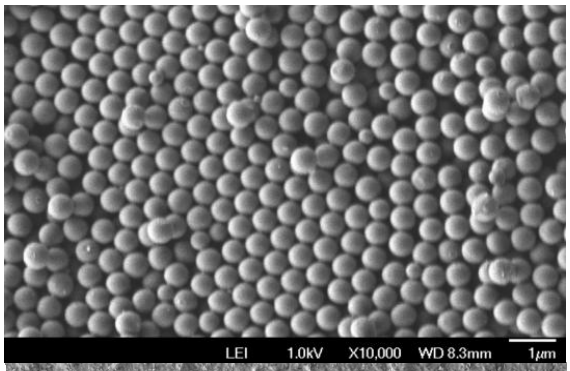


C ) -

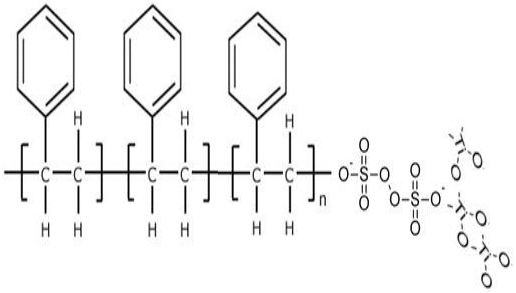

D ) -

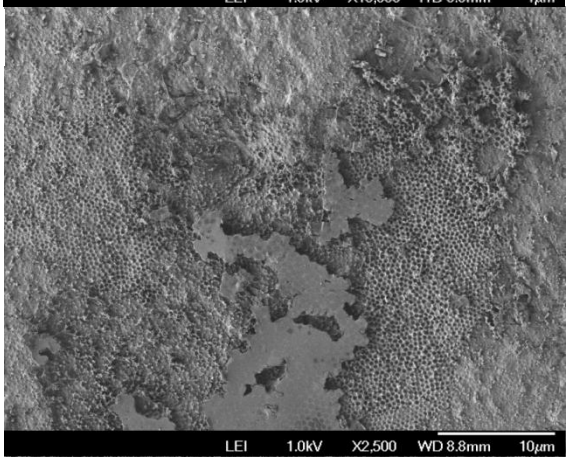


**Figure 01 –** Steps for the formation of meso-macroporous titania: A ) – polymerization of styrene; B ) – self assembly of latex beads; C ) – titania incorporation; D ) – generation of meso-macroporous titania after remotion of latex beads by heat treatment.

## RESULTS AND DISCUSSION

The results show that the polymerization of styrene resulted in latex beads with size distribution at the range of 400 – 500 nm (Figures 1A and 1B). The presence of $SO_4^-$ ions induces the attachment of $TiO_4^-$ molecules along latex beads surfaces (Figure 1C). This attachment extends along the whole self assembly structure replicating the inverse porous architecture after heat treatment at slow heating rate (Figure 1D).

## CONCLUSION

The preparation of meso-macroporous titania can be obtained using latex beads synthesized without $N_2$ gas. This synthesis route allows to produce latex beads in a fast and inexpensive way which can be interesting for an industrial generation of functional devices based on titania oxide. However, some features must be improved to apply latex beads without $N_2$ gas at industrial scale like: control of speed rotation; concentration of chemical reagents; long time for heat treatment; adherence to the substrate.

## CITATIONS AND REFERENCES

[1] - P. Jiang,J. F. Bertone,K. S. Hwang, and, and V. L. Colvin. Single-Crystal Colloidal Multilayers of Controlled Thickness,Chem. Mater., 1999 11 (8), 2132-2140, DOI: 10.1021/cm990080+

[2] - S. Choi, M. Mamak, N. Coombs, N. Chopra, and G. Ozin. Thermally Stable Two-Dimensional Hexagonal Mesoporous Nanocrystalline Anatase, Meso-nc-TiO2: Bulk and Crack-Free Thin Film Morphologies. Adv. Funct. Mater., 2004, 14: 335-344. doi:10.1002/adfm.200305039

# LAYERED DOUBLE HYDROXIDES FOR MEDICAL APPLICATIONS: STUDY OF DRUG DELIVERY SYSTEM BASED ON $M_2Al$-CIPROFLOXACIN (M: $Zn^{2+}$ and $Mg^{2+}$)

N. Fodil Cherif [a,b,c], F. Leroux [a], V.R.L. Constantino [d], C. Taviot-Guého [a]

[a] *ICCF, Univ. Clermont Auvergne – CNRS, Clermont-Ferrand, France .* [b] *C.R.A.P.C., Tipaza, Algérie.* [c] *LEE, Univ. Annaba, Algérie.* [d] *DQF, Univ. São Paulo, São Paulo, Brazil.*

**nawal.fodil_cherif@uca.fr*

Nowadays, biomedical efforts try to join therapeutic and diagnostic activities using one unified material. These materials are able to deliver the drugs to the target site effectively. Inorganic compounds such as layered double hydroxides (LDH) are being extensively studied to develop carriers for drugs and bioactive molecules due to their biocompatibility. In order to achieve carriers of controlled size and high degree of dispersion in physiological media, a deep investigation on synthetic parameters such as reagents concentration, pH value, temperature etc. is needed.

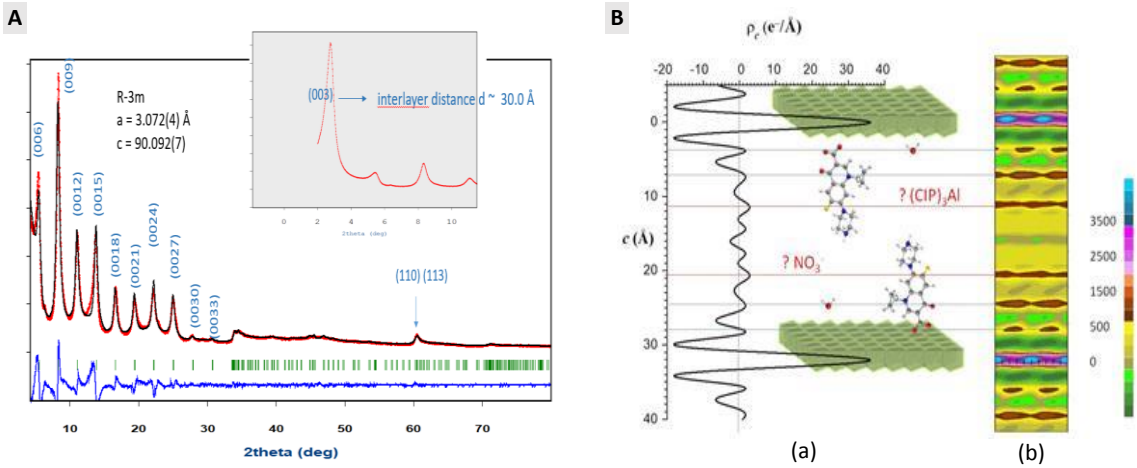


*Figure 1 : (A) Profile analysis of the XRD pattern of $CIP_1ZnAl$ sample: experimental X-ray diffraction (black dots), calculated (red line), Bragg reflections (ticks), and difference profiles (bottom). (B) Schematic representation of the interlayer arrangement of CIP for $CIP_1ZnAl$: (a) One-dimension electron density distribution along the c-stacking direction; (b) contoured Patterson map; the electron density scale is given on the right in arbitrary units.*

The aim of this study is to explore the intercalation of ciprofloxacin (CIP), a BCS class IV into MgAl / ZnAl LDH structures and to assess to their main properties by PXRD, $^{13}C$ MAS NMR, TGA, TEM and SEM techniques. The intercalation of CIP into LDH has already been reported in the literature but results are inconsistent and contradictory [1-2]. Our results show a competition between the complexation reaction of CIP towards $Al^{3+}$ and the formation of $M_{1-x}Al_x(OH)_2$ hydroxide layers. Depending on the amount of CIP with respect to $Al^{3+}$, we observed two different structures, one with only CIP for CIP/Al = 0.5 and the other intercalated both with CIP and $(CIP)_3Al$ complex for CIP/Al=1.

**Keywords: Layered double hydroxide, fluoroquinolone, complexation**.

[1] M. Silion, M.I. Popa, G. Lisa, D. Hritcu. *Rev. Roum. Chim.,* 53, 2008, 827.
[2] Z. Rezvani, M. Shahbaei. *Polym. Composites,* 36, 2015, 1819.

# OXIDATIVE DEGRADATION OF HERBICIDE DCMU OVER LAYERED DOUBLE HYDROXIDES

**D. M. CAIADO[1a], A. S. OLIVEIRA[2], R. ROSSETO[1b]**

[1] Campus Anápolis de Ciências Exatas e Tecnológicas, BR 153 Km 98, Universidade Estadual de Goiás, Brazil. [a)] dancaiado@outlook.com [b)] renato.rosseto@ueg.br
[2] Instituto Federal de Educação, Ciência e Tecnologia de Goiás, Av. Pedro Ludovico, Brazil. alessandro.oliveira@ifg.edu.br

## ABSTRACT

The objective of the present research was to investigate the degradation of DCMU [3-(3,4-dichlorophenyl)-1,1-dimethylurea] using two different oxidants, hydrogen peroxide ($H_2O_2$) and sodium hypochlorite (NaClO) over Mg/Fe layered double hydroxides (LDHs). Adsorbents and products adsorption were characterized by infrared spectroscopy, scanning electron microscopy (SEM-EDS), and the evaluation of herbicide removal in aqueous solution was analyzed by UV-Vis spectrophotometry. The calcined LDH combined with hydrogen peroxide showed good ability to remove DCMU, reaching the equilibrium within 4 h, degradation capacity and removal ability of 347 mg $g^{-1}$ and 85%, respectively.

Keywords: organic pollutants, remediation, anionic clays.

## INTRODUCTION

For decades, the contamination of soil and water by herbicides has aroused general concern, since it affects drinking water quality and impacts on crop safety. DCMU is a phenyl urea herbicide widely used for pre and early post-emergent control of perennial broadleaf and grassy weeds [1]. Since its commercialization, several studies have been worldwide reported evidencing high toxicity and environment persistent [2].

Advanced oxidation processes (AOPs) using layered double hydroxides (LDHs) as heterogeneous catalyst might be an affordable approach for water decontamination due to efficiency to remove residuals of agrochemicals in waters [3]. LDHs exhibit favourable characteristics for the adsorption of recalcitrant organic pollutants such as large surface areas, good thermal stabilities and regeneration efficiencies [4].

## MATERIALS AND METHODS

### Preparation and characterization of Mg/Fe-LDH and adsorption experiments

Magnesium iron layered double hydroxide (ratio 3:1) was prepared via co-precipitation method [4] and calcined LDH samples were prepared at 500 ºC for 4 h. The LDHs were characterized by infrared spectroscopy and scanning electron microscopy (SEM-EDS).

### Kinetic removal of DCMU

The removal studies were performed using 100 mL of DCMU solution (40 mg $L^{-1}$) and 10 mg of LDH at 65 ºC in the presence of hydrogen peroxide ($H_2O_2$, 0.1 mol $L^{-1}$) or sodium hypochlorite (NaClO, 0.02 mol $L^{-1}$). The adsorption kinetic data was analysed by UV-Vis spectroscopy at a maximum absorption wavelength from 215 to 245 nm.

## RESULTS AND CONCLUSION

The Mg/Fe LDH calcined showed much better ability to remove the herbicide compared to Mg/Fe LDH, independently of the employed conditions. The influence of the oxidants on the degradation of DCMU are compiled on Table 1. The calcined LDH combined with sodium hypochlorite showed good ability to remove DCMU at 65ºC and near-neutral pH, reaching the equilibrium removal capacity close to 347 mg $g^{-1}$ and removal efficiency higher than 85% within 24 h. On the other hand, when combined with hydrogen peroxide, the same LDH showed much better ability to remove DCMU from solution, reaching removal capacity close to 85% within 4 h.

Table1. Herbicide removal. Kinetic parameters data at 65ºC and near-neutral pH.

| **Time (h)** | **Removal capacity (%)** | | | |
|---|---|---|---|---|
| | **Mg/Fe-LDH** | | **Mg/Fe-LDH calcined** | |
| | NaClO | $H_2O_2$ | NaClO | $H_2O_2$ |
| 4 | 34.7 | 60.2 | 50.5 | 84.9 |
| 24 | 40.6 | 65.4 | 86.1 | 89.2 |

The obtained results give us insights on the structure-property relationship of these materials for removal of environmental contaminants. Details of the synthesis, characterization and removal kinetic studies will be presented.

## CITATIONS AND REFERENCES


[1] M. Jirı, S. Pavel, M. Jana, F. Jan, K. Karel, M. Jan, Eco. Env. Saf., v. 74, 2011, p. 117–122.

[2] W. Chen, T. M. Young, Environ. Sci. Technol., v. 42, 2008, p. 1072-1077.

[3] R. S. Ribeiro, A. M. T. Silva, J. L. Figueiredo, J. L. Faria, H.T. Gomes, Appl. Catal. B, v.187, 2016, p. 428-460.

[4] L. Conceição, S. B. C. Pergher, C. C. Moro, L. C. A. Oliveira, Quím. Nova, v. 30, 2007, p. 1077-1081.



The authors thank CAPES, Programa de Bolsa de Incentivo à Pesquisa e Produção Científica (PROBIP/UEG), PrP/UEG (Pró-Eventos/UEG), PBIT/UEG and FAPEG for sponsorships.

# Upconversion Phosphor Based on $Yb^{3+}$; $Er^{3+}$ Doped Dion-Jacobson Layered Perovskite $KCa_2Nb_3O_{10}$

**VICTOR VENDRUSCOLO, LUIDGI GIORDANO, VERA R. L. CONSTANTINO, LUCAS C. V. RODRIGUES**

Institute of Chemistry, University of São Paulo, Av. Prof. Lineu Prestes, 748, 05508-000, São Paulo, SP, Brazil, victor.vendruscolo@usp.br; luidgi@iq.usp.br ,vrlconst@iq.usp.br; lucascvr@iq.usp.br

## ABSTRACT

Materials with efficient upconversion emission have been of a great interest in order to explore new photoluminescent compounds for optical devices. Dion-Jacobson layered niobium perovskites are taking in account as host matrices for ions that present upconversion emission. The main objective of this work was prepared an upconversion material based on $KCa_2Nb_3O_{10}$ codoped with $Er^{3+}$ and $Yb^{3+}$ cations. Herein, this material was successfully synthesized *via* ceramic method from their respective oxides and carbonates. The crystallinity and phase purity of isolated niobate was attested by the X ray diffraction (XRD) analysis. Raman spectra of the doped layered material showed a low phonon energy loss by absorption at frequencies lower than 1000 $cm^{-1}$. Scanning electron microscopy (SEM) images showed morphological modifications promoted by the isomorphic substitution of $Ca^{2+}$ ions by the rare earth ions. The Yb/Er-codoped niobate was evaluated with respect of the influence of molar concentration of the doping ions on the upconversion luminescence response. The obtained material is a green emitter when excited at 980 nm. The energy absorbed by the $Yb^{3+}$ ion is transferred to the $Er^{3+}$ site in a mechanism known as *energy transfer upconversion.* The upcoming effect is the non-radiative relaxation in the $Er^{3+}$ ion to mainly the $^2H_{11/2}$ and $^4S_{3/2}$ states followed to a radiative relaxation to the fundamental state by emission of green light. The $Yb^{3+}$:$Er^{3+}$ molar ratio was considered to interpreted the energy transfer mechanism and the emission process.

**Keywords***:* Upconversion, Layered Perovskite, Energy Transfer, Photoluminescence.

## INTRODUCTION

Optical materials that work as high energy converter or energy storage, especially at the near infrared (NIR) region, have been widely studied due to the applicability in biological and technological areas.[1] Upconversion emission is a special case, in this sense, since materials with this property are passive to absorb photons in the NIR region and emit in the UV/Vis region in a multiphotonic non-linear anti-Stokes process.[2]

Trivalent lanthanides such as $Er^{3+}$, $Tm^{3+}$, $Ho^{3+}$ and $Nd^{3+}$ are good examples of ions that could be used in infrared emission or anti-Stokes upconversion by itself or sensitized by other ions as $Yb^{3+}$.[3] Layered perovskites are potential host matrices for these infrared sensitive ions. Dion-Jacobson calcium-niobium layered perovskite $KCa_2Nb_3O_{10}$ is a great example. $Ca^{2+}$ is a good ion to be exchanged for rare earths because of the close ionic radii value in several coordination sites, and the chemical similarity between them.[4]

Therefore, this work aims to synthesize an upconversion material based on the layered niobium perovskite $KCa_2Nb_3O_{10}$ codoped with $Yb^{3+}$ and $Er^{3+}$ and evaluate the influence of the dopant ions concentration in the luminescence properties.

## EXPERIMENTAL

The synthesis of the Yb/Er-codoped layered niobium perovskite was performed according to the literature.[4] Metal oxides or carbonates were mixed using acetone in a crucible for 20 min. Once homogenized, the solid mixture was heated at 1473 K for 5 h in a Pt-crucible. The obtained product was then washed with deionized water and dried under reduced pressure.

## RESULTS AND DISCUSION

XRD patterns of the layered materials were assigned to the anhydrous $KCaNb_3O_{10}$. No evidence of phase segregation was observed. According to SEM images, undoped and codoped matrices showed microscopic structural modifications in the crystal organisation such as different patterns for crystal agglomeration. Raman spectra of doped layered materials showed absorption at frequencies lower than 1000 $cm^{-1}$, which stands for a low phonon matrix, ideal for luminescent systems involving rare earth ions. Raman spectra showed bands at 1000 - 700 $cm^{-1}$ assigned to high-distorted [$NbO_6$] octahedra, 600 - 400 $cm^{-1}$ attributed to low-distorted [$NbO_6$], 400 - 200 $cm^{-1}$ associated to [$NbO_6$] bending, and at 200 - 50 $cm^{-1}$ range assigned to the phonon assisted vibrations.[5]

With respect to the luminescent property of the doped $KCaNb_3O_{10}$, all synthesized materials presented a well-defined and intense green emission when excited with a diode 980 nm laser. The emission spectra of doped $KCaNb_3O_{10}$ samples showed also a very low intensity red emission despite of Yb:Er molar ratio variation. $Er^{3+}$ doped materials usually show two colours region of emission: a green emission, which is attributed to $^2H_{11/2}\rightarrow{}^4I_{13/2}$ and $^4S_{3/2}\rightarrow{}^4I_{13/2}$ relaxations and a red emission assigned to $^4F_{9/2}\rightarrow{}^4I_{13/2}$ radiative relaxation.[3] The relative intensity between these bands depends on the $Er^{3+}$ concentration and, in a case of codoped systems, of $Yb^{3+}$ ions amount.

The proposed mechanism for energy transfer from $Yb^{3+}$ ions to $Er^{3+}$ sites follows the model already reported in the literature:[6] the exciting radiation in the NIR region is resonant with the $^2F_{7/2}\rightarrow{}^2F_{5/2}$ ($Yb^{3+}$) energy level transition and with the $^4I_{13/2}\rightarrow{}^4I_{11/2}$ ($Er^{3+}$) transition (a two photon-assisted process is assumed). The energy absorbed by the $Yb^{3+}$ ion is transferred to the $Er^{3+}$ site in a mechanism called *energy transfer upconversion*, in which metastable superexcited state is populated. The upcoming effect is the non-radiative relaxation in the $Er^{3+}$ ion to mainly the $^2H_{11/2}$ and $^4S_{3/2}$ states followed to a radiative relaxation to the fundamental state by emission of green light.

## CONCLUSION

Ceramic method was effective to the preparation of Yb/Er-codoped $KCaNb_3O_{10}$ matrix with phase purity. The material luminescence can be characterized as an attractive green emitter when excited in the NIR region, with perspective of applications in bioimaging or technological devices such as lighting emitting diodes (LED) and optical sensors.

## REFERENCES


(1) Wu, S.; Butt, H. J. *Phys. Chem. Chem. Phys.* 2017, *19*, 23585–23596.
(2) Haase, M.; Schäfer, H. *Angew. Chemie Int. Ed.* 2011, *50*, 5808–5829.
(3) Auzel, F. *Chem. Rev.* 2004, *104*, 139–173.
(4) Bizeto, M. A.; Constantino, V. R. L.; Brito, H. F. *J. Alloys Compd.* 2000, *311*, 159–168.
(5) Jehng, J.-M.; Wachs, I. E. *Chem. Mater.* 1991, *3*, 100–107.
(6) Khan, M. A.; Idriss, H. *Wiley Interdiscip. Rev. Energy Environ.* 2017, *6*, 1–23.

# Comparative characterization of $M^{2+}/M^{3+}$ ($M^{2+}$= $Mg^{2+}$ or $Zn^{2+}$ and $M^{3+}$= $Al^{3+}$ or $Ga^{3+}$) carbonate-intercalated Layered Double Hydroxides

**VAGNER R. MAGRI, PAULO A. C. LOUREIRO, VERA R. L. CONSTANTINO**

Departamento de Química Fundamental, Instituto de Química, Universidade de São Paulo, Av. Prof. Lineu Prestes 748, 05508-000, São Paulo, SP, Brazil, vrmagri@usp.br, paulo.loureiro@usp.br, vrlconst@iq.usp.br

## ABSTRACT

Layered Double Hydroxides (LDH) are very versatile materials which properties are interesting to diversified scientific and technological fields. Modifying the LDH chemical composition, it is possible achieve a range of materials with distinct properties and potential applications. In this work, well crystalized LDH constituted by $M^{2+}/M^{3+}$ ($M^{2+}$= $Mg^{2+}$ or $Zn^{2+}$ and $M^{3+}$= $Al^{3+}$ or $Ga^{3+}$) intercalated with carbonate anion were synthesized and characterized by a set of physicochemical techniques. Results indicated that zinc-gallium sample presents superior crystallinity, higher particle size and the lower thermal stability compared to the other materials.

**Keywords:** Layered Double Hydroxides, gallium, thermal analysis.

## INTRODUCTION

LDH are very versatile brucite-like materials which properties are interesting to diversified scientific and technological fields such as environmental remediation, catalysis, energy storage, polymer nanocomposites and medicine. Modifications in the layer metal cations (as well the cations molar ratio) and the interlayer guest species, allow to achieved a range of materials with distinct properties.[1,2] The knowledge of such properties can guide the LDH application. Materials with magnesium-aluminium chemical composition are intensely investigated. In this work, LDH constituted by $M^{2+}/M^{3+}$ ($M^{2+}$= $Mg^{2+}$ or $Zn^{2+}$ and $M^{3+}$= $Al^{3+}$ or $Ga^{3+}$) intercalated with carbonate anion were synthesized aiming to investigate the differences in their structural, textural, thermal and spectroscopic properties.

## EXPERIMENTAL

LDH materials were synthesized by co-precipitation method, without any thermal treatment and denominated as $M^{2+}_RM^{3+}$-$CO_3$, where $M^{2+}$ is $Mg^{2+}$ or $Zn^{2+}$, $M^{3+}$ is $Al^{3+}$ or $Ga^{3+}$, and R is 2 ($M^{2+}/M^{3+}$ molar ratio). Materials were characterized by powder X ray diffraction (XRD), scanning electron microscopy (SEM), attenuated total reflectance Fourier transform infrared (ATR-FTIR) and Fourier transform Raman (FT-Raman) spectroscopies, elemental chemical analysis, and mass coupled thermal analysis. Crystallite sizes (L) were calculated by Scherrer equation.

## RESULTS AND DISCUSSION

XRD patterns of synthesized materials (**Fig. 1a**) presented profiles typical of LDH intercalated with carbonate anions with rhombohedral symmetry. LDH basal spacing ($d_{00l}$) values were not sensitive to the trivalent cation but were lower to zinc LDH due to a minor electrostatic repulsion between layers compared to the magnesium analogous matrices.[2] Peaks attributed to (110) plane and related to the distance between cations in the layer were shifted to low angles in $Ga^{3+}$ and $Zn^{2+}$ materials, indicating the incorporation of these

cations into the layer. This tendency agrees with the ionic radii of metal cations ($Zn^{2+}$ > $Mg^{2+}$ > $Ga^{3+}$ > $Al^{3+}$). Gallium and zinc incorporation improved the materials crystallinity (**Fig. 1b**). In addition, parameters calculated from Scherer equation indicated that these cations favor the increase of crystallite size in both *c* and *ab* directions. Materials presented $M^{2+}/M^{3+}$ molar ratio very close to the nominal ratio. SEM micrographs (**Fig. 1c**) revealed remarkable differences in LDH morphologies and particles sizes according to cation composition. Magnesium-LDH presented morphology like *desert rose stone*, whereas zinc-LDH showed flakes platelets without a defined morphological organization. Furthermore, gallium-LDH samples exhibited largest platelets, in agreement with XRD data. LDH thermal behavior is mainly related to $M^{2+}$ cation and slightly dependent of $M^{3+}$(**Fig. 1d**). Indeed, $Mg_2Al$-$CO_3$ showed be the most stable phase for which dehydroxylation occurs at higher temperatures. The observation may be related to Gibbs free energy of respectively hydroxide-oxide transition.

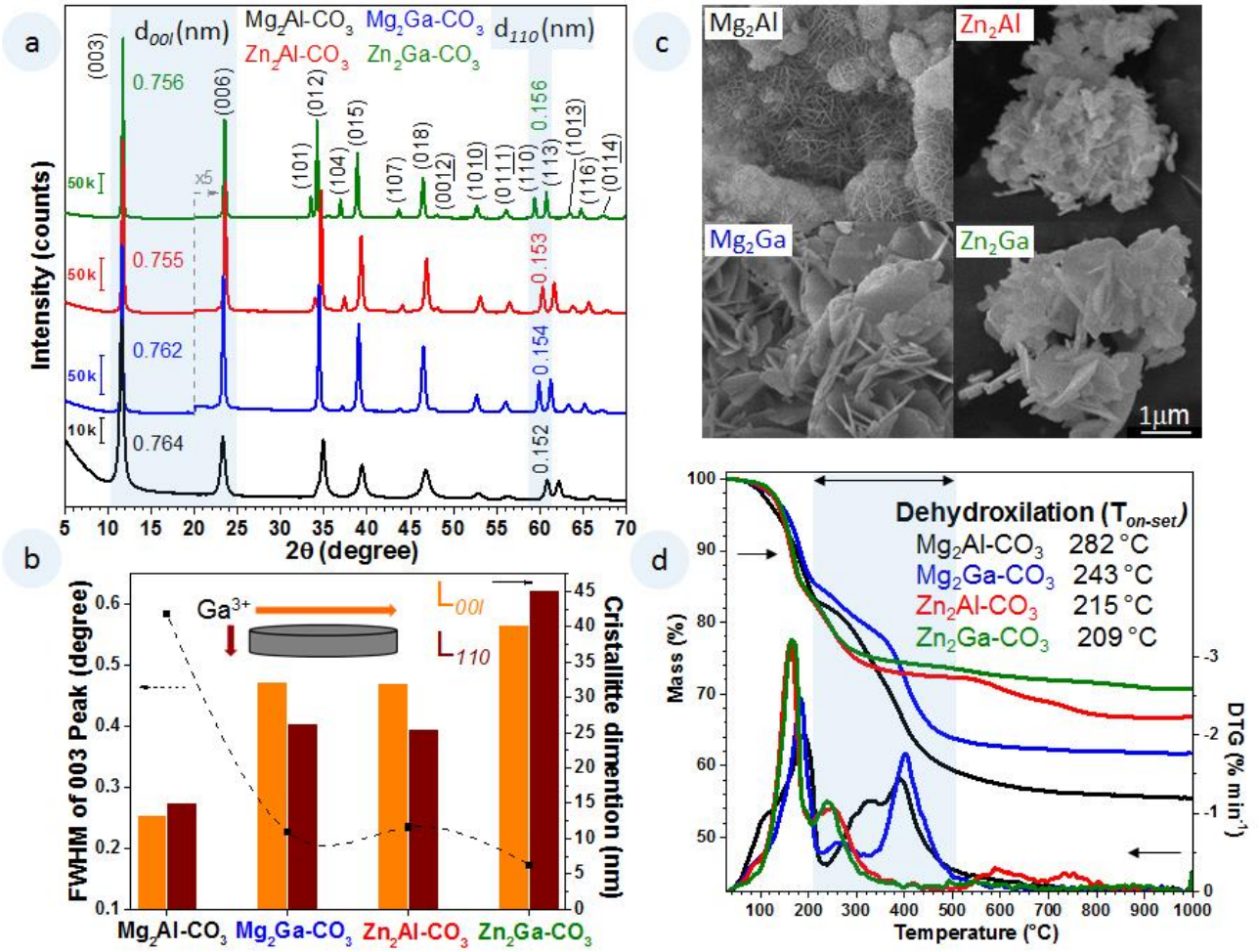


**Figure 1.** XRD patterns **(a)**; FWHM and crystallite parameters calculated from Scherrer equation **(b)**; SEM micrographs at x20k magnification; and TGA-DTG curves **(d)** of indicated samples.

## CONCLUSION

Well crystallized LDH materials were isolated in the used experimental conditions. Comparing the samples, $Zn_2Ga$-$CO_3$ presents the highest crystallinity and largest crystallites size while $Mg_2Al$-$CO_3$ shows major thermal stability. This work opens perspective to preparation of gallium based catalysts.

## REFERENCES


[1] Cavani, F.; Trifirò, F.; Vaccari, A. *Catal. Today* **1991**, 11, 173.
[2] Troutier-Thuilliez, *et al*. *Prog. Org. Coatings* **2009**, 64, 182.

# MATERIALS DERIVED FROM THERMAL DECOMPOSITION OF HYDROCALUMITE-TYPE COMPOUNDS: CATALYSTS FOR TRANSESTERIFICATION REACTIONS

**PRADO R.G.[1,2*], CORRÊA A.G.S.[1], RODRIGUES J.F.[1], SCALDAFERRI C.A.[2], SOUZA F.P.[2], PASA V.M.D.[2], CONSTANTINO V.R.L.[3], PINTO F.G.[1], TRONTO J.[1]**

[1] Laboratory of Layered Compounds, Institute of Exact and Technological Sciences, Federal University of Viçosa, BR 354, km 310, CEP: 38810-000, Rio Paranaíba - MG, Brazil. E-mail: robertagprado@gmail.com
[2] Fuel Testing Laboratory, Department of Chemistry, Federal University of Minas Gerais, Antônio Carlos Avenue 6627, CEP: 31270-901, Belo Horizonte - MG, Brazil
[3] Department of Fundamental Chemistry, Institute of Chemistry, University of São Paulo, Lineu Prestes Avenue 748, CEP: 05508-000, São Paulo - SP, Brazil

## ABSTRACT

The performance of a catalyst is a relevant factor in biodiesel production because it can affect the efficiency of the process. This work provides a study of the synthesis of heterogeneous catalysts for the biodiesel production derived from thermal treatments performed on hydrocalumite-type compounds intercalated with chloride or nitrate anions. The aims of this work were: (*i*) synthesis and characterization of the hydrocalumite-type compounds intercalated with $NO_3^-$ or $Cl^-$ anions; (*ii*) application of thermal treatments in these materials at different temperatures (500°C, 600°C, 700°C, 750°C); and (*iii*) evaluation of the performance of these materials as catalysts in transesterification reactions with soybean oil and methanol. The materials were characterized by X-ray diffraction (XRD), vibrational spectroscopy (FTIR-ATR), thermogravimetric analysis coupled to mass spectrometry (TGA-DSC-MS), specific surface area, temperature-programmed desorption of carbon dioxide (TPD-$CO_2$), etc. The results of transesterification reactions showed that the materials thermally treated from hydrocalumite intercalated with chloride presented high catalytic activity for biodiesel conversion, and particularly if treated at 700°C.

***Keywords:*** hydrocalumite, biodiesel, transesterification, heterogeneous catalyst.

## 1. INTRODUCTION

The technology of biodiesel production has been the subject of studies in several countries[1]. These studies aim to reduce the dependence and environmental impact of the use of fossil fuels. Biodiesel is a biodegradable fuel produced by means of transesterification reaction, from renewable sources such as vegetable oils or animal fats. In this reaction, the use of catalysts is highly recommended[1]. Ca-Al layered double hydroxide (LDH) intercalated with chloride anions, known as a hydrocalumite-type compound ($Ca_2Al$-Cl-LDH), and its thermal derivatives , are interesting materials to be evaluated as catalysts in transesterification reactions[2]. When thermally treated, $Ca_2Al$-Cl-LDH decomposes into oxides and/or oxyhydroxides of calcium and aluminium which exhibit basic properties. The aims of this work were: (*i*) synthesize and characterize compounds of the hydrocalumite-type intercalated with $NO_3^-$ or $Cl^-$ anions, named as $Ca_2Al\_Cl$ and $Ca_2Al\_NO_3$; (*ii*) calcine or activate these materials at different temperatures (500-750°C); and (*iii*) evaluate the thermal treated materials as catalysts in transesterification reactions using soybean oil and methanol.

## 2. EXPERIMENTAL

The synthesis of $Ca_2Al\_Cl$ and $Ca_2Al\_NO_3$ were performed by the coprecipitation method at a constant pH value[3]. These materials were calcined in tubular furnace in $O_2$ atmosphere with flow of 150 $cm^3 \cdot min^{-1}$ at different temperatures (500°C, 600°C, 700°C and 750°C). Different

techniques of analysis were used to characterize the produced materials such as XRD, FTIR-ATR, TGA-DSC-MS, TPD-$CO_2$, and specific surface area mesuarement.

The transesterification reactions were performed using commercial soybean oil (Liza®) and 3% of catalyst (thermally treated materials) in mass relative to the mass of the oil. The methanol:oil molar ratio was 14:1, and the reaction occurred for 4 h at reflux temperature. The concentrations of the methyl esters were determined by nuclear magnetic resonance of hydrogen ($^1$H NMR).

## 3. RESULTS

The diffractograms of the $Ca_2Al\_Cl$ and $Ca_2Al\_NO_3$ show characteristics profile of hydrocalumite-type compounds[3]. After the thermal treatment, the lamellar structures were decomposed giving rise to new phases attributed mainly to the presence of oxides of the mayenita-type ($Ca_{12}Al_{14}O_{33}$) and of calcium (CaO).

The results of TPD-$CO_2$ for calcined materials showed an intense $CO_2$ desorption in high temperatures, indicating the presence of strong basic sites in all these materials. Moreover, the samples obtained from $Ca_2Al\_NO_3$ showed two different types of basic sites, whereas for those from $Ca_2Al\_Cl$ only one type was observed. There was no direct relation between the temperature of thermal treatment and $CO_2$ desorption. The results of the transesterification reactions for the conversion of soybean oil to methyl esters as a function of time, using the calcined materials are presented in Figure 1.

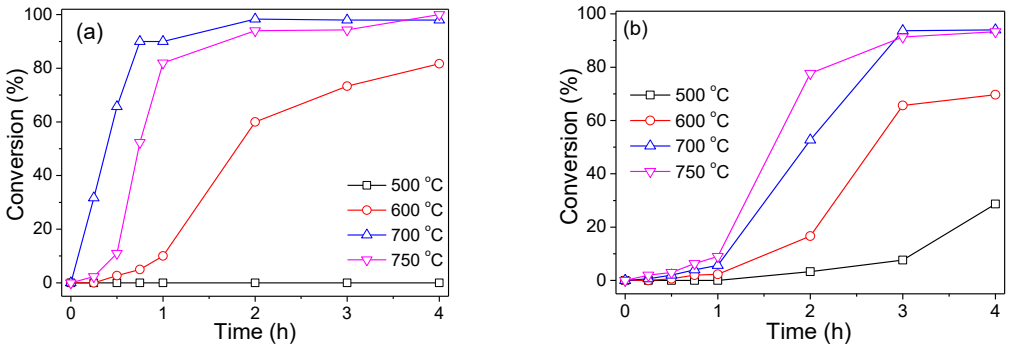


**Figure 1**: Conversion of soybean oil to methyl esters as a function of time using (a) $Ca_2Al\_Cl$ and (b) $Ca_2Al\_NO_3$ thermally treated at the indicated temperatures.

The materials derived from $Ca_2Al\_Cl$ showed the higher conversion percentages in a shorter time than the nitrate analogous systems, especially if treated at 700°C (Figure 1). The differences of composition and basicity may justify the better performance of the materials derived from $Ca_2Al\_Cl$ as catalysts in the transesterification reactions. The results obtained for the materials synthesized in this work present a superior catalytic performance when compared to other catalysts commonly reported in the literature as CaO for example[4].

## 4. CONCLUSIONS

The synthesis of the hydrocalumite-type compounds intercalated with chloride and nitrate anions were efficient. The thermal treatments applied in $Ca_2Al\_Cl$ and $Ca_2Al\_NO_3$ produce $Ca_{12}Al_{14}O_{33}$ and CaO. TPD-$CO_2$ results showed the presence of two basic sites for $Ca_2Al\_NO_3$ and only one type for $Ca_2Al\_Cl$. The $Ca_2Al\_Cl$ thermally treated at 700°C presented the best rate of conversion among the studied materials.

**REFERENCES**

[1] M. R. Avhad and J. M. Marchetti, *Renew. Sustain. Energy Rev.*, vol. 50, pp. 696–718, 2015.
[2] R. G. Prado *et al.*, *Energy & Fuels*, vol. 30, pp. 6662–6670, 2016.
[3] L. Vieille *et al.*, *Chem. Mater.*, vol. 15, no. 23, pp. 4361–4368, 2003.
[4] M. Kouzu and J.-S. Hidaka, *Fuel*, vol. 93, pp. 1–12, 2012.

***Acknowledgments:*** FAPEMIG, CAPES and CNPq.

# TERBIUM (III) BASED INFINITE COORDINATION POLYMER AND CARBOXYMETHYL CELLULOSE COMPOSITE MEMBRANES FOR LIGHT-EMITTING APPLICATIONS

**GUILHERME ARROYOS, REGINA CÉLIA GALVÃO FREM**

Department of General and Inorganic Chemistry, Institute of Chemistry, São Paulo State University (UNESP), Araraquara, Brazil. E-mail: guiarroyos@gmail.com

## ABSTRACT

A new terbium (III) based infinite coordination polymer was obtained (**Tb-M**) by microwave-assisted synthesis in water, using 3,5-pyrazoledicarboxylate and malonate linkers. The **Tb-M** sample consists of spherical particles with sizes ranging between 2,0 – 3,0 μm. The compound shows bright green luminescence under 280 nm excitation due to the antenna-effect between linkers and $Tb^{3+}$ ion. **Tb-M** was then combined with carboxymethyl cellulose in water to produce a composite gel, which was then dried on a Petri dish to form a flexible transparent membrane. The membrane still shows the characteristic bright green emission of under 280 nm excitation and has great potential for light-emitting applications.

*Keywords*: coordination polymer, metal-organic framework, luminescence, membrane.

## INTRODUCTION

The infinite coordination polymers (ICPs) are compounds similar to metal-organic frameworks (MOFs). They are synthesized using metal ions combined with bridging polydentate organic ligands. The key difference between these classes of compounds is that MOFs usually display high crystallinity and ICPs are low crystallinity compounds. ICPs can also show a higher array of different particle morphologies (spherical, rods, fibers, coin-shapes).[1] Both types of coordination polymers can display similar properties, like permanent porosity, high surface areas and high thermal stability. When synthesized using lanthanide (III) ions like europium or terbium, these compounds can show luminescence due to antenna-effect. This phenomenon consists of absorption of radiation by the organic part of the polymer (mainly chromophore molecules) and transfer to the lanthanide ion. This energy transfer causes population of the lanthanide emissive levels, leading to *f-f* forbidden transitions observable as photon emission.[2]

Since coordination polymers are usually obtained in the form of crystals or powders, the potential applications are hampered by the particle size. In order to enhance applicability of these compounds, they are commonly synthesized as thin films or composites. In this work, a composite made of a luminescent terbium (III) based ICP[3] and carboxymethyl cellulose was produced. Carboxymethyl cellulose is an edible cellulose derivative, which forms emulsions and gels in water. When dried, it forms flexible transparent membranes.[4] The luminescent composite membrane obtained in this work shows great potential for light-emitting applications.

## EXPERIMENTAL

For the synthesis of the terbium based ICPs, terbium (III) chloride hexahydrate, 3,5-pyrazoledicarboxylic and malonic acids were dissolved in water, with pH adjusted to 4.0 using sodium hydroxide. The mixture was heated to 150 ºC using microwave-assisted synthesis, yielding a white powder (**Tb-M** compound), which was then centrifuged and washed with water/ethanol.

For the membrane preparation, 500 mg of sodium carboxymethyl cellulose and 10 mg of **Tb-M** were mixed in water under vigorous stirring for 1h. The mixture was then transferred to a Petri dish and dried for 4 days under 60 ºC. The resulting membrane is easily detached from the glass.

## RESULTS AND DISCUSSION

*Characterization of **Tb-M***. **Tb-M** compound presents itself as spherical particles with sizes between 2,0 – 3,0 µm, as can be seen in Fig. 1. Powder XRD data shows that the compound has low crystallinity, characteristic of similar ICPs. FT-IR presents shifting of carboxylate bands from the ligands from 1701 $cm^{-1}$ to 1361 (symmetric stretching) and 1583 $cm^{-1}$ (antisymmetric stretching), indicating that the ligands had coordinated to $Tb^{3+}$ ion. Thermogravimetric analysis shows that the compound is stable up to 450 ºC. The empirical formula of **Tb-M** is believed to be $[Tb_3(C_3O_4)(C_5N_2O_4)(H_2O)_4]$.

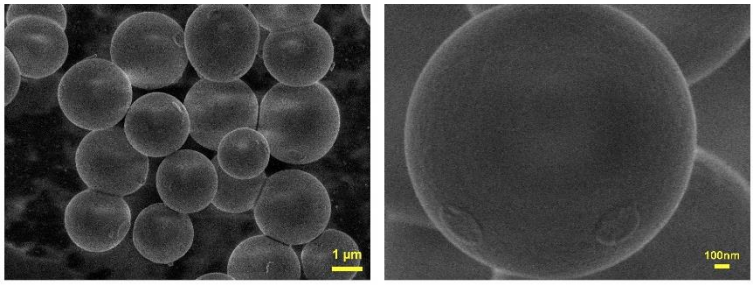


**Fig.1. Tb-M** compound observed by scanning electronic microscopy.

*Luminescence studies*. The excitation spectrum (λem = 624 nm) shows a broad band, with a maximum at 280 nm. Terbium (III) intraconfigurational transition bands also appear. The broad band is assigned to ligand transitions, evidencing the antenna-effect, since characteristic $Tb^{3+}$ emission bands can be observed when excitation is fixed at 280 nm. The green emission is very intense and observable by naked eye.

*Composite membrane*. The membrane obtained by mixing **Tb-M** with carboxymethyl cellulose can be observed in Fig. 2. It retains luminescence properties from the powder, indicating that **Tb-M** has not decomposed during the process. The scanning electronic microscopy confirms that **Tb-M** spheres are still present and dispersed in the cellulose matrix.

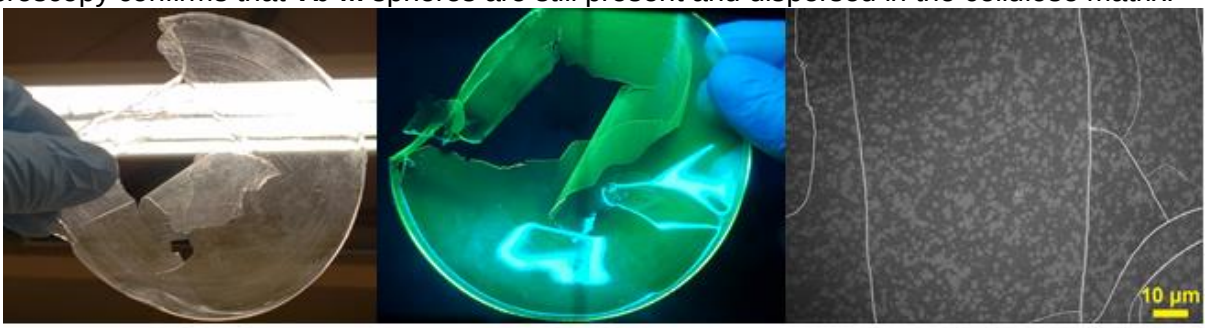


**Fig. 2. Tb-M** + carboxymethyl cellulose membrane under: artificial light (left); under 254 nm lamp (center); scanning electronic microscopy (right).

## CONCLUSION AND PERSPECTIVES

A composite membrane of **Tb-M** and carboxymethyl cellulose was obtained, with carboxymethyl cellulose serving as a supportive substrate for **Tb-M** microspherical particles. The composite combines properties from both precursors, like transparency and luminescence. Different proportions of the coordination polymer and cellulose are in study in order to further improve these properties. The membrane shows great potential for light-emitting applications.

### Citations and References

[1] A. M. Spokoyny, D. Kim, A. Sumrein and C. A. Mirkin, ***Chem. Soc. Rev.***, 2009, 38, 1218.
[2] Y. Cui, B. Chen and G. Qian, ***Coord. Chem. Rev.***, 2014, 273–274, 76–86.
[3] G. Arroyos and R. C. G. Frem, ***New J. Chem.***, 2018, 42, 19070–19075.
[4] A. A. Altam *et al.*, ***Carbohydr. Polym.***, 2017, 168, 240–246.

| FULL NAME | INSTITUTION | CITY | COUNTRY |
|---|---|---|---|
| Alfredo Duarte | IQ-USP | São Paulo | Brazil |
| Ana Alcântara | UFMA | São Luís | Brazil |
| Ana Carolina Cruz da Silva | Instituto de Química- USP | São Paulo | Brazil |
| Ana Luiza Gomes | Universidade Federal de Viçosa | Rio Paranaíba | Brazil |
| Ana Paula Benevides | Universidade do Estado do Rio de Janeiro | Rio de Janeiro | Brazil |
| Bernd Marler | Ruhr University Bochum | Bochum | Germany |
| Bruna Usuginu | Instituto de Química USP | Sao Paulo | Brazil |
| Bruna Carla Santos Silveira | Universidade Federal de São João del Rei | Ouro Branco | Brazil |
| Bruna Nádia Silva | Universidade Federal de Juiz de Fora | Juiz de Fora | Brazil |
| Bruno Manduca | Universidade de São Paulo | São Paulo | Brazil |
| Caio Sartorato Fava | Institute of Chemistry - UNICAMP | Campinas | Brazil |
| Carla Grijó Fonseca | Universidade Federal de Juiz de Fora | Juiz de Fora | Brazil |
| CAROLINA LUCHETTA | UNICAMP | Campinas | Brazil |
| Carolina Torres | IQ USP | São Paulo | Brazil |
| Caroline Silva | UNESP/IQAr | Araraquara | Brazil |
| Cecilia Lopes | Universidade de São Paulo (USP) | São Paulo | Brazil |
| Chiara Bisio | Università del Piemonte Orientale "A. Avogadro" | Alessandria | Italy |
| Claudia Manuela Santos Calado | Universidade Federal de Alagoas | Maceió | Brazil |
| Danilo Caiado | Universidade Estadual de Goiás | Anápolis | Brazil |
| Danilo Losito | Unifesp | S PAULO | Brazil |
| Denis de Araujo | Universidade de Franca | Franca | Brazil |
| Denise Eulálio | Instituto de Química | São Paulo | Brazil |
| Doy Why Justin Leung | University of Oxford | Oxford | United Kingdom |
| Eliene Santos | UNIFRAN | Franca | Brazil |
| Emanoel Hottes | Universidade Federal Rural do Rio de janeiro | Seropédica | Brazil |
| Fabrice Leroux | Chemical Institute of Clermont-Ferrand UMR 6296 | Aubière | France |
| Fernanda Romeiro | Unesp | Araraquara | Brazil |
| Fernando Wypych | Universidade Federal do Paraná | Curitiba | Brazil |
| Gabriel de Biasi Báfero | Institute of Chemistry, University of Campinas | Campinas | Brazil |
| GABRIEL MACHADO | USP | São Paulo | Brazil |
| Geovanne Lemos de Assis | Universidade de São Paulo | SÃO PAULO | Brazil |
| Gilmar Pinheiro | Universidade de São Paulo | São Paulo | Brazil |
| Giorgio Gatti | Università Piemonte Orientale | Alessandria | Italy |
| GISELLY CAVALCANTE | IFAL MACEIÓ | São Miguel dos Campos | Brazil |
| Guilherme Arroyos | Institute of Chemistry, São Paulo State University (UNESP) | Araraquara | Brazil |
| Guilherme Pires de Campos | Unicamp - Campinas State University | Campinas | Brazil |
| Hipassia Moura | TUWien | Vienna | Austria |
| Irlan Santos Lima | IQ USP | São Paulo | Brazil |
| Jader Ferreira | Universidade Federal de Viçosa - Campus Rio Paranaíba | Rio Paranaíba | Brazil |
| Jairo Tronto | Universidade Federal de Viçosa | Rio Paranaíba | Brazil |
| Jalusa Konzen Albiero | Grupo Guaçu | Londrina | Brazil |
| Jéssica Arjona | Universidade de São Paulo (USP) | Osasco | Brazil |
| jingfang yu | University of Oxford | Oxford | United Kingdom |
| João Paulo Pereira Duarte | Universidade Federal do Rio de Janeiro | | Brazil |
| Jocelyne Brendlé | Institut de Science des Matériaux de Mulhouse | Mulhouse | France |
| José Renato Lanzi Martini | Grupo Guaçu | Estiva Gerbi | Brazil |
| Josué Gonçalves | IQ-USP | São Paulo | Brazil |
| Joyce Fabiula Rodrigues | Universidade Federal de Viçosa | Rio Paranaíba | Brazil |
| Klara Melanova | Institute of Macromolecular Chemistry, AS CR | Pardubice | Czech Republic |
| Kleyton Ritomar Monteiro da Silva | Universidade Federal de Alagoas | União dos Palmares | Brazil |
| Larissa Bonfim | Universidade de Franca | Franca/SP | Brazil |

| FULL NAME | INSTITUTION | CITY | COUNTRY |
|---|---|---|---|
| Larissa Oliveira | Universidade Federal de São Paulo | Campinas | Brazil |
| Leonardo Miguel Menedez | UNICAMP | Campinas | Brazil |
| Lilian Amaral | Universidade Federal do Paraná | Curitiba | Brazil |
| Lister Pronestino Bianconi | Universidade Federal de São Paulo (UNIFESP) / Universidade de São Paulo (USP) | São Paulo | Brazil |
| Lorrana Vietro Barbosa | Universidade de Franca | Franca | Brazil |
| Lorranny Lemes | Universidade Estadual de Goiás | Goiânia | Brazil |
| Lucas Fonseca Quartarolli | University of São Paulo | São Paulo | Brazil |
| Lucas José | Universidade de São Paulo | São Paulo | Brazil |
| Ludvik Benes | University of Pardubice | Pardubice | Czech Republic |
| Manoel Vítor Borel Gonçalves | Universidade Federal de Ouro Preto | Florestal | Brazil |
| Marcos Bizeto | Federal University of São Paulo | Diadema | Brazil |
| Margarita Zimmermann | Universidade de São Paulo (USP) | São Paulo | Brazil |
| Mariana Dessimone | Universidade estadual paulista- Unesp | | Brazil |
| Mariana Veiga Rodrigues | Institute of Chemistry - UNICAMP | Campinas | Brazil |
| Matheus Ireno da Silva | University of São Paulo - USP | Osasco | Brazil |
| Maximillian Nascimento da Costa | Instituto Federal de Educação, Ciência e Tecnologia do Amazonas | Manaus | Brazil |
| Meng Lyu | University of Oxford | Oxford | United Kingdom |
| Michele Aparecida Rocha | Instituto de Química da USP | São Paulo | Brazil |
| Monica Pica | University of Perugia | Perugia | Italy |
| Nathalia da Silva Schiavi | Grupo Guaçu | Estiva Gerbi | Brazil |
| Otávio Gil | Universidade de São Paulo | São Paulo | Brazil |
| Paulo Loureiro | IQUSP | São Paulo | Brazil |
| Pedro Ivo Rodrigues Moraes | Universidade Federal de Juiz de Fora | Juiz de Fora | Brazil |
| Philippe Alexandre Divina Petersen | Universidade de São Paulo | São José dos Campos | Brazil |
| Rafael Macedo | USP- Escola Politécnica | São Paulo | Brazil |
| Rafael Trinca | University of São Paulo - USP | São Paulo | Brazil |
| Rafaela Bechara Soares | Universidade de São Paulo | São Paulo | Brazil |
| Sebastien CAHEN | Université de Lorraine | Nancy | France |
| Sergio Tavares | Universidade Federal de Juiz de Fora | Juiz de Fora | Brazil |
| Shuangde Li | Institute of Process Engineering, Chinese Academy of Sciences | Beijing | China |
| Suelen Souza | Unifran | Franca | Brazil |
| Tamires Silva | Universidade Federal de Alagoas | Maceió | Brazil |
| Telma de Oliveira Zacharias | UNICAMP | Campinas | Brazil |
| Thiago Monteiro | Universidade de São Paulo | São Paulo | Brazil |
| Tiago Honorato da Silva | Universidade de Franca | Franca | Brazil |
| Tierui Zhang | Technical Institute of Physics and Chemistry, Chinese Academy of Sciences | Beijing | China |
| Vagner Magri | Chemistry Institute, University of São Paulo | São Paulo | Brazil |
| Valber Duarte | Federal University of Viçosa | Rio Paranaíba | Brazil |
| Vander Alencar de Castro | UFV | Rio Paranaíba | Brazil |
| Vanessa Rodrigues da Cunha | Instituto de Química - Universidade de São Paulo | São Paulo | Brazil |
| Victor dos Santos Azevedo Leite | Universidade Federal de Viçosa | Rio Paranaíba | Brazil |
| Victor Vendruscolo | Institute of Chemistry - University of São Paulo | São Paulo | Brazil |
| Vítezslav Zima | Inst. Macromolecular Chemistry As CR, Prague | Pardubice | Czech Republic |
| Wing Lam Joyce Kwok | University of Oxford | Oxford | United Kingdom |